TOPOGRAPHICAL DISTRIBUTION AND MORPHOLOGICAL FEATURES OF SECOND ORDER PROJECTIONS FROM IDENTIFIED SUBDIVISIONAL AREAS OF RAT TRIGEMINAL NUCLEUS ORALIS

VOLUME I

By

Lizabeth Ann Smith

A DISSERTATION

Submitted to
Michigan State University
in partial fulfillment of the requirements
for the degree of

DOCTOR OF PHILOSOPHY

Department of Anatomy

1992

ABSTRACT

TOPOGRAPHICAL DISTRIBUTION AND MORPHOLOGICAL FEATURES OF SECOND ORDER PROJECTIONS FROM IDENTIFIED SUBDIVISIONAL AREAS OF RAT TRIGEMINAL NUCLEUS ORALIS

By

Lizabeth Ann Smith

This study examines the overall course, distribution and morphology of efferent axons and their terminal arborizations originating from neurons in rat trigeminal nucleus oralis (Vo) and innervating the spinal cord, cerebellum, cranial nerve nuclei and diencephalon. Unilateral deposits of Phaseolus vulgaris leucoagglutinin (PHA-L) were made iontophoretically into each Vo subdivision. Labeled terminal arborizations of a single type were observed bilaterally throughout the dorsal column nuclei while terminal arborizations of three morphologically distinct types were found bilaterally throughout laminae II-X of all levels of the spinal cord. Vo efferents projected bilaterally and were of three types in the granule cell layer of Crus I, Crus II, PML and the uvula of the cerebellum. Two morphologically distinct types of mossy fibers terminated in the Purkinje cell layer in these same orofacial tactile areas. A single type of axon collateral innervating the deep cerebellar nuclei emanated from parent mossy fibers destined for the cerebellar cortex. Vo efferents to the thalamus were of several types. Vo efferents of a single type innervated the oculomotor, trochlear, abducens, trigeminal motor, Edinger Westphal and dorsal vagal nuclei while two types of Vo efferents terminated in the

triger

Based

projec

nocice

horn

motor

reflex

other

spinal

direct

trigeminal sensory complex, facial motor, hypoglossal and solitary nuclei. Based on the results of this study, ascending and descending Vo efferent projections may contribute to the modulation of nociceptive and non-nociceptive input in the thalamus, dorsal column nuclei, spinal cord dorsal horn and cranial nerve sensory nuclei; influence output of cranial nerve motor nuclei; modulate spinal cord motor output involved in withdrawl reflexes (e.g., trigemino-neck reflex); and/or contribute to the expression of other reflexes involving the integration of trigeminal sensory input with spinal autonomic systems. Vo efferents to the cerebellum are positioned to directly and indirectly influence final cerebellar output.

DEDICATION

To my family: Although they never understood my quest for knowledge, they accepted it.

Fa
th
my
Pys
con

Dep
Uni
supp
grad
the
genu

unfa
pleas
wish
bestow
Dr. Di

Osteop
Traini
Veroni

ACKNOWLEDGMENT

I wish to express my sincere appreciation to Dr. William McKenzie Falls, my advisor, for his patience, encouragement and guidance throughout the course of this study. I also wish to thank the members of my guidance committee, Drs. John Johnson, David Kaufman, Joseph Pysh, John Thornburg and Charles Tweedle for their advice, support and constructive criticism regarding this thesis.

I wish to extend my gratitude to the faculty and staff of the Department of Anatomy as well as the staff of the Student Affairs Office and Unit III Clerkship Office in the College of Osteopathic Medicine for their support, encouragement and patience during the entire length of my graduate and medical student training. A special indebtedness is owed to the Osteopathic medical students at Michigan State University for their genuine interest and unwavering support of my efforts.

Although many individuals are remembered for their generosity and unfailing friendship, a certain few will forever be a part of my most pleasurable memories during my training at Michigan State University. I wish to state my gratitude and heartfelt thankfulness for the kindness bestowed upon me by the following persons and friends: Dr. Kay E. White, Dr. Diane Sayers, Kathy Assiff and Diane Batten.

Lastly, I wish to acknowledge financial support from the College of Osteopathic Medicine given to me as a member of the Medical Scientist Training Program under the direction of Drs. Justin McCormick and Veronica Maher.

TABLE OF CONTENTS

Table of Contents (Continued)

LIST OF FIGURES

CHAPTER I

CHAP

Figure

Figure

Figure

Figur

Figur

CHA

Figu

Figu

Figu

Figu

Figu

Fig

Fig

Fig

Fig

CHAPTER I (CONTINUED)

CHAPTER II

CHAPTER II (CONTINUED)

CHAPTER III

CHAPTER III (CONTINUED)

CHAPTER IV

CHAPTER IV (CONTINUED)

CONCLUDING REMARKS

NUM

III

IV

VI

VII

VIIg

VIIn

XII

X

I-X

1-10

3V

LETTE

BZ

CC

CE

CeC

CG

CL

CM

cp

CRUS I

ABBREVIATIONS

NUMERALS

III	oculomotor nucleus
IV	trochlear nucleus
VI	abducens nucleus
VII	facial motor nucleus
VIIg	genu of the facial nerve
VIIn	facial nerve
XII	hypoglossal motor nucleus
X	dorsal vagal nucleus
I-X	spinal cord laminae
1-10	cerebellar lobules
3V	third ventricle

LETTERS

BZ	border zone Vo
CC	cerebellar cortex
CE	cervical enlargement
CeC	central cervical nucleus
CG	central gray
CL	centrolateral thalamic nucleus
CM	central medial thalamic nucleus
cp	cerebral peduncle
CRUS I	crus I ansiform lobule

CF

Cu

DA

DC

dC

dfu

dlfu

DM

dsc

EP

EW

F

f

fr

G

GCL

Gr

HRP

IBN

ic

icp

IML

IMM

INT

IO

IS

LAT

CRUS II	crus II ansiform lobule
Cu	cuneate nucleus
DAB	3,3' diaminobenzidine
DCN	dorsal column nuclei
dCN	deep cerebellar nuclei
dfu	dorsal funiculus spinal cord
dlfu	dorsolateral funiculus spinal cord
DM	dorsomedial Vo
dsc	dorsal spinal commissure
EP	entopeduncular nucleus
EW	accessory oculomotor nucleus
F	nucleus fields of Forel
f	fornix
fr	fasciculus retroflexus
G	gelatinosus thalamic nucleus
GCL	granule cell layer
Gr	gracile nucleus
HRP	horseradish peroxidase
IBN	intermediate basilar nucleus
ic	internal capsule
icp	inferior cerebellar peduncle
IML	intermediolateral cell column
IMM	intermediomedial cell column
INT	interposed cerebellar nucleus
IO	inferior olive
IS	injection site
LAT	lateral cerebellar nucleus

LC

LC

LE

LR

MI

MD

MD

MD

MEI

MF

MG

ML

ml

mlf

mt

PB

PCL

PF

PHA-

PML

P_0

PVP

R

RCC

R_e

Rf

RF_g

LC	locus coeruleus
LCN	lateral cervical nucleus
LE	lumbar enlargement
LRt	lateral reticular nucleus
MD	mediodorsal thalamic nucleus
MDH	medullary dorsal horn
MDMd	middle dorsomedial, dorsal Vo
MDMv	middle dorsomedial, ventral Vo
MED	medial cerebellar nucleus
MF	mossy fiber
MG	medial geniculate nucleus
ML	molecular layer, cerebellar cortex
ml	medial lemniscus
mlf	medial longitudinal fasciculus
mt	mammillothalamic tract
PB	parabrachial nucleus
PCL	Purkinje cell layer
PF	parafascicular thalamic nucleus
PHA-L	Phaseolus vulgaris leucoagglutinin
PML	paramedian lobule
Po	posterior thalamic nuclear group
PVP	posterior paraventricular thalamic nucleus
R	red nucleus
RCC	rostral cervical cord
Re	reuniens thalamic nucleus
Rf	retrofacial nucleus
RFg	reticular formation, gigantocellularis

RFp

RRI

SI

SC

SIM

SNR

SO

Sol

STh

SVC

SVN

svt

TC

vfu

Vi

VL

Vmo

Vms

Vo

VPL

VPM

vsc

WGA

wm

ZI

RFp	reticular formation, parvocellular
RRF	retrorubral field
SI	SI somatosensory cortex
SC	superior colliculus
SIM	simplex lobule
SNR	substantia nigra, reticular
SO	superior olive
Sol	nucleus solitary tract
STh	subthalamic nucleus
SVC	spinal trigeminal complex
SVN	spinal trigeminal nucleus
svt	spinal trigeminal tract
TC	thoracic cord
vfu	ventral funiculus spinal cord
Vi	trigeminal nucleus interpolaris
VL	ventrolateral Vo
Vmo	trigeminal motor nucleus
Vms	main sensory trigeminal nucleus
Vo	trigeminal nucleus oralis
VPL	ventral posterolateral thalamic nucleus
VPM	ventral posteromedial thalamic nucleus
vsc	ventral spinal commissure
WGA	wheat germ agglutinin
wm	white matter, cerebellar cortex
ZI	zona incerta

INTRODUCTION

Trigeminal nucleus oralis (Vo) is thought to play an important role in the reception, central processing, modification and the transmission of nociceptive information to the brainstem and spinal cord from tooth pulp, oral and perioral areas as well as mechanoreceptive information from the face and oral cavity. Rat nucleus oralis (Vo) can be subdivided into dorsomedial (DM), ventrolateral (VL) and border zone (BZ) subdivisions based on differences in morphological and functional criteria. DM receives terminal arborizations of a group of large diameter primary trigeminal axons. Included within the DM neuropil are five additional types of trigeminocerebellar projection neurons, all of which innervate one or more of the orofacial portions of tactile areas (Crura I and II, the paramedian lobule, and the uvula) in the rat cerebellar cortex (Falls et al., '86; Hu and Sessle, '84; Tamarova et al., '73). In addition to these cells, in the cat, are two morphologically distinct types of projection neurons innervating the trigeminal motor nucleus (Sessel et al., '77), of which one type responds to stimulation of intraoral low threshold mechanoreceptors while the other is activated following stimulation of the tooth pulp. Rat DM also contains a small population of trigeminospinal and trigeminohypoglossal projection neurons (Borke et al., '83; Falls, '84b).

The neuropil of VL is comprised of terminal arborizations of a population of small myelinated primary trigeminal axons (Falls, '86; Falls, '88) and two groups of ascending intratrigeminal axons (Falls, '84a) originating from neurons in the medullary dorsal horn (MDH). Additional

retrogr
studies
Falls,
project
trigemi
al., '87
et al.,
Kruger
neuron
innerva
trigemi
of five
neuropi
fibers (
myelina
while th
to the d
BZ cont
axons fr
and Alb
single p
MDH p
subdivis
trigemir
trigemin
number

retrograde horseradish peroxidase (HRP) and fluorescent dye and Golgi studies have demonstrated a subpopulation of Golgi type II interneurons (Falls, '83), three morphologically distinct types of intratrigeminal MDH projection neurons (Falls, '84), morphologically distinct populations of trigeminospinal (Falls, '84b; Ruggiero et al., '81), trigeminotectal (Bruce et al., '87; Huerta et al., '83), trigeminothalamic (Bruce et al., '87; Erzurumlu et al., '80; Fukushima and Kerr, '79; Kruger et al., '77; Silverman and Kruger, '85) and trigeminofacial (Erzurumlu and Killackey, '79) projection neurons. Trigeminospinal projection neurons are most numerous and innervate all levels of the rat spinal cord while trigeminotectal and trigeminothalamic neurons are fewer in number. Terminal arborizations of five populations of primary trigeminal axons are found within the BZ neuropil, three of which arise from different types of large myelinated fibers (Falls, '87). Of the remaining two types, one is derived from small myelinated parent branches (Falls and Alban, '86; Falls, '87; Falls, '88) while the other originates from unmyelinated parent fibers and is confined to the dorsal one-half of the subdivision (Falls, '86; Falls, '88). Additionally, BZ contains the terminal arbors of one group of ascending intratrigeminal axons from MDH neurons (Falls '84) as well as trigeminocerebellar (Falls and Alban, '86) and descending MDH projection neurons (Falls, '84a). The single population of trigeminocerebellar cells is found dorsally in BZ, while MDH projection neurons are situated more ventrally within the subdivision. Throughout BZ are morphologically distinct populations of trigeminospinal (Falls, '84b), trigeminotectal (Bruce et al., '87), and trigeminothalamic (Bruce et al., '87) projection neurons which are few in number with trigeminothalamic cells being found least frequently.

In
within e
to the su
afferent
projectio
and are
the neu
and or
arboriza
allowing
neural e
contacts
glomeru
dendrite
endings
A
to disc
anatom
electro
central
nocicep
numero
target
the pri
was to
mechan
by pri

In general, the morphologically distinct populations of neurons within each Vo subdivision of have most of their dendritic arbors confined to the subdivision and are in a position to receive primary and non-primary afferent inputs terminating within the neuropil. The second-order projection neurons provide the efferent outflow from each Vo subdivision and are able to affect the synaptic activity within numerous locations along the neuraxis. Axons of neurons which remain within each Vo subdivision and/or give off intranuclear collaterals as they leave Vo, have their arborizations primarily confined to that subdivision of the parent cell allowing for interaction with neighboring neuronal processes. Many neural elements within each of the three subdivisions of Vo form synaptic contacts in well-defined structures referred to as glomeruli, with each glomerulus containing a primary trigeminal afferent axonal ending, dendrites of projection and interneuronal Vo cells and non-primary axonal endings.

Although a number of electrophysiological studies have been devoted to discerning the functional organization of Vo, only recently have anatomical analyses provided structural substrates underlying these electrophysiological events. Vo has been implicated in the reception, central processing as well as modification and transmission of orofacial nociceptive and mechanoceptive information suggesting a role in numerous chronic pain states (e.g., trigeminal neuralgia). Vo is a major target of primary trigeminal neurons which innervate the tooth pulp where the primary sensation elicited in man is pain. The purpose of this study was to delineate the synaptic circuitry in Vo in order to understand possible mechanisms involving orofacial pain and tactile information transmitted by primary trigeminal neurons is processed and relayed by Vo to other

areas of
anterogra
determine
axons fro
brain and
for an und
which Vo
under nor

areas of the neuraxis. This light microscopic study utilized the anterograde technique of Phaseolus vulgaris leucoagglutinin (PHA-L) to determine the overall pattern, organization, and morphology of efferent axons from projection neurons in each Vo subdivision to targets in the brain and spinal cord. The knowledge gained from this study will provide for an understanding of the anatomical framework and circuitries through which Vo processes orofacial nociceptive and mechanoceptive information under normal and pathological circumstances.

DESC
SPIN
TRIG

!

al., '85
experi
oralis
primar
influen
neuron
three V
zone (B
the ne
electrop
trigemi
spinal t
Vi and
rat (Bu
Ruggier
(Burton
Kuypers

CHAPTER I

DESCENDING PROJECTIONS TO RAT DORSAL COLUMN NUCLEI AND SPINAL CORD FROM IDENTIFIED SUBDIVISIONAL AREAS WITHIN TRIGEMINAL NUCLEUS ORALIS UTILIZING THE METHOD OF PHA-L

INTRODUCTION

Neuroanatomical studies in our laboratory (Falls, '83a; 84a-c; Falls et al., '85) and electrophysiological investigations (Hayashi,'82) have provided experimental evidence that each subdivision of rat trigeminal nucleus oralis (Vo) receives morphologically and functionally distinct groups of primary and non-primary afferent axons which are positioned to directly influence the activity of different groups of second order Vo projection neurons. These projection cells provide the efferent outflow from each of three Vo subdivisions; dorsomedial (DM), ventrolateral (VL) and border zone (BZ), and affect synaptic activity in the numerous target areas along the neuraxis. Several investigations utilizing anatomical and electrophysiological methodology have established the existence of a direct trigeminospinal projection originating from neurons in each portion of the spinal trigeminal nucleus (SVN), i.e., Vo, trigeminal nucleus interpolaris (Vi) and the medullary dorsal horn (MDH; trigeminal nucleus caudalis) in rat (Burton and Loewy, '76; Burton and Loewy, '77; Leong et al., '84; Ruggiero, '81; Satoh, '79; Falls, '83b), hamster (Bruce et al., '84), cat (Burton et al, '79; Burton and Loewy, '76; Craig, '78; Hayashi et al., '84; Kuypers and Maisky, '75; Matsushita et al., 80; Matsushita et al, '81;

Matsus
(Cabana
Loewy,
VL subc
to the e
and by v
interme
activity
internu
transpor
that inn
Falls et a

To
morpholo
from neu
the dorsa
leucoaggl
from diffe
been iden
This techn
features o
in each Vc
motor and
anatomica
destinatior
axonal con
examined

Matsushita et al., '82; Tohyama et al., '79), dog (Craig, '78), opossum (Cabana and Martin, '84; Crutcher et al., '78), and monkey (Burton and Loewy, '77). Vo trigeminospinal (Vo-TS) projection neurons situated in the VL subdivision have been shown in retrograde studies to project bilaterally to the entire length of the spinal cord (Leong et al., 84; Ruggiero et al., '81) and by virtue of their position in the dorsal and ventral horns as well as the intermediate gray (Lamina VII) have been suggested to influence the activity of somatosensory relay neurons, motoneuronal cell pools and internuncial cells throughout the spinal cord. Previous retrograde transport studies have shown that rat VL contains large multipolar cells that innervate cervical, thoracic and lumbar spinal cord levels (Falls '84b; Falls et al.'90).

To date, no anatomical studies have been undertaken to examine the morphological features of efferent axons and their terminal arbors arising from neurons in each Vo subdivision and innervating the spinal cord and the dorsal column nuclei (DCN). The anterograde Phaseolus vulgaris leucoagglutinin (PHA-L) technique allows for comparison of projections from different neuronal populations, eg., spinal cord neurons, which have been identified previously using retrograde transport methods (Falls, '84b). This technique also allows for further characterization of morphological features of parent axons and terminal arborizations arising from neurons in each Vo subdivision and terminating in anatomically identified sensory, motor and autonomic areas in the spinal cord. Detailed quantitative anatomical information about precise spatial features including source, destination, patterns of termination, and morphological details of Vo-TS axonal connections is non-existent. In the present study, we have closely examined and compared the distribution, relative densities and

morph

horns

thorac

well a

each

publis

morphological features of Vo-TS axons terminating in dorsal and ventral horns of the rostral cervical segments (RCC), cervical enlargement (CE), thoracic segments (TC) and lumbar enlargements (LE) of the spinal cord as well as efferent axons innervating DCN following injections of PHA-L into each Vo subdivision. A preliminary report of these findings has been published (Smith and Falls, '88).

MATERIAL AND METHODS

Nine adult male Sprague Dawley albino rats (250-300g) were anesthetized with sodium pentobarbital (35-40 mg/kg) and placed in a stereotaxic apparatus (Kopf). All surgeries employed aseptic technique. A small opening was made in the occipital bone and the dura matter incised. Glass micropipettes (inside tip diameter 20-30 um) filled with 2.5% PHA-L (Vector Labs) in 0.05 M phosphate buffered saline (pH 7.4) were lowered into Vo passing through the cerebellum at an angle of approximately 90° with respect to the horizontal plane. A pulsed (7 seconds on, 7 seconds off) positive current of 5 mA (Midgard, Transkinetics model CS3) was employed to iontophoretically deliver PHA-L for 45-60 minutes into each Vo subdivision; DM (Cases 734, 741 and 824), VL (Cases 739, 751, 860 and 866) and BZ (Cases 750 and 826) utilizing coordinates obtained from the stereotaxic atlas of Paxinos and Watson ('86). The choice of the injection sites was based on the results of previous anterograde PHA-L studies (Smith and Falls, '88) of Vo efferents. The micropipette was left in place for and additional 5 minutes following termination of current and then withdrawn. At the completion of the experiment, the scalp was sutured and the animal returned to its cage. All animals were housed, maintained and cared for according to federally prescribed guidelines (NIH Guide, '85). After postinjection survival periods of 10-14 days animals were deeply anesthetized and perfused transcardially using a two stage procedure (Berod, '81) with solutions of 250 ml of 150 mM acetate buffer (pH 6.5) with 4% paraformaldehyde followed by 750 ml of 65 mM borate buffer (pH 9.5) containing 4% paraformaldehyde and 0.05% gluteraldehyde at 4° C. The brain and spinal cord were removed and postfixed overnight at 4° C in the

last perfusate solution. The pons-medulla and spinal cord was blocked and 20-30 um thick transverse sections were cut using an Oxford vibratome into Tris buffered saline (TBS, pH 7.6) at room temperature (RT). Sections were collected in tissue trays filled with TBS and processed immediately for immunocytochemistry according to a modification of the method of Gerfen and Sawchenko ('84). After three rinses in TBS with 0.5% Triton X-100 (TBS-TX) at RT, sections were placed in a solution of 3% normal rabbit serum in TBS-TX for 30 minutes and then briefly rinsed (5 minutes) in TBS-TX at RT. Sections were then incubated for 24-48 hours at 4° C in goat anti-PHA-L (1:2000; Vector Labs) diluted in TBS-TX. To visualize the PHA-L stain, sections were processed with the avidin-biotinylated HRP (HRP-ABC) technique (Hsu et al., '81) using a vectastain ABC kit (Vector Labs). The final peroxidase reaction was performed with a solution of 0.15 M Tris Buffer containing 100 mg% 3,3' diaminobenzidine or DAB (Sigma), 40 mg% ammonium chloride, 200 mg% B-D-glucose, and 38 mg% imidozole. Sections were incubated in this solution for 45-60 minutes. After several rinses in TBS-TX, sections were mounted onto gelatin-coated slides, counterstained with cresyl violet and coverslipped. Detailed light microscopic evaluation of each section was undertaken in order to determine the overall course, distribution, organization and morphology of efferent axons and their terminal arbors originating from neurons in each Vo subdivision. Schematic drawings illustrating the distribution and overall pattern of termination of parent axons and their terminal arbors were made using an Aus Jena Documator at a magnification of 17.5X. Drawings illustrating the position of parent fibers and their terminal arborizations within schematic drawings were made using a 2.5X objective lens attached to a Leitz Laborlux 12 microscope fitted with a drawing tube at

a mag

their t

objecti

corresp

compos

density

encount

Within

their te

of serial

of serial

distinct

neuropil

segment

similar

terminati

a magnification of 31X. The morphological features of parent axons and their terminal arborizations were illustrated using a 100X oil immersion objective lens at a magnification of 1,250X. Photomicrographs of corresponding sections were taken to illustrate morphological details. All composite drawings, Figures 5-7, illustrate the course, distribution and density of labeled Vo-TS efferent axons and terminal arborizations encountered in fifteen consecutive sections through a spinal cord segment. Within the confines of each segment analyzed, labeled parent axons and their terminal arborizations were mapped out through a successive series of serial sections and cataloged by terminal type. Through the same series of serial sections spanning approximately 450-500 um, each of the three distinct types of Vo-TS efferents were followed as they coursed through the neuropil to assess direction as well as length of trajectory within each segment in dorsoventral, mediolateral and rostrocaudal dimensions. A similar method was utilized to examine the single type of Vo efferent terminating in DCN.

INJE

each
neuro
projec
injecti
neuron
V tract
which
transpo
problem
other s
significa
without
the labe
spinally
84b).

Mo
caudally
reticular
bilaterall
caudally t
DCN. Alt
fibers of p
not though

RESULTS

INJECTION SITES

Unilateral PHA-L deposits were localized in discrete areas within each Vo subdivision (Figure 2). Only areas containing densely filled neurons were considered to be effective zones from which efferent projections originated. Weak anterograde label was observed following injections in which PHA-L deposits only sparsely filled Vo projection neurons. In several cases (824, 826 and 750) PHA-L diffused into the spinal V tract (svt) and labeled numerous svt axons as far caudally as the MDH which serves to indicate that PHA-L may have been subject to uptake and transport by at least some fibers of passage. However, the potential problems of retrograde transport of PHA-L by fibers of passage published in other studies (Cliffer and Giesler, '88; Schofield, '90) did not play a significant role in the results of this study since cases of PHA-L deposition without spread into svt yielded similar results. The potential does exist that the labeled fibers found in svt originate from VL neurons giving rise to spinally projecting parent axons described in an earlier study by Falls (' 84b).

Most Labeled Vo-TS efferent axons coursed ventromedially and caudally through the gigantocellular (RFg) and parvocellular (RFp) reticular formation on their way to the medial longitudinal fasciculus (mlf) bilaterally. In addition, a small contingency of Vo efferents coursed caudally through Vi and MDH as they descended to the spinal cord and DCN. Although the potential exists for possible labeling of intertrigeminal fibers of passage originating from neurons located in Vi and MDH it was not thought to be significant in this study. The pattern of distribution and

morphologies of labeled Vo-TS efferents to the spinal cord were not identical in characteristics as described previously for Vi efferents to the spinal cord (Cook and Falls, '90; '91), while no published reports exist for SVN projections from rat Vi or MDH to DCN.

In this study all nine experiments resulted in injections of PHA-L largely restricted to either DM, VL or BZ. Three of the brains examined (Cases 734, 860 and 750) were used to illustrate representative DM, VL and BZ injection sites respectively in Figure 1 A-C, schematically and Figures 2 A-C, photographically. The DM injection site, Case 734 (Figures 1,2 A), was situated in middle DM and partially filled dorsal and ventral zones with slight spread into dorsal BZ. The injection site measured 1180 um rostrocaudally, 850 um dorsoventrally and 400 um mediolaterally. The VL injection site, Case 860 (Figures. 1,2 B), was located approximately midway along the rostrocaudal length of Vo. The PHA-L deposit extended a short distance into BZ and measured 720 um rostrocaudally, 525 um dorsoventrally and 700 um mediolaterally. The BZ injection site, case 750 in Figures. 1,2 C was located in the dorsal two-thirds of the subdivision with some spread into the dorsal portion of VL. The injection site was located midway along the rostrocaudal extent of Vo and extended 1080 um rostrocaudally, 700 um dorsoventrally, and 300 um mediolaterally. In the additional six experiments injections were made at other locations in Vo subdivisions (Cases 739, 741, 751, 824, 826, and 860) and the injection sites were similar in size to those illustrated above and yielded similar results.

PROJECTIONS TO THE DORSAL COLUMN NUCLEI

PHA-L labeled efferent axons and terminal arborizations were visible in the DCN following injections into DM, VL and BZ. Injections restricted

to DM

caudal

dorsola

MDH w

Termina

Upon re

paralleli

off and

and MD

Upon re

arborizat

entered r

while a f

DCN. D

solitary r

while at r

hypogloss

caudal po

terminal

labeling fo

824, term

projections

efferents il

density of t

of labeling

when comp

positioned i

to DM (Figure 5 A, B) resulted in labeling of parent axons that passed caudally in axon bundles through the ipsilateral dorsal cap and dorsolateral regions of Vi and the dorsomedial portion of lamina III-V of MDH with the greatest density of labeled efferents in laminae III and IV. Terminal arbors were not observed in any of these regions of Vi and MDH. Upon reaching the rostral pole of DCN and for the rest of their trajectory paralleling the rostrocaudal extent of DCN, many parent axons would peel off and leave the axon bundles dorsomedially and proceed through the Vi and MDH neuropil to exit the dorsal and dorsomedial borders of SVN. Upon reaching ipsilateral DCN many parent fibers gave rise to terminal arborizations (parent axons coursed dorsally to nucleus cuneatus (Cu) and entered nucleus gracilis (Gr) by weaving around the medial portion of Cu) while a few others continued on, decussated and innervated contralateral DCN. Decussating fibers took a path through the dorsal portion of the solitary nuclei (Sol) to terminate in rostral portions of contralateral DCN while at more caudal levels the decussating axons crossed through Sol and hypoglossal nuclei (XII) to form terminal arbors in successively more caudal portions of the contralateral nuclei. The densest population of terminal arbors was found ipsilaterally in Cu and Gr with less dense labeling found contralaterally in the same nuclei. In two cases, (734 and 824), terminal arborizations were observed in Cu bilaterally while bilateral projections to Gr were only found in Case 734. The distribution of DM efferents illustrated in Figure 5 B from Case 734 suggests that the greatest density of terminal arborizations was ipsilaterally in DCN with a gradient of labeling suggesting a greater number of arborizations in ipsilateral Cu when compared to Gr. Labeled Vo efferent terminal arborizations were positioned in the ventral three-fourths of Cu throughout its rostrocaudal

exter

Gr al

Vo ef

numb

the ip

ventro

concen

unbran

the res

axons v

medial

DCN. S

and Gr

density

with labe

diffusely

Fol

spread in

axons wer

region of i

MDH. As

rise to term

DCN levels

and proceed

terminal a

ventrally in

extent whereas, labeled terminal arbors were found scattered throughout Gr also along the rostrocaudal extent of the nucleus. In Case 741, labeled Vo efferents were sparsely distributed in ipsilateral Cu.

PHA-L injections restricted to VL (Figures 6 A,B) resulted in a small number of labeled parent axons that descended in axon bundles through the ipsilateral ventrolateral magno-and parvocellular regions of Vi and the ventrolateral portion of laminae III-V of MDH, with the heaviest concentration of fibers in laminae III and IV. The parent axons were unbranched throughout their course reaching the rostral pole of DCN. For the rest of their trajectory, along the rostrocaudal extent of DCN, parent axons would leave the bundles, turn and course dorsomedially along the medial borders of Vi and MDH to form terminal arborizations in ipsilateral DCN. Sparse terminal arbors were observed in the rostral two-thirds of Cu and Gr with a greater density always observed in Cu. Terminal arbor density was considerably less than that observed following DM injections with labeled terminal arborizations situated ventrally in Cu and scattered diffusely within Gr.

Following an injection in the dorsal two-thirds of BZ, with some spread into dorsal VL (Figures 1,2 C; 7 A,B), a few PHA-L labeled parent axons were observed to descend in axon bundles through the dorsolateral region of ipsilateral Vi and the dorsolateral portion of lamina I of rostral MDH. As described for the parent axons above, DCN efferents did not give rise to terminal arborizations along their course. Continuing to descend at DCN levels, the parent fibers left the axonal bundles, turned dorsomedially and proceeded through Vi and MDH to ipsilateral DCN where they formed terminal arborizations. Labeled Vo efferents were widely scattered ventrally in the rostral two-thirds of Cu and diffusely in rostral Gr.

Termin

Gr. H

and Gr

L

appear

into all

to 1.0

relative

passant

end bo

fields i

other fo

PROJE

P

gray ma

subdivis

their lar

fibers an

La

matter, t

and disti

labeled a

fibers tr

arborizat

were few

and origi

Terminal arborizations were most dense in Cu when compared to those in Gr. However, these terminal arbors were considerably less dense in Cu and Gr when compared to those arising from DM and VL neurons.

Labeled parent axons and terminal arborizations in Cu and Gr appeared to be of a single morphological type following PHA-L injections into all three Vo subdivisions (Figures 9 A,B; 17 E). Each parent axon (0.8 to 1.0 um in diameter) terminated in a thin (0.5 to 0.8 um in diameter) relatively unbranched terminal strand containing widely spaced boutons en passant (0.5 to 0.8 um in diameter). A few short side branches capped by an end bouton emanated from the terminal strand. Within their terminal fields in Cu and Gr, terminal strands frequently intertwined with each other forming a delicate plexus of interlacing terminal fibers.

PROJECTIONS TO THE SPINAL CORD

PHA-L labeled parent axons and terminal arbors were visible in the gray matter of the RCC, CE, TC and LE following injections into Vo subdivisions. The course of Vo efferent axons, their levels of termination, their laminae and nuclei of distribution and the morphology of the parent fibers and terminal arborizations were not uniform.

Labeled Vo-TS efferents, destined for specific regions of spinal gray matter, traversed the brainstem and spinal cord primarily by two separate and distinct routes. An additional route containing a small grouping of labeled axons was observed in C1-C2 segments of ipsilateral RCC. Parent fibers traveled along these routes without giving rise to terminal arborizations. Labeled parent axons taking the first route (trans SVN) were fewer in number when compared to those utilizing the second route and originated from neurons in each Vo subdivision. They also projected

bilaterally to the spinal cord with an ipsilateral predominance. Parent axons following the ipsilateral path joined deep axonal bundles traversing each Vo subdivision and descended through Vo and comparable portions of Vi and laminae III-V of MDH. At caudal MDH levels the labeled parent axons, still in the axonal bundles, shifted medially and entered the spinal dorsal horn. As the parent axons descended in the dorsal horn, axonal bundles containing the labeled fibers were located primarily in laminae V with some situated along the ventral aspect of lamina IV. Labeled parent axons arising from these bundles formed terminal arborizations of one type, Type 1, in the dorsal horn and intermediate gray. Parent fibers descending to the contralateral dorsal horn and intermediate gray followed the same route through deep axonal bundles in contralateral Vo, Vi and MDH as did the descending ipsilateral parent axons. These axons arose form neurons in each Vo subdivision and decussated through the reticular formation and caudal pontine levels to enter the same Vo subdivision contralaterally. Within these contralateral Vo subdivisions the parent axons emitted collaterals which formed terminal arborizations within the subdivisions before entering the deep axonal bundles to descend spinal levels.

The second and largest path (trans mlf/ventral funiculus (vfu) consisted of parent axons which left each Vo subdivision ventromedially and caudally, traversed RFp and RFg and formed distinct axonal bundles which descended bilaterally in the mlf with an ipsilateral predominance (Figures 5-7). In the spinal cord these bundles of labeled axons were located in the ventromedial portion of vfu bilaterally. Labeled parent axons exited these bundles, coursed dorsally and medially or laterally in the spinal gray matter and formed terminal arbors of two types (Types 2 and 3)

primarily in the ventral horn and intermediate gray. Type 2 arborizations were also observed to arise from parent axons extending into lamina III of the dorsal horn bilaterally. Labeled Vo-TS parent axons giving rise to Type 2 arborizations were observed to emanate from the vfu bilaterally while parent axons giving rise to Type 3 arborizations were only observed in ipsilateral vfu. The parent axons with Type 3 arbors destined for the contralateral spinal gray would course through the ventral spinal commissure (vsc). At C1 and C2 levels some labeled parent fibers were observed to leave vfu laterally, course dorsally and laterally adjacent to the ventral horn spinal gray matter in the lateral funiculus (lfu) and enter ipsilateral laminae III-V of the dorsal horn where they formed Type 2 terminal arborizations.

The additional route (trans RF) contained only a few labeled parent axons. The fibers left Vo ventromedially and caudally at caudal pontine levels, decussated and descended to the spinal cord through the RFp. In the reticular formation the labeled parent axons are widely scattered and did not form any discernable bundles. Upon entering RCC at the C1 and C2 levels the axons formed a small bundle in the dorsal funiculus (dfu) adjacent to laminae II-IV of the dorsal horn. Parent arbors left the bundle and gave rise to collateral terminal arborizations in ipsilateral laminae IV-VI medially and the intermediate basilar nucleus (IBN) before decussating in the dorsal spinal commissure to terminate in these same areas contralaterally. These terminal arborizations fell into the Type 1 category.

PROJECTIONS TO ROSTRAL CERVICAL SPINAL CORD

Following DM, VL and BZ injections, numerous labeled parent axons and terminal arborizations were observed to innervate RCC (C1-C4). Vo-TS

efferents are of three morphologically distinct types (Types 1, 2 and 3). Two types, Types 1 and 2, terminated in the dorsal horn and intermediate gray and Types 2 and 3 arborized in the ventral horn and intermediate gray. All three types were seen bilaterally in varying proportions after injections made in all three Vo subdivisions.

The Density and Morphology of Vo Efferent Terminal Arborizations, Rostral RCC

The density of labeled Vo-TS terminal arbors was greatest in the ipsilateral dorsal horn following VL and DM injections and decreased significantly in density following BZ injections. The intermediate gray (lamina VII) was observed to be less densely innervated and received terminal arborizations in approximately equal numbers from DM and VL neurons. Cells located in BZ projected to the intermediate gray (lamina VII). The projection was sparse and bilateral. The density of labeled Vo-TS efferents, from DM and VL neurons, terminating in the ipsilateral ventral horn was observed to be almost equal to the density seen in the ipsilateral dorsal horn. BZ neurons projected only sparingly to this area. Vo-TS efferents terminating in the contralateral ventral horn were most numerous from VL neurons followed by DM and BZ cells. In all three cases, the density of labeled terminal arborizations was most pronounced at C1-C2 segments and decreased significantly in C3-C4 segments.

The terminal arborizations of Type 1 Vo-TS efferents (Figures 10; 13; 14; 18 A,B) in the dorsal horn and intermediate gray (lamina VII) of RCC were observed following injections placed in all three Vo subdivisions and consisted of a sparsely branched thin terminal strand (0.8 to 1.0 um in diameter) with widely spaced boutons en passant 0.6 X0.8 um in diameter.

These te
coursed r
the termi
after the
dorsolater
small gro

Typ
the ventra
and were
made in a
thick pare
tertiary c
These brar
1.5 to 3.5 X
were obse
bilaterally,
1 and 2 V
within the
density belo

The
ipsilateral v
in these sa
laminae VII
The terminal
large diamet
sinuous cours
12, 16; 18 E,

These terminal arbors were direct continuations of the parent fiber and coursed rostrocaudally before ending in a terminal bouton. The trajectory of the terminal arborizations was primarily dorsolaterally and dorsomedially after the parent fibers exited deep axonal bundles within the dorsal horn or dorsolaterally and ventromedially after the parent axons emerged from the small grouping of fibers in dfu.

Type 2 Vo-TS efferents gave rise to collateral arbors terminating in the ventral horn, intermediate gray and laminae III-VI of the dorsal horn and were present in approximately equal densities following injections made in all three Vo subdivisions. These efferents were characterized by a thick parent fiber (1.5 um in diameter) which underwent secondary and tertiary collateral branching along its trajectory (Figures 11; 15; 18 C,D). These branches displayed large boutons en passant and end boutons (1.3 X 1.5 to 3.5 X 2.5 um in diameter). Parent fibers of the Type 2 Vo-TS efferent were observed in RCC to shift laterally from the fiber bundles in vfu bilaterally, being of greater density ipsilaterally, and course in dlfu. Types 1 and 2 Vo-TS efferent terminal arborizations were observed to coexist within the same portions of the same dorsal horn laminae with the greatest density belonging to the Type 1 arborizations.

The Type 3 Vo-TS efferent terminated predominately in the ipsilateral ventral horn and intermediate gray and decussated to terminate in these same areas contralaterally. Its greatest density was within laminae VIII and IX of spinal cord enlargements and the thoracic cord. The terminal arborization of the Type 3 Vo-TS efferent is characterized by a large diameter parent fiber (1.8 to 2.0 um in diameter) which follows a sinuous course after entering the ventral horn from ipsilateral vfu (Figures 12: 16: 18 E,F). Occasionally, side-branches emanate from the parent fiber

which gave rise to large end boutons (3.0 X 4.0 to 3.0 X 5.0 um in diameter). Very few boutons en passant were observed. Collateral branches from parent strands were observed to course dorsomedially, decussate in vsc, and terminate in homonymous areas within the contralateral spinal gray. Type 3 efferents were labeled in their greatest density after DM injections followed by VL injections, with sparse labeling observed following BZ injections.

Distribution and Density of Vo Efferents to Rostral Segments C1-C2 of RCC Following DM Injections

The pattern in which labeled Vo-TS efferents terminated in the dorsal horn laminae following a DM injection (Case 734) is illustrated in Figure 5 C. In all cases studied the density of labeled Vo efferents to the dorsal horn was always greatest ipsilaterally. Type 1 Vo efferent terminal arbors were observed in their greatest density in medial portions of ipsilateral laminae II-IV, including IBN while Type 2 terminal arborizations were fewer in number and were scattered medially and laterally in lamina IV. Terminal arbors of both types were observed throughout lamina V and within some of the dorsalmost part of lamina VI. The density of Type 1 and Type 2 Vo-TS efferents innervating contralateral laminae II-VI was significantly less with only a few sparsely distributed labeled terminal arbors in the medial portions of laminae II-V along the lateral border of lamina V and dorsally in lamina VI. Contralateral IBN received a similar density of labeled Vo efferents to that found ipsilaterally and they were located in approximately the same regions along the rostocaudal extent of C1-C2.

Throughout the ipsilateral intermediate gray were found the terminal arbors of Types 1 and 2 Vo-TS efferents. In addition, this area received sparse innervation from the terminal arborizations of Type 3 Vo-TS efferents. The density of innervation was similar to that found in lamina V, except that here terminal arborizations of Type 2 Vo-TS efferents were more numerous. Type 1 and Type 2 Vo-TS efferents were observed in equal density throughout the Central cervical nucleus (CeC). Contralateral lamina VII received slightly fewer labeled terminal arbors from the same three types of Vo-TS efferents and they were spread throughout its mediolateral extent. Contralateral CeC was less densely innervated with Type 1 and Type 2 terminal arbors found only in its ventral portion.

Lamina X contained numerous terminal arborizations of Type 1 and Type 2 Vo-TS efferents which were arranged along its lateral borders following several DM and VL injections (Figures 5,6 C). No terminal arborizations were observed in this lamina following BZ injections.

Terminal arborizations of Types 2 and 3 Vo-TS efferents were observed in the ventral horn bilaterally with their greatest density ipsilaterally. The terminal arbors were principally located in lamina VIII and medial, ventral and lateral motoneuronal cell groups in lamina IX. Terminal arbors of Type 2 Vo-TS efferents predominated. The density of Type 3 Vo-TS efferents was low at this level of the cervical cord and a few of these terminal arborizations were observed to extend beyond lamina VIII into lamina VII. For other cases involving DM injections (Cases 824 and 741) the topographical distribution and density of labeled Vo-TS efferents was similar to that described above (Case 734) in dorsal and ventral horns as well as the intermediate gray.

Distribution and Density of Vo Efferents to Rostral Segments C1-C2 of RCC Following VL Injections

Following a VL injection (Case 860; Figure 6 C) the density of Vo-TS efferent terminal arbors in C1 and C2 segments was greater than that observed following a DM injection. In all cases studied, the density of labeled Vo-TS efferent terminal arbors was always greatest on the ipsilateral side. Along with differences in density of labeling, the topographical pattern of termination was also different in comparison to that seen following DM injections. In addition, all three types of Vo-TS efferents were observed following VL injections and were restricted to approximately the same laminae and nuclei as described following DM injections.

Labeled terminal arborizations of Types 1 and 2 Vo-TS efferents were observed within ipsilateral laminae II-VI. They formed dense terminal plexuses in central and lateral portions of laminae II-IV and in the lateral portion of lamina V. These two types of Vo-TS efferents became more diffuse in lamina VI. Type 1 terminal arbors were observed within ventral portions of ipsilateral IBN while both Types 1 and 2 coexist in lamina VI. Only a few labeled Vo-TS efferent terminal arbors were observed contralaterally with most of them limited to laminae IV and V.

Labeled terminal arborizations of Types 1, 2 and 3 Vo-TS efferents were observed to be distributed both medially and laterally along the ventral borders of the ipsilateral intermediate gray and the density of labeling was comparable that observed following DM injections. Ipsilateral CeC was also innervated by Types 1 and 2 Vo-TS efferents but the density of labeling was somewhat less than that following a DM injection, and the area of innervation was shifted to lateral portions of the nucleus. The density of

labeled Vo-TS efferents was slightly less on the contralateral side with labeled terminal arbors observed more ventrally in lamina VII. Contralateral CeC was innervated in approximately the same density as ipsilaterally with labeled terminal arbors again located along the lateral edge of the nucleus.

Bilaterally, ventral horn laminae VIII and IX received numerous Type 2 and some Type 3 Vo-TS efferents in greater density than observed following DM injections. For all cases studied dense plexuses of labeled terminal arborizations were observed primarily in medial and ventral motoneuronal cell pools. The same general pattern and density of labeling in rostral RCC was observed following other VL injections.

Distribution and Density of Vo Efferents to Rostral Segments C1-C2 of RCC Following BZ Injections

Figure 7 C illustrates the density and distribution of labeled Vo-TS efferent terminal arborizations following a BZ injection (Case 750). These results reflect a markedly reduced projection from this Vo subdivision to C1 and C2 segments when compared to those arising from neurons in DM and VL. Additional BZ injections, which labeled known target structures in other parts of the neuraxis, labeled only a few terminal arborizations in RCC. The populations of Vo-TS efferents innervating RCC were similar with Types 1 and 2 observed in the dorsal horn and intermediate gray while Types 2 and 3 were predominately found in the ventral horn. Type 3 axons also terminated in the intermediate gray. A sparse projection to the dorsal horn resulted in labeled terminal arbors limited primarily to the medial and central portions of lamina V bilaterally. No labeled arbors were seen in IBN or CeC on either side. The intermediate gray also received a few

labeled terminal arbors which were located centrally in lamina VII bilaterally. Labeled terminal arbors in the ventral horn were bilateral, sparse and were located predominately in lamina VIII in similar density. A small plexus of labeled terminal arbors was observed in the contralateral lateral motoneuronal cell pool.

The Density and Morphology of Vo Efferent Terminal Arborizations in Caudal Segments of RCC

The distribution and density of innervation of more caudal sections of RCC (C3-C4) by Vo-TS efferents differed dramatically from rostral sections following DM and VL injections but not after BZ injections. In the cases analyzed (734 and 739; Figure 8 A,B) there is a significant reduction in number of terminal arborizations as well as a shift in the bilateral pattern of innervation. The populations of Vo-TS efferent types followed the same basic pattern of innervation as described for rostral RCC except that in these cases, the numbers of Types 1 and 2 Vo-TS efferent terminal arborizations in the ventral horn decreased in comparison to rostral sections while the numbers of Type 3 arborizations increased in density through the level of the cervical enlargement with the greatest densities observed in the ipsilateral ventral horn following DM injections.

The Distribution and Density of Vo Efferents to Caudal Segments C3-C4 of RCC Following DM Injections

Following DM injections, (Figure 8 A-2; Case 734) the dense plexuses of labeled Vo-TS efferent terminal arborizations that occupied a position in medial portions of laminae II-IV of the ipsilateral dorsal horn in C_1 and C_2 segments were no longer present. The only areas of labeled Vo-TS efferent

terminal arbors in the ipsilateral dorsal horn were located laterally in laminae II, III and V, a continuation of the pattern seen rostrally, as well as a few scattered labeled Vo-TS efferent terminal arbors centrally placed in lamina VI. Contralaterally, only a few labeled terminal arbors were observed in lateral regions of laminae II and V.

Lamina VII and CeC, bilaterally, were observed to be innervated in approximately the same density as they were in rostral RCC (Figure 8 A-1). Labeled terminal arbors in contralateral CeC shifted slightly being positioned more medially (Figure 8 A-2) and not ventrally as observed at rostral levels.

Ventral horn laminae, bilaterally, were observed to be innervated by slightly fewer Vo-TS efferents. The positions of the majority of the terminal arborizations were somewhat different than in rostral RCC in that ipsilateral medial and ventral motoneuronal cell pools received the densest projections while contralaterally the majority of labeled terminal arbors were located in the ventral and lateral motoneuronal cell pools.

The distribution and Density of Vo Efferents to Caudal Segments C_3-C_4 of RCC Following VL and BZ Injections

The changes in density as well as distribution of innervation of C3 and C4 segments following a VL injection (Case 739) is illustrated in Figure 8. A significant reduction in the numbers of Vo-TS efferents innervating the dorsal horn bilaterally was observed. Terminal arbors were restricted to medial portions of laminae III and IV and the lateral portion of lamina V.

Only a few labeled terminal arborizations were observed in the intermediate gray. Ipsilateral CeC contained a few terminal arborizations centrally. Contralaterally, an extremely sparse distribution of labeled Vo-

TS efferent terminal arborizations was observed with labeling seen centrally in lamina IV and VII. No Vo-TS efferents terminated in contralateral CeC.

A significant reduction in the number of labeled Vo-TS efferents arborizing in ventral horn laminae was observed bilaterally. Ipsilateral laminae VIII and IX received the densest projections. As described for the ventral horn in the upper limits of RCC, labeled terminal arborizations were confined to the medial, ventral and lateral motoneuronal cell pools ipsilaterally and only the ventral motoneuronal cell pool contralaterally (Figure 8 B-2).

The distribution and density of Vo-TS efferents to segments C3 and C4 following BZ injections was similar to that found in C1 and C2 segments.

PROJECTIONS TO CERVICAL ENLARGEMENT

Labeled Vo-TS efferents arborized in CE (C6-C8) following DM, VL and BZ injections. Vo-TS efferents forming terminal arborizations in CE included Types 1 and 2 which were found in the dorsal horn and intermediate gray and Types 2 and 3 found in the ventral horn. Type 3 Vo-TS efferents had some input to the intermediate gray.

Distribution and Density of Vo Efferents to CE following a DM Injection

Labeled Vo-TS efferents innervating dorsal horn laminae following a DM injection (Figure 5 D; Case 734) followed a general pattern of significantly decreasing input at more successively caudal segments of the cervical spinal cord. A sparse number of labeled terminal arborizations were observed in medial portions of ipsilateral laminae II-IV with labeled

arbors spreading into the central portion of lamina IV. These same laminae in ipsilateral RCC received Vo-TS efferent terminal arborizations. A very sparse projection was also noted in the extreme medial portion of lamina I in Case 824. Ipsilateral lamina V and VI received a sparse Vo-TS efferent input with terminal arbors scattered both medially and laterally in these laminae. Slightly fewer labeled Vo-TS efferent terminal arborizations were observed in the same laminae of the contralateral dorsal horn and were distributed in a pattern similar to that found ipsilaterally.

The intermediate gray of ipsilateral CE was diffusely innervated by Vo-TS efferents with terminal arbors clustered in the medial portion of the lamina. The contralateral intermediate gray received a sparse contingent of Vo-TS efferents whose terminal arbors were scattered throughout. Only a very sparse projection is shown to terminate in the ipsilateral area of lamina X. In additional experiments (Cases 824 and 741) as well as experiments involving VL (Cases 751 and 739) and BZ injections (Case 750) several labeled Vo-TS efferents were seen to terminate in the dorsal and ventral portions of this lamina.

The density of labeled Vo-TS efferent terminal arborizations in the ipsilateral ventral horn was greater than that found contralaterally and was primarily concentrated medially in laminae VIII and IX. Terminal arborizations were observed in medial, ventral and lateral motoneuron cell pools ipsilaterally and in medial and ventral motoneuron cell pools contralaterally. A similar pattern of density and distribution of labeled Vo-TS efferents was observed following other DM injections (Cases 824 and 741) in dorsal and ventral horns of CE as well as the intermediate gray.

Distribution and Density of Vo Efferents to CE Following VL Injections

Fewer Vo-TS efferent parent axons were observed to course caudally and terminate in CE when compared to DM injections. VL injections (Case 860; illustrated in Figure 6 D) labeled very few Vo-TS efferent terminal arborizations in CE dorsal horn and those observed were limited to central portions of ipsilateral laminae II-IV. Likewise, very few Vo-TS efferents terminated in the ipsilateral intermediate gray. Those present were located mostly in the most dorsal portions of the lamina. The densest projection was to the ventral horn with terminal arbors located bilaterally in lamina VIII and the medial and ventral motoneuronal cell pools of lamina IX.

A similar pattern for density of labeling and distribution of labeled Vo-TS efferent terminal arborizations in CE was found in all of the additional cases with VL injections with the exception of Case 739, which demonstrated a slightly more robust labeling of Vo-TS efferent terminal arborizations in laminae VIII and IX bilaterally and in contralateral laminae III-V laterally and lamina VI medially.

Distribution and Density of Vo Efferents to CE Following BZ Injections

The density and distribution of labeled Vo-TS efferent terminal arborizations in CE following a BZ injection (Figure 7 D; Case 750) could be characterized as being more like that described for the innervation of CE following a DM injection (Figure 5 D). A sparse, diffusely scattered array of labeled Vo-TS efferent terminal arborizations were found centrally and medially in ipsilateral laminae IV-VI. The density in the dorsal horn was approximately equal bilaterally. Vo-TS efferents terminated centrally in the intermediate gray bilaterally in about equal density. The numbers of labeled terminal arborizations in the ventral horn bilaterally were greater

in CE than those observed bilaterally in RCC following BZ injections. In CE the densest groupings of labeled terminal arborizations were located in medial and lateral motoneuronal cell pools ipsilaterally.

PROJECTIONS TO THORACIC SPINAL CORD

Labeled Vo-TS efferent terminal arborizations were observed in mid thoracic spinal cord segments (T5-T7) in substantial numbers following DM injections (Figure 5 E). Few, if any terminal arborizations were observed subsequent to VL and BZ injections. Following DM injections, numerous labeled arborizations of Types 1 and 2 Vo-TS efferents were found in the dorsal horn. They occupied the more medial portions of ipsilateral laminae III-V and were located medially in contralateral lamina III and centrally in contralateral lamina V. Labeled Vo-TS efferent terminal arborizations were observed in the intermediolateral cell column (IML) bilaterally with an ipsilateral predominance. The intermediate gray was diffusely innervated bilaterally with the greatest density of labeled terminal arborizations seen ipsilaterally. Types 1 and 2 Vo-TS efferents formed the terminal arborizations observed in IML and lamina VII. Type 1 and Type 2 Vo-TS efferents formed terminal arbors laterally in lamina X following DM injections. Numerous Types 2 and 3 Vo-TS efferents innervated the ventral horn bilaterally. The general pattern of density and distribution of Vo-TS efferent terminal arborizations in the ventral horn was continued at this level of the spinal cord in that a greater density was observed ipsilaterally in laminae VII and IX with the majority of terminal arbors positioned in the medial motoneuronal cell pools. In another experiment, with a DM injection (Case 824), the pattern of innervation was similar but the density of labeling was slightly less in all regions.

PROJECTIONS TO LUMBAR ENLARGEMENT

Vo-TS efferent terminal arborizations were observed in LE (L5-L6) only following DM injections. Labeled Vo efferents innervated LE bilaterally with the greatest density seen ipsilaterally (Figure 5 F). The density and distribution of Vo-TS efferents terminating in the dorsal horn was similar to that seen for the dorsal horn of CE with Types 1 and 2 Vo-TS efferents forming the terminal arborizations. A sparse, diffusely arranged projection was observed laterally in lamina III and laterally and medially in laminae IV-VI of the ipsilateral dorsal horn. A similar distribution of labeled terminal arborizations was observed in the contralateral dorsal horn except that the density of labeling was slightly less. A few scattered Types 1, 2 and 3 Vo-TS efferent terminal arborizations were observed bilaterally within the intermediate gray in approximately equal numbers. Labeled Vo-TS efferents terminating within lamina X consisted of Type 1 and Type 2 arborizations which arborized primarily in ventral portions bilaterally and the lateral aspect of this lamina ipsilaterally. In an additional experiment, with a DM injection (Case 824), several labeled terminal arbors were located in dorsal and ventral portions of lamina X. Numerous Type 2 and some Type 3 Vo-TS efferents innervated the ipsilateral ventral horn with the greatest density of terminal arbors located within lamina VIII and the medial motoneuronal cell pool. Contralaterally, labeled Vo-TS efferent terminal arbors were fewer in number and were observed in approximately equal density within VIII and the medial and lateral motoneuronal cell pools.

PROJECTIONS TO LATERAL CERVICAL NUCLEUS

Following DM and VL injections a plexus of loosely arranged Vo-TS efferent terminal axonal arborizations was observed in cervical segments C_1 and C_2 of RCC beyond the lateral borders of ipsilateral laminae I-IV. Vo-TS efferents of the Type 1 and Type 2 varieties extended into the dorsolateral funiculus and arborized in the lateral cervical nucleus (LCN). Although the density of labeling of the Type 1 arborizations was less, there was an obvious somatotopy with Type 1 arbors limited to the most dorsal aspect of LCN while Type 2 arbors were in greater numbers ventrally. The greatest density of innervation was observed following VL injections (Figures 6 C; 8 B1). The pattern in which these collections of labeled Vo-TS efferents terminated within LCN differed depending on which Vo subdivision was injected. For VL injections at least two dense aggregates of terminal arbors were seen directly adjacent to laminae I-II and laminae III-IV. As illustrated in Figures 6 C; 8 B1, a small collection of labeled terminal arborizations was also seen in contralateral LCN adjacent to laminae I-II and laminae III-IV. A significantly smaller projection to ipsilateral LCN adjacent to laminae III and IV was observed following DM injections (Figure 5 C). Labeled terminal arbors could also be seen in the dorsolateral funiculus at more caudal levels of the spinal cord adjacent to laminae III-IV at TC and LE levels.

DISCUSSION

The results in this study demonstrate the contributions made by each Vo subdivisional area to previously described projections of the sensory trigeminal nuclei to rat spinal cord (Leong et al., '84; Ruggiero et al., '81). Our findings support previous retrograde experiments (Falls, 83; '84b) indicating that cells situated in VL provide direct secondary trigeminospinal efferents to the entire length of the rat spinal cord. Present data extend the above findings to indicate that the neurons projecting to the spinal cord are more widespread throughout Vo than previously thought (Falls, '84b). Not only are they located in the VL subdivision of Vo but they are also found in DM and BZ subdivisional areas as well. Furthermore, Vo-TS projections are bilateral to second order primary afferent receptive cells and motoneuronal cell pools within the dorsal and ventral horns, respectively. Taken together, these findings indicate that the rat Vo-TS projection is more substantial and more highly organized within spinal cord laminae than previously defined by virtue of its distribution to dorsal horn laminae containing second order sensory projection neurons as well as the IML cell column of the thoracic cord and motoneurons within the ventral horn of the spinal cord. By virtue of its connections with the DCN and spinal cord, Vo must play an important role in conveying orofacial tactile information to these medullary tactile centers and spinal somatic and autonomic areas for sensorimotor processing and modulation of complex reflex activities.

Methodological Considerations

The uptake and subsequent transport of PHA-L were originally shown to be restricted to cell bodies and dendrites at the site of injection (Gerfen and Sawchenko. '84). Thus the utilization of PHA-L once taken up by cell bodies and proximal dendrites of Vo neurons within the identified subdivisional areas would allow for the complete filling of axons and their terminal arborizations and permit the visualization of efferent axons to target nuclei as well as the determination of morphological detail of terminal arborizations within those nuclei. However, recent studies indicate that PHA-L may be taken up by fibers of passage within the spinal cord (Cliffer and Giesler, '99; Schofield, '90). Although neither injections of PHA-L into the white matter of svt nor deposits of PHA-L into the Vo neuropil, which failed to result in cellular uptake, produced any observable anterograde uptake, the mechanism of uptake by fibers of passage can not be completely negated in this study. In addition, extensive axon labeling has been thought (Schofield, '90) to be the result of increased uptake secondary to axonal damage produced by administration of PHA-L by a continuous current (not pulsed every 7 seconds). When utilizing parameters similar to those used in this study of small tipped micropipettes and pulsed current the number of labeled fibers was low (Schofield, '90). The potential exists for uptake of PHA-L by intratrigeminal axons due to the extensive interconnections made by trigeminal internuclear collaterals and the trajectory of Vo axons through Vi and MDH to reach spinal cord dorsal horn laminae and nuclei (Rhoades et al.; '89; Jacquin, '90). This is also suggested by the ability of trigeminal primary afferent axons to incorporate and transport PHA-L to upper cervical spinal cord levels bilaterally (Jacquin, '90). Such situations necessitate the processing of the trigeminal

sensory ganglion for PHA-L immunoreactivity as well as future parallel studies utilizing autoradiographical techniques, which are not subject to transport by fibers of passage. The differences observed in the morphologies of Vo-TS axonal arborizations in this study compared with afferents/efferents originating from trigeminal sensory ganglion cells, Vi and MDH neurons as well as differences observed in the pattern of termination within spinal cord laminae for Vo-TS efferents suggests that most, if not all, of the terminal labeling observed in the spinal cord arose from cells located within the confines of Vo PHA-L injection sites and not from fibers of passage.

The localization of cells filled with PHA-L was used to determine the limits of the effective site within Vo from which anterograde transport occurred. This ability to make well defined and restricted PHA-L injection sites facilitated the delineation of the topographical organization of Vo efferent projections, both within and across the cytoarchitecture of this nucleus. In most instances in this study it was possible to limit the uptake of PHA-L to cells situated within the myelo-and cytoarchitectonically defined DM and VL subdivisions of Vo (Falls, 84a-c; Falls and Alban, '86). However, deposits of PHA-L restricted to cells comprising BZ could seldom be achieved without some slight spread of reaction product into DM and VL. This was apparently due to the narrow width of BZ and the fact that injections could not be contained within such a small area.

Target regions which exhibited a comparable density of labeling after discretely placed injections within Vo subdivisions i.e., cranial nerve nuclei and cerebellum (Smith and Falls, '87;'91) have been shown in retrograde tracing studies to receive Vo afferents (Erzurumlu and Killackey, '79; Falls, et al. '85, Falls and Alban, '86; Falls, '87). Conversely, studies which have

demonstrated only weakly retrogradely labeled cells in Vo following retrograde double labeling or HRP injections in the ventrobasal nucleus of the rat (Kruger et al., '77; Mantle-St. John and Tracey, 87) have been shown with the use of PHA-L to be more substantial than originally thought (Smith and Falls. '90). The ability to recognize morphological features associated with terminal axonal arborizations at the light microscopic level represents a significant advantage of the PHA-L method over other anterograde techniques (Gerfen and Sawchenko, '84; Wouterlood and Groenewegen, '85). In the present study, it was often possible to distinguish between axon terminal arbors and fibers of passage in Vo target sites for which previously existing data were incomplete. The unequivocal demonstration of Vo terminations onto target cells requires electron microscopic verification. The PHA-L anterograde tracing method appears to be more sensitive than autographic techniques, particularly with regard to minor projections (Ter Horst, '84). This study observed a number of efferent projections from Vo which, to the best of our knowledge, have previously been unreported in the rat eg., DCN, LCN, IBN, IML, spinal cord lamina X. Furthermore, the PHA-L method permitted a more detailed examination of projections which had been recognized by some investigators (Ruggierio et al., '81; Falls, '84b; Falls et al, '90), but otherwise went uncharacterized.

MODULATION OF MEDULLARY SOMATOSENSORY NUCLEI CUNEATUS AND GRACILIS

The DCN are considered a major relay station for ascending somatosensory information from the upper and lower limbs and trunk to the thalamus. The afferent sources from spinal cord dorsal roots have been

demonstrated in opossum (Culberson, '87), cat (Rustioni and Macchi, '68; Keller and Hand, '70), monkey (Ferraro and Barrera, '35: Shriver et al., '68; Rustioni et al., '79). Afferent sources have also been demonstrated from second order fibers within the dorsal columns and dorsolateral funiculus (Rustioni, '73, '74), trigeminal primary afferents (Jacquin et al., '83b), red nucleus (Edwards, '72) and cerebral cortex (Kuypers and Tuerk, '64). Efferent thalamic projections have been demonstrated to the ventroposterolateral nucleus of the thalamus (VPL) in cat (Burton and Craig, '79; Burton et al., '79; Berkley, '75; Hand and Van Winkle, '77; Berkley and Hand, '78; Berkley et al., '80; Blomqvist, '80; Berkley et al., '86; Hockfield and Gobel, '78; Peschanski and Ralston, '85), rat (Lund and Webster, '67a; Fukushima and Kerr, '79), monkey (Boivie, '78; Ganchrow, '78; Burton and Craig, '79; Kalil, '81), hedgehog (Ring and Ganchrow, '78), and raccoon (Ostapoff and Johnson, '88). Considerable evidence exists to demonstrate that the DCN do more than simply relay sensory input to the thalamus. In addition to VPL, other efferent targets include the inferior olive, superior and inferior colliculi, red nucleus, medial geniculate body, posterior thalamus, zona incerta, fields of Forel, pretectal area, pontine nuclei, cerebellum and spinal cord (Hand and Liu, '66; Lund and Webster, '67; Ebbesson, '68; Boivie, '71; Cooke et al., '71a,b; Dart, '71; Burton and Loewy, '77; Berkley, '75; Cheek et al., '75; Kuypers and Maisky, '75; Rivnik and Walberg, '75; Kuypers and Maisky, '75; Robards et al., '76; Burton and Loewy, '76; Burton and Loewy, '77; Hand and Van Winkle, '77; Berkley and Hand, '78a,b; Blomqvist et al., '78; Armstrong et al., '79; Nagata and Kruger, '79; Somana and Walberg, '79; Feldman and Kruger, '80; Kosinski et al., '82; Bjorkeland, '83; Budell and Berkley, '83; May and Berkley, '83;

Bull and Berkley, '84; Molinari, '83, '84; Berkley, '86; Ostapoff and Johnson, '88).

Clusters of labeled neurons have been described in cat DCN (Kuypers and Tuerk, '64) and also have been suggested in rat (Tan and Wong, '82) where the clusters are described as slabs or bricks (Basbaum and Hand. '73). Reports have also been published to indicate that a "true nest" region, as demonstrated in cat, does not exist in rat (Valverde, '66; Gulley, '73). Recent experiments utilizing axonal degeneration (Hand and Van Winkle, '77) and retrograde HRP transport techniques (Berkley, '75; Cheek et al., '75; Berkley, '83; Berkley et al., '80; Blomqvist et al., '78; Ellis and Rustioni, '81; Tan and Lieberman, '78) have demonstrated thalamic projections originating from the cell clusters.

As a result of stimulation of rat skin and movement of body hairs, electrical discharges have been recorded to suggest that the arrangement of cells within DCN is related to the location of receptive fields on the body surface. Fibers from tail receptors project to the most medially placed cells and fibers of receptors in more rostral body regions project to more laterally located cells. A dorsoventral axis is also revealed which is reverse in order so that the back is ventrally located in DCN while the limbs extend dorsally (Nord, '67). Histologic evidence following evoked discharges revealed stimulation induced responses in limbs, trunk, neck, posterior face and pinna (Nord, '67; Millar and Basbaum, '75). Studies in monkey suggest that dorsal root fibers terminating in Gr are organized such that lower thoracic and upper lumbar roots project lateral to the core region, lumbar enlargement roots project to the central core of the nucleus and sacral and coccygeal dorsal roots project to dorsomedial parts of Gr (Carpenter et al., '68). Neurons located in Cu also demonstrate a similar pattern of

organization with respect to incoming dorsal root afferents. Fibers from C1-C4 terminate in ventrolateral regions, fibers from C5-C8 terminate in a central core and fibers from T1-T7 terminate in dorsomedial regions (Shriver et al., '68). The somatotopic organization for primary afferent fibers in DCN suggests that fibers from the tail region run close to the midline while while fibers from the hindlimb, trunk and forelimb are successively added laterally at more rostral levels. In rat degeneration techniques were used to differentiate the manner in which cervicothoracic dorsal roots terminate in Cu (Basbaum and Hand, '73). Dorsal roots C1 and C2 were not found to terminate in Cu. However, roots C3 and C4 were found to be distributed primarily in the rostral portion whereas C5-T1 roots distributed rostrally and caudally within the nucleus. T2 roots were seen to project primarily to the caudal portion of the nucleus. Dorsal roots C1 and C2 which did not project to Cu innervated the neck region and were considered to be important in the mediation of tonic neck reflexes (Ranson et al., '32). This finding is not incompatible with the finding of Torvik, ('56) of a slight projection to rostral Cu from the first three dorsal roots following a combined rhizotomy of the three roots. Keller and hand ('70) have shown large terminal fields in the rostral and caudoventral regions of Cu were shown to have greater intersegmental overlap of cervical and thoracic root fibers. These areas correspond to regions corticofugal fibers (Andersen, et al., '64; Kuypers and Tuerk, '64) suggesting that these areas may function as sites of integration for peripheral and central input.

A somatotopic organization in the distribution of labeled cells is observed in DCN (Burton and Loewy, '77) after HRP injections at different spinal cord levels. Injections into caudal and sacral spinal cord segments labeled neurons concentrated in the medial part of Gr, lumbar injections

labeled neurons more laterally in Gr and upper thoracic and lower cervical injections label the lateral extreme of Gr and parts of Cu.

The density and distribution of different cell types within DCN has been shown to vary rostrocaudally so that a basic mammalian pattern exists which allows both Cu and Gr to be subdivided into three major regions: Rostral reticular zone, middle cell nest zone and caudal region (Cajal, '09; Ferraro and Barrera, '35; Taber, '61; Kuypers and Tuerk, '64; Hand, '66; Biedenbach, '72; Basbaum and Hand, '73; Gulley, '73; Berkley, '75). However, rat Cu and Gr have been subdivided into rostral, middle and caudal thirds based on cytoarchitecture as well as afferent and efferent connectivity (Burton and Loewy, '77). In addition, Basbaum and Hand ('73) refer to only rostral and caudal halves of Cu based cytoarchitectonics and dorsal root projections. Spinally projecting neurons in rat DCN are situated in the middle cell nest zone ventrally (Burton and Loewy, '79) and not dorsally where thalamic projection neurons are located (Tan and Lieberman, '78; Kemplay and Webster, 89). Cells lying in the rostral reticular zone in cat project to the cerebellum (Rinvik and Walberg, '75; Cheek et al., '75). Projections to rat and cat pretectum have been described to ensue from neurons in the rostral portion of DCN (Lund and Webster, '67a; Berkley et al., '86; Bjorkeland and Boivie, '84) and although these projections are predominately contralateral, a sparse ipsilaterally projecting group of neurons has been labeled (Norris and Killackey, '88). The pars rotunda in monkey, equivalent to the cluster region in cat, receives dorsal root afferents from segments supplying distal extremities (Shriver et al., '68) while the cell cluster region in cat receives the highest density of dorsal root afferents (Kuypers and Tuerk, '64; Keller and Hand, '70). Second order neurons (Rustioni, '73), fibers originating from the

cerebral cortex (Kuypers and Turek, '64; Hayes and Rustioni, '79; Rustioni and Hayes, '81), laminae IV and VI of the spinal cord (Rustioni and Kaufman, '77) and projections from the reticular formation (Scheibel and Scheibel, '58; Odutola, '77; Sotgiu and Marini, '77) terminate chiefly in the rostral part of DCN.

The termination of PHA-L labeled Vo efferents from all three subdivisions was shown to be densest in ventral portions of the rostral division of ipsilateral Cu. Vo projections from DM cells projected in greatest density to Cu and were found bilaterally along the rostrocaudal extent with an ipsilateral predominance. The greatest number of labeled DM terminal arbors were observed in the ventral half of rostral and caudal portions of Cu and fewer numbers were found along the ventral border of the middle portion of Cu bilaterally. Sparse labeling of Vo terminal arborizations was observed to be restricted to ipsilateral Cu along its rostrocaudal extent following VL injections and more limited to the ventral half of the rostral two-thirds of Cu following BZ injections. Vo projections to Gr were primarily observed following DM injections with labeled terminal arborizations found scattered bilaterally throughout Gr along its rostrocaudal axis. Only slight labeling was evident in the ventral border of Gr ipsilaterally following VL injections. BZ neurons did not project to Gr. In a series of carefully placed injections of HRP into rostral, middle and caudal Cu (Weinberg and Rustioni, '89) labeled cells were illustrated in all three Vo subdivisions with the greatest number of labeled neurons seen in DM and the dorsomedial half of BZ after middle Cu injections. The density of labeled cells was less in these Vo areas following rostral Cu injections. Fewer and more widely spread labeled cell bodies within the middle third of Vo were illustrated when injections were placed caudally in Cu. Only a

few cells situated in contralateral DM were labeled following rostral and caudal Cu HRP injections. Based on the density of Vo efferent terminal arborizations in the middle portion of Cu in the present study, only a moderate to sparse number of labeled cell bodies would be expected following an HRP injection placed in middle Cu. The greater density of retrogradely labeled cell bodies following the middle Cu injection illustrated by Weinberg and Rustioni ('89) may be due to reported spread of HRP into the dorsomedial portion of caudal Vo and rostral Vi.

Anatomical studies utilizing the retrograde transport of HRP have demonstrated primary (Jacquin et al., '82) and secondary trigeminal (Weinberg and Rustioni, '89) projections in rat. The results shown in the present study, demonstrating the pattern of termination of Vo efferent projections both rostrally and caudally in Cu and Gr, suggest that Vo efferents have the potential to affect DCN efferents destined for the spinal cord and cerebellum. According to the autoradiographic studies of Burton and Loewy ('77), spinally projecting neurons from DCN, situated in the ventral aspect of Cu and Gr, project primarily to ipsilateral laminae IV and V, and possibly in lamina I, with the greatest concentration of silver grains distributed over the fiber bundles in the reticulated portion of lamina V in cervical levels C1-C6. The predominate pattern of Vo efferent projections terminating in the ventral and ventrolateral aspects of Cu may relate to the fact that roots carrying information from more proximal body regions, C1-C4, may be situated in the lateral portions of rat Cu (although a projection from roots C1-C2 has not been demonstrated in rat by Basbaum and Hand, '73) as are the upper cervical roots in monkey (Shriver et al., '68). A similar pattern may exist for Vo efferent projections to ventral and ventrolateral portions of Gr since afferent information from the proximal

part of the body, carried by the lower thoracic and upper lumbar dorsal roots, is found to terminate in ventrolateral portions of monkey Gr (Carpenter et al., '68) and in rat, lumbar spinal cord HRP injections labeled cells primarily laterally in Gr and thoracic cord injections labeled cells in the lateral extreme of Gr (Burton and Loewy, '77). It is likely that Vo efferent projections are terminating in areas within DCN which allow for modulation of incoming input from dorsal roots transmitting afferent tactile information from proximal body regions and may also be positioned to affect the output of DCN cells projecting from these same areas.

Vo-TS efferent projections confirm and extend the results found for trigeminal secondary projections to Cu (Weinberg and Rustioni, '89) and suggest for possible modulation or interaction with spinally projecting efferents from DCN to laminae IV at V of the RCC and CE levels. Further studies must be made to determine if trigeminal primary afferent projections in Cu (Jacquin et al., '82) are terminating in the same or similar manner as secondary Vo efferents.

Conflicting reports have been made with respect to rostrocaudal differences within the DCN. Physiologic studies in cat have suggested that neurons in Gr exhibit rostrocaudal differences for size of the peripheral receptive fields (Gordon and Paine, '60; McComas, '63) and segregation of sensory modality (Gordon and Jukes, '64; Kuhn, '49; Winter, '65). Rostral portions of the nucleus are thought to be concerned with reception of deep pressure and joint movement while caudal regions are concerned with hair and skin receptors. Other, contradictory, data (Kruger et al., '61) has not provided support for a rostrocaudal differentiation in terms of either somatotopy or modality segregation. However, recently, Ostapoff et al., ('88) has shown that raccoon basal cuneate nucleus may be somatotopically

organized dorsoventrally with responses to projections of deep tissues of the forelimb situated most ventrally, ventral to the cutaneous body representation. In this ventral border area, cells were observed to respond to kinesthetic stimulation of the head and humerus. Vo-TS input into the more ventral portions of DCN may supply cutaneous information to "kinesthetic" cells within rat Cu and Gr, similar electrophysiological studies must be performed to verify this supposition.

DIFFERENTIAL PROJECTIONS TO DORSAL, INTERMEDIATE AND VENTRAL HORN LAMINAE CONTAINING IDENTIFIED TRACT CELLS

Somatosensory input via cutaneous mechanoreceptors, nociceptors, thermoreceptors, muscle receptors and visceral receptors arriving in the spinal cord dorsal horn is compartmentalized with pain and temperature information conducted by small (Ad) and unmyelinated (C) fibers entering the dorsal horn through the lateral division of the dorsal root and terminating on neurons primarily located in laminae I, II and V (Light and Perl, '79 a,b). Large myelinated (Aa and Ab) fibers conveying discriminative touch and proprioceptive information enter the dorsal horn from the medial division of the dorsal root to terminate in laminae III-VI. Neurons positioned within these dorsal horn laminae project through the spinocervical (Brown and Franz, '69; Cervero et al., '77; Hong et al., '79; Brown, '81), post-synaptic dorsal column (Rustioni and Kaufman, '77; Rustioni et al., '79; Bennett et al., '83; Giesler et al., '84), spinoreticular (Abols and Basbaum, '81; Andrezik et al., '81; Chaouch et al., '83; Kevetter and Willis, '83) or spinothalamic (Trevino et al., '72; Trevino et al., '73;

Albe-Fessard et al., '74; Kerr, '75 a; Carstens and Trevino, '78; Giesler et al., '79 a; Willis et al., '79) pathways.

A close association exist between the functional type of peripheral mechanoreceptor, the morphology of their terminal arbors and the area of termination in the dorsal horn (Brown, '81). Large Ab fibers project to laminae III-V and the dorsal part of VI. Hair follicle primary afferents (Ab and Ad), forming "flame-shaped terminal arbors" (Ramon y Cajal, '09) are confined to lamina III with occasional spread to lamina II and the dorsal part of lamina IV. Primary axons originating from other cutaneous mechanoreceptors distribute their terminal arbors over a wider area in the dorsal horn from the inner part of lamina II to the dorsal part of lamina VI (Brown, '81). No primary afferent projections from low-threshold mechanoreceptors with myelinated axons are observed within laminae I or the outer part of II. Most cutaneous C fibers probably terminate in lamina II, with the inner part of this lamina the most likely target (Light and Perl, '79a,b). Some neurons within lamina II are driven by "slow Brush' cutaneous stimulation with the suggestion that the input is from C fiber mechanoceptors (Light et al., 79). Mechanoreceptive neurons are principally located in laminae III and IV and are of two types, class 1 and class 2. The first type is exclusively mechanoreceptive driven by mechanoreceptive, low threshold receptors in skin, while the second type, the latter, stimulated by other types of cutaneous receptors, is characterized as being multireceptive with a wide dynamic range. Tactile information is forwarded to higher brain centers by long ascending axons from some of these mechanoreceptive neurons through either the spinocervical, post-synaptic dorsal column, spinoreticular or spinothalamic tracts.

Nociceptive input from the skin arrives in the dorsal horn through small A-d fibers originating from mechanonociceptors which terminate in laminae I and V (Light and Perl, '79b) and C fibers ensuing from polymodal nociceptors ending primarily in the outer portion of lamina II (Light and Perl, '79a). Two groups, (class 2 and 3) of nociceptive neurons can be distinguished based on differences in responses to noxious skin stimulation. Class 3 (a and b) neurons are nociceptor specific in that they are exclusively driven by cutaneous nociceptors. Class 3a cells receive input from mechanonociceptors only while class 3b neurons have input both from mechanonociceptors and polymodal nociceptors. The class 2 cells are multireceptive, have a wide dynamic range response and are excited by other types of cutaneous receptors. Nociceptive neurons are found predominately in lamina I, consisting of large marginal type cells (Molony et al., '81). Pain information is relayed from these cells by axons running in the spinoreticular and spinothalamic tracts (Willis and Coggeshall, '78).

Central endings of visceral primary afferent axons provide another source of sensory information to dorsal horn neurons. Visceral primary afferents have been demonstrated to terminate in laminae I and V (Morgan et al., '81; Cervero and Connell, '84) and can be classified into two groups: Somatic primary neurons, which are only excited by stimulation of somatic receptive fields, and viscerosomatic primary neurons which are driven by somatic and visceral input concomitantly. Both cell types give rise to A-d and C fibers (Pomeranz et al., '68; Gokin, '70; Guilbaud et al., '77; Foreman and Ohata, '80; Milne et al., '81; Cervero, '82, '83a,b). No dorsal horn neurons have been identified that respond exclusively to visceral input. Second order somatic and viscerosomatic responding neurons are distributed in different locations within the gray matter. Somatic neurons,

the majority of which are activated by mechanoreceptive input are located primarily in laminae II-IV while viscerosomatic cells stimulated by either nociceptive or multireceptive information are situated in laminae I and V as well as the ventral horn. Somatic input reaches higher brain centers via spinocervicothalamic and post-synaptic dorsal column pathways (Cervero and Iggo, '78; Cervero, '83b) while viscerosomatic neurons project to higher brain centers through spinothalamic and spinoreticular tracts (Hancock et al., '75; Foreman and Weber, '80; Cervero, '83b).

Cutaneous thermoreceptors conduct their information to the dorsal horn via small A-d and C primary afferent fibers (Iggo, '69). In the dorsal horn, neurons responding to cold intermingle in the superficial dorsal horn with neurons which receive input from both thermoreceptors and nociceptors (Christensen and Perl, 1970; Hellon and Misra, '73).

Proprioceptive information is conveyed to the spinal cord from several sources: Primary endings in muscle spindles utilizing group Ia axons (A-a), secondary afferents in muscle spindles and Golgi tendon organs using group II (A-b) and Ib (Aa) axons, respectively. Although dorsal horn neurons receiving proprioceptive primary input are found primarily in lamina VI, the areas of distribution of these axons within the spinal cord laminae is more extensive. Collateral branches of group Ia primary axons terminate in laminae VI, VII and IX. Collaterals of group II primary axons project to laminae IV-VI and lamina IX while group IB primary axons terminate in laminae V-VII (Brown, '81). Group III, A-d fibers and group IV, C fibers from muscle nociceptors have been shown (Mense et al., '81; Craig and Mense, '83) to project to laminae I and V. Neurons positioned within these laminae project through the spinothalamic tract (Willis and Coggeshall, '78).

Studies utilizing several mammalian species have demonstrated the distribution of neurons in the dorsal horn that project to the intralaminar thalamic nuclei, ventrobasal thalamus (Giesler et al, '79a; Carstens and Trevino, '78; Willis et al., '79) and reticular formation (Abols and Basbaum, '81; Andrezik et al., '81; Corvaja et al., '77; Kevetter et al., '82; Kevetter and Willis, '83; Menetrey et al., '83; Chaouch et al., '83). Cell bodies are found to overlap laterally in the neck of lamina V and in the intermediate gray. Collaterals to two or more of these thalamic or reticular areas have been shown to emanate from axons of lamina V neurons (Giesler et al., '81b; Kevetter and Willis, '83). Further studies have shown that spinothalamic cells, projecting to the medial thalamus (intralaminar), originate predominately from cell bodies located in the intermediate gray and ventral horn while cells projecting to the lateral thalamus (ventrobasal) are situated in the superficial (laminae I-V) dorsal horn (Giesler et al., '79a; Giesler et al, '81a,b; Kevetter and Willis, '83). Electrophysiological studies show that the dorsalmost two-thirds of the dorsal horn contains neurons capable of coding tactile and nociceptive information (Giesler, '76; Menetrey et al., '77) while cells located in the intermediate gray and ventral horn respond to stimuli delivered to subcutaneous tissues (Giesler, '79).

The results of this study show that Vo-TS efferent terminal arbors end primarily in laminae III-V throughout the rostrocaudal extent of the spinal cord, most often bilaterally. Very few Vo-TS efferent terminal arborizations are observed in lamina II of the dorsal horn which has been shown to contain class 2 and class 3 neurons that receive terminals from fine Ad and C primary afferent fibers, and respond maximally or exclusively to noxious cutaneous inputs (Iggo, '74; Menetrey et al., '77). Likewise, relatively few retrogradely labeled rat spinothalamic (Giesler et

al., '76), spinomesencephalic (Menetrey et al., '80) and spinoreticular (Menetrey et al., '83) tract cells have been identified within these laminae. Deeper in the dorsal horn, primarily lamina V, but including laminae III and IV, bilateral Vo-TS efferent terminal arbors are observed from all three subdivisions in RCC and although they decrease greatly in density at lower levels of the cervical cord following injections located in VL and BZ subdivisions, the density of projections remains significant from DM cells at more caudal levels of TC and LE. The neck of the dorsal horn has been shown to contain class 1 or class 2 cells driven exclusively by noxious cutaneous input and driven by both noxious and non-noxious cutaneous stimuli respectively, that respond to inputs from both large Ab fibers and fine Ad and C fibers. This area has been demonstrated to contain the majority of tract cells giving rise to spinothalamic (Giesler et al., '79a), spinomesencephalic (Menetrey et al., '80; Menetrey et al, '82; Lima and Coimbra' 89) and spinoreticular (Menetrey et al., '83) pathways in rat.

In monkey, spinothalamic cells projecting to the medial thalamus (central lateral nucleus and portions of the medial dorsal nucleus) have been shown to be located in the intermediate gray or ventral horn while neurons projecting to the lateral thalamus were found primarily in the marginal zone, lateral nucleus proprius and medial portion of the intermediate gray (Giesler et al., '81a). Medial spinothalamic tract cells were characterized as having excitatory receptive fields that included parts of several limbs or even the entire surface of the body and face. Lateral spinothalamic tract cells were described to have excitatory receptive fields restricted to the ipsilateral hindlimb. Studies utilizing rat demonstrate a similar differentiation with respect to the location of medially and laterally projecting spinothalamic neurons. Medial spinothalamic tract cells are

located in more ventral levels of the spinal gray and are concentrated in laminae V-VIII while lateral spinothalamic tract cells are concentrated more dorsally in laminae I-V, with a second dense population contained within laminae VII-VIII (Kevetter and Willis, '83; Giesler et al., '79a).

In studies to determine laminar differences with respect to the location of spinoreticular tract cells. HRP injections in the medial reticular nucleus labeled cells situated primarily in lamina V and laminae VII and VIII at all levels of the spinal cord. Injections made in the lateral reticular nucleus labeled cells common to all spinal segments and were found in the ventromedial parts of laminae VII, VIII and X (Chaouch et al., '83; Menetrey et al., '83). It is possible that Vo-TS efferent projections, especially those originating from DM neurons, may target spinothalamic and spinoreticular tract cells differently, i.e., conveying non-noxious tactile input to one type of tract cell and projecting noxious information to the other type. It has already been demonstrated that three morphologically distinct types of terminal arborizations arising from Vo neurons are located within the areas occupied by these tract cells.

PROJECTIONS TO THE INTERMEDIATE BASILAR NUCLEUS

IBN is considered a caudal extension of Cu in the spinal cord (Torvik, '56) and has been reported to project to the thalamus, mesencephalic tegmentum and adjacent structures (Lund and Webster, '67; Nagata and Kruger, '79; Feldman and Kruger, '80). This nucleus is observed to be predominately composed of spindle shaped neurons and extends caudally to the C3 spinal cord segment (Giesler et al., , '79). Rosen ('67) reported that IBN receives input from group 1 afferents of forelimb muscles. IBN cells were reported to be densely labeled at C1 and C2 levels following multiple

injections of HRP extending into the mediolateral thalamus at two anterior-posterior planes that included the middle portions of VPL and VPM (Giesler et al., '79a). The major thalamic pathway from IBN has been identified following single injections of HRP. Injections made in anterior and posterior medial thalamus resulted in light labeling of cells in contralateral IBN at C1 and C2 levels. Whereas, an injection placed specifically in the lateral thalamus resulted in extremely dense retrograde labeling of contralateral IBN cells, with a few cells labeled in ipsilateral IBN. Following an injection of HRP into the cuneiformis area and ventrolateral part of the central gray, a dense population of ipsilaterally labeled IBN cells was observed with scant labeling in the contralateral nucleus and was most prominent at the C1 cord level.

The importance of IBN projections to the mesencephalic tegmentum suggests an involvement in spinal modulation of pain transmission since destruction of the central gray has been reported to reduce (Melzack et al., '58) or alter (Liebman et al., '70) painful reactions while electrical stimulation in the dorsal portion of the central gray has been observed to induce pain-like reactions or sensations in animals and man. Analgesic effects have been induced by stimulation of the ventral central gray (Basbaum, '80) which has been shown to be rich in endogenous opiates (Hokfelt et al., '77; Simantov et al., '77; Sar et al., '78; Uhl et al., '79). Responses to light touch, hair movement, pressure, changes in skin temperature which are both noxious, and non-noxious and noxious mechanical stimuli have been demonstrated in spinothalamic tract neurons which project to the lateral thalamus (Giesler et al., '79). It is possible that IBN neurons may play a major role in transmitting information regarding skin-impinging stimuli (Giesler et al., '79). Webster

and Kemplay ('87) have suggested that the IBN, or internal basilar column, which lies on the medial side of the base of the dorsal horn in cervical segments C1-C4 (as well as thoraco-lumbar segments T12-L4) acts as a "whole body" relay in the same manner as the LCN, with the suggestion that the cervical part of IBN is involved with forelimb afferents.

Vo-TS efferent projections to IBN, observed to terminate bilaterally from DM neurons and ipsilaterally from VL neurons, may serve to transmit cutaneous noxious and non-noxious input from the face and oral cavity which is further integrated with forelimb input at the rostral cervical levels in IBN and relayed to higher centers as a composite map of tactile input from the total body.

PROJECTIONS TO THE CENTRAL CERVICAL NUCLEUS

CeC has been described in cat (Matsushita and Ikeda, '75; Snyder et al., '78; Wilksten, '79a-c, '83), dog (Nakano, '70; Cummings and Petras, '77), monkey (Snyder et al., '78) and rat (Snyder et al., '78; Matsushita and Hosoya, '79). Cec is an unevenly distributed collection of cells, occurring in clumps along the rostrocaudal extent of the nucleus (Snyder et al., '78), that extends through cervical segments C1-C4. CeC receives afferents from the upper and lower dorsal roots in cat (Papez, '29; Ranson et al., '32; Corbin and Hinsey, '35; Escolar, '48; Kerr, '61; Petras, '65, '66; Imai and Kusama, '69), rabbit (Yee and Corbin, '39), monkey (Corbin et al., '37; Shriver et al., '68), rat (Torvik, '56; Basbaum and Hand, '73), dog (Cummings and Petras, '77). Afferents have also been demonstrated from the vestibular nuclei (Hirai et al.,'79).

The efferent projections from CeC cell bodies located in provide information from receptors in joints and adjacent ligaments of the upper

cervical vertebra (Matsushita and Hosoya, '79; Hirai et al., '79) to the contralateral anterior lobe and parts of the posterior vermis and paramedial lobule (PML) of the cerebellum (Grant, '62; Hirai, et al., '79). In more recent HRP studies, afferent projections have been demonstrated to arise from rat longus capitis and sterno-mastoid muscles (Mysicka and Zenker, '81). It is suggested by Hirai et al. (79) that the afferent input from the neck probably arises from the same afferents that initiate tonic neck reflexes (McCouch et al., '51), and influence extraocular motoneurones (Hikosaka and Maeda, '71). Thus, neurons situated in CeC play an important role in the reflex regulation of balance of the body as well as eye movements.

Vo-TS projections from DM and VL subdivisions terminate throughout the rostrocaudal extent of CeC. These projections provide a pathway whereby tactile stimuli applied to the head, face and oral cavity can assist in the coordination of movement of the head and eyes to avoid aversive outcomes. In addition, these projections help the animal to negotiate objects or food in the ambient environment through bilateral innervation of this nucleus as well as motoneurones situated ventrally in RCC and connections with cranial nerve nuclei III, IV and VI (discussed in Chapt 4).

PROJECTIONS TO THE LATERAL CERVICAL NUCLEUS

LCN has been demonstrated in man (Ha and Morin, '64; Truex et al., '70), monkey (Gardner and Morin, '57; Ha and Morin, '64; Mizuno et al., '67; Kircher and Ha, '68; Shriver et al., '68; Ha, '71) cat (Rexed, '51; Rexed and Brodal, '51: Brodal and Rexed; '53), dog (Kitai et al., '65), raccoon (Ha et al., '65) and rat (Giesler et al., '79b; Gwyn and Waldron, '68). The rat LCN

comprises a group of diffusely scattered cells located along the lateral and ventrolateral border of the cervical dorsal horn between C1 and C2 (Giesler et al., '79b). In cat, this nucleus has been shown to receive afferents from all levels of the spinal cord laminae III-V via the spinocervical tract (Brown and Franz, '69; Bryan et al., '73; Brown et al., '76; Craig, '76; Cervero et al., '77). LCN has been shown to project via the cervicothalamic tract to the contralateral ventrobasal thalamus, specifically VPL (Landgren et al., '65; Bovie, '70; Ha, '71; Millar, '73; Craig and Burton, '79; Giesler et al., '79a ; Boivie. '79, '80; Berkley, '80) as well as the posterior complex (Berkley, '80; Boivie, '80). The termination zone of the cervicothalamic projection to VPL overlaps with projections from DCN but terminations from each pathway end predominately on separate populations of VPL neurons (Berkley, '80). However, Landgren et al. ('65) have shown that some VPL neurons receive convergent input from both pathways. LCN has also been shown to receive afferents from the reticular part of DCN (Craig, '78; Burton and Loewy, '77) and project to the midbrain tegmentum (Menetrey et al., '80, '82). The cells of origin contributing to the spinocervical tract are located predominately in laminae III-V (Craig, '76; Brown, '81). Dorsal horn cells contributing to the spinocervical tract receive monosynaptic excitatory input from thick, myelinated cutaneous fibers and polysynaptic excitatory input from thin myelinated and unmyelinated afferents from muscle and skin (Brown, '73; Bovie and Perl, '75). Some of these cells are activated by mechanoreceptors while others receive convergent inputs from both mechanoreceptors and nociceptors (Brown, '81; Brown and Franz, '69; Cervero et al., '77; Hong et al., '79). The predominant input is from various types of hair follicle receptors. Electrophysiological studies (Craig, '78; Craig and Tapper, '78; Craig and

Burton, '79; Giesler et al., '79b; Horrobin, '66; Kitai et al., '65; Oswaldo-Cruz and Kidd, '64) have shown that LCN neurons are excited by sensitive mechanoreceptors while nociceptive responses were also be recorded in some neurons. Craig and Tapper ('78) have shown that nociceptive cells in the medial part of the nucleus do not project to the thalamus. In rat, many of these cells show nociceptive responsiveness (Giesler et al., '79b). Stimulation of the cortical sensorimotor area inhibits transmission in the spinocervicothalamic pathway in a selective manner with input from nociceptors strongly inhibited while input from hair follicle afferents is unaffected (Brown et al., '76) Cells within cat LCN have been demonstrated to be somatotopically organized (Craig and Tapper, '78),with hindlimbs represented dorsally, forelimbs ventromedially and the face represented in the medialmost part of the nucleus. Although this somatotopic organization has not been found for rat, receptive fields have frequently been shown to include two or more body quadrants and in some cases covered 90% of the available body surface, including the entire head. Input to the head area is presumably derived from input from the trigeminal system with cell responsiveness to noxious cutaneous, thermal, or visceral stimuli located widely throughout the nucleus (Giesler et al., ' 79b). This cellular grouping which continues caudally beyond C2 in the spinal cord dlfu (Gwyn and Waldron, 68; Giesler et al., '79b) also projects to the ventrobasal thalamus (Giesler et al., '81a) and mesencephalon (Menetrey et al., '82) and is referred to as the lateral spinal nucleus. Webster and Kemplay ('87) have referred to this area as a "whole body" relay for somatosensory information projecting to the thalamus.

Vo-TS efferent projections terminate in the medial aspect of LCN along the lateral border of the dorsal horn spanning the corresponding

laminae I-IV levels. Terminal grains have been found distributed on medially directed dendrites of LCN neurons following injections of a mixture of tritiated amino acids into DCN (Burton and Loewy, '77). A somatotopic arrangement is demonstrated with DM neurons projecting to the ventral one-half of the LCN ipsilaterally and VL neurons projecting to the dorsal and ventral halves bilaterally. Furthermore, this somatotopy is suggested with Type 1 terminal arbors limited to the dorsal half of LCN while Type 2 endings were limited to the ventral half of the nucleus. The spinocervical thalamic pathway is thought to be of great importance to nociception in carnivores. The high degree of spatial convergence in LCN in light of the large receptive fields suggest a role in nociception that is not to localize the source of input but to contribute to other aspects of pain perception (Giesler et al., '79) in the thalamus. Projections to the midbrain have been demonstrated in monkey (Trevino, '78) and cat (Blomqvist, '78) which is though to subserve reflex movements to turn the head toward a tactile stimulus (Bjorkeland and Boivie, '85).

The majority of neurons within the lateral spinal nucleus at the lumbar spinal cord level have been shown electrophysiologically (Menetrey et al., '80) to respond only to subcutaneous, articular or muscular stimulation. These characteristics are quite different from those reported for LCN neurons. In their study, Menetrey et al. ('82) showed that only two cells responded maximally to noxious cutaneous stimuli. Neurons in the lateral spinal nucleus at cervical, thoracic and lumbar spinal core levels have been retrogradely labeled bilaterally with HRP following injections made into the caudal periaqueductal gray, cuneiform nucleus and parabrachial nuclei (Lima and Coimbra, '89; Menetrey et al., '82). Lateral spinal nucleus neurons in rat cervical, thoracic and lumbar segments have

also been retrogradely labeled bilaterally with HRP following injections made into the lateral reticular nucleus, nucleus gigantocellularis, nuclei reticularis pontis pars oralis and caudalis and nuclei raphe magnus (Chaouch et al., '83; Menetrey et al., '83). More sparsely HRP labeled cells were seen contralaterally in rat lateral spinal nucleus following HRP injections into the medial and lateral thalamus (Giesler et al., '79, '81). Vo-TS efferent projections are observed from DM neurons in the ipsilateral lateral spinal nucleus at thoracic and lumbar spinal cord levels. Like DM neuron projections to LCN in the most rostral levels of the spinal cord, terminal arborizations following DM injections were observed in the ventral half of the lateral spinal nucleus at lower cervical levels as well as thoracic and lumbar cord segments. The role of this input is not obvious at this time but based on the results presented above, Vo-TS efferent projections may participate in relaying possible whole body information of noxious and non-noxious origin conveyed by the lateral spinal nucleus. This region contains very dense substance P terminals of peripheral origin (Barber et al., '79; Hokfelt et al., '76) and may be involved in the transmission of nociceptive input to the mesencephalon, where stimulation produces fear-like or pain-like behavior in rats (Kiser et al., '78; Liebman et al., '70).

Vo PROJECTIONS TO THE CENTRAL CORE OF THE SPINAL CORD GRAY MATTER

Cells in ventral areas of the dorsal horn, intermediate gray and ventral horn, are responsive to a variety of stimuli ranging from noxious to non-noxious from cutaneous and subcutaneous tissues (Fields et al., '75, '77 a,b; Maunz et al., '78). In addition, some cells are impinged upon by both somatic and visceral afferent fibers and are participants in the

"convergence-projection" theory of referred pain (Ruch, '47). Viscerosomatic information is thought to project through pathways in the ventrolateral funiculus via the spinothalamic and spinoreticular tracts (Hancock et al., '75; Foreman and Weber, '80; Cervero, '83b). Most of the cells are described to have complex excitatory or inhibitory cutaneous receptive fields while others have excitatory fields in deep structures such as joints, muscles and tendons. Many recent studies utilizing neuroanatomical and electrophysiological techniques have demonstrated a substantial population of rat spinothalamic and spinoreticular neurons in laminae V, VII and VIII at cervical, thoracic and lumbar spinal cord levels (Giesler, '79; '81a; Menetrey et al. '82; '83). Bilateral Vo-TS efferent projections to these laminae suggests a potential of modulating viscerosomatic as well as somatic neurons. In the thoracic cord this is perhaps most obvious with the clinical symptom of referred pain to the jaw as well as the left arm during episodes of coronary ischemia. Somatic and viscerosomatic neurons in the thoracic cord has been demonstrated for the most part to be segregated with somatic neurons occupying laminae II-IV and viscerosomatic neurons positioned in laminae I, V, VII and VII (Cervero, '83b). A convergence of visceral nociceptive input from the heart via the vagus nerve with trigeminal tactile input onto the same spinal cord neurons in laminae V, VII or VII that project through somatosensory pathways may provide for the transmission of noxious signals to VPM. Vo input onto viscerosomatic neurons could play a prominent role in the arousal of diffuse visceral sensations occurring in some forms of visceral pain. It has been demonstrated in cat that vigorous responses to splanchnic nerve stimulation in the intact state are abolished after cold block of the spinal cord (functional reversible cordotomy) suggesting that

supraspinal loops are an important component of visceral afferent input onto viscerosomatic neurons (Cervero, '83b).

Lamina V is a prime area for tract cells conveying noxious and non-noxious cutaneous primary input and there exists the potential for modulating interactions with respect to pain and tactile input between Vo-TS efferent fibers and second order cells of the spinothalamic (especially the medial spinothalamic tract cells), spinomesencephalic and spinoreticular tracts. Spinothalamic tract neurons within cat LE have been shown to receive descending excitatory input from the trigeminal region (McCreery et al., '79) and noxious stimulation of tooth pulp in cats has been demonstrated to cause a decrease in the response threshold to foot shock (Anderson et al., '76).

CONVERGENCE OF TRIGEMINAL AND SPINAL CORD DORSAL ROOT PROJECTIONS IN ROSTRAL CERVICAL DORSAL HORN

Previous degeneration studies have shown that primary trigeminal afferents project not only to the spinal trigeminal nucleus but also to the cervical dorsal horn (Torvik, '56; Kerr, '61; Grant and Arvidson, '75; Arvidson and Grant, '79). Utilizing the transganglionic transport of HRP a bilateral projection from primary trigeminal neurons to the cervical cord has been confirmed and extended (Arvidsson and Gobel, '81; Marfurt, '81; Arvidsson, '82; Jacquin et al., '82, '83b; Marfurt and Turner, '84; Nishimori et al., '86; Shigenaga et al., '86, Jacquin et al., '90). Projections of muscle afferents of trigeminal ganglion origin were observed to terminate in the medial portion of laminae I and V of upper cervical segments C1-C3 (Shigenaga et al., '88). Jacquin et al., ('90) have utilized the PHA-L technique to demonstrate morphological detail of primary trigeminal

afferents to the cervical dorsal horn. The fact that primary trigeminal afferents project bilaterally to rostral cervical spinal cord levels raises important questions concerning the relationship between the central termination sites of primary trigeminal afferents and trigeminal afferents arising from Vo-TS projection neurons which also project bilaterally to the cervical spinal cord as well as to more caudal cord levels. Primary afferent trigeminospinal projections in rat have been described as far caudally as the C6 or C7 segments (Jacquin et al., '82; Pfaller and Arvidsson, '88), although the amount of HRP labeling becomes very sparse caudal to C3 (Pfaller and Arvidsson, '88). However, other groups (Torvik, '56; Clark and Bowsher, '62, Jacquin et al., '83, '90) have reported primary trigeminal afferent projections that end only in the first three cervical segments. Taken together, these studies report substantial amounts of labeling down to the caudal limit of C3. The pattern of terminal labeling described in these studies is described to be primarily contained dorsomedially in dorsal horn laminae I, II and V bilaterally following injections into the mandibular division of the trigeminal ganglion (Jacquin et al., '82; Panneton et al., '91). Terminal labeling is described as extensive contralaterally in the ventrolateral portions of laminae III-V following injections into the ophthalmic-maxillary portion of the trigeminal ganglion (Jacquin et al., '90; Panneton et al., '91). Following total trigeminal ganglion injections (Pfaller and Arvidson, '88) heaviest labeling was demonstrated in the medial half of the dorsal horn in ipsilateral laminae I-IV bilaterally. The pattern of labeling of Vo-TS efferents in the present study is greatest in the medial aspect of laminae III-V of cervical segments C1 and C2 with a greater density ipsilaterally following DM injections and greatest in the lateral aspect of laminae III-V of cervical segments C1 and

C2 with a greater density ipsilaterally following VL injections. At more caudal cervical levels Vo-TS efferents are still concentrated within ipsilateral laminae III-V but the lateralization is not maintained. It has been shown that primary trigeminal afferents are organized somatotopically with cell bodies of axons in mandibular division neurons innervating the lower face and ventral half of the oral cavity occupying the posterolateral portion of the trigeminal ganglion and terminating dorsally in ipsilateral SVN, while cell bodies of the ophthalmic branches supplying the dorsal third of the face are located anteromedially and end ventrally within SVN. Maxillary division primary neurons innervating the upper lip, vibrissae, rhinarium, facial pads, and dorsal oral cavity terminate in an area of SVN interposed between the previously described two (Allen, '24; Darian-Smith and Mayday, '69; Darian-Smith et al., '65; Beaudreau and Jerge, '68; Zucker and Welker, '69; Lende and Poulos, '70; Mazza and Dixon, '72; Gregg and Dixon, '73; Arvidsson, '75; Anderson and Rosing, '77; Arvidson, '77; Pearl et al., '77; Aldskogius and Arvidsson, '78; Morgan et al., '78; Aker and Reith, '80; Westrum et al., '80; Arvidsson and Gobel, '81; Marfurt, '81a; Porter and Spencer, '82; Jacquin and Zeigler, '83). The results in this study suggest a convergence of trigeminospinal projections from Vo-TS neurons in DM and VL subdivisions with primary trigeminal afferent projections from mandibular and ophthalmic divisions of the ophthalmic nerve in laminae III-V of C1 and C2 segments which is in register with defined trigeminal somatotopy for the lateralization of mandibular and ophthalmic projections to the dorsal horn. While lateralization is lost at C3 and C4 levels, it is again picked-up in CE and TC levels following DM injections.

To the above discussion must be added the question of convergence of primary afferent input from neurons in cervical dorsal root ganglia (DRG) with Vo-TS efferents in the cervical spinal cord. The central projections of upper cervical DRG neurons in the rat have been studied previously with degeneration techniques (Torvik, '56; Basbaum and Hand, '73), by ganglion injections of wheat germ agglutinin conjugated to HRP (WGA-HRP), (Imamura et al., '86, Pfaller and Arvidsson, '88), and with combined electrophysiologic and retrograde transport of HRP methodology (Abrahams et al., '79). The central projections terminating in the dorsal horn have been described in these studies to vary in their level of origin from cervical DRGs C1 to C8. The Vo-TS projection to the dorsal horn is similar to spinal segments in which bilateral projections of primary afferents have been demonstrated (Culberson and Kimmel, '75; Proshansky and Egger, '77; Culberson et al., '79; Light and Perl, '79b; Mesulam and Brushart, '79; Rethelyi et al., '79; Matsushita and Tanami, '83; Smith, '83; Ritz et al., '85; Pfaller and Arvidsson, '88) with the consensus that these bilateral projections terminate most heavily in laminae III-V of the extreme medial and lateral aspects of the dorsal horn. A trend toward somatotopic organization was reported for trigeminal and upper cervical afferent projections to the dorsal horn at C1-C3 levels (Pfaller and Arvidson, '88) which were best observed in the densely labeled areas of lamina II-IV at C2 and C3 levels. The preferential termination of these bilaterally terminating fibers predominately, but not exclusively, in laminae III-V, with sparser projections reported to laminae I and II, is consistent with a role in pain processes (Light and Pearl, '79b). The representation of masticatory muscle afferent information in lamina I (and lamina V)

suggests that primary muscle afferent neurons of ganglionic origin primarily mediate muscle pain (Shigenaga et al., '88).

Other studies in our laboratory (Cook and Falls, '90, '91) suggest a somatopic pattern of distribution of efferent projections originating from different subdivisional areas within Vi to the dorsal horn of C1-C5 spinal cord levels. Projections originating from cell bodies located in the ventrolateral portion of Vi (ventrolateral magnocellular subdivision) are illustrated to terminate primarily in the lateral two-thirds of lamina III and IV bilaterally, with an ipsilateral predominance. Projections arising from dorsomedial portions of Vi were observed to be of greater density in more caudal ipsilateral sections and were distributed along the mediolateral extent of the ipsilateral dorsal horn in C1 with a shift to the lateral aspect of the ipsilateral dorsal horn in lower cervical levels. In addition, terminal arborizations arising from Vi dorsomedial injections did distribute more medially in the contralateral dorsal horn at the C1 level. The extent of literature demonstrating not only primary afferent but secondary Vo-TS, Vi (Cook and Falls, '90,'91) and MDH (Burton and Loewy, '76) trigeminospinal efferent projections as well as projections from the trigeminal mesencephalic nucleus neurons within the masseter and deep temporal muscles and afferent projections from the cervical spinal cord to C1 and C2 segments in a discrete somatotopic manner suggest that perhaps this area may be a caudalization of MDH. Previous studies have demonstrated functional and physiological similarities between MDH and the dorsal horn of the cervical spinal cord (Torvik, '56; Darian-Smith, '73; Yakota, '76; Gobel et al., '77; Dubner et al., '78; Gobel, '79; Gobel et al., '81) suggesting that MDH extends caudally to the second cervical level.

Wise et al. ('79) have shown corticotrigeminal efferent projections to arise exclusively from neurons located in the head, muzzle and vibrissal representations of the primary sensory cortex (SI) while corticospinal cell bodies in this cortical area target the cervical spinal cord in a differential manner. Corticospinal projections to RCC originate from posterior head and neck representations of SI primarily and those projections observed to continue more caudally in CE originating from the forelimb area of SI and primary motor cortex (MI). That the corticospinal system may subserve a functional role in the sensory system of rodents is supported in a degeneration study by Brown ('71) illustrating a pattern of degenerating debris in the dorsomedial area of the neck of the dorsal horn, predominately in layers II-IV, following unilateral sensorimotor cortex ablation.

Perhaps rostral segments of the cervical spinal cord represent a unique area, between the trigeminal orofacial system and the spinal cord upper/lower limb system, where strict modulation of afferent and efferent activities is needed to keep the head upright and synchronized with peripheral events affecting the face and limbs. The main terminal fields of jaw muscle afferents are observed to be in laminae I and V of MDH and the upper cervical cord (Shigenaga, '88). It is thought that the overlapping representation of jaw muscles and facial and intraoral regions, including tooth pulp, may explain the specific patterns of referred pain and help explain the existence of a trigger area in the masticatory muscles (Dubner et al., '78).

TRIGEMINAL MODULATION OF MEDIAL AND LATERAL AUTONOMIC CENTERS

Labeled cellular groupings of sympathetic preganglionic neurons have been identified in the spinal cord intermediate gray following application of HRP to the paravertebral ganglia in cat (Chung et al., '75), dog (Petras and Faden, '78) and HRP treated adrenal medulla in rat (Schramm et al., '75). These separate studies concluded that the majority of sympathetic preganglionic cells in various mammals were found in the IML (Cummings, '69; Petras and Cumings, '72) with the remainder situated in the lateral funiculus, middle region of the intermediate gray (Petras and Cummings, '72), and occasionally along the dorsal and dorsolateral border of lamina X (Cummings, '69; McDonald and Cohen, '70; Petras and Cumings, '72; Hancock and Peveto, '79). Several other collections or groupings of sympathetic preganglionic neurons have been demonstrated (Petras and Cummings, '72).

Afferent inputs arriving from baroreceptors and chemoreceptors, receptors in the atria or ventricles of the heart, kidney, gastrointestinal tract, pelvic viscera and other organs as well as skin and muscle afferents elicit excitatory or inhibitory influences on preganglionic neurons through spinal and supraspinal pathways. (Koizumi and Brooks, '72,'80). Inhibition of preganglionic and postganglionic cells occurs following stimulation of baroreceptors (Kirchheim, '76; Spyer, '81) while changes in respiration are mediated by excitation of chemoreceptors (Korner, '71; Koizumi and Brooks, '72). Hypoxia or hypercapnia stimulation of arterial chemoreceptors causes mixed effects on preganglionic neurons in the thoracic cord (Preiss and Polosa, '77). Central chemoreceptors located in the ventral medulla have been shown to modulate sympathetic neurons

(Schlafke and See, '80; Hanna et al., '81). Excitation of visceral afferents produces powerful sympathetic reflex responses. Receptors in the atria and ventricles of the heart (Coleridge et al., '64; Paintal, '73; Koizumi et al., '75; Linden, '75; Kollai et al., '78a; Hainsworth et al., '79) which are stimulated by chemical and mechanical changes evoke cardiovascular reflexes involving sympathetic nerves, receptors in the lungs and great veins also affect the autonomic system (Coleridge and Coleridge, '79). Most of these reflexes are mediated through vagal afferents entering the medulla to influence supraspinal modulation of preganglionic neurons in the spinal cord. However, afferents, excited by mechanical changes i.e., occlusion of the coronary arteries, distention of the aorta, have been shown to run in sympathetic cardiac nerves to the spinal cord that eventually evoke excitatory of inhibitory changes in sympathetic neurons acting on the cardiovascular system (Malliani, '79; Malliani et al., '81). Somatosympathetic reflexes mediated by myelinated and unmyelinated afferent fibers affect preganglionic sympathetic neurons in the spinal cord (Koizumi and Brooks, '72; Sato and Schmidt, '73). The excitation of preganglionic neurons by stimulation of somatic afferents has been shown to result in an initial excitation followed by a long lasting inhibition of tonic discharge (Polosa, '67; Koizumi and Brooks, '72; Sato and Schmidt, '73;) in spinal preganglionic neurons. Afferent fibers, types II-IV, have been shown to produce this biphasic reflex response, excitation then inhibition (Koizumi et al., '70; Koizumi and Brooks, '72; Sato and Schmidt, '73; Horeyseck and Janig, '74). Certain reflexes i.e., chemoreceptor reflex, temperature regulation reflex, have been shown to produce differential discharges in sympathetic neurons (Simon and Riedel, '75; Kollai and Koizumi, '77; Kollai et al., '78b; Iriki and Korner, '79; Riedel and Iriki, '79;

Kollai and Koizumi, '80) and suggests that preganglionic fibers have differentially controlled discharge patterns. Janig and Kummel ('81) and Janig and Szulczyk ('81) have shown that four groups of postganglionic fibers from skin and muscle vasoconstrictors and sudomotor and pilomotor fibers are controlled by four groups of neurons situated in the lumbar spinal cord. In a histochemical analysis utilizing retrograde fluorescent dyes, Appel and Elde, ('88) demonstrated an anatomical substrate in rat IML reflecting selective regulation of sympathetic neurons to different system target organs. Retrograde labeling of preganglionic sympathetic neurons was achieved after simultaneous exposure of the cervical sympathetic trunk and adrenal medulla to Fluoro Gold and True Blue. This study revealed two populations of sympathetic preganglionic neurons in IML with greatest overlap in distribution at T1-T4 segments in the spinal cord. In areas of overlap sympathoadrenal preganglionic neurons occupied the more lateral aspect of IML, with cervical sympathetic trunk preganglionic neurons positioned more medially. In this same study, equal proportions of identified cervical sympathetic trunk and sympathoadrenal preganglionic neurons were identified as being apposed by varicosities immunoreactive for either somatostatin or serotonin. However, oxytocin immunoreactive varicosities were limited to cervical sympathetic trunk preganglionic neurons and avoided sympathoadrenal preganglionic neurons. The suggestion was made that different portions of the sympathetic outflow may be regulated independently of one another. Central nervous system administration of somatostatin or a somatostatin-like peptide blunted epinepherine secretion in response to simultaneous administration of neuroactive peptides while it had little or no effect on norepinepherine secretion in response to the coadministered neuroactive

peptides (Fisher and Brown, '80). Appel and Elde ('88) explain the differences observed in their study for equal distribution of somatostatin varicosities on distinct cell populations in IML as possibly due to the existence of two different forms of somatostatin, which have been identified in the spinal cord that could be acting or regulating the two identified IML subnuclei in a different manner. Neuropeptide somatostatin-like activity has been illustrated (Bowker, '88) while substance P and Met-enkephalin reactivity has been observed (communication by R. Bowker) for Vo neurons in the subdivisional area that has been shown in this study to project in close approximation to preganglionic neurons in IML.

Trigeminal reflexes consisting of the diving reflex (elicited by facial immersion) and nasopharyngeal reflex (from non-noxious stimulation of the olfactory mucosa) are associated with a reflex induced bradycardia (Kumada et al., '77).

Vo PROJECTIONS TO IDENTIFIED MOTONEURONAL CELL POOLS IN THE VENTRAL HORN

Cell bodies of motoneurons to skeletal muscles are found within lamina IX in the spinal cord ventral horn (Rexed, '54). They are arranged in somatotopically organized longitudinal columns of motoneuronal cell pools, spanning 1-3 spinal segments (Romanes, '51). Motoneuronal cell pools are observed medially, laterally and dorsolaterally within the ventral horn depending upon the spinal cord segment being viewed (Mollander et al., '84,). A general pattern for cat has been shown to exist within lumbosacral cell groups innervating hindlimb musculature (Romanes, '51) with medial pools supplying proximal muscles e.g., hip, intermediate pools supplying the limbs e.g., thigh and leg, and lateral pools supplying distal

muscles e.g., foot. A similar pattern would also be found in the cervical enlargement for forelimb musculature. These pools are further organized with ventrally lying neurons projecting to limb extensors and dorsally situated cell bodies supplying limb flexors. Cytologic studies utilizing silver and Nissl stains (Angulo y Gonzales, '40; Schroder, '80), degeneration studies (Goering, '28; Grant and Ygge, '81) studies utilizing the retrograde transport of HRP (Kitamura and Sakai, '82; Goshgarian and Rafols, '81; Smith and Hollyday, '83; Smith '83; Ygge and Grant, '83; Nicolopoulos-Stournas and Iles, '83; Peyronnard and Charron, '83; Janjua and Leong, '84; Brink et al., '79) and studies using fluorescent retrograde tracers (Brunner et al., '80) have demonstrated in rat, cat, and monkey the relative positions within the spinal cord of motoneuronal cell pools and the muscles that these cell pools innervate. Vo-TS efferents may be involved in larger issues of respiratory function as evidenced by the participation of the trigeminal system in sneezing and the cardiovascular component of the diving reflex (Andersen, '66).

Motor neuronal cell columns of CE have been studied with the utilization of discretely placed lesions of brachial plexus nerves (Goering, '28). Motor neuronal cell columns containing neurons innervating forelimb muscles are positioned at various segmental levels of rat CE. Goering ('28) reported that the dorsolateral portion of CE ventral horn contains five cell columns. Three of these are situated most laterally (from dorsal to ventral they are referred to as C', D and S) and two are positioned more medially in the dorsolateral aspect of the ventral horn (designated C and M, from dorsal to ventral). Varying proportions of these five motoneuronal cell columns are contained within different CE segments. At rostral levels of CE, i.e., C6, the medially placed cell groups predominate

with a gradual enfolding of the more laterally situated cell groups in more caudal segments C8 and T1 containing all five motoneuronal cell groups. The localization of motoneuronal cell pools within the described columns from C6 to T1 was further characterized according to the various nerves utilized in the distribution of their efferent axons. Cells in column C contributed to nerves musculocutaneous, median, ulnaris and axillary; cells in column C' utilized nerves radial, median and ulnar; cells in column D were associated with nerves radial, axillary and anterior thoracalis and cells in column M were involved with nerves suprascapularis, axillary and anterior thoracalis. The functional significance attributed to the organization of these cell columns within different segmental levels was principally that cells in column C subserve partly or principally a flexor function while cells in columns C' and D innervate muscles which are chiefly or partly extensors and cells in column M are connected to muscles which are chiefly rotators. Motoneurons in column S are probably functionally correlated with adduction. Vo-TS efferents were observed to be densest to the ipsilateral medial cell pools following DM injections and were concentrated almost entirely within the medial motoneuronal cell pools bilaterally following VL injections. Terminal arborizations were scattered more diffusely among medial and lateral cell pools bilaterally following BZ injections. The diagramatic illustrations by Goering ('28) of the dorsolateral cell pools illustrated their positions to be more medially displaced and more expansive than those noted in the tissues used in the present study. Perhaps this can be accounted for in the fact that by virtue of the age range of rats used in Goering's study, 50-100 days of age, the developmental organization of motoneuronal cell pools is more diffuse in the young rat in

comparison to the adult. Vo-TS efferents were observed to project ipsilaterally to the dorsolateral motoneuronal cell pools contained within CE following DM injections and bilaterally to the same cell pool following a BZ injection while no projections to the dorsolateral motoneuronal cell pools were demonstrated for VL neurons. It is clear that there are subdivisional differences observed for cells lying within DM and BZ in comparison to those lying in VL with the implication that VL neurons are more aligned with affecting functions involving the proximal musculature with a possible role in subserving balance. Neurons situated in DM and BZ project in a more diffuse or generalized manner to medially as well as laterally situated cell pools.

Motoneurons innervating hindlimb musculature have been identified in rat (Brink et al., '79; Brushart and Mesulam, '80; Ha et al., '80; Schroder, '80; Brunner et al., '81; Nicolopoulos-Stournaras and Iles, '83; Janjua and Leong, '84), cat (Romanes, '51, '64), and monkey (Janjua and Leong, '84). Motoneurons innervating muscles derived from the dorsal muscle mass (psoas, quadriceps, gluteal, and anterolateral groups) are situated more lateral in the ventral horn than those motoneurons innervating muscles derived from the ventral muscle mass (Lance-Jones, '79). A similar somatotopic relationship has been reported in adult rat (Nicolopoulos-Stournaras and Iles, '83). Utilizing the retrograde transport of HRP the columnar organization of motoneuronal cell groups has been shown to persist at lumbar levels in six major groupings of motoneuronal cell pools spanning L2-L5 or L4-L7 segments (Janjua and Leong, '84; Nicolopoulos-Stournaras and Iles, '83). Based on their locations in the ventral horn these six motoneuronal cell groups are identified as medial, ventromedial, anterolateral, central, posterolateral and post-posterolateral

cell columns (Janjua and Leong, '84), or have been illustrated in diagrams and simply referred to by group number (Nicolopoulos-Stournaras, '83). When femoral, sciatic, common peroneal and tibial nerves were severed and treated with HRP labeled neurons were observed in these cell groups in the following arrangement: HRP treated sciatic nerve labeled cells in post-posterolateral, posterolateral, central and anterolateral motoneuronal cell groups in caudal parts of L3 to rostral S1 segments; tibial nerve treatment labeled cell bodies in central, anterolateral, posterolateral and post-posterolateral motoneuronal cell groups from rostral L4 to caudal L6; neurons labeled by application of HRP to the common peroneal nerve were in anterolateral, posterolateral and post-posterolateral motoneuronal cell groups from caudal L3 to rostral L6; femoral nerve HRP exposure labeled neurons in anterolateral, posterolateral and central motoneuronal cell groups in rostral L2 to middle L4 segments (Janjua and Leong, '84). Nicolopoulos-Stournaras and Iles ('83), referred to these six motoneuronal cell columns by numbers. Although the position of the motoneuronal cell pools varied with respect to segmental level in the spinal cord in both studies, cell columns 1,4, 3/6 roughly correspond to anterolateral, posterolateral and post-posterolateral motoneuronal cell pools referred to by Janjua and Leong ('84) respectively and cell columns 2 and 5 corresponding to ventromedial and central motoneuronal cell pools respectively. According to Nicolopoulos-Stournaras and Iles, '83) at L2 and L3 segment levels columns 1, 3 and 4 were located most laterally in the dorsal horn with columns 2 and 5 placed more medially in the lateral portion of the ventral horn. At more caudal segments, L4 and L5, columns 1, 5 and 6 occupied the most lateral area of the ventral horn while column 2 remained more medially positioned in the lateral aspect of the ventral horn. The

motoneuronal cell columns innervated specific muscle groups: column 1 in lower L1 and in L2 segments innervated the psoas-iliacus group of muscles and more caudally at the L3 level innervated the gluteal group. Column 2 in L1, L2 and upper L3 segments innervated the adductor group and more caudally in lower L3 and L4, L5 segments innervated the hamstring group. Column 3 at lower L2 and L3 segments innervated the quadriceps group, while column 4 at L3 and L4 segments innervated the anterolateral crus muscles. Column 5 at L3 and L4 segments innervated the posterior crus muscles and column 6 at L4 and L5 segments innervated the intrinsic muscles of the foot. Medial and ventromedial motoneuronal cell columns mentioned by Janjau and Leong, ('84) were not labeled by either the femoral, sciatic, common peroneal or tibial nerves in the study of Nicolopoulos-Stournaras and Iles, '83). Following injections of HRP into lateral longissimus and transverso-spinalis muscles most labeled cells were located in the medial motoneuronal cell pool of the ventral horn in the lumbar enlargement (Brink et al., '79). Only Vo-TS efferents originating from DM cell bodies projected as far caudally as the lumbar enlargement. Terminal arbors were almost equally distributed within medial, ventral and lateral cell columns ipsilaterally and were located in medial and lateral motoneuronal cell columns contralaterally. A large number of Vo-TS efferents were aggregated in lamina VIII surrounding the ipsilateral medial motoneuronal cell pool. DM neurons project to the ventral horns of the lumbar enlargement in a manner to suggest a diffuse, generalized affect on motoneuronal cell pools supplying axial and distal musculature. However, the density of label in ipsilateral lamina VIII suggests a more significant role in the innervation of ipsilateral postural muscles, perhaps

those of the tonically active transverso-spinalis muscles which are important in the maintenance of balance and posture.

Motoneuron cell pools in rat lumbosacral transition area (L6) consist of dorsomedial, ventral, dorso-lateral and retrodorso-lateral groups (Schroder, '80). Utilizing the retrograde transport of HRP, Schroder injected pelvic muscles and treated the ischiadicus. Following injections into the bulbocavernosus and sphincter ani muscles labeled neurons were found in the dorsomedial motoneuronal cell pool while injections into the sphincter urethrae and ischiocavernosus muscles labeled neurons in the dorsolateral cell pool. HRP injections in levator ani muscle labels motoneurons in the ventral cell column. Neurons were found to be situated in the retrodorso-lateral and dorsal part of the lateral cell pools following application of HRP to the cut end of the ischiadicus nerve. The pelvic muscles are somatic muscles under voluntary control. However, they are also intimately coupled with visceral functions. Innervation of motoneurons supplying the pelvic musculature by Vo neurons that are stimulated by tactile and nociceptive input from the oral cavity could take place during the act of eating in reflexively preparing the alimentary tract for digestion and elimination of digested wastes in a manner similar to the gastrocolic reflex. Vo-TS efferents are positioned in the appropriate areas of the L6 segment to make this suggestion a possibility.

The tail flick reflex has been widely used to study neural mechanism of analgesia. The underlying anatomy has been demonstrated with tail flick motoneurons present from L4 to coccygeal 3 levels (Grossman et al., '82). Following the injection of HRP in tail flick muscles (extensor caudae medialis, extensor caudae lateralis and abductor caudae dorsalis) labeled motoneurons were found in lumbar segments L4-L6 and caudally in sacral

and coccygeal levels. Extensor caudae medialis motoneurons were concentrated ventromedially at L4-L6 cord levels, abductor caudae dorsalis motoneurons were located ventrally in lumbar cord levels L5-L6 and extensor caudae lateralis motoneurons were not demonstrated in the lumbar cord. Dorsolateral tail nerve and the ventrolateral tail nerve which innervate the skin of the tail labeled afferent terminals in the lateral half and medial half of dorsal horn laminae I-II, respectively. Vo-TS projections to the ventral horn of lumbar segments L4-L6 places Vo in a position to affect muscles involved with tail flicking movements. It is not inconceivable to suggest that in the exploration of space the rat may use tactile input gained by vibrissal hairs to modulate ventral horn motoneuronal cell output in the maintenance of balance through tail movements.

FUNCTIONAL CONSIDERATIONS

Descending trigeminospinal projections from Vo reported here may be related to reflex swallowing mechanisms via projections to the cervical and upper thoracic cord levels. It is conceivable that sensory stimulation of receptors in the oral cavity during swallowing could reflexively inhibit phrenic and intercostal activity through trigeminospinal projections.

The main terminal fields of jaw muscle afferents are observed to be in laminae I and V of MDH and the upper cervical cord (Shigenaga, '88). It is thought that the overlapping representation of jaw muscles and facial and intraoral regions, including tooth pulp, may explain the specific patterns of referred pain and help explain the existence of a trigger area in the masticatory muscles (Dubner et al., '78). A similar suggestion has been made for the nociceptive neurons in the spinal dorsal horn receiving

widespread convergent inputs from cutaneous, visceral and muscle afferents (Pomeranz et al., '68; Cervero et al., '76; Foreman et al., '79a,b; Cervero, '82).

In an electrophysiological study in cat which also utilized the retrograde transport of HRP (Abrahams et al., '79), an extensive convergence of information from neck muscle afferents (originating from splenius, biventer cervicis and complexus) and input from the face onto cells located in C1 to C4 spinal cord segments with about 40% of isolated single units investigated in dorsal and ventral horns demonstrating input from both areas simultaneously. Following stimulation of the infraorbital nerve small sharp movements of face hairs, vibrissae and supraorbital sinus hairs resulted in unit discharge as far caudally as C3. In laminae V and VI ipsilateral and contralateral neck muscle nerves evoked unit discharge. Isolated units investigated in MDH demonstrated that units activated by cutaneous stimulation of the face dominated in the dorsomedial regions of lamina IV while units activated by muscle afferent stimulation were restricted to the ventrolateral regions of lamina IV and extending across the border of lamina V. About 40% of units between the obex and C1 were activated by either infraorbital nerve stimulation or by hair movement and were also activated by neck muscle afferent stimulation. When convergence could not be found a functional relationship was shown to exist between neck muscle and trigeminal afferents by the demonstration that prior stimulation of one modality strongly inhibited the normal multiunit response of the second modality.

The present study suggests the existence of a strong functional relationship between neck cutaneous and muscle afferents and primary and secondary trigeminal input in RCC. It has been shown physiologically

that monosynaptic projections from neck muscle afferents exist but that they are difficult to elicit under conditions which would normally result in monosynaptic reflex production in the lumbosacral cord (Ezure et al., '78; Abrahams, '75). It is possible that in the execution of head movements, trigeminal sensory afferent input may play a role in the simple reflex aversion to noxious stimuli as well as in head movements involved with feeding, grooming, exploration, aggression, suckling and orientation to environmental cues.

Some of the earliest elicited fetal reflex responses demonstrated in rat (Angulo y Gonzales, '40) and man (Humphrey and Hooker, '59) involve stimulation to the snout or perioral area of facial skin. From a functional standpoint, rat fetuses at the late stages of fifteen days of age respond to light stimulation of the snout with a contralateral flexion of the head (neurogenic reflex) or to ligation of the umbilical cord with lateral flexion of the head (neuromotor activity). A few hours later they are seen to give lateral flexion of the trunk with forelimb movement spontaneously or upon stimulation of the snout. The manner in which motor behavior begins in the rat fetus is first with the most medial motoneuron cell groups, innervating axial muscles, and proceding to lateral motoneuronal cell columns, innervating the muscles of the limbs (Angulo Y Gonzalez, '40). In human fetuses light exteroceptive stimulation, with pressure calibrated esthesiometers, to the perioral facial skin at 7 1/2 week gestation results in flexion of the neck and upper trunk region toward the contralateral side. In the next week, stimulation of the face spreads caudally to involve the entire trunk in a generalized response of lateral flexion, pelvic rotation and extension of the upper extremities at the shoulders. At 10 1/2 weeks response changes to trunk extension. Beyond these generalized reflexive

movements, local reflex responses are observed beginning at 9 1/2 weeks with facial stimulation producing mouth opening followed by contraction of the obicularis occuli and concomitant squint in response to stimulation of the eyelid. Other local responses documented are deglutition, contraction of the corrugator supercilii resulting in scowling and lip closure. Later, at 13 weeks circumoral stimulation can also produce contraction of the obicularis oculi. At approximately 14 weeks, double simultaneous stimulation of the upper lip and palm of the hand results in finger flexion elicited by the proximal stimulus, facial stimulation and approximately 1/2 week later each stimulus producing the characteristic reflex response. It was thought by these authors that as lip closure becomes more common and the suctorial reflex appears, facilitation of the palmer reflex may occur (Humphrey and Hooker, '59) partly based on the work of Prechtl ('53) who reported that neonates have a stronger grasp while sucking than at other times. One of the suggested underlying factors was thought to involve the transmission of a large volume of sensory impulses, set off by vigorous and continued sucking, to motoneurons within CE that facilitate the grasp reflex. The complete replacement of contralateral trunk flexion/extension responses upon stimulation of the face by local reflexes is thought due to newly functioning anatomical connections. Impulses set up by circumoral stimulation that results in contralateral neck flexion are suggested to be carried by descending fibers of the spinal trigeminal tract to commissural neurons in the upper cervical cord levels (Humphrey, '52). Humphrey and Hooker ('59) suggested that commissural neurons transmit impulses to the contralateral ventral horn motoneurons that innervate the cervical muscles resulting in head bending laterally with extension of the reflex contraction caudally to involve trunk flexion, brachial extension and rump

rotation through the utilization of propriospinal fibers or the reticulospinal tracts or both. Simultaneous face and palm stimulations that elicited responses to the proximal stimulus is thought due to impulses descending to the upper cervical levels of the spinal cord coursing ipsilaterally to motoneurons innervating flexor muscles of the fingers as well as contralaterally to motoneurons stimulating neck and trunk muscles. Following simultanous stimulation of both face and palm impulses reach the spinal cord as the result of perioral stimulation and evidently distribute ipsilaterally to motoneurons responsible for finger flexion in a manner to prevent the palmer reflex. It is thought by these authors that both he reticulospinal pathways or spinal trigeminal tract may transmit impulses to the cervical cord in response to circumoral stimulation. The developmental changes responsible for the failure to suppress palmer reflex of older fetuses involve structural changes in the development of branches of the trigeminal nerve and svt leading to the SVN and the establishment of internuclear connections between this nucleus and the cranial nerve nuclei to complete the reflex arcs for local reflexes. Prior to 9 1/2 weeks gestational age when no local responses are observed to stimulation of the face fibers of the svt have made is thought due to the possibility that functional terminations exist in only the caudal portion or MDH, differentiated by 8 1/2 weeks (Brown, '56a,'58). Later, at 14 weeks, when the local reflex type of response predominates, Vi and Vo are differentiated as far rostrally as the cochlear nerve (Brown, '56b), such that a cervicorostral sequence of development occurs for SVN. With the possible differentiation of cranial nerve motor nuclei in a cervicorostral sequence, as is the case for chick (Windle and Austin, '36) and cat (Windle, '33) the developmental order of appearance for local reflexes following trigeminal

stimulation (starting with mouth opening, obicularis oculi contraction, deglutition to mouth closure) indicate a cervicorostral sequence for the establishment of connections with SVN to the brainstem motor nuclei (Humphrey, '54; Hooker, '54; Humphrey and Hooker, '59). With the establishment of more functional internuclear connections between SVN and cranial motor nuclei it is thought that impulses coursing through svt are distributed in greater number to these nuclei with fewer passing to the spinal cord. This decrease in number of impulses reaching the spinal cord may account for sporadic neck and trunk movements and loss of inhibition of the palmer reflex finger closure observed during double simultaneous stimulation tests. It is thought that the changes in response to double simultaneously delivered stimuli to the face and palm occurs at approximately the same time that local reflexes predominate over the earlier neck and trunk flexion/extension following perioral stimulation. A further suggestion is that during the early developmental period a few impulses coursing caudally to reach trunk or neck motoneurons also reach distal flexor motoneurons.

The observations in rat and human fetus described above suggest an expansive establishment of trigeminal efferent projections throughout the spinal cord and with brainstem motor nuclei at an early stage of development. It is possible that these trigeminal efferent connections are part of an exuberant pathway that gradually receds as supraspinal and spinal motor systems develop and also as the SVN matures to establish functional differences among the different subdivisions as well as the formation of internuclear connections established between SVN and other trigeminal and brainstem nuclei.

Neck motoneurons can be recruited by trigeminal nerve activation (Manni et al., '75; Sumino and Nozaki, '77; Abrahams et al., '79). The results of this study and data presented in Chapter 4 establish an anatomical pathway whereby perioral and snout stimulation can result in each of the generalized and local behavioral responses documented in rat and human fetuses. The possibility exists for generalized and double simultaneous stimulus responses (perioral/palmer) resulting from stimulation of Vo-TS neurons subserving perioral imput which project bilaterally to the dorsal and ventral horns of RCC, CE, TC and LE segments of the spinal cord, as well as the additional input made by VL and BZ neurons to caudal cervical levels. The circuitry underlying the squinting reflex, illustrated in chapter 4, is present in the bilateral projections of Vo neurons to the facial motor nucleus.

Recent studies regarding descending systems projecting to neck motoneurons suggest that these cells are subject to several influences unique to the upper cervical cord (Wilson and Peterson, '78; Anderson et al., '71,'72) and that the structure of neck muscles displays an organization and complexity not seen in hindlimb muscles (Richmond and Abrahams, '75a). Futhermore, it is suggested that some of the mechanisms underlying the control of head movements may differ from those involved in the control of hindlimb movements. The trapezius muscle, although not considered a neck muscle (shoulder muscle), has been thought to contribute its cranial portion, clavotrapezius, to the functional support of head movements involving flexion and twisting. The motoneuronal cell pool that contains alpha motoneurons which innervate the trapezius muscle is located in the dorsolateral portion of the ventral horn (Pearson, '38; Gura and Limanskii, '77).

Ezure et al. ('78), demonstrated that monosynaptic reflexes were rarely seen in neck motoneurons and if present, only occurred if the level of spontaneous activity was high. These results suggest that with respect to monosynaptic synapses, muscle afferent projections to neck muscle motoneurons are much weaker that those found in the lumbosacral spinal cord and further suggests that segmental influences are mediated by polysynaptic connections which may involve tectospinal and reticulospinal pathways (Anderson et al., '71, '72; Abrahams and Rose, '74; Rose and Abrahams, '78). A close functional relationship has been shown to exist between the trigeminal system and the upper cervical spinal cord. Stimulation of trigeminal primary afferents have been shown (Kerr and Olafsson, '61) to excite ventral horn cells in the upper cervical spinal cord and Manni et al. ('75) and Sumino and Nozaki ('77) established the existence of the "trigemino-neck reflex" with the demonstration that neck muscle motoneurons were excited by electrical stimulation of several trigeminal primary afferents. Not only were extensor muscles of the neck shown to be influenced by stretching extraocular muscles, stimulating the medial part of the semilunar ganglion, stimulating the ophthalmic and maxillary branches of the trigeminal nerve and stimulating supraorbital and infraorbital nerves but they were also activated by such cutaneous input as pinching and rubbing the skin of the face, particularly the eyelids. Intracellular responses of biventer cervicis-complexus, splenius and trapezius motoneurons have been shown following stimulation of the infraorbital nerve, which has its receptors in the nose, and supraorbital nerve that receives sensory input from the forehead (Rose and Sprott, '79). Infraorbital nerve stimulation elicited a powerful excitation bilaterally of biventer cervicis-complexus and splenius motoneurons and either initially

ex
an
mo
ne
inh
inh
tra
sti
mo
stir
the
wou
hav
the
'61).
neck
leve
stim
(Fall
large
conv
demo
anato
degre
motor
media
in the

excited or inhibited trapezius motoneurons. Biventer cervicis-complexus and splenius motoneurons bilaterally were excited while trapezius motoneurons were inhibited by ipsilateral stimulation of the supraorbital nerve. Stimulation of the contralateral supraorbital nerve induced inhibitory responses in biventer cervicis-complexus motoneurons, inhibition and excitation of splenius motoneurons and excitation of trapezius motoneurons. It is thought that as a result of infraorbital nerve stimulation, the response of neck motoneurons is consistent with a movement which would raise the animal's head to perhaps avoid a stimulus received on the nose while a more complex movement of twisting the head away from the stimulus and raising the head toward the stimulus would result from stimulation of the supraorbital nerve. These movements have many similarities to suckling and orientation reflexes and have led to the suggetion that SVN may be involved in such behavior (Wall and Taub, '61). It has been shown that svt is partly responsible for the generation of neck movements (Sumino and Nozaki, '77) since after sectioning svt at the level of the obex abolished the response of neck muscle motoneurons to stimulation of the ipsilateral infraorbital nerve. Earlier studies in our lab (Falls, '83, 84b; Falls et al.'90) have demonstrated axonal trajectories of large spinally projecting VL neurons in svt. Although pathways which convey trigeminal input to neck muscle motoneurons have been demonstrated (Ruggierio et al., '81; Schenigaga, '88), the present study anatomically demonstrates a possible trigeminspinal pathway with a high degree of morphological detail. Vo-TS projections to upper cervical motoneurons are potentially supported through Vo projections to the medial cerebellar nucleus (MED; discussed in Chapt 2). Neurons situated in the rostroventral portion of Dieters' (lateral vestibular) nucleus which

pro

hea

dor

act

'74

late

MEI

tran

MEI

dorso

were

super

the ce

here

innerv

caudo

observ

project

sparsel

for furth

providir

respons

(cerebell

the head

Sor

brain cer

spinothala

project to the cervicothoracic region are frequently activated by ipsilateral head tilt and inhibited by head tilt to the opposite side, while neurons in the dorsocaudal part of the nucleus, which project to lumbosacral levels, are activated in response to head tilt in either direction (Peterson, '70; Precht, '74). Cerebellar projections to the rostroventral (forelimb) region of the lateral vestibular nucleus have been shown to originate from contralateral MED (Brodal, '74), discussed in Chapt 2, (Figs. 4, 5:B, C). Retrograde transport techniques have been used (Beitz, '82) to determine the origin of MED efferent connections. Large cells of the rostral portion and dorsolateral protuberance and small cells of the caudomedial subdivision were labeled contralateral to HRP injections made in the lateral and superior vestibular nuclei. Ipsilateral labeling was found in cells located in the central and ventrolateral part of MED. DM neurons, which are shown here to project to caudal levels of the lumbar cord, are illustrated to innervate contralateral MED (Chapter 2). They terminate in the caudomedial portion and dorsolateral protuberance while some are observed to reach the rostral portion of the nucleus. Contralateral projections provided by VL and BZ neurons are either non-existent or sparsely limited to the centromedial portion. This additional data suggests for further support for a possible indirect pathway utilized by Vo neurons in providing for a syncronous performance of head movements or postural responses consistent with the activities of other systems (cerebellovestibular, vestibulospinal) with regard to the relative position of the head in space.

Somatosensory information is relayed from the spinal cord to higher brain centers via four major routes: dorsal column-medial lemniscal, spinothalamic, spinoreticulothalamic and spinocervicothalamic pathways.

The spinothalamic tract, thought to play an important role in pain transmission (Kuru, '49; Morin et al., '51; Yoss, '53; White and Sweet, '55; Noordenbos and Wall, '76), has been shown to have most (94%) of its cells inhibited by noxious pinch or heat applied to the tail, contralateral hindlimb, trunk, forelimbs or face (Gerhart et al., '81). Inhibitory mechanisms impacting on spinothalamic tract neurons in rat is thought to be the result of diffuse noxious inhibitory controls (LeBars et al., '79a,b). This mechanism for inhibitory control operates through dorsal horn interneurons which possess widespread cutaneous inhibitory receptive fields which require noxious mechanical, thermal or transcutaneous electrical stimulation to produce inhibition. Following upper cervical spinal cord transection in monkeys a background of inhibition persists and does not require a supraspinal loop. (Gerhart et al., '81) However, the inhibitory effects from noxious stimulation of the face were no longer seen. Therefore, the partial participation of supraspinal pathways can not be completely ruled out. Another study (Wilcox et al., '80) has shown that, in monkey, some neurons in nucleus raphe magnus are excited following stimulation of the upper and lower extremities as well as the tail and face. Stimulation of nucleus raphe magnus cells produces a powerful inhibition of spinothalamic tract cells (Willis et al., '77; McCreery et al., '79; Gerhart et al., '81). Potential pathways exist from the nucleus raphe magnus and other brainstem pathways,i.e., trigeminal, that participate in the inhibition of spinothalamic tract cells. The underlying neural mechanism of inhibition caused by noxious cutaneous stimulation may be involved in acupuncture, trans-cutaneous nerve stimulation and some forms of manual medicine i.e., counterpressure and myofascial release techniques. It is thought that the existence of inhibitory receptive fields may also be

imp
from
of th
rece
'81).
could
path
over
activ

and
electr
onto
possib
cardio
and cu
angina
Descer
swallo
recept
phreni

important in coding stimulus location and intensity so that noxious input from one part of the body can inhibit spinothalamic tract cells in other parts of the body to enhance the signal at thalamic and other higher order cells receiving convergent input from spinothalamic tract cells (Gerhart et al., '81). The possible role of Vo-TS descending projections to the dorsal horn could be inhibitory or excitatory feedback onto other somatosensory spinal pathways so that trigeminal neural activity in the thalamus is emphasized over the projections from other ascending systems that are simultaneously activated by a peripheral stimulus.

Spinothalamic tract cells have been shown to receive both somatic and visceral input (Blair et al., '81; Ammons et al., '85). These electrophysiological studies have described afferent input from the heart onto thoracic spinothalamic tract cells of anesthetized monkeys. It is possible that the convergence of visceral input from the heart and cardiopulmonary region with somatic input from the left chest and arm and cutaneous input from Vo provide a neural basis for the referred pain of angina pectoris which is often discribed to radiate to the neck and jaw. Descending Vo-TS projections to ventral horn may also play a role in reflex swallowing mechanisms since its conceivable that sensory stimulation of receptors in the oral cavity during swallowing would reflexively inhibit phrenic and intercostal activity through trigeminospinal connections.

Figure 1

rat trige

(A) dors

subdivis

Figure 1: Schematic drawings of representative coronal sections through rat trigeminal nucleus oralis (Vo) illustrating three injections made into (A) dorsomedial (DM), (B) ventrolateral (VL) and (C) border zone (BZ) subdivisions. svt, spinal trigeminal tract; VII, facial motor nucleus.

Figure
L injec
site si
zones
in VL
An inj
extens
tract;

Figure 2: Low power photomicrographs (A-C) showing the location of PHA-L injection sites in each of the three subdivisions of rat Vo. A. An Injection site situated in the middle portion of DM partially filling dorsal and ventral zones with slight spread into dorsal BZ (Case 734). B. An injection located in VL with a small extension into the ventral portion of BZ (Case 866). C. An injection site positioned within the middle two-thirds of BZ with partial extension into the dorsal portion of VL (Case 750). svt, spinal trigeminal tract; VII facial motor nucleus.

FIGURE 2

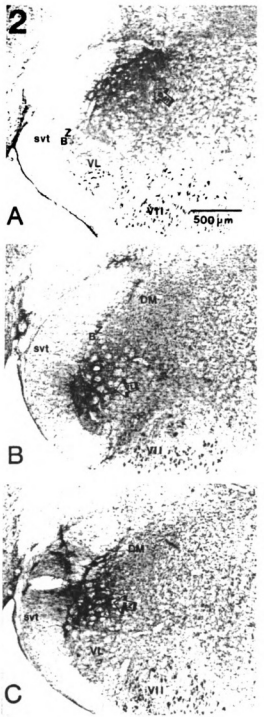

Figu
the l
A-D.
the
illust
from

Figure 3: A composite of low power photomicrographs (A-L) illustrating the location of PHA-L injection sites for supporting experiments in rat Vo.. A-D. Inection sites from four experiments illustrating deposits of PHA-L in the DM subdivision. E-H. Injection sites from four experiments illustrating deposits of PHA-L in the VL subdivision. I-L. Injection sites from four experiments illustrating deposits of PHA-L in the BZ subdivision.

FIGURE 3

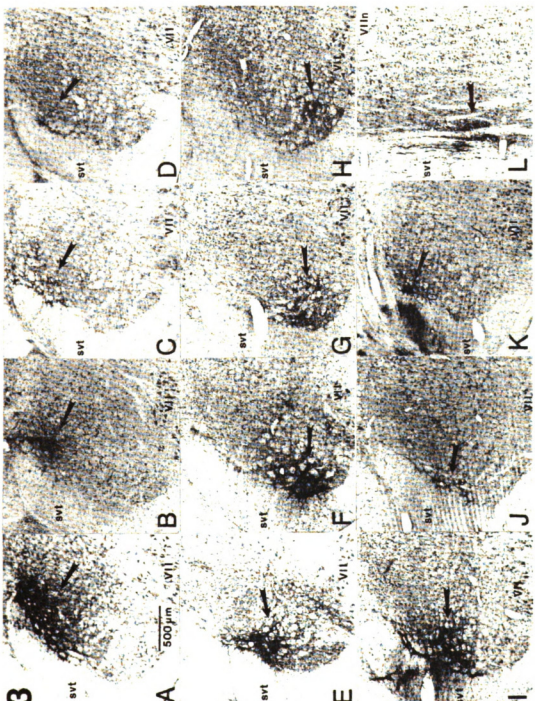

Figur

sectio

Lower

E. L

patter

Figure 4: Camera lucida drawing illustrating representative transverse sections through the rat spinal cord. A. Upper rostral cervical cord. B. Lower rostral cervical cord. C. Cervical enlargement. D. Thoracic cord. E. Lumbar enlargement. Drawings in A-F illustrating Rexed's ('54) pattern of lamination in the spinal cord as it applies to the rat.

FIGURE 4

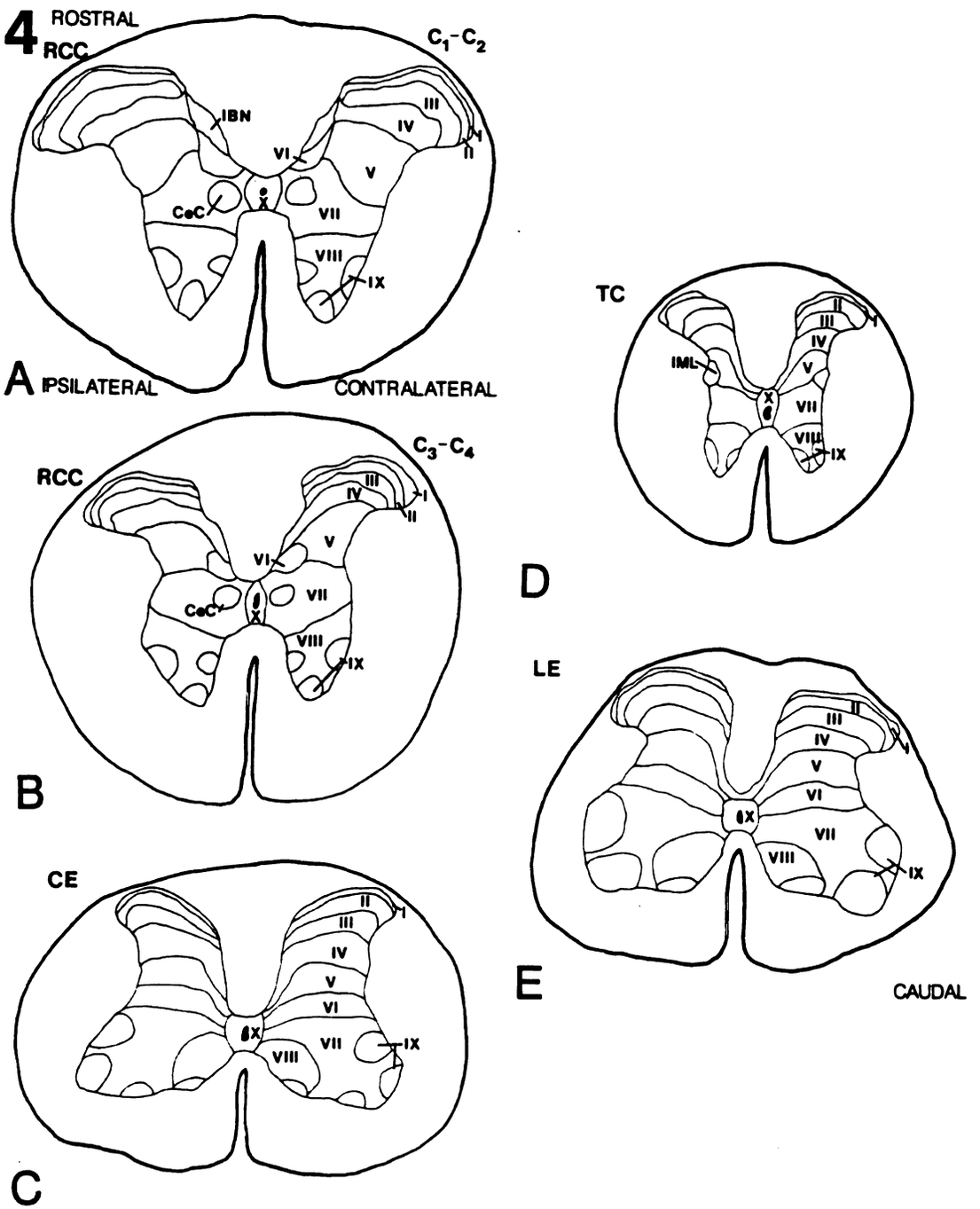
4
ROSTRAL
RCC
C1-C2
IBN
III
IV
VI
II
V
CoC
VII
VIII
IX
A
IPSILATERAL
CONTRALATERAL
C3-C4
RCC
III
IV
I
II
V
VI
CoC
VII
X
VIII
IX
B
CE
II
III
IV
V
VI
X
VII
IX
VIII
C
TC
II
III
IV
IML
V
X
VII
VIII
IX
D
LE
II
III
IV
V
VI
X
VII
VIII
IX
E
CAUDAL

Figure 5: Camera lucida drawings illustrating representative coronal and transverse sections through the rat pons (A), medulla (B), and spinal cord (C-F). Drawing (A), a coronal hemisection through Vo, illustrates the DM injection site. Drawings (B-F) illustrate the distribution and relative density of anterogradely labeled fibers and terminal arborizations. Numerous axons form dense terminal plexuses primarily in the ventral and ventrolateral portions of nucleus cuneatus (Cu) and nucleus gracilis (Gr) bilaterally throughout rostrocaudal sections (1-3). Labeled terminal arborizations were also observed bilaterally in the rostral cervical cord (RCC), cervical enlargement (CE), thoracic cord (TC) and lumbar enlargement (LE). In RCC, the greatest density of labeling was in the medial two-thirds of the dorsal horn laminae II-VI and medially in ventral horn laminae VIII-IX with an ipsilateral predominance. The density of labeled terminal strands decreased in more caudal sections with a similar pattern of topographical termination. Approximate anterior/posterior (AP) levels shown in (B1-3) utilize the coordinates of Paxinos and Watson ('86). svt, spinal trigeminal tract; MDH, medullary dorsal horn; Vi, trigeminal nucleus interpolaris. The magnification scale indicated in C is the same for schematics D and F.

FIGURE 5

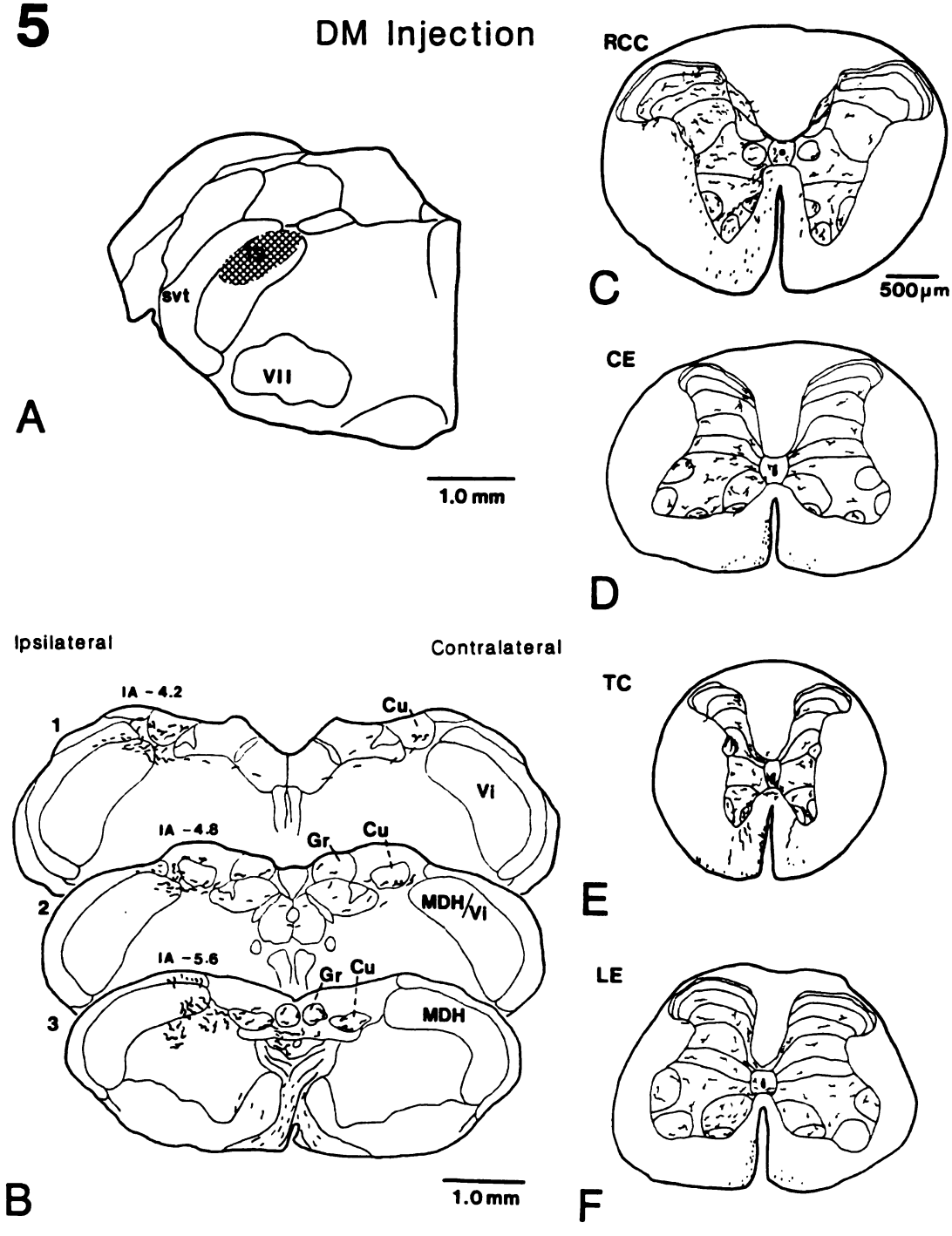
5
DM Injection
svt
VII
A
1.0 mm
RCC
C
500µm
CE
D
Ipsilateral
Contralateral
IA - 4.2
1
Cu
VI
IA - 4.8
Gr
Cu
2
MDH/VI
IA - 5.6
Gr
Cu
3
MDH
B
1.0mm
TC
E
LE
F

Figu
trans
(C-F
injec
densi
collec
ventr
arbor
sectio
bilate
the l
media
labele
patter
were l
the sa

Figure 6: Camera lucida drawings illustrating representative coronal and transverse sections through the rat pons (A), medulla (B), and spinal cord (C-F). Drawing (A), a coronal hemisection through Vo, illustrates the VL injection site. Drawings (B-F) illustrate the distribution and relative density of anterogradely labeled fibers and terminal arborizations. Sparse collections of axonal terminal plexuses were found in the ventral and ventrolateral portions of Cu and Gr ipsilaterally with labeled terminal arbors found throughout rostrocaudal Cu sections and limited to rostral Gr sections (B1-3). Labeled terminal arborizations were also observed bilaterally in RCC and CE. In RCC, the greatest density of labeling was in the lateral two-thirds of dorsal horn laminae II-VI ipsilaterally and medially in ventral horn laminae VIII-IX bilaterally. The density of labeled terminal strands decreased in more caudal sections with a similar pattern of topographical termination Most labeled terminal arborizations were limited to the ventral horn. The magnification scale indicated in C is the same for the schematic in D.

FIGURE 6

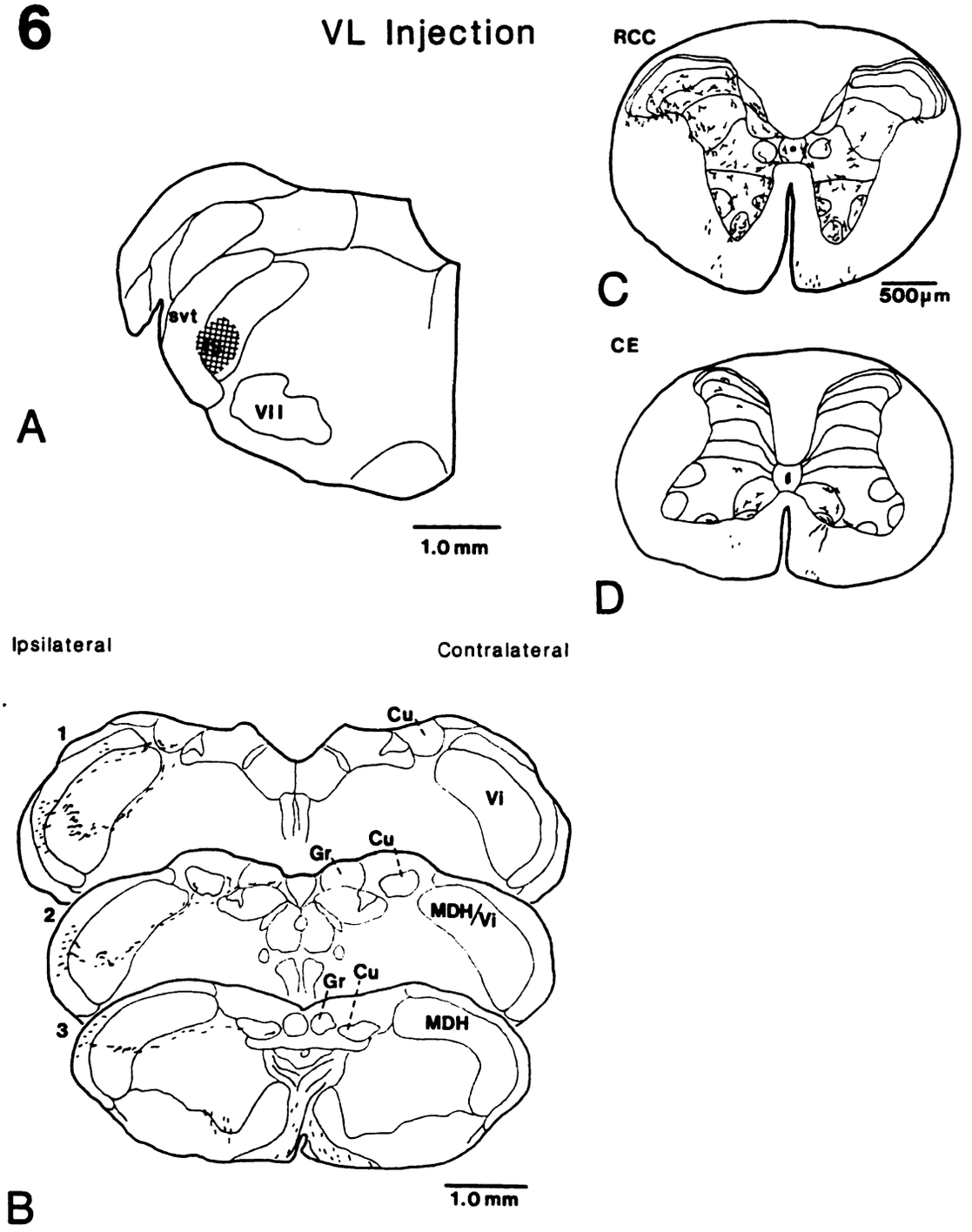
6
VL Injection
svt
VII
A
1.0 mm
RCC
C
500µm
CE
D
Ipsilateral
Contralateral
1
2
3
Cu
Vi
Gr
Cu
MDH/Vi
Gr
Cu
MDH
B
1.0 mm

Figu
tran
(C-F
injec
dens
Colle
and
Spar
RCC
were
bilat
densi
simil
termi
scale

Figure 7: Camera lucida drawings illustrating representative coronal and transverse sections through the rat pons (A), medulla (B), and spinal cord (C-F). Drawing (A), a coronal hemisection through Vo, illustrates the BZ injection site. Drawings (B-F) illustrate the distribution and relative density of anterogradely labeled fibers and terminal arborizations. Collections of axonal terminal plexuses were found primarily in the ventral and ventrolateral portions of rostral sections of Cu ipsilaterally (B1-3). Sparsely labeled terminal arborizations were also observed bilaterally in RCC and CE of the spinal cord. In RCC, labeled terminal arborizations were found in the central portions of dorsal horn laminae V and VII bilaterally and were diffusely scattered in the ventral horn bilaterally. The density of labeled terminal strands persists in more caudal sections with a similar pattern of topographical termination, although most labeled terminal arborization were limited to the ventral horn. The magnification scale indicated in C is the same for the schematic in D.

FIGURE 7

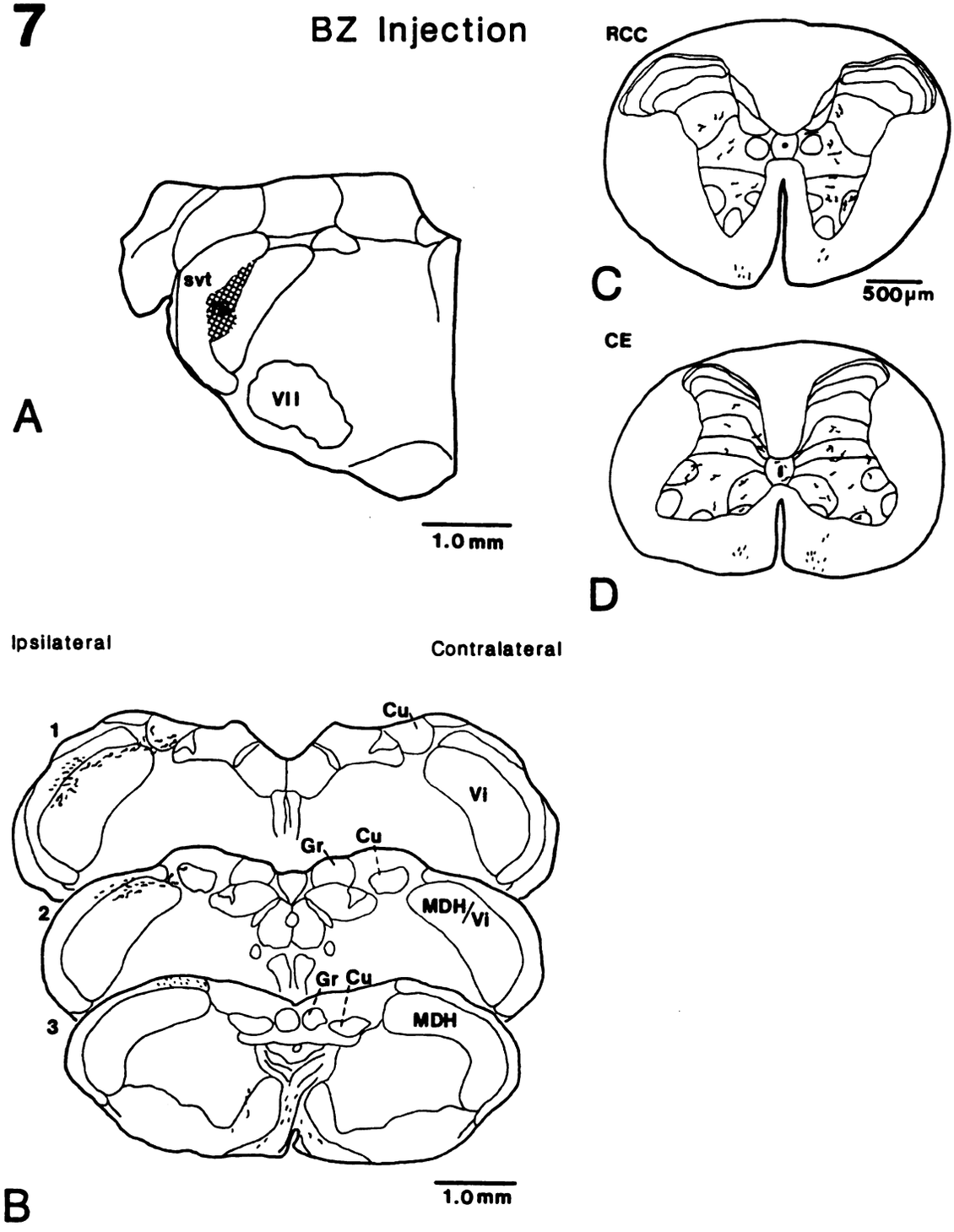
7
BZ Injection
RCC
svt
VII
A
1.0 mm
C
500µm
CE
D
Ipsilateral
Contralateral
1
Cu
Vi
Gr
Cu
2
MDH/Vi
Gr Cu
3
MDH
B
1.0 mm

Figure 8: Camera lucida drawings illustrating representative transverse sections through RCC (C1-C4) of rat spinal cord. Drawings A1 and B1 illustrate the distribution and relative density of anterogradely labeled fibers and terminal arborizations in C1-C2 cord segments after a DM and VL injection, respectively. Drawings A2 and B2 illustrate the distribution and relative density of anterogradely labeled fibers and terminal arborizations in C3-C4 cord segments after a DM and VL injection, respectively. In A1, numerous axons form dense terminal plexuses ipsilaterally in the medial two-thirds of the dorsal horn; while in B1, dense plexuses of labeled terminal arbors are found predominately in the lateral two-thirds of the dorsal horn. The density of labeling decreases significantly in C3-C4 cord segments. In A2 and B2, collections of anterogradely labeled terminal arbors are found, in greatest density, medially in the ventral horn laminae VIII-IX with an ipsilateral predominance. The density of labeled terminal strands decreases in more caudal sections A2 and B2 with a similar pattern of topographical termination except that an ipsilateral predominance was found following both injections. The magnification scale indicated in A is the same for schematics A2-B2.

FIGURE 8

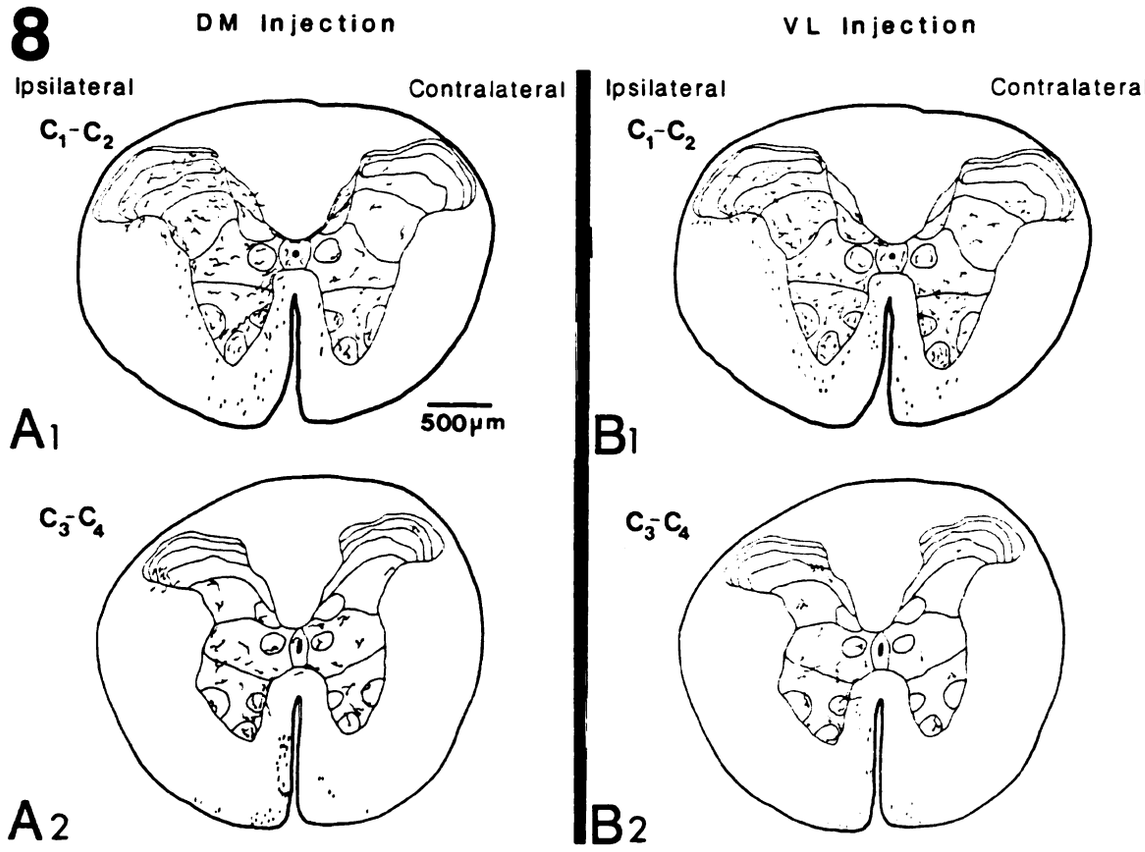
8
DM Injection
VL Injection
Ipsilateral
Contralateral
Ipsilateral
Contralateral
C1-C2
C1-C2
500µm
A1
B1
C3-C4
C3-C4
A2
B2

Figure 9: A: Camera lucida drawing of a transverse section through rostral Cu illustrating the single type of Vo efferent terminal arborization found throughout rostrocaudal levels of the dorsal column nuclei. B: This single type of efferent has a terminal arborization characterized by a thin terminal strand (ts) that terminates in widely spaced boutons (b) en passant. A terminal bouton caps the side branches emanating from the terminal strand.

FIGURE 9

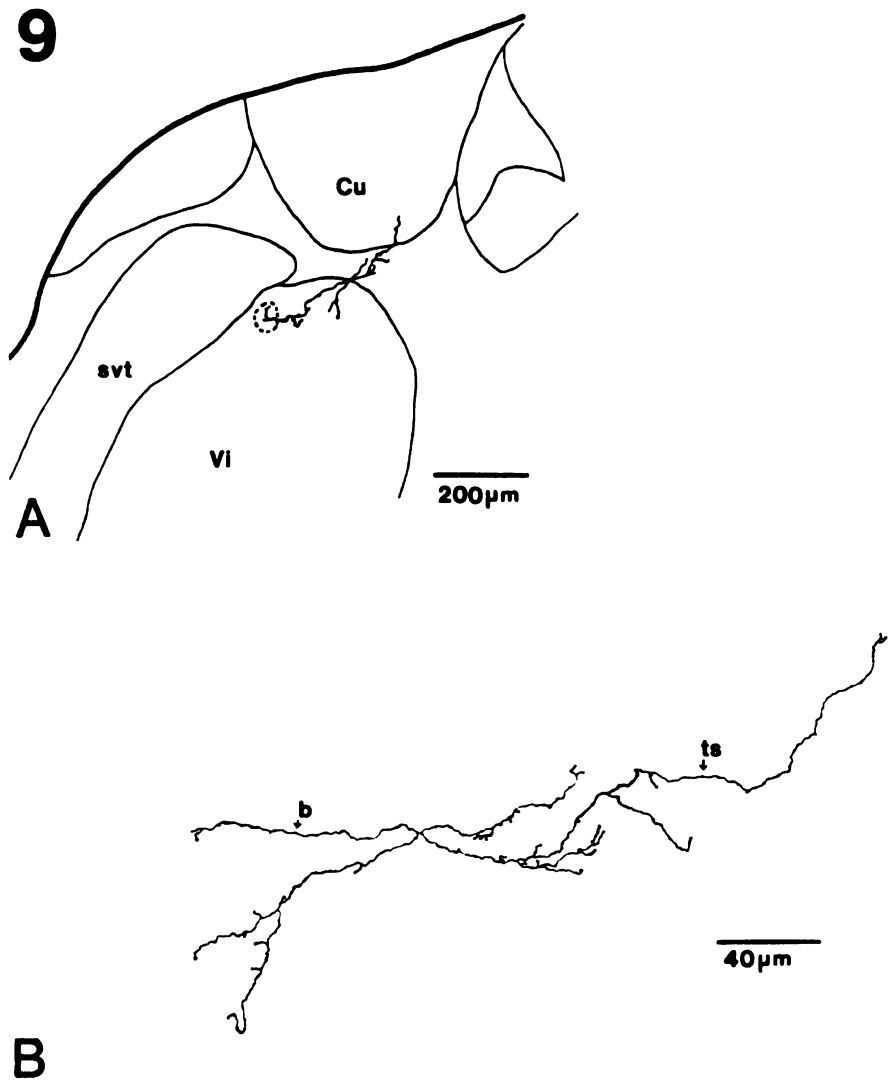

Fig
me
eff
B:
dia
cap

Figure 10: A: Camera lucida drawing of a transverse section through the medial portion of the dorsal horn in RCC illustrating a Type 1 Vo-TS labeled efferent terminal arborization which arises from the dorsal funiculus (dfu). B: Type 1 Vo-TS terminal arborizations are characterized by long thin diameter terminal strands (ts) that give rise to only a few side branches capped by terminal boutons (b).

FIGURE 10

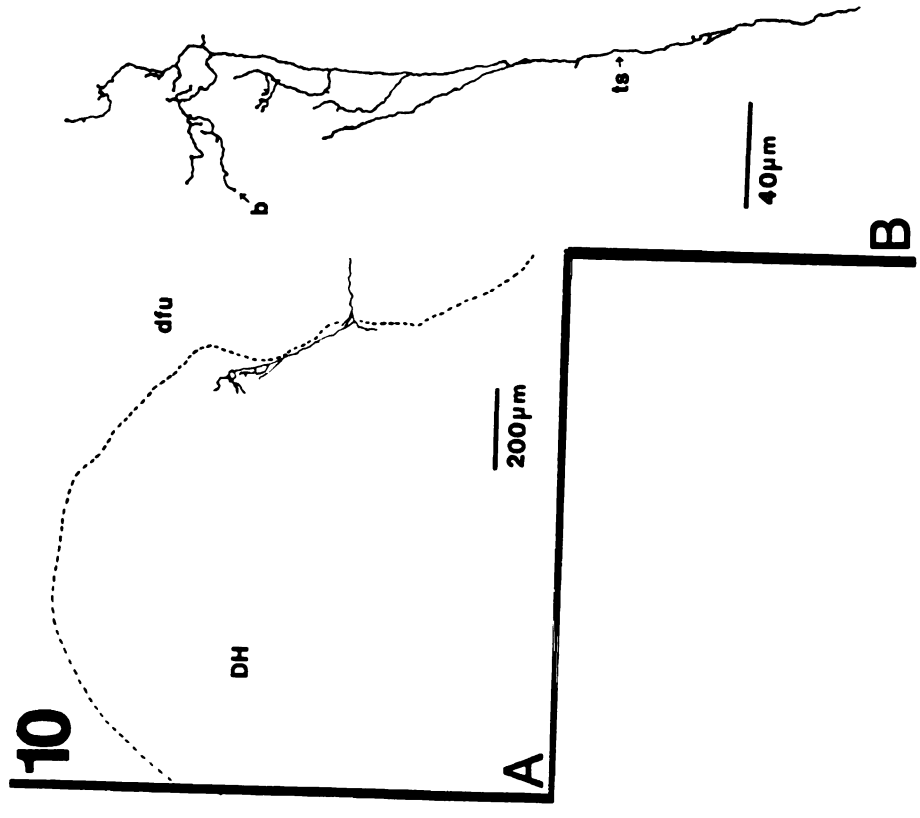

Figure 11: A: Camera lucida drawing of a transverse section through LE illustrating Type 2 Vo-TS labeled efferent terminal arborization which arises from the ventral funiculus (vfu). B: Type 2 Vo-TS terminal arborizations are characterized by medium diameter bouton bearing terminal strands (ts) that course for varying lengths and occassionally giving rise to secondary side branches capped by bulbous end boutons (b).

FIGURE 11

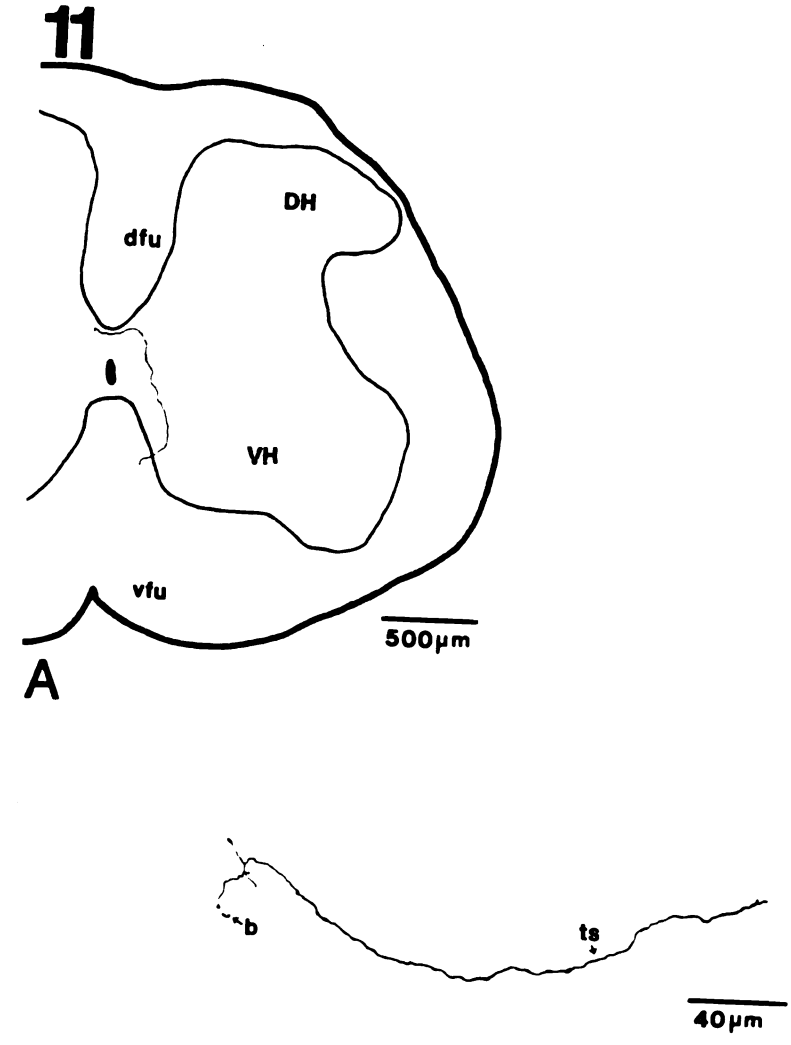

Figure 12: A: Camera lucida drawing of a transverse section through CE illustrating a Type 3 Vo-TS labeled efferent terminal arborization which arises from vfu. B: Type 3 Vo-TS terminal arborizations are characterized by large diameter terminal strands (ts) which course long distances often giving rise to secondary and tertiary side branches ending in globular shaped end boutons (b).

FIGURE 12

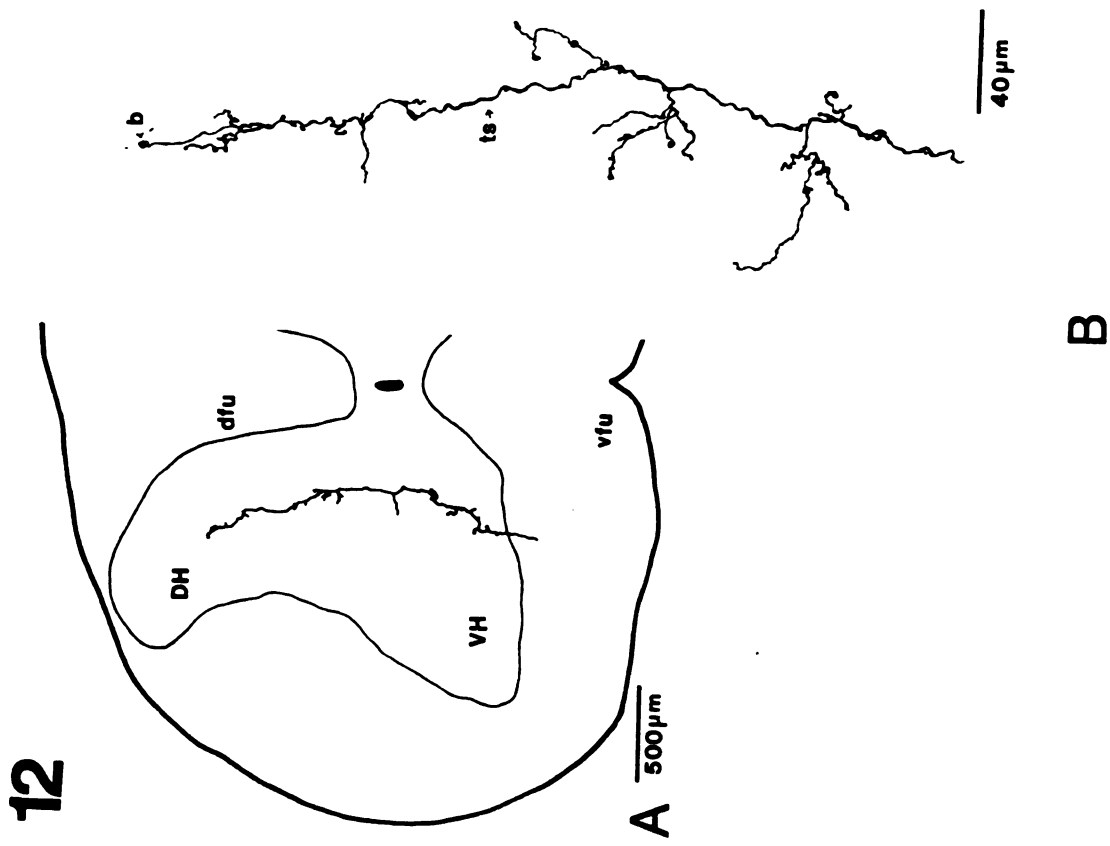

Figure 13: A: Camera lucida drawing of a transverse section through CE illustrating a Type 1 Vo-TS labeled efferent terminal arborization which arises from rosrtocaudal oriented axonal bundles in the dorsal horn. B: Type 1 Vo-TS terminal arborizations are characterized by long thin diameter terminal strands (ts) that give rise to few side branches. The terminal strand is characterizedby several boutons en passant and the side branches are capped by terminal boutons (b).

FIGURE 13

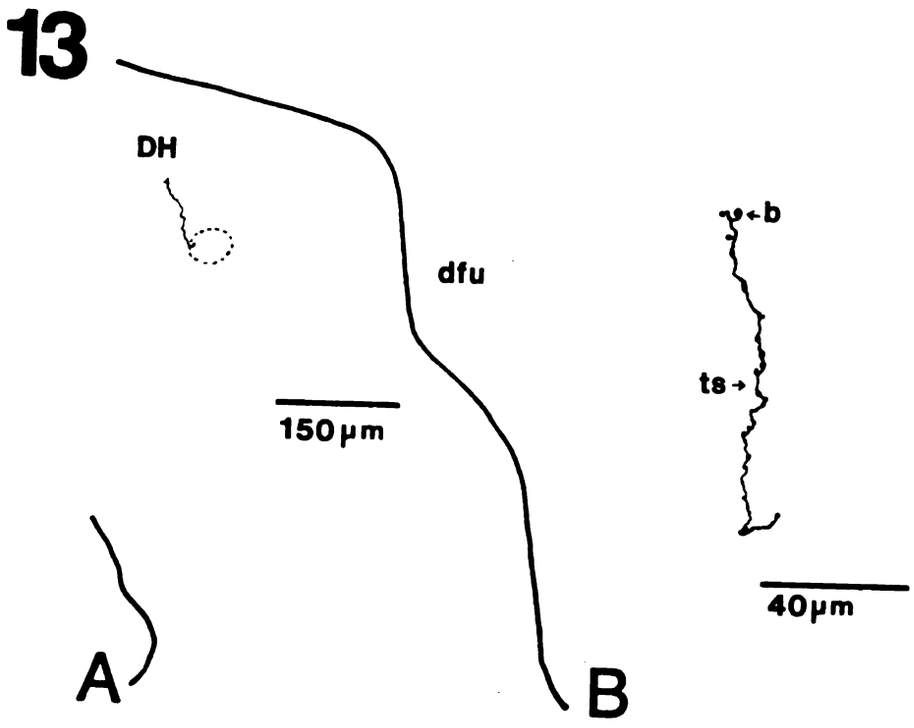

Figure 14: Representative drawings of Type 1 Vo efferent terminal axonal arborizations located in laminae of the dorsal horn and ventral horn. Type 1 is characterized by a thin terminal strand (ts) that terminates in widely spaced boutons (b) en passant. A terminal bouton caps the side branches emanating from the terminal strand.

FIGURE 14

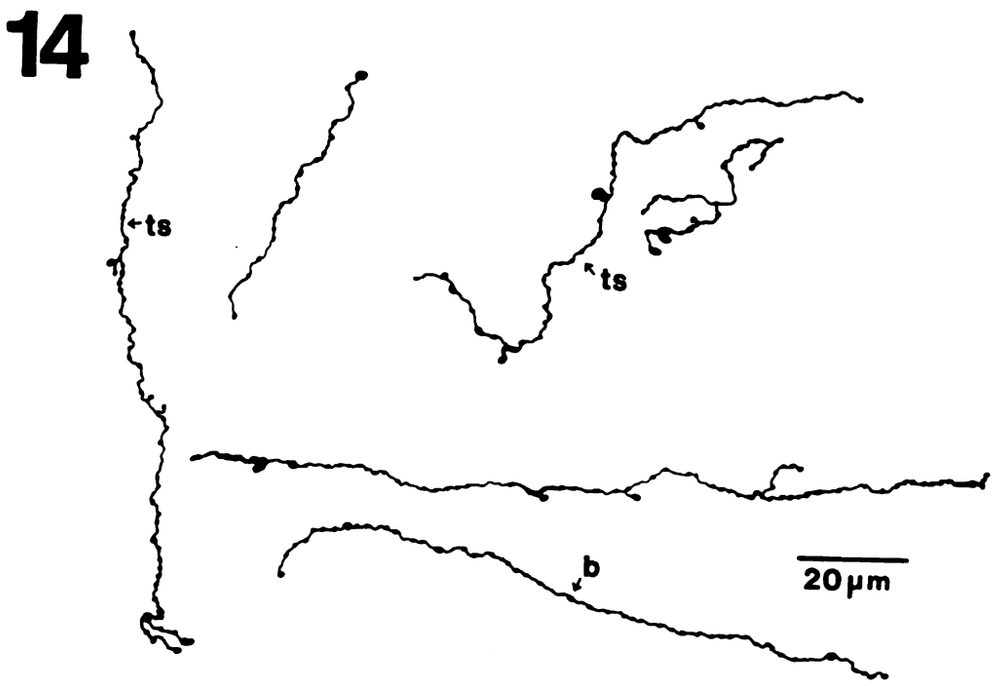

Figure 15: Representative drawings of Type 2 Vo efferent terminal axonal arborizations located in laminae of the dorsal horn and ventral horn. Type 2 Vo-TS terminal arborizations are characterized by medium diameter terminal strands (ts) that course for varying lengths and occassionally giving rise to secondary side-branches capped by bulbous end boutons (b).

Figure 16: Representative drawings of Type 3 Vo efferent terminal axonal arborizations located in laminae of the dorsal horn and ventral horn. Type 3 Vo-TS terminal arborizations are characterized by large diameter terminal strands (ts) which course long distances often giving rise to secondary and tertiary side branches ending in irregularly shaped end boutons (b).

FIGURE 16

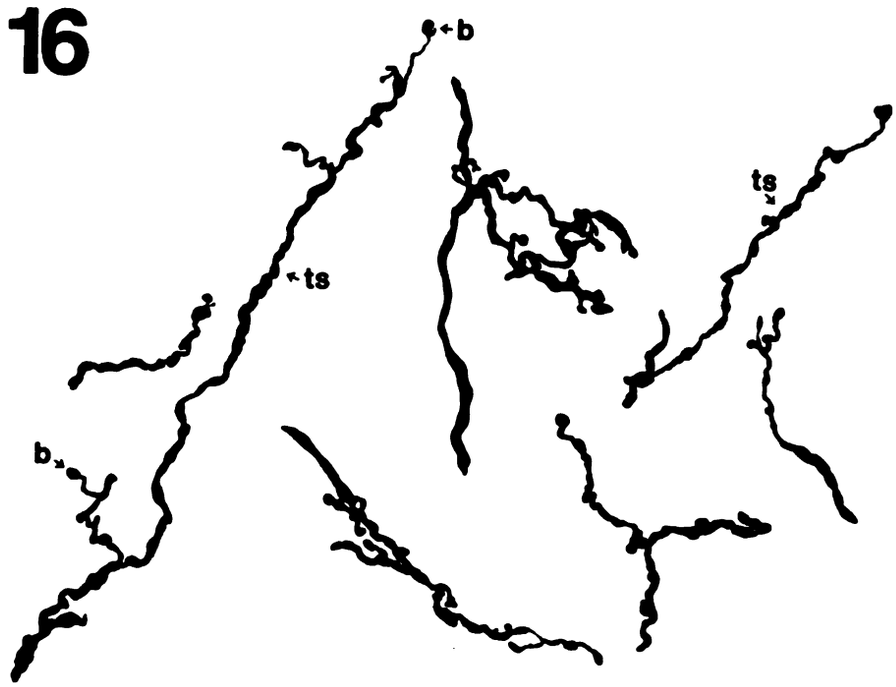

Figure 17: Photomicrographs that document the morphological characteristics of each type of Vo efferents found in the dorsal column nuclei and spinal cord. A-B: Representative trajectory of Vo-TS fiber tracts coursing from vfu toward the medial aspect of the ventral horn. C-D: Course and morphology of Vo-TS efferent terminal arbors in close approximation to lateral cervical nucleus neurons. E: The type of morphologically distinct terminal strand (ts) found in Cu. F: One type of terminal strand (ts), Type 2 Vo-TS found in the central cervical nucleus. G: A Type 1 Vo-TS terminal strand (ts) found in the intermediate basilar nucleus. The magnification scale indicated in D is the same for photomicrographs E and F.

FIGURE 17

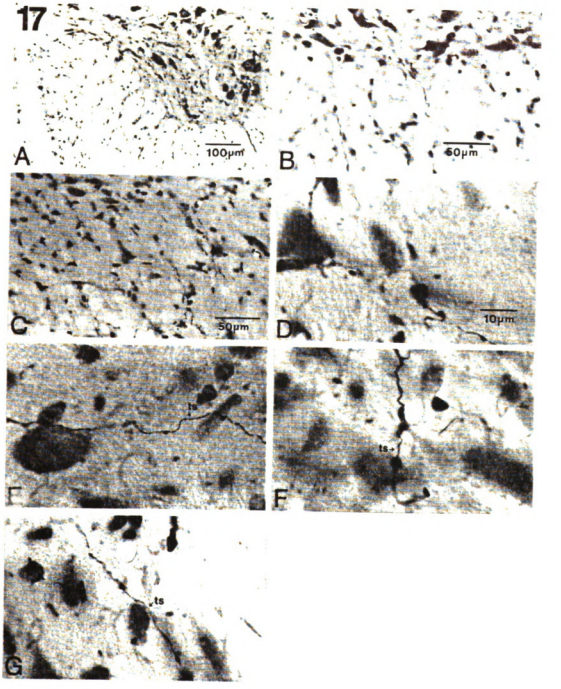

Figure 18: Photomicrographs that document the morphological characteristics of each type of Vo efferents found in various regions of the spinal cord. A-F: Types of morphologically distinct Vo-TS efferent terminal arbors found in spinal cord dorsal and ventral horns. A-B: Type 1 Vo-TS efferent. C-D: Type 2 Vo-TS efferent. E-F: Type 3 Vo-TS efferent. The magnification indicated in D is the same for photomicrographs E and F.

FIGURE 18

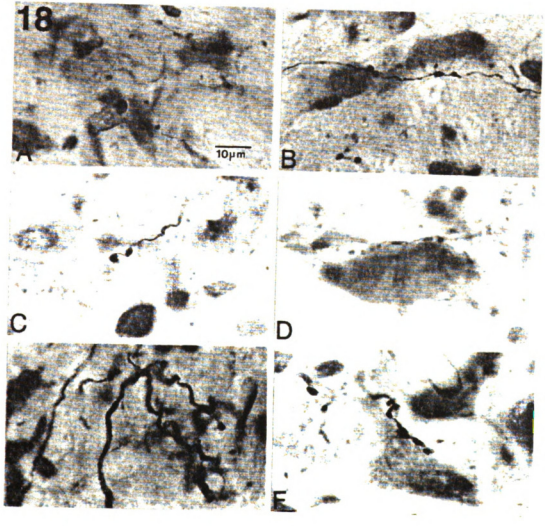

CHAPTER II

TOPOGRAPHICAL ORGANIZATION AND MORPHOLOGY OF TRIGEMINOCEREBELLAR PROJECTIONS FROM IDENTIFIED SUBDIVISIONAL AREAS WITHIN RAT TRIGEMINAL NUCLEUS ORALIS UTILIZING THE PHA-L ANTEROGRADE TECHNIQUE

INTRODUCTION

Anatomical studies (Falls, '83, '84, '86; Falls et al.,'85; and Falls and Alban, '86) and electrophysiological investigations (Hayashi, '82) have provided experimental evidence that each subdivision of rat trigeminal nucleus oralis (Vo), receives morphologically and functionally distinct groups of primary and non-primary afferent axons, conveying orofacial tactile information, which are positioned to directly influence the activity of different groups of second-order projection neurons. These second-order cells provide the efferent outflow from each Vo subdivision and affect synaptic activity at numerous locations along the neuraxis including the ventral posterior medial (VPM) nucleus of the thalamus (Burton and Craig, '79; Carpenter and Hanna, '61; Dunn and Matzke, '67; Fukushima and Kerr, '79; Erzurumlu et al., '80; Matsushita et al., '82; Shigenaga et al., '83; Silverman and Kruger, '85; Bruce et al., '87; and Smith and Falls, '90), the trigeminal, facial and hypoglossal motor nuclei (Carpenter and Hanna, ' 61; Dubner et al., '78; Erzurumlu and Killackey, ' 79; Greenwood and Sessle, '76; Ramon y Cajal, '09; Sessle and Kenny, '73; and Smith and Falls, '90), the superior colliculus (Huerta et al., '83; and Killackey and

Erzurumlu, '81), the spinal cord (Falls, '83; Matsushita et al., '81; Matsushita et al., '82; Ruggiero et al., '81; and Smith and Falls, '88), and the cerebellum (Falls and Van Wagner, '84, '85; Huerta et al., '83; Mantle-St. John and Tracey, '87; Matsushita et al., '82; and Smith and Falls, '90).

Previous anatomical studies utilizing retrograde transport of horseradish peroxidase (HRP) have identified the neurons of origin of direct trigeminocerebellar projections in cat (Ikeda, '79; Somana et al., '80; and Matsushita et al., '82), mouse (Steindler, '77), rat (Watson and Switzer, '78; Huerta et al., '83; and Falls and Van Wagner, '84, '85), sheep (Saigal et al., '80), and tree shrew (Patrick and Haines, '82). Until recently, most projections, in the rat, to the orofacial tactile areas of crura I and II, the paramedian lobule (PML), and the uvula have been shown to originate from neurons in ipsilateral trigeminal nucleus interpolaris (Vi) and the main sensory nucleus (Vms), with a small contingent of projections from a few scattered cells located in contralateral Vi and Vms. In addition, Vo has been shown to provide some input to orofacial portions of these four areas (Watson and Switzer, '78; and Huerta et al., '83). Recent studies utilizing retrograde HRP (Falls and Van Wagner, '84, Falls et al., '85) suggest that rat Vo trigeminocerebellar projections (Figure 1) are more substantial and more complex than originally thought and that they primarily originate from neurons located in dorsomedial (DM) and border zone (BZ) subdivisions of Vo.

Several lines of experimentation have focused on the role that orofacial mechanoceptive (tactile) information plays in the function of the cerebellar cortex (CC). Electrophysiological studies in rat have shown that four major areas of the cerebellar hemispheres and vermis contain highly organized yet fractured tactile maps of the body surface within the granule

cell layer (GCL) (Joseph et al., '78; Shambes et al., '78a,b; Kassel, '80; Bower et al., '81; and Woolston et al., '81). Tactile representation areas are located in Crus Ia-Ic, Crus IIa-IIb, PML of the cerebellar hemisphere, and a small region of the uvula (lobule 9) of the vermis. A major portion of each of these areas in Crus I, PML and uvula is related to the ipsilateral head and face, while a greater part of the tactile representation area in Crus II is devoted to the ipsilateral oral cavity.

The orofacial tactile portions of rat crura I and II as well as PML have been shown to receive convergent tactile inputs from the somatosensory (SI) cortex (Bower et al., '81), superior colliculus (Kassel, '80), inferior olivary nucleus (Brown, '80; Armstrong et al., '82; and Huerta et al., '83), and trigeminal sensory nuclei (Watson and Switzer, '78; Shambes et al., '78a,b; Huerta et al., '83; and Falls and Van Wagner, '84, '85). Trigeminal sensory nuclei have also been shown to provide a major portion of the tactile input to the orofacial portion of the uvula (Joseph et al., '78; Watson and Switzer, 78; and Falls and Van Wagner, '84, Falls et al. '85).

Electrophysiological studies in rat (Josephs et al., '78; and Shambes et al., '78a,b) suggest a patch theory of well defined, patch-like, spatial patterns of orofacial tactile projections for axons terminating in GCL of Crus I, Crus II, PML and the uvula. An anatomical study employing the Golgi method and examining the sagittal organization of mossy fiber (MF) terminals in rat cerebellum (Scheibel, '77), suggests a zone theory of patterns of mossy fiber (MF) terminations in discrete longitudinal strips. Many retrograde (Walberg and Brodal, '79; Brodal, '80; Brodal and Kawamura, '80 and Walberg, '80) and anterograde studies (Groenewegen

et al., '77 and Groenewegen et al., '79) support a zonal configuration of olivocerebellar projections to CC.

These separate and distinct (patch vs. zone) configurations may not be necessarily exclusive patterns with respect to the manner in which the mammalian cerebellum is compartmentalized by incoming afferents. A major question to be investigated in this study is the manner in which tactile orofacial information, originating from discrete recipient areas of Vo which receive different types of primary input, is organized within the present concepts of zonal and patch theories of mossy fiber input into the cerebellar cortex. The anterograde Phaseolus vulgaris leucoagglutinin (PHA-L) technique allows for the comparison of projections from different neuronal populations which have been identified previously using retrograde transport methods (Falls et al., '85; Falls and Alban, '86; and Falls, '87). This technique permits close examination and comparison of the distribution, relative densities and morphological features of Vo trigeminocerebellar axons terminating in the four major orofacial tactile areas of CC as well as in the deep cerebellar nuclei (dCN) following injections of PHA-L into each of the three Vo subdivisions. A preliminary report of these findings has been published elsewhere (Smith and Falls, '90).

METHODS

Unilateral deposits of PHA-L were made iontophoretically under stereotaxic guidance into each Vo subdivision; DM (cases 734, 741, 824 and 840), VL (Cases 739, 751, 825, and 860) and BZ (Cases 750, 753 and 826). The choice of the injection sites was based on the results of previous anterograde PHA-L studies (Smith and Falls, '90) of Vo efferents utilizing coordinates obtained from the stereotaxic atlas of Paxinos and Watson ('86). Details concerning anesthesia, surgical procedure and injections have been described previously (Chapter 1). All animals were housed, prepared for surgery and cared for postoperatively according to NIH prescribed guidlines (NIH Guide, '85). After 10-14 days survival each animal was deeply anesthetized and perfused according to a modification of the pH-shift method of Berod et al. ('81). The cerebellum was immediately removed, blocked and stored in fresh fixative at 4°C. Later, the cerebellum blocks were sectioned serially at 20-30 um thick sagittal, horizontal or transverse sections on an Oxford vibratome. For the visualization of PHA-L reaction product the sections were incubated 48 hours in antibodies against PHA-L (1:2000) and processed using the Vectastain kit (Vector Laboratories) according to the method of (Hsu et al. ('81). The sections were processed in a solution of 0.05% 3,3' diaminobenzadine or DAB (Sigma) in Tris buffer (0.05 M, pH 7.6) for 60 minutes, rinsed mounted onto gelatin-coated slides, stained with cresyl violet and coverslipped for light microscopic analysis. Detailed light microscopic evaluation of each section was undertaken in order to determine the overall course, distribution, organization and morphology of efferent axons and their terminal arbors originating from neurons in each Vo subdivision. For data presentation, the course,

distribution and density of labeled Vo axons were illustrated in schematic drawings using an Aus Jena documator at a magnification of 17.5X onto which drawings of parent fibers and terminal arbors were positioned utilizing a 2.5X objective lens attached to a Leitz Laborlux 12 microscope fitted to a drawing tube at a magnification of 31X. The morphological features of parent axons and their terminal arborizations were illustrated using a 100X oil immersion objective lens at a magnification of 1,250X. Photomicrographs of corresponding sections were taken to illustrate morphological details. All composite drawings, Figures 4-9, illustrate the course, distribution and density of labeled Vo efferent axons and terminal arborizations encountered in fifteen consecutive sagittal sections through six specifically identified areas, some which contained dCN, identified in Figure 3, all spanning the vermal, paravermal and lateral zones of the cerebellum.

RESULTS

INJECTION SITES

Deposits of PHA-L were localized to discrete areas within each of the three subdivisions of rat Vo (Figure 2). Only areas containing densely filled neurons were considered to be effective zones from which efferent projections originated. PHA-L deposits which sparsely labeled neurons at the injection sites often resulted in weak anterograde label. In two cases (734, 840) a total of two PHA-L labeled cells were located two or more millimeters from the central zone of the injection site. The possibility exists that these cells were labeled as a result of retrograde lectin transport. In several cases (824, 826 and 750) PHA-L diffused into the spinal V tract (svt). In these instances injections labeled numerous svt axons as far caudal as the medullary dorsal horn (MDH) and served to indicate that PHA-L was subject to uptake and transport by at least some fibers of passage. The potential problems of retrograde transport and transport of PHA-L by fibers of passage as reported earlier by Cliffer and Giesler ('88) and Schofield ('90) probably did not influence the results of this study since cases of PHA-L deposition without spread into svt yielded the same results and only two retrogradely labeled cells have been seen from a total of eleven experimental cases. Labeling of parent axons and terminal arborizations in the cerebellum following Vo-PHA-L injections would not involve the main axons of trigeminocerebellar projection neurons in more caudal brainstem areas, eg. Vi and MDH, since most of the axons do not course through Vo as they ascend to the cerebellum. In this study all eleven experiments resulted in injections of PHA-L largely restricted to either DM, VL, or BZ. Of the brains examined, six (cases 741, 824, 751, 825, 750, and 826) were chosen for detailed analysis of trigeminocerebellar projections (Figures 4-

9). at levels indicated in Figure 3. Three of these (cases 741, 751, and 750) were used to illustrate representative injection sites (Figure 2). The DM injection site (Figure 2A) was situated in middle DM and partially filled its dorsal and ventral zones. This injection site measured 390 um rostrocaudally, 250 um dorsoventrally and 500 um mediolaterally. The VL injection site (Figure 2B) was approximately two-thirds the distance along the rostrocaudal length of Vo. It measured 570 um rostrocaudally, 520 um dorsoventrally, and 480 um mediolaterally. The BZ injection site (Figure 2C) was located in the dorsal two-thirds of the subdivision with some spread into dorsal VL. The injection site was midway along the rostrocaudal extent of Vo and extended 1080 um rostrocaudally, 700 um dorsoventrally, and 300 um mediolaterally.

OVERALL DISTRIBUTION OF PHA-L LABELED Vo TRIGEMINOCEREBELLAR AXONS

Based on the results of these experiments, trigeminal efferents were observed to distribute to the cerebellum in a pattern which is illustrated in the composite drawings for all subdivisional injections in Figure 4-9. In each case, labeled Vo parent fibers were observed to course rostrally from Vo at the level of mid-facial nucleus, enter and course in the ventrolateral portion of the ipsilateral inferior cerebellar peduncle (icp) and terminate in either ipsilateral CC and dCN or decussate in the cerebellum and enter contralateral CC and dCN. Ascending efferent axons from neurons in each Vo subdivision resulted in anterograde labeling in specific areas of crura I and II, PML and uvula.

Following DM injections, numerous axons formed dense terminal arborizations in ipsilateral vermis with the density of labeled arborizations

decreasing in Crus I, Crus II and PML, as well as simplex lobule (SIM). Labeled efferent fibers were also observed in dCN (Figure 4; A-F). Slightly fewer fibers terminated in these same areas contralaterally (Figure 5; A-F).

Injections into VL resulted in labeling of terminal arbors ipsilaterally in vermis, Crus I, Crus II, PML, SIM and dCN (Figure 6; A-F). Very few labeled terminal arborizations were found contralaterally (Figure 7; A-F). The densities of the arbors appeared to be less than those observed following DM injections for ipsilateral Crus I and Crus II and were of greatest concentration at locations in the more lateral portion of the cerebellum (compare Figure 4 with Figure 6).

Following an injection contained within the middle one-third of BZ along its dorsoventral axis of Vo only a few scattered fibers were observed in CC bilaterally and no labeling was observed in dCN. However, BZ injections with slight spread into VL, labeled efferent axons that were distributed throughout the cerebellum ipsilaterally in a pattern showing relatively greater labeling in sections from the lateral half of CC. This was similar to that found following a VL injection except that the total density of labeled fibers was far less (Figure 8; A-F). The density and general pattern of distribution of labeled terminal arbors in ipsilateral dCN was comparable in density to that found following a VL injection. Terminal arborizations were only observed posteriorly in the middle one-third of the contralateral cerebellar hemisphere (Figure 9; A-F).

DIFFERENTIAL PROJECTIONS TO THE VERMIS

Following DM, VL, and BZ injections, parent fibers coursed through icp and bifurcated at or medial to the level of the medial cerebellar (MED)

nucleus into many ascending branches which coursed medially to enter the ten lobules of the vermis (vermal zone) bilaterally.

Deposits of PHA-L in DM resulted in terminal arborizations found throughout the mediolateral extent of the ten lobules of the ipsilateral vermis, (Figures 4; A-C) with the exception of lobule 4 (Figure 4 B). The greatest density of terminal labeling was observed medially in lobules 9 and 10, the uvula and nodule respectively. The greatest density of contralateral labeling was observed medially in the vermis (Figures 5; A-C), particularly in posterior lobules 6-10.

Figures 6 and 7 illustrate efferent axons labeled by an injection in VL. A sparser projection in comparison to that reported for DM was observed bilaterally with the greatest density of labeling located in the lateral one-half of ipsilateral CC. In the ipsilateral vermis (Figures 6; A-C) labeled fibers were found in lobules 3-5 and lobules 7-9. In the contralateral cerebellum (Figures 7; A-C) only a few labeled fibers arborized in vermal lobules 4, 6 and 7.

Following a BZ injection, with some spread into VL, a few labeled efferents were found predominately positioned in ipsilateral CC. Medially, terminal sites included lobules 5-7 and lobule 9 (Figure 8; A-B) while at a more lateral level (Figure 8 C) projections shifted and were concentrated in the anterior one-half of the vermal lobules. This is in contrast to DM projections which arborized predominately posteriorly and VL efferents which were scattered through anterior and posterior halves.

Labeled Vo trigeminocerebellar efferents to ipsilateral folium 9a are densest following DM injections. The pattern in which DM and VL efferents projected onto folium 9a and 9b was distinct with very little overlap of terminal arbors from neurons in the two subdivisions. DM terminal

arbors were predominately located in the most medial portion of folium 9a and b (Figure 4; A-B). Terminal arbors were observed in lobule 9 at the most lateral extent in the vermal cortex (Figure 4 C). VL terminal arbors, in their greatest density, were restricted to medial aspects of folium 9a, in the folial crown and were not observed to extend farther laterally (Figure 6; A-B). There were no projections to folium 9b. Only sparse BZ terminal arborizations were distributed to folium 9a along its medial extent (Figure 8 B).

Labeled efferents were observed to distribute in lesser density in contralateral folium 9a than in folium 9b and in greater density in more lateral sections (Figure 5; A-C) following DM injections. No labeled efferent fibers were seen contralaterally following VL and BZ injections (Figures 7,9; A-C).

DIFFERENTIAL PROJECTIONS TO SIM

Parent axons of DM, VL and BZ neurons were observed to exit the icp and either course rostrally in the ipsilateral cerebellar hemisphere or decussate at the levels of the interposed (INT) and lateral (LAT) nuclei and course laterally to terminate in the contralateral hemisphere.

Labeled Vo trigeminocerebellar efferents to ipsilateral SIM were densest in the lateralmost portion, lateral zone, following VL injections while fewer fibers labeled by DM injections were positioned in the medialmost portion, paravermal zone. Only a few scattered fibers were found after BZ injections (Figures 4,6,8; D-F). Contralateral Vo projections for the most part were only observed to arise from DM neurons. The pattern in which neurons located in each of the three subdivisions projected onto SIM was distinct with very little overlap of terminal arbors from the

different subdivisions. DM terminal arbors in ipsilateral SIM were located predominately in SIMa at the level of INT and at the level of LAT (paravermal and lateral zones, respectively). At the most lateral levels (Figure 4 F), very few labeled terminal arbors were observed in SIM. VL terminal arbors were confined to the lateral zone in SIM in approximately equal number in SIMa and SIMb (Figure 5E). Axons of BZ neurons gave rise to a few terminal arborizations in SIM situated in the lateral zone (Figure 7E).

An efferent projection of similar density to that found ipsilaterally was observed to originate from DM neurons and to terminate in contralateral SIM. However, the pattern in which labeled fibers distributed in contralateral SIM was different compared to the pattern found ipsilaterally. Efferent fibers were observed to terminate predominately in SIMb in the paravermal and lateral zones with only a few labeled terminal arborizations located at the most lateral extreme of the lateral zone (Figure 5 F). No substantial Vo projection was found to contralateral SIM from VL and BZ neurons.

DIFFERENTIAL PROJECTIONS TO CRUS I

Labeled parent axons coursed through ipsilateral icp from DM, VL and BZ to either course dorsally toward the ipsilateral LAT or decussate at the level of LAT and run toward contralateral LAT. Labeled fibers ran dorsolaterally in the white matter of the ansiform lobule in the lateral one-half of the cerebellar hemispheres bilaterally to enter Crus I medially at the level of INT (Figures 4-7 D). Fibers also entered Crus Ia-Ic at the level of and more lateral to LAT (Figures 4-9; E-F).

Following DM injections labeled terminal arbors were found in the lateral zone in ipsilateral Crus Ia and Ib at the level of LAT and most laterally were restricted to Crus Ia (Figures 4; D-F). Terminal arbors of parent fibers labeled following VL injections were observed in ipsilateral Crus Ia and Ic in the lateral zone only (Figure 6; D-F). Following BZ injections, the density of labeling was greater in ipsilateral Crus Ia and extended laterally throughout the lateral zone. The pattern of terminal labeling in contralateral Crus I following DM injections was observed both in the paravermal and lateral zones in Crus Ib and Ic (Figure 5; D-F). At the most medial levels, terminal arbors were localized in the folial wall of Crus I. Laterally, labeled fibers were observed to terminate predominately in the folial crown of Crus Ib, with a few terminal arborizations in Crus Ic. No Vo trigeminocerebellar axons (Figures 7,9; D-F) were observed in contralateral Crus I following VL and BZ injections.

Although labeled Vo efferents were found most medially in contralateral Crus I following DM injections, terminal arborizations from labeled efferents were not observed in the medial portions of ipsilateral Crus I from neurons in any of the three Vo subdivisions (Figures 4-6,8; D-F). DM and BZ efferent terminal arborizations extended further laterally in Crus I than VL efferent terminal arbors. The pattern of projection for BZ terminal arborizations was similar to that of DM terminal arbors in that the greatest density of labeling was in Crus Ia.

DIFFERENTIAL PROJECTIONS TO CRUS II

The trajectory of parent fibers to Crus II followed the same route to the cerebellar hemispheres as did those described for Crus I following injections into DM, VL and BZ. At the LAT level, parent axons exited

ipsilateral icp and either ascended to ipsilateral Crus II or decussated and coursed through the cerebellar white matter toward contralateral Crus II.

Trigeminocerebellar efferent projections were observed throughout the mediolateral extent of ipsilateral Crus II in both paravermal and lateral zones following DM and VL injections, and only a sparse projection was observed after BZ injections in the paravermal zone (Figures 4,6,8; D-F). Although the labeled parent axons and terminal arbors were observed bilaterally in Crus II following DM and VL injections, the densest projection was always ipsilateral (Figures 4-9; D-E).

Following DM injections labeled terminal arborizations were found at the most medial extent of ipsilateral Crus II in the paravermal zone. Labeled axons coursed laterally in Crus II with the greatest density of labeled terminal arbors located in Crus IIb in the lateral zone and were observed to extend more laterally in Crus IIb than axons from VL and BZ subdivisions (Figures 4,,6,8; D-F). No substantial number of labeled efferent fibers were observed in ipsilateral Crus IIa in the lateral zone (Figure 4; D-E). Labeled efferents following VL injections terminated along the mediolateral axis of ipsilateral Crus II. However, the density was much less than that observed following a DM injection. At lateral levels fibers were observed in both Crus IIa and Crus IIb with a greater density of projections in Crus IIa (Figure 6 E). Aside from finding a few labeled terminal arborizations in ipsilateral Crus II in the paravermal zone, trigeminocerebellar axons arising from BZ neurons did not project substantially to Crus II ipsilaterally.

The pattern of distribution for labeled arbors originating from DM neurons in contralateral Crus II was observed in the paravermal zone and extended laterally to the lateral zone where terminal arbors were observed

in Crus IIa and IIb. The density of labeled Vo efferents was approximately the same as that observed ipsilaterally. Scattered labeled terminal arbors were found in contralateral Crus II in the paravermal zone following VL injections (Figure 7 D). Injections made into BZ did not label mossy fibers in contralateral Crus II.

DIFFERENTIAL PROJECTIONS TO PML

In the lateral one-half of the ipsilateral cerebellum, parent axons of DM, VL and BZ neurons were observed to exit icp and either course caudally in the ipsilateral cerebellar hemisphere or decussate at the LAT level and course medially and laterally to terminate caudally in the contralateral hemisphere.

Trigeminocerebellar efferent terminal arbors were found in ipsilateral PML in both the paravermal and lateral zones following injections in all three Vo subdivisions (Figures 4,6,8; D-F). Labeled terminal arborizations were observed to be concentrated principally in the ventral portions of PML in the lateral zone. Terminal arborizations were observed to be oriented in different planes and were found in approximately equal density in ipsilateral PML following DM and VL injections. Labeled terminal arbors were sparse following BZ injections and were located medially in ipsilateral PML in both the paravermal and lateral zones.

Although the labeled parent axons and terminal arbors were observed bilaterally following DM injections, the densest projection was always ipsilateral (Figures 4; D-F). No significant Vo projections were observed from VL or BZ neurons to contralateral PML.

In summary, the above results from multiple injections in each Vo subdivision suggest that there may be a more precise arrangement of Vo

efferents originating from specific regions of each subdivision. Further studies utilizing different, more precise techniques are needed to more fully characterize regional subpopulation differences in Vo trigeminocerebellar projections.

TERMINAL ARBORIZATIONS TO THE GRANULE CELL LAYER

Individual sprays of MF's were observed (Figure 14 A) to emerge from labeled axons in the white matter of single folia and terminate in each of three major types in the GCL of the vermis, SIM, Crus I, Crus II and PML The first type, GCL-Simple, was found throughout the mediolateral extent of the cerebellum bilaterally following injections made in each Vo subdivision and was found to course in all directions within GCL. Following DM injections, GCL-Simple terminal arbors were observed in higher frequency than after VL and BZ injections. Thin (0.8-1.3 um in diameter) relatively unbranched terminal strands characterized this first type of terminal arbor (Axons 1-2, Figures 10,14B). Widely spaced boutons 1.2-1.5 um in diameter were found along the strands which terminated in bulbous fusiform-shaped end boutons ranging in size from 4.0-5.0 um to 5.0-6.0 um in diameter. A few finger-like projections, terminating in a swelling, emanated from the end boutons. The second type of GCL-MF terminal arbor, GCL-Complex, was observed more medially and was primarily positioned in the posterior one-half of the cerebellum (lobules 6-10) with the highest density occurring in the vermis following a DM injection. GCL-Complex terminal arbors were only occasionally observed following VL injections and were limited to medial portions of the posterior one-half of the cerebellar hemisphere. No GCL-Complex MF's were found following BZ injections. The GCL-Complex terminal arbor (Axons 3-4,

Figures 10,14C) is characterized by massive irregularly shaped boutons (5.0 X 6.0 to 6.0 X 8.0 um in diameter) from which twisted and angular appendages ensue. These boutons may be seen along the course of the terminal strands and as end boutons (Figures 10,14C). The terminal strand is thicker in diameter in comparison to GCL-Simple (1.3-2.0 um in diameter) and is generally unbranched (Figures 10,14C). The third type of GCL-MF terminal arborization, GCL-Filamentous, is primarily localized within the medial portion of the posterior one-half of the cerebellum and is observed to originate predominately from DM neurons. The GCL-Filamentous MF's course through deep portions of GCL and terminate in the outer one-third of this layer beneath the Purkinje cell layer (PCL) (Axon 5, Figures 10,14D). Thick terminal strands (1.3-2.0 um in diameter) similar in diameter to those of GCL-Complex MF's are characterized by several multi-shaped boutons en passant and side branches terminating in an irregularly-shaped boutons. In addition, the terminal strands usually terminate in an elongated irregularly-shaped end bouton which emit several recurving thin bouton bearing filamentous processes which closely approximate Purkinje cell somata. Often times these end boutons have internal open areas surrounded by bouton cytoplasm.

TERMINAL ARBORIZATIONS IN THE PURKINJE CELL LAYER

Labeled terminal arborizations were also found within PCL predominately following DM injections. These terminal arbors were found bilaterally with an ipsilateral predominance, and many of them were located in posterior lobules of the vermis. Many of the terminal arborizations in PCL resembled MF's (Figure 11). The first type, PCL-Simple, (Axons 1-2, Figures 11,14; E) was less complex in structure than

the second type and was characterized by thin terminal strands (0.5-0.8 um in diameter) which traversed the border between GCL and PCL to terminate in either several short side branches capped by an end bouton (1.5-2.0 um in diameter) or as a single bouton bearing branch (Figures 11,14; F) measuring 2.0-2.5 um in diameter. The second type, PCL-Complex, (Figure 11) can be characterized as being morphologically similar to the GCL-Filamentous terminal arborization except that they occurred in PCL. These arborizations had several recurving filamentous processes arising from the elongated terminal expansion (Axons 3-4, Figures 11,14; E) which extended well into PCL. These processes were thin and twisting and terminated in a spherical knob.

TERMINAL ARBORIZATIONS IN THE DEEP CEREBELLAR NUCLEI

A single population of PHA-L labeled Vo axons and terminal arborizations were found bilaterally in dCN after DM and VL injections and ipsilaterally after BZ injections with the densest labeling of Vo axons observed after DM injections. The terminal arborizations were more prominent ipsilaterally than contralaterally. Following DM injections the densest population of terminal arbors was found bilaterally in MED (i.e., fastigial nucleus) with less dense labeling in INT and LAT (i.e., dentate nucleus). Following VL and BZ injections the majority of labeled efferent fibers were found more laterally in the INT and LAT. The density of labeled terminal arbors decreased greatly in the contralateral cerebellum for all three dCN (Figures 5,7,9; B-E). Single collateral terminal strands branched from parent MF's (1.3-2.0 um in diameter) as they coursed through dCN on their way to CC (Axon 1, Figures 12,14; G). Single terminal strands measured approximately 0.3-0.5 um in diameter and were characterized by

widely spaced boutons en passant (0.5-1.0 um in diameter). The terminal strands usually issued several bouton bearing side branches of varying lengths capped by an end bouton (0.8-1.3 um in diameter) (Figures 12,14; H).

DISCUSSION

This study demonstrates the unique and differential contribution that each Vo subdivision makes with respect to direct projections to orofacial tactile portions of rat CC. The results extend previous findings to indicate that neurons projecting to orofacial portions of each of these tactile areas are more widespread throughout Vo than previously described (Falls et al., '85; and Falls and Alban, '86). Not only are they found in DM and dorsal one-half of BZ, but they are also located in VL and ventral BZ. Furthermore, Vo MF efferents distribute tactile input to the cerebellum in a manner which suggests both a patch-like organization as well as a zonal pattern. Lastly, trigeminocerebellar projections to dCN have been described anatomically for cat and monkey (Carpenter and Hanna, '61; and Somana et al., '80) and show that INT is the main recipient for axons originating from the spinal trigeminal nucleus (SVN). A projection to cat INT has also been demonstrated in physiological studies (Cody and Richardson, '78b; and Richardson et al., '78). Our data is the first to demonstrate the morphology of terminal arborizations of trigeminocerebellar efferents within INT as well as in MED and LAT. Taken together, these findings indicate that the rat Vo trigeminocerebellar projection is more substantial and more highly organized than previously defined and by virtue of its distribution must play an important role in conveying orofacial tactile information to the cerebellum for sensorimotor processing.

Methodological Considerations

Although the uptake of PHA-L was originally shown (Gerfen and Sawchenko, '84; and Wouterlood and Groenewegen, '85) to be restricted to

cell bodies and dendrites at the injection site, recent studies indicate that the lectin may be taken up by axons within the spinal cord (Lee, '87), or within svt or icp (Schofield, '90). Although Schofield reported that MF's were labeled after injections placed in icp, other sources of MF input (reticulocerebellar, cuneocerebellar) may have contributed to his finding. Transport of PHA-L by fibers of passage is not likely to account for the present findings since PHA-L injections, with spread into svt failed to result in any distribution pattern different from deposits restricted to subdivisional boundaries. In addition, injections which failed to label cells in the Vo neuropil failed to produce anterograde labeling in Vo target nuclei.

The effective injection site allowing for anterograde transport was restricted to localized areas of cells filled with PHA-L within Vo subdivisions. In most instances, in this study, it was possible to limit the uptake of PHA-L to cells situated within the myelo- and cytoarchitectonically defined DM and VL subdivisions (Falls, '83; '84a-c; Falls et al., '85). However, deposits of PHA-L restricted to cells comprising BZ could seldom be achieved without slight spread of reaction product into DM and VL. This was apparently due to the narrow width of BZ and the fact that injections could not be contained within such a small area. Target regions along the neuraxis, which have been shown in retrograde tracing studies to receive Vo efferents, i.e., cerebellum, cranial nerve nuclei and spinal cord (Falls, '85; Falls, '86; Erzurumlu and killackey, '79; Ruggiero et al., '81; Falls, '83) exhibited a comparable density of anterograde labeling after discretely placed injections within Vo subdivisions. Projections with only weakly retrogradely labeled cells in Vo after partial and large VPM injections (Kruger et al., '77) have been shown to be more robust (Smith and

Falls, '90) than previously described which is attributed to a more intense uptake of PHA-L by neuronal cell bodies.

The fact that the PHA-L method permitted a more detailed examination of trigeminocerebellar efferent projections which had been recognized but went uncharacterized by investigators (Chan-Palay and Palay, '77), reflects the significant advantage of the PHA-L method over other anterograde techniques in its ability to demonstrate morphological features associated with terminal axonal arborizations at the light microscopic level (Gerfen and Sawchenko, '84; Wouterlood and Groenewegen, '85). In addition, a number of efferent projections from Vo which have previously been unreported in the rat eg., PCL and dCN were observed in this study. However, the possibility that labeled terminal arbors could result from PHA-L uptake by fibers of passage in Vo target sites for which previously existing data were incomplete, e.g., dCN, can only be revealed by the unequivocal demonstration of Vo terminations onto target cells with electron microscopic verification.

PHA-L injections in DM, VL, and BZ required that the micropipette be lowered through either SIM or the junction between SIM and Crus I when the angle of entry was limited to 90° with respect to the brain surface. Several of the cases in this study had evidence of necrotic neuropil destruction in the medial and middle portions of Crus I which sometimes included Crus II. Thus, the characterization of Vo projections to Crus I and Crus II in this study was based on cases in which necrotic destruction was minimal or analysis was limited to the pattern of terminal labeling in lateral areas of Crus I and Crus II and represents, at least, a modest reflection of the extent and density of Vo efferents to these orofacial tactile areas. For the purpose of a more complete evaluation of the distribution of

Vo trigeminocerebellar projections to Crus I and Crus II in the future, different angles of micropipette placement must be considered.

SOMATOTOPIC ARRANGEMENT OF TRIGEMINOCEREBELLAR EFFERENTS

Electrophysiological studies in cat, recording climbing fiber responses following natural mechanical stimulation, have revealed the existence of functionally defined parasagittal zones (zone configuration) primarily in vermal cortex (Robertson, '84; Robertson et al., '82; Robertson, '85; Rushmer, '80) as well as the coexistence of a patch-like representation (patch configuration) of various body surfaces. Functional studies in monkeys have also shown that there is some evidence for a dual representation of parasagittal zones (zone configuration) and patch-like organization (patch configuration) in a discrete portion of the intermediate zone in lobule 5 (Robertson and Laxer, '81). Patch configuration electrophysiological studies in rat (Josephs et al., '78; and Shambes et al., '78a,b) suggest well defined, patch-like, spatial patterns of orofacial tactile projections for MF terminations in the GCL of Crus I, Crus II, PML and uvula. Conversely, a zone configuration has been proposed in an anatomical study which demonstrates a sagittal organization of MF terminals in rat cerebellum (Scheibel, '77) with terminal endings organized in discrete longitudinal strips. Trigeminocerebellar axons from DM, VL, and BZ neurons terminate in CC in a manner which suggests a pattern closely resembling the patch-like organization of tactile representation of body parts described by Shambes et al. ('78a and b) and Joseph et al. ('78). However, the manner in which Vo-MF's terminate in CC also supports a zonal pattern of organization for trigeminocerebellar MF terminations.

Crus Ia-Ic, which have receptive fields primarily for information arising from the head and upper face, are shown here to receive efferents from specific Vo subdivisions. In the ipsilateral cerebellar hemisphere the paravermal zone of Crus Ia receives efferents predominately from cells located in BZ while the lateral zone of Crus Ia receives a majority of efferents from DM and BZ neurons. Terminal arbors were only observed in Crus Ia ipsilaterally. Crus Ib contains labeled terminal arbors predominately from axons of DM neurons bilaterally with the greatest density observed contralaterally in the medialmost portion of the lateral zone with extension to the lateralmost portion. Crus Ic receives a small trigeminocerebellar projection terminating in the medialmost portion of the lateral zone specifically from VL and BZ neurons ipsilaterally with VL neurons innervating the medialmost and BZ neurons innervating the lateralmost portions. Contralateral Crus Ic was innervated in only the medialmost portions of the lateral zone by DM neurons.

Vo trigeminocerebellar efferents terminating in Crus II are also partitioned in a specific manner. The medial and lateral portions of ipsilateral Crus IIa, within the lateral zone, receive a small input from VL neurons while labeled terminal arbors arising from DM cells are found to be the predominant efferents terminating along the mediolateral axis of ipsilateral Crus IIb. Contralateral Crus IIa and IIb at their medialmost extent received a majority of efferents from DM neurons in approximately equal density with no labeled efferents observed in the most lateral regions. A small contribution of labeled efferents from VL neurons was found situated paravermally in Crus II. Ipsilateral PML receives efferents from each of the three Vo subdivisions with the greatest contribution made by DM, followed by VL and then BZ. Labeled terminal arbors are distributed

primarily in the medialmost portion of the lateral zone. The medialmost portion of contralateral PML received a small population of labeled efferents from DM neurons and only a sparse number from BZ neurons.

Of all the regions studied the ipsilateral uvula, in the vermal zone, receives the greatest number of labeled trigeminocerebellar efferents which originate from neurons in all three Vo subdivisions with DM cells providing the densest input. The contralateral uvula also receives trigeminocerebellar efferents with most of these arising from DM neurons.

The pattern of organization of orofacial receptive fields in Crus Ia based on electrophysiological data (Shambes et al., '78a,b) suggests that a substantial amount of mystacial vibrissae input is located in patch-like complexes in this region. The medial and lateralmost portions of ipsilateral Crus Ia receives significant input as a result of a BZ injection which had some spread into dorsal portion of VL. This latter subdivision receives vibrissal primary afferent input (see below). Taken together, these findings suggest that vibrissae input comprises a major portion of the trigeminocerebellar input to the medial and lateral halves of Crus I.

A ratculus for the rat head and snout can be superimposed upon SVN which illustrates that Vo neurons are situated in such a way as to receive primary trigeminal afferent inputs in a pattern that is inverted and medially oriented (Torvik, '56; Nord, '67; Bates et al., '85; Arvidsson and Gobel, '81; Arvidsson, '82; and Erzurumlu and Killackey, '80). Because of this organization, the majority of maxillary (vibrissae) input terminates ventrolaterally in Vo while mandibular and peri- and intraoral input is predominately ending dorsomedially. The fact that neurons in dorsal VL send the major input to vibrissae specific areas of Crus I fits with the type of primary afferent information being received by these cells. The maxillary-

ophthalmic divisions of the trigeminal nerve have been shown (Arvidsson, '82; Belford and Killackey, '79) to convey sensory information from mystacial vibrissae, guard hairs and hairy skin to the ventrolateral portions of SVN. Neurons located more ventrally in VL receive periorbital input (Nord, '67). The trigeminocerebellar projection to the medial one-half of Crus Ib can also be accounted for on the basis of primary afferent specific information arriving to cells located in DM. Although a majority of vibrissae input is targeted for VL, the potential exists for some vibrissae input to be carried to ventrally situated DM neurons which are also receiving sensory information from the upper and lower lips.

Several points can be discussed concerning the pattern of Vo trigeminocerebellar input terminating in Crus II. Although Crus II has been described as receiving the majority of the peri- and intraoral tactile input, a small amount of vibrissae input is also terminating within the medial portion of Crus IIa (Shambes et al. '78b). In this study, Crus IIa contains the terminal arbors of VL neurons which are more than likely receiving vibrissae inputs. Crus IIb, which consists of tactile maps of predominately lip and incisor origin (Shambes, et al.. '78b) receives efferents from DM neurons receiving primarily peri- and intraoral primary afferent information. PML has been described to contain granule cells which respond to stimulation applied to the whole body with a predominant input coming from the snout and head (Shambes et al., '78b). This study supports these findings and shows PML to receive projections from all three Vo subdivisions with cells in DM and VL contributing the majority of Vo efferents.

Contralateral and bilateral areas of orofacial receptive fields have been reported in Crus II and PML (Shambes et al., '78b). These previous

findings are supported here for efferents arising primarily from DM neurons. It is interesting that contralateral, as well as ipsilateral, Crus I, which has has been shown by Shambes to have lip and incisor receptive fields represented medially, also has a substantial input medially from contralateral DM which has been shown to receive information from the same orofacial areas. The uvula, folium 9a of the vermis, has been described (Shambes et al., '78b) to receive a majority of its inputs ipsilaterally from neurons conveying sensory information from mystacial vibrissae and the upper lip. In the present study, sensory information received by neurons in all three Vo subdivisions, was conveyed by efferent projections to folium 9a bilaterally with the pattern made by cells located in DM being the densest.

An ipsilateral area of orofacial receptive fields (predominately gingival) has been reported for SIMb (Shambes et al., '78a). VL efferents, originating from neurons receiving predominately vibrissal and upper snout tactile information, project to ipsilateral SIMb while projections from DM neurons, which are receiving predominately intraoral and perioral tactile information, are essentially contralateral suggesting a discrete pattern of input to SIMb that is received on both sides and not solely ipsilaterally or contralaterally as indicated previously in electrophysiological studies (Shambes et al., '78a). The findings in the present study, also suggest that it is possible that more vibrissal tactile projections are received by SIMb than previously thought. According to the illustrations of Shambes et al. (78 'a) a small amount of vibrissal input is located primarily in SIMb at its medial one-half and more posterior levels. The results of this study indicate that vibrissal input may be more extensively represented in SIMb, to extend more laterally and to be

positioned more anteriorly in both a and b portions of the lobule. In addition, SIMa also receives intraoral and perioral tactile information from MF's arising from Vo.

Somatotopically arranged trigeminal input to the cerebellar hemisphere is supported by studies in Vi (Arends, '90; Cook and Falls, '90). Cook and Falls ('90) suggest that the ventrolateral magnocellular region projects in a somatotopically specific pattern similar to that seen for the VL subdivision of Vo. It may be that mosaics containing patches of tactile information are formed by efferents from similar areas i.e., VL subdivisions within Vo and Vi which receive similar sensory input, namely vibrissal. As for the zonal patterns of vermal, paravermal and lateral portions described for projections from Vo subdivisions, a similar pattern has been noted for projections from Vi (Cook and Falls, '90). As observed following Vo injections, restricted to VL, the lateral zone of the ipsilateral cerebellar hemisphere is devoid of Vi projections and the densest projections are contained within a vermal zone. Although primary trigeminal afferents were reported (Jacquin et al., '82, '83) to innervate the ipsilateral Crus I and Crus II and dentate nucleus following HRP application to the transected mandibular division of the rat trigeminal ganglion, it is not clear whether a pattern similar to the one demonstrated for DM neurons, reception area for mandibular input, was found. Future studies must be conducted since additional knowledge of the pattern of SVN trigeminocerebellar and extranuclear inputs is necessary for an accurate interpretation of the electrophysiological and anatomical evidence of the relationships existing between the somatotopically organized input and the zonal pattern of output systems of the rat cerebellum.

LATERALITY 0F Vo PROJECTIONS TO OROFACIAL TACTILE AREAS IN THE CEREBELLAR CORTEX

The data from this study suggest that crura I and II, PML, and the uvula receive different proportions of direct efferent axons from ipsilateral and contralateral Vo subdivisions. The greatest number of labeled parent axons and terminal arborizations found in the orofacial portions of these four major tactile areas arise from neurons in ipsilateral Vo following injections into each of its three subdivisions. These observations agree with previous retrograde HRP studies in rat (Falls and Van Wagner, '84; Falls et al., '85; Falls and Alban, '86; and Falls, '87). Electrophysiological studies (Shambes et al., '78a,b; and Joseph et al., '78) have generated additional evidence for a strong ipsilateral rat trigeminocerebellar projection. These studies have shown that peripheral orofacial tactile stimuli elicit short-latency responses from GCL neurons in ipsilateral orofacial portions of crura I and II, PML, and the uvula. Small contralateral zones have been reported immediately lateral to the vermis. Bilateral trigeminocerebellar projections are principally reported from the rostral face and perioral structures (Shambes et al., '78a). Retrograde transport studies in cat (Ikeda, '79; Matsushita et al., '82; and Somana et al., '80) describe an almost exclusive ipsilateral Vo trigeminocerebellar projection following injections into Crus II, PML, and the simple lobule and sublobule 9A. From this aspect of the present study, it can be concluded that, even though projections from rat Vo to orofacial tactile portions of the four major tactile areas of CC are bilateral, they have their most significant involvement in sensorimotor processing in ipsilateral CC.

Based on the density of terminal labeling and distribution of terminal arbors in CC, trigeminocerebellar projection neurons in ipsilateral Vo are

situated primarily in DM with some cells in VL and only a few neurons in BZ. This assumption is supported by the findings of previous retrograde transport studies in rat (Falls et al., '85; Falls and Alban, '86 and Falls, '87) which show the greatest number of trigeminocerebellar projection neurons are located in DM. Projections to CC from VL are supported by studies in cat (Matsushita et al., '82) which suggest that Vo trigeminocerebellar neurons are less strictly confined and have a tendency to be situated in more ventral portions of the nucleus.

COLLATERAL Vo PROJECTIONS TO THE DEEP CEREBELLAR NUCLEI

Cerebellar corticonuclear projections have been studied with degeneration, HRP, and autoradiographic methods, in rat (Goodman et al., '63; and Schild, ' 78a,b), cat (Dietrichs and Walberg, '79,'80; Voogd and Bigare, '80; and Dietrichs, '81a,b), rabbit (van Rossum, '69), opossum (Haines et al., 76; and Klinkhachorn et al., '84a,b) tree shrew (Haines and Whitworth, '78; Haines and Patrick, '81) and primate (Haines and Rubertone, '77, '79). Previous studies in cat, rabbit and monkey (Jansen and Brodal, '40, '42) have provided evidence for a high degree of topographical localization. Corticonuclear projections are arranged in three ipsilateral longitudinal zones: vermal, paravermal or intermediate, and lateral zones projecting to MED, INT and LAT nuclei respectively. Rat corticonuclear projections also suggest a zonal organization (Goodman et al., '63; Armstrong and Schild, '78a,b; Haines and Koletar, '79; Umetani et al., '86). Armstrong and Schild ('78a,b) using autoradiography reported a mediolateral localization in rat dCN with regard to projections from the vermis and hemisphere. Furthermore, projections from the vermal cortex

(Haines and Koletar, '79) have been described which suggest a zonal compartmentalization of that cortex into medial and lateral subdivisions.

The location of nuclear areas along the rat neuraxis (pontine reticulotegmental nucleus, inferior olive, trigeminal nuclear complex, rostral portion of the lateral reticular nucleus, perihypoglossal nuclei, dorsal parabrachial body, locus coeruleus, and raphe nuclei) contributing efferents which terminate specifically in LAT have been identified by the retrograde HRP methodology following injections in dCN (Eller and Chan-Palay, '76). Projections from cat reticulotegmental nucleus (Gerrits and Voogd, '81; and Gerrits et al., '84a), and lateral reticular nucleus (Russchen et al., '76) as well as rat nucleus raphe magnus (Chan-Palay et al., '77) have been confirmed by anterograde methods. In addition to direct projections to rat dCN, double labeling techniques (Huisman et al., '83) have revealed terminal arborizations of collaterals from rubrospinal axons which end in INT while autoradiographic studies (Chan-Palay et al., '77) have shown collaterals of olivocerebellar axons terminating within dCN with parent axons continuing on to terminate within sagittal bands in the molecular layer of CC.

In a double labeling study of rat dCN (Bentivolgio and Kuypers, '82) utilizing fluorescent dye injections cells within the lateral, magnocellular part of LAT were shown to project to the thalamus with collaterals given to superior colliculus, reticular formation and spinal cord. Diencephalic projections with collaterals to the superior colliculus were also shown to originate from cells within the central and caudal part of MED and some of the large cells in the ventral portion of MED were also shown to project as far as the spinal cord. In another study utilizing retrograde transport techniques (Beitz, '82) HRP injections were made into the lateral and

superior vestibular nuclei. This study demonstrated that large cells in the dorsal part and small cells in the caudal part of MED were labeled contralaterally and cells in the central and ventrolateral part of MED were labeled ipsilaterally. Based on the results in this study the potential exists for Vo modulation of dCN output to the thalamus, superior colliculus and spinal cord in LAT and MED by virtue of Vo MF collateral arborizations in the lateral part of LAT and central, caudal and ventral portions of MED. It is interesting that DM-MF's terminate in MED in a manner which suggests modulation of rostral portions ipsilaterally and caudal portions contralaterally thereby affecting those areas containing cells of origin for fastigiobulbar connections.

Terminal arborizations in the present study were found in each of the dCN bilaterally with an ipsilateral predominance, following DM and VL injections. BZ injections yielded only ipsilateral labeling in dCN. Collaterals were observed to emanate from parent MF axons coursing through or in close proximity to dCN on their way to CC. The above findings suggest that efferents destined for specific portions of the vermis and hemisphere, vermal, paravermal and lateral zones, send collateral branches to specific portions of MED (Figures 4-9; A-B), INT (Figures 4-9; C-D), and LAT (Figures 4-9; E) nuclei which underly the cortical area in which the parent fibers terminate. In this study a small amount of overlap occurs between vermal and paravermal sections. Terminal arborizations ending in the vermis and vermal cortex were analyzed in Figures 4-9; A-C even though these sections show that the INT nucleus is starting to appear while labeled arborizations terminating in the cerebellar hemisphere overlying INT, paravermal cortex, were assessed in Figures 4-9 D.

No collaterals were observed to terminate in portions of dCN located immediately below those areas of cortex which did not receive trigeminocerebellar efferents. For instance, a lateral zone of contralateral Crus I receives a sparse projection from DM cells.and the underlying LAT also receives a sparse DM projection. No afferents were observed in these same areas from VL or BZ neurons. The vermal zone, lobules 1-10, receives the densest projection, from axons of cells located primarily in DM and VL subdivisions which terminate in its ipsilateral cortex. The underlying ipsilateral MED receives the densest input as collaterals from parent fibers originating from neurons in these two subdivisions terminate within its boundaries. Conversly, a dense projection is also seen in the vermal zone and MED contralaterally following a DM injection while no Vo efferents are found in these receptive areas following a VL injection.

Simply stated, these findings suggest that collaterals of MF axons terminating within each dCN originate from parent axons which continue on to terminate within zonal bands in the granule cell layer of the vermis and cerebellar hemispheres overlying each of the respective dCN. This pattern of zonal trigeminocerebellar efferent terminations within dCN and CC resembles the zonal organization of the corticonuclear output system of the cerebellum.

CLASSIFICATION OF Vo TRIGEMINOCEREBELLAR TERMINAL AXONAL ARBORIZATIONS

Although a large variety of mossy fiber formations have been described (Palay and Chan-Palay, '74, Brodal and Drablos, '63) for axons terminating in GCL of the rat cerebellar cortex only one simple and two complex formations, have been recognized as the predominant

morphological types (Palay and Chan-Palay, '74). Simple MF formations have been characterized as a simple fusiform enlargement emitting a few short finger-like extensions. Complex MF formations of the first type have been characterized as being more complicated with a massive central expansion from which filiform appendages project. The second type of complex formation, usually found in the outer one-third of the GCL beneath PCL, has been described to consist of an elongated cone expanding into a flower-like figure which gives off recurving filamentous processes.

Several studies have suggested that MFs originating from different areas of the neuraxis have different morphologies (Brodal and Drablos. '63) and different areas of distribution in GCL (Eccles et al., '67;). While different lines of investigation have been attempted through lesion experiments (Mugnaini, '67) and histochemical studies (Hebb, ' 59; Csillik et al., '63; Shute and Lewis, '65) to determine whether the differences in morphology of MF's can be attributed to neurons originating from different areas (eg., pons and spinal cord) the results have been generally inconclusive. The three major types of MF's have been reported to terminate in equal frequency in all lobules of CC (Palay and Chan-Palay, '74). However, Brodal and Drablos ('63) have suggested that a large contingent of MF's in the nodulus, flocculus, ventral uvula, and ventral paraflocculus differ from those in other areas in that they are more massive and coarser. These MF's are presumably of the complex variety.

All three morphologically distinct types of MF's described by Palay and Chan-Palay ('74) were observed to terminate in the cerebellum from axons of Vo trigeminocerebellar projection neurons. GCL-Simple MF's were observed in all lobules innervated by trigeminal efferents. Both types

of complex MF's, GCL-Complex and GCL Filamentous, were limited to the medial portion of the posterior one-half of CC.

The results of this study support the idea that the frequency in which the three types of MF's are observed in CC is dependent upon which Vo subdivision is giving rise to them. DM neurons have been reported in retrograde HRP studies to have the major Vo projection to the cerebellum (Falls and Van Wagner, '84; Falls et al., '85; and Falls and Alban, '86). These cells give rise to all three types of GCL-MF's in the greatest density. Axons of VL neurons are less dense and predominately terminate as GCL-Simple MF's. Although a sparse number were observed to terminate as GCL-Complex MF's. Axons of BZ neurons are the fewest and give rise primarily to GCL-Simple MF's. These findings also support the studies of Brodal and Drablos ('63) in that more GCL-simple MF's are located throughout the CC while the complex MF's are limited to the posterior one-half of the cerebellum. The morphological description of trigeminocerebellar efferents which terminate in PCL is without previous characterization in the literature.

FUNCTIONAL CONSIDERATIONS

Longitudinal Zones and Spatial Patterns of Organization of Vo Input

A longitudinal corticonuclear zone theory of cerebellar function has been applied to rat (Goodman et al. '63) consisting of a medial zone (vermal cortex and medial nucleus), intermediate zone (paravermal cortex and interposed nucleus), and a lateral zone (cerebellar hemisphere and dentate nucleus). In an earlier study Goodman and Simpson ('61) described, in rat, three postural patterns following cerebellar stimulation. First, a vermal

zone pattern observed following stimulation of the vermis with postural patterns of flexion and adduction of the ipsilateral limbs and extension and abduction of the contralateral limbs. A second postural pattern, paravermal-zone pattern, was elicited by stimulation of an area subadjacent to the vermis laterally, medial hemisphere, and consisted of mirror images of movements observed following stimulation of the vermal zone. The third postural pattern, lateral zone pattern, was observed following stimulation of the cerebellar hemisphere lateral to the paravermal zone and consisted primarily of ipsilateral forelimb flexion and adduction with occasional contralateral limb extension and abduction. Frequently, stimulation of the cerebellum was reported to cause a concomitant head turning and head rotation to the contralateral side. Vo trigeminocerebellar efferents project to dCN in a manner suggesting a longitudinal pattern of collateral input from parent MF's destined for cortical areas overlying each of the respective dCN. That Vo may have the potential for modulating outgoing postural patterns occurring in the forelimbs and hindlimbs bilaterally and in the head through its connections with the output nuclei of the cerebellum, the dCN, is not surprising. SVN has been implicated in the modulation of spinal cord motor activity by retrograde (Ruggerio et al., '81) and anterograde studies (Smith and Falls, '88) which show a descending projection along the entire length of the spinal cord which terminates in the dorsal and ventral horns. It is possible that the cerebellum is receiving input from Vo neurons also projecting to the spinal cord or neighboring Vo neurons to alert the cerebellum on a moment to moment basis of the ongoing modulation of motor output taking place in the ventral horns.

The receptive fields for climbing fibers in rats (Logan and Robertson, '86) and cats (Rushmer et al., '80) have been shown to have a coexisting patch-like representation of various body regions, similar to that described for MF's in the CC (Shambes et al., '78a,b), and a zonal representation for the same information (Logan and Robertson, '86). A similar pattern of dual representation of somatotopic tactile input was found for rat trigeminocerebellar MF's in this study. Perhaps longitudinal arrays of patches corresponding to vermal, paravermal, and lateral zones are organized in such a manner that smaller mosaics of orofacial, head, trunk as well as limb areas are represented within these longitudinal zones with each receiving a specific type of input depending upon where in the hemisphere the receptive field of the patch is situated (Crus I, Crus II, PML, and uvula).

Morphologically Distinct Cell Types and Mossy Fiber Terminals

DM has been shown to provide a significant amount of tactile efferents to the cerebellar hemispheres bilaterally giving rise to three morphologically distinct MF's in the GCL (GCL-MF's) and two morphologically distinct MF's in the PCL (PCL-MF's). Data from Nissl, Golgi and retrograde HRP studies (Falls and Van Wagner, '84 and Falls et al., '85) have demonstrated that rat DM contains five morphologically distinct neuronal cell types which project to one or more of the orofacial portions of the four major tactile areas of CC. It is possible that each of the five neuronal cell types gives rise to one of the five morphologically distinct MF's entering GCL and PCL. Further studies need to be done to clarify this possibility.

The fact that terminal arborizations of the axon collaterals arising from MF's of DM, VL and BZ neurons terminating in DCN have an appearance that is different from the morphology of the terminal arborizations of the MF parent axons in the cerebellar hemisphere further suggests that two morphologically different terminal axonal arbors can originate from the same neuronal cell body depending on their area of termination. Whether they are functionally different awaits electron microscopic and electrophysiological analyses.

Vo Control and Regulation of Tactile Consequences

The basic circuitry in the cerebellum includes three external inputs consisting of climbing fibers (from the inferior olive), MF's (from vestibular nuclei, SVN, spinal cord, and cerebral cortex), and aminergic fibers, discerned with the use of histofluorescent methods (Chan-Palay, '75; Hokfelt and Fuxe, '69 and Takeuchi et al., '82b). Purkinje cell axons are the only route out of CC projecting to dCN which in turn give rise to cerebellar efferents. A major neural circuit, a loop from the cerebral cortex to the cerebellum and back to the cerebral cortex (motor and premotor cortex) provides the circuitry for cerebellar hemisphere involvement in the planning of movements, acting to influence efferent output of the motor cortex. The need for ongoing sensory input, to the cerebellum, regarding evolving changes with respect to the animal and its environment, is essential for enabling adjustments in motor patterns to be made. Not only do Vo trigeminocerebellar efferents provide sensory information from the orofacial region by way of MF's which terminate in GCL but they are also able to affect cerebellar output by inputs directly to PCL and dCN, the last and critical part of the output system. Trigeminocerebellar efferents may

contribute to the control and regulation of tactile consequences generated by movements of vibrissal and perioral structures through circuits relaying information about spatial location of peripheral stimuli directly through trigeminal-PCL and trigeminal-dCN routes and indirectly by way of trigeminal-GCL and by the trigeminal-VPM-SI-Pons-GCL route suggested by Bowers et al. ('81). The possibility also exists that convergence of indirect input occurs within the same GCL tactile patches, allowing for a greater complexity of outputs via parallel fibers.

A new proposal has been made (Welker, '90) which supports the individual folium of the cerebellar cortex as a distinct structural and functional entity responsible for independent processing of afferent inputs and control of output through its characteristic set of target neurons. In this study, Vo trigeminocerebellar efferents have been shown to project to the folia of the vermis and cerebellar hemispheres in a distinct and differential manner that implies probable functional differences. For instance, Vo MF's from all three subdivisions tend to be located within the folial crown and ventral folial wall within ipsilateral PML whereas in contralateral PML these MF's are primarily situated in the dorsal folial crown. Each folia has been hypothesized (Welker, '90) to receive source specific information which is processed and organized for efferent outflow to the dCN to proceed along a medial to lateral topographical plan. To what extent Vo trigeminocerebellar tactile information is being compartmentalized into the various morphologic sites of individual folia of the vermis and cerebellar hemisphere is not known at this time. Preliminary results published in this study suggests that future studies need be performed to address this issue.

In conclusion, this study shows that orofacial tactile input arising from cutaneous mechanoceptors is routed through Vo to the GCL as well as the motor output areas contained both within the PCL and the dCN simultaneously which suggests a higher degree of complexity in trigeminocerebellar circuitry than has been presently thought. To what extent Vo information is equally or preferentially relayed over a single Vo input path is still unknown, nor is it known if certain types of sensory information , tactile or pain, vibrissal or intraoral, have preferential paths to GCL, PCL, or dCN.

Putative Neurotransmitters for Vo Mossy Fibers

The MF, arising from a variety of sources, has been the subject of many detailed anatomical and electrophysiological studies and although neuroimmunohistochemical studies have identified several putative transmitters, none have been clearly demonstrated to act as neurotransmitter at the MF-granule cell synapse. Early neurochemical and histochemical studies (McIntosh, '41; Feldberg and Vogt, '48; Burgen and Chipman, '51; and Hebb and Silver, '56) demonstrating acetlycholine (ACh), acetylcholinesterase (AChe) and choline acetyltransferase (ChAT) activity in the cerebellum suggested ACh as a possible neurotransmitter. Later, immunohistochemical staining of rabbit cerebellum with antisera against ChAT revealed ChAT positive MF's (Kan et al., '78). Studies of catecholamine and serotonin distribution within the cerebellum have indicated their presence in association with MF's. However, these terminals are only demonstrated (Hockfelt and Fuxe, '69; Chan-Palay, '75; Beaudet and Sotelo, '80) when the tissue is pretreated with the putative neurotransmitter. Histofluorescence preparations of untreated cerebellum

for either norepinepherine or serotonin fail to show MF staining (Hockfelt and Fuxe, '69). A few reports of immunohistochemical staining of MF's by antisera directed against neuropeptides have shown substance P-like activity (Korte et al., '80), enkephalin-like immunoreactivity (Schulman et al., '81) and somatostatin-like immunoreactivity (Renaud et al., '75) in the cerebellum. However, only substance P has been demonstrated to be a neurotransmitter (Otsuka and Konishi, '75) in the central nervous system. Neuropeptide somatostatin-like activity in rat Vo has been illustrated, but not specifically discussed by Bowker et al. ('88). Somatostatin-like activity has been observed to exist predominately in DM, while substance P-like activity occupies neurons in the area of dorsal BZ and Met-enkephalin-like activity rest within cells in the ventral aspect of VL (unpublished observation made with materials stained by Dr. R. Bowker). The role of peptides in cerebellar function is further obscured in that both enkephalin and somatostatin have predominately inhibitory actions, while inhibitory MF's have not been reported. It is quite possible that Vo MF's terminating in the dCN may utilize inhibitory neuropeptides to achieve a similar response to that of the Purkinje cell-inhibitory pathway which is purported to use GABA in its inhibitory projections to Dieter's nucleus of cats and rats (Otsuka et al., '71; McLauglin et al., '74). Identification of the neurochemical mediating synaptic transmission via Vo-MF's is necessary for a complete understanding of the relationship between neuronal activity and cerebellar function with such elicudation awaiting future studies.

Figure 1: Schematic drawings of a representative coronal section through rat trigeminal nucleus oralis (Vo) and dorsal view of rat cerebellum illustrate the results of previous retrograde studies (Falls and Wagner, '85; Falls and Alban, '86; Falls, '87) showing the major Vo trigeminocerebellar efferent projections. BZ, border zone Vo; Crus I, crus I ansiform lobule; Crus II, crus II ansiform lobule; DM, dorsomedial Vo; MDMd, middle dorsomedial, dorsal Vo; MDMv, middle dorsomedial, ventral Vo; VL, ventrolateral Vo; VII, facial motor nucleus.

FIGURE 1

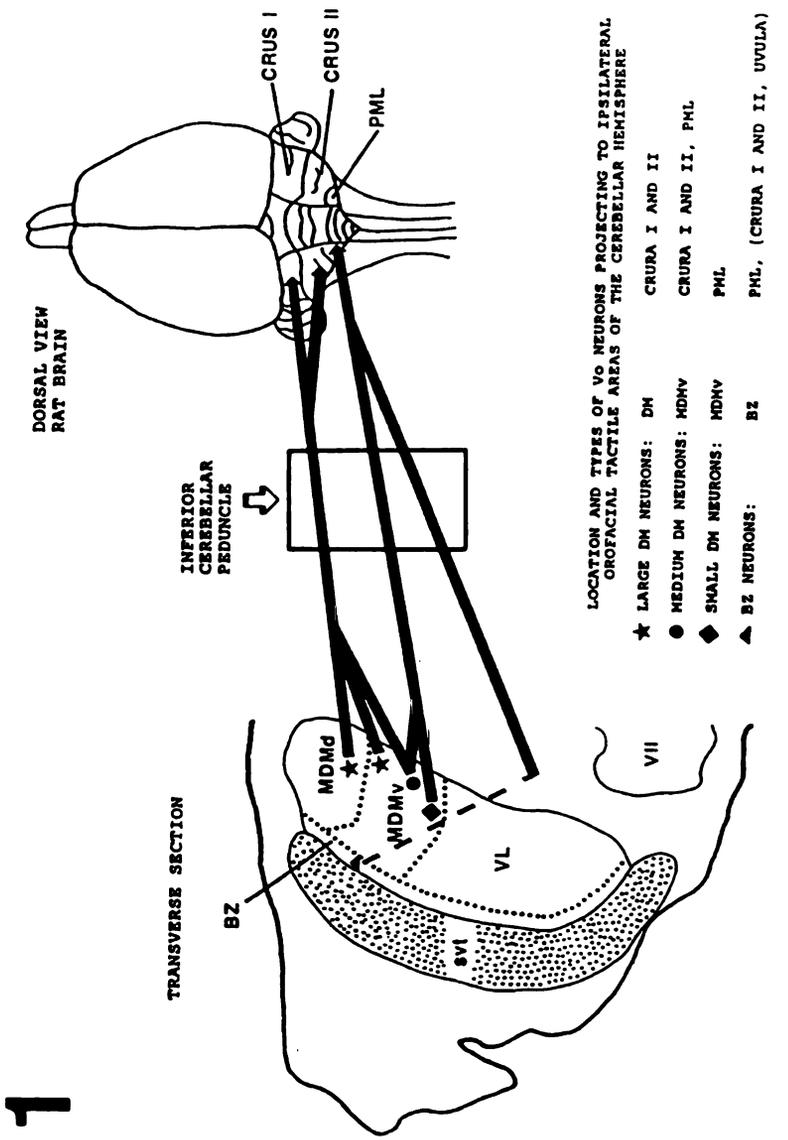
DORSAL VIEW
RAT BRAIN
CRUS I
CRUS II
PML
INFERIOR
CEREBELLAR
PEDUNCLE
TRANSVERSE SECTION
MDMd
MDMv
VL
VII
BZ
svl
LOCATION AND TYPES OF Vo NEURONS PROJECTING TO IPSILATERAL
OROFACIAL TACTILE AREAS OF THE CEREBELLAR HEMISPHERE
★ LARGE DM NEURONS: DM CRURA I AND II
● MEDIUM DM NEURONS: MDMv CRURA I AND II, PML
◆ SMALL DM NEURONS: MDMv PML
▲ BZ NEURONS: BZ PML, (CRURA I AND II, UVULA)

1

Figure 2: Low-power photomicrographs (A-C) showing the location of PHA-L injection sites in each of the three subdivisions of rat Vo. Dotted lines indicate the limits of Vo as well as its dorsomedial (DM), ventrolateral (VL), border zone (BZ) subdivisions. A. An injection site situated in the middle portion of DM (MDM), partially filling its dorsal (MDMd) and ventral (MDMv) zones (case 741). B. An injection site located in VL (case 751). C. An injection site positioned within BZ with some spread into dorsal VL (case 750). svt, spinal trigeminal tract; VII facial motor nucleus.

FIGURE 2

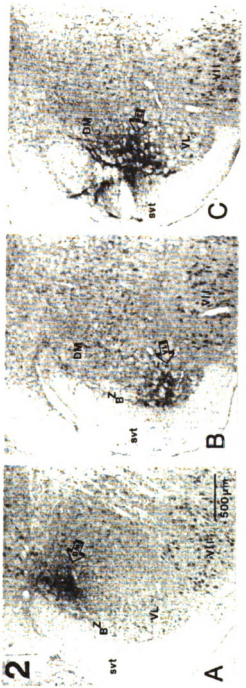

FIGURE 3: Schematic drawing of a dorsal view of the left one-half of the cerebellum. Lettered lines illustrate the approximate mediolateral level at which sagittal drawings in figures 4-9: A-F are taken.

FIGURE 3

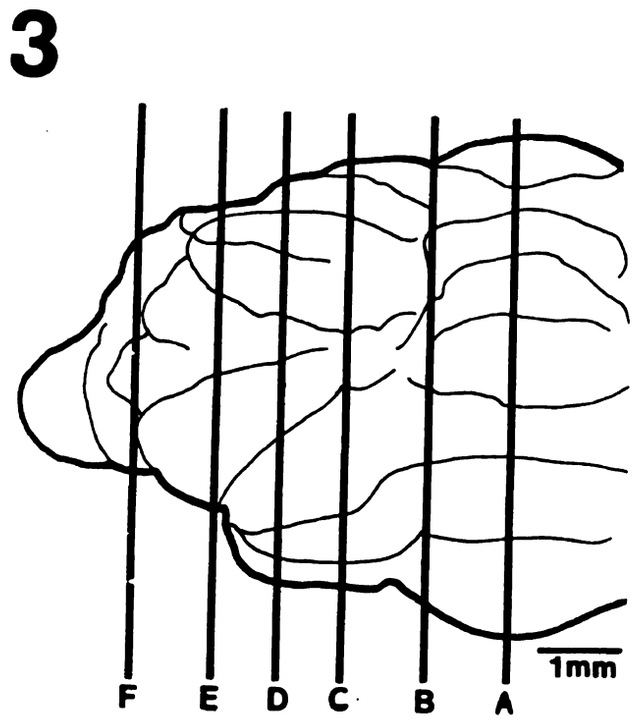

Figure 4: Camera lucida drawings of representative sagittal sections through the medial third (A, B), middle third (C, D), and lateral third (E, F) of ipsilateral rat cerebellum. These drawings illustrate the distribution and relative density of anterogradely labeled fibers and terminal arborizations after DM injections. Numerous axons form dense terminal plexuses throughout the mediolateral extent of the 10 vermal lobules. Labeled terminal arborizations were also observed medially in Crus Ib and laterally in Crus Ia. In Crus II the greatest density of labeling was in Crus IIb. Labeled fibers were restricted to the medial two-thirds of the ventral folial wall of PML. Dense terminal arborizations were observed in MED with fewer arbors found laterally in INT and LAT. The magnification scale indicated in F is the same for schematics A-F in this Figure and in Figures 5-9.

FIGURE 4

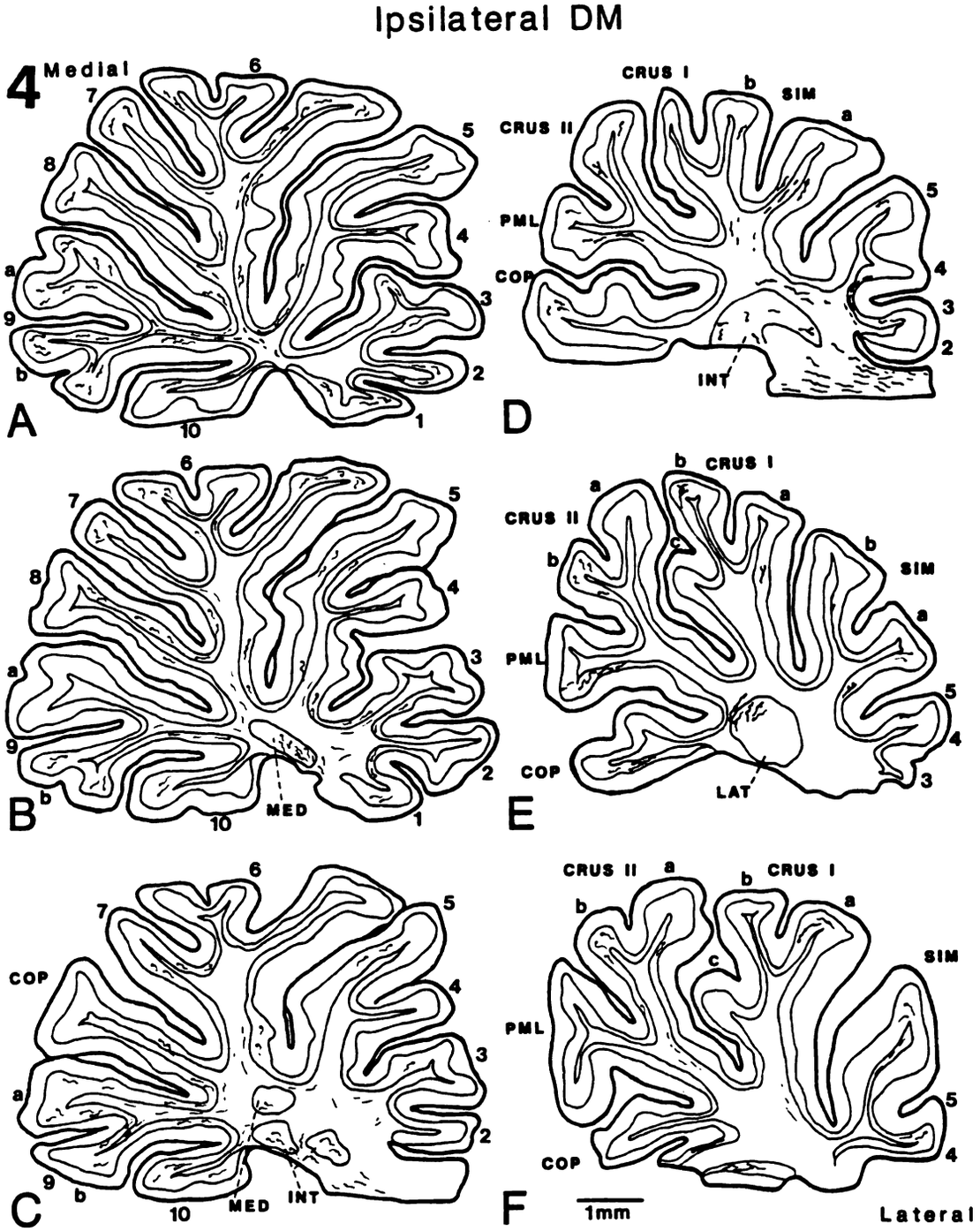
Ipsilateral DM
4
Medial
A
B
C
D
E
F
CRUS I
CRUS II
SIM
PML
COP
INT
MED
LAT
1mm
Lateral

Figure 5: Camera lucida drawings of representative sagittal sections through the medial third (A, B), middle third (C, D), and lateral third (E, F) portions of contralateral rat cerebellum. These drawings illustrate the distribution and relative density of anterogradely labeled fibers and terminal arborizations after DM injections. Numerous axons form dense terminal plexuses throughout the mediolateral extent of the 10 vermal lobules. Labeled terminal arborizations were also observed in Crus I, in the mediolateral extent of Crus Ib and medially in Crus Ic. In Crus II the greatest density of labeling was in the medial two-thirds and was observed in approximate equal density in Crus IIa and Crus IIb. Labeled fibers were restricted to the middle one-third of the folial crown of PML. Dense terminal arborizations were observed in MED with fewer arbors found laterally in INT and LAT.

FIGURE 5

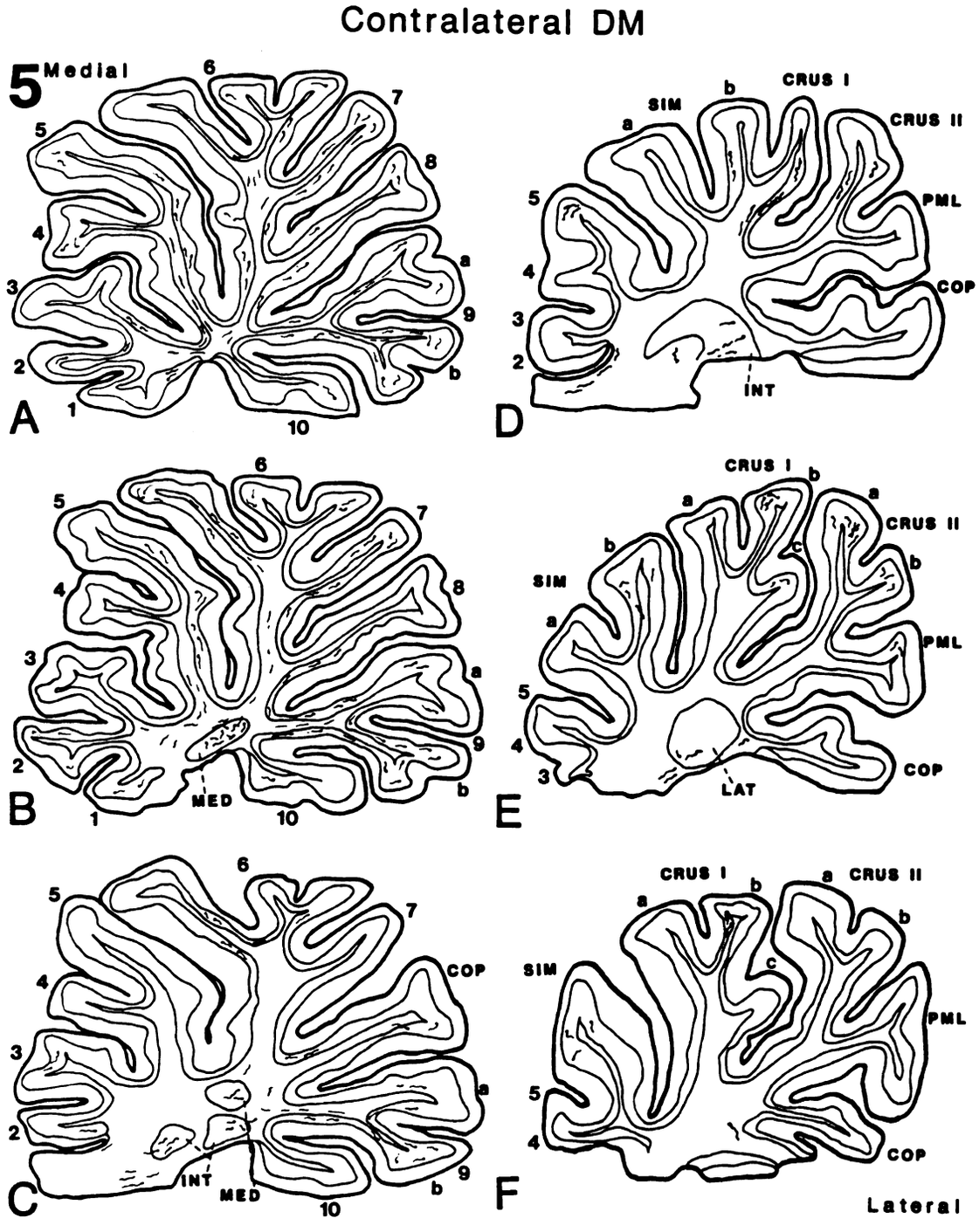
Contralateral DM
5
Medial
A
B
C
D
E
F
CRUS I
CRUS II
SIM
PML
COP
INT
MED
LAT
Lateral

Figure 6: Camera lucida drawings of representative sagittal sections through the medial third (A, B), middle third (C, D), and lateral third (E, F) portions of ipsilateral rat cerebellum. These drawings illustrate the distribution and relative density of anterogradely labeled fibers and terminal arborizations after VL injections. Numerous axons form dense terminal plexuses in several vermal lobules. Labeled terminal arborizations were sparse in Crus I and were restricted primarily to Crus Ic. In Crus II the greatest density of labeling was in the middle one-third and was observed predominately in Crus IIa. Labeled fibers were restricted to the medial two-thirds of the ventral folial crown medially and wall laterally of PML. Terminal arborizations were observed in MED, INT and LAT in approximately equal density.

FIGURE 6

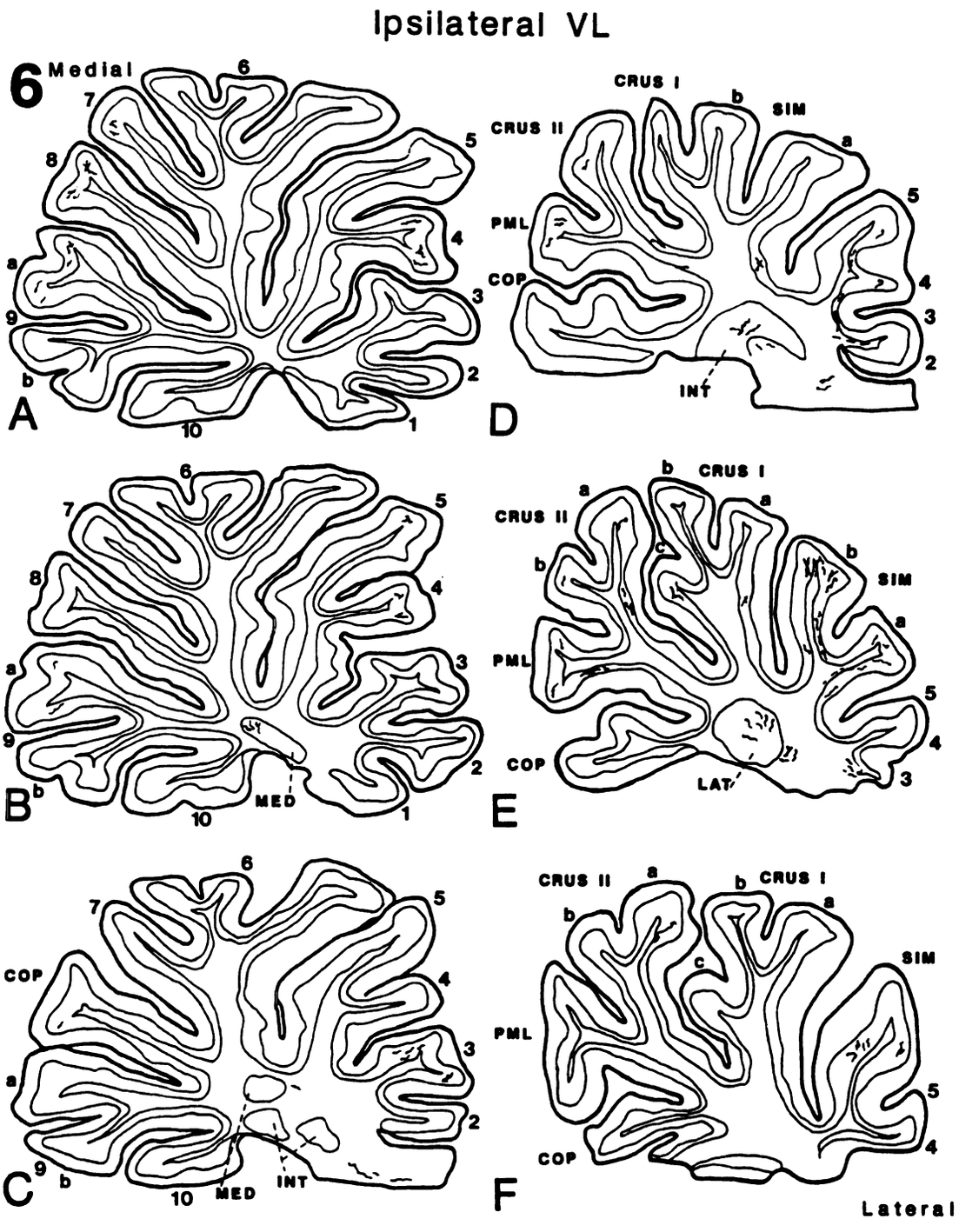
Ipsilateral VL
6
Medial
A
B
C
D
E
F
CRUS I
CRUS II
SIM
PML
COP
INT
MED
LAT
Lateral

Figure 7: Camera lucida drawings of representative sagittal sections through the medial third (A, B), middle third (C, D), and lateral third (E, D) portions of contralateral rat cerebellum. These drawings illustrate the distribution and relative density of anterogradely labeled fibers and terminal arborizations after VL injections. Sparse collections of axonal terminal plexuses are found in several vermal lobules. In Crus II a sparse collection of labeled fibers was observed medially. Terminal arborizations were sparsely distributed in MED and INT.

FIGURE 7

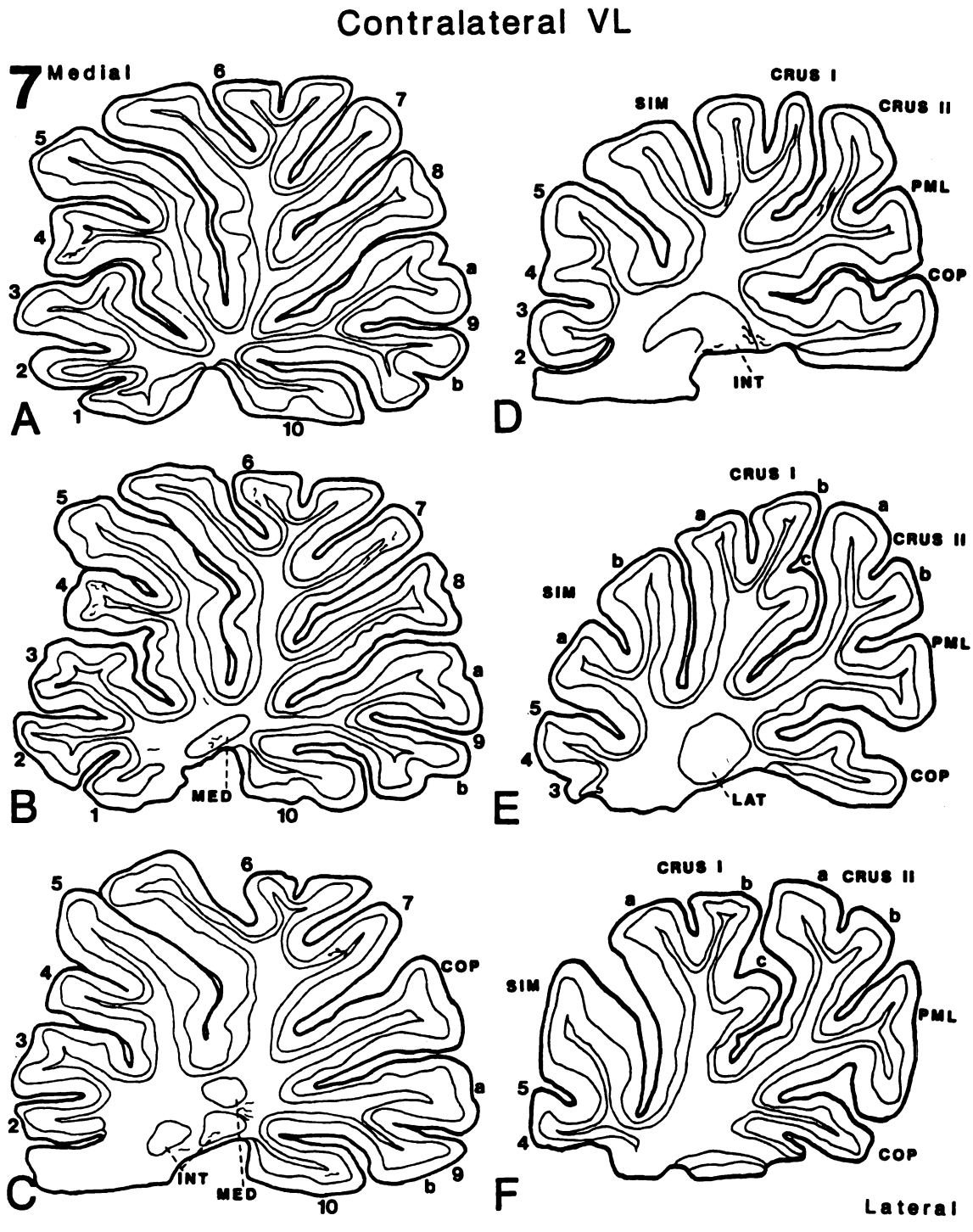
Contralateral VL
7
Medial
A
B
C
D
E
F
CRUS I
CRUS II
SIM
PML
COP
INT
MED
LAT
Lateral

Figure 8: Camera lucida drawings of representative sagittal sections through the medial one-third (A, B), middle one-third (C, D), and lateral one-third (E, F) portions of ipsilateral rat cerebellum. These drawings illustrate the distribution and relative density of anterogradely labeled fibers and terminal arborizations after BZ injections with some spread into dorsal VL. Sparse collections of axonal terminal plexuses are found in several vermal lobules. Labeled terminal arborizations were also observed laterally in Crus Ia and Crus Ic. In Crus II labeled fibers were few and limited to the posterior folial wall. Labeled fibers were restricted medially to the folial crown and laterally to the folial wall of PML. Terminal arborizations were observed in INT and LAT in approximately equal density.

FIGURE 8

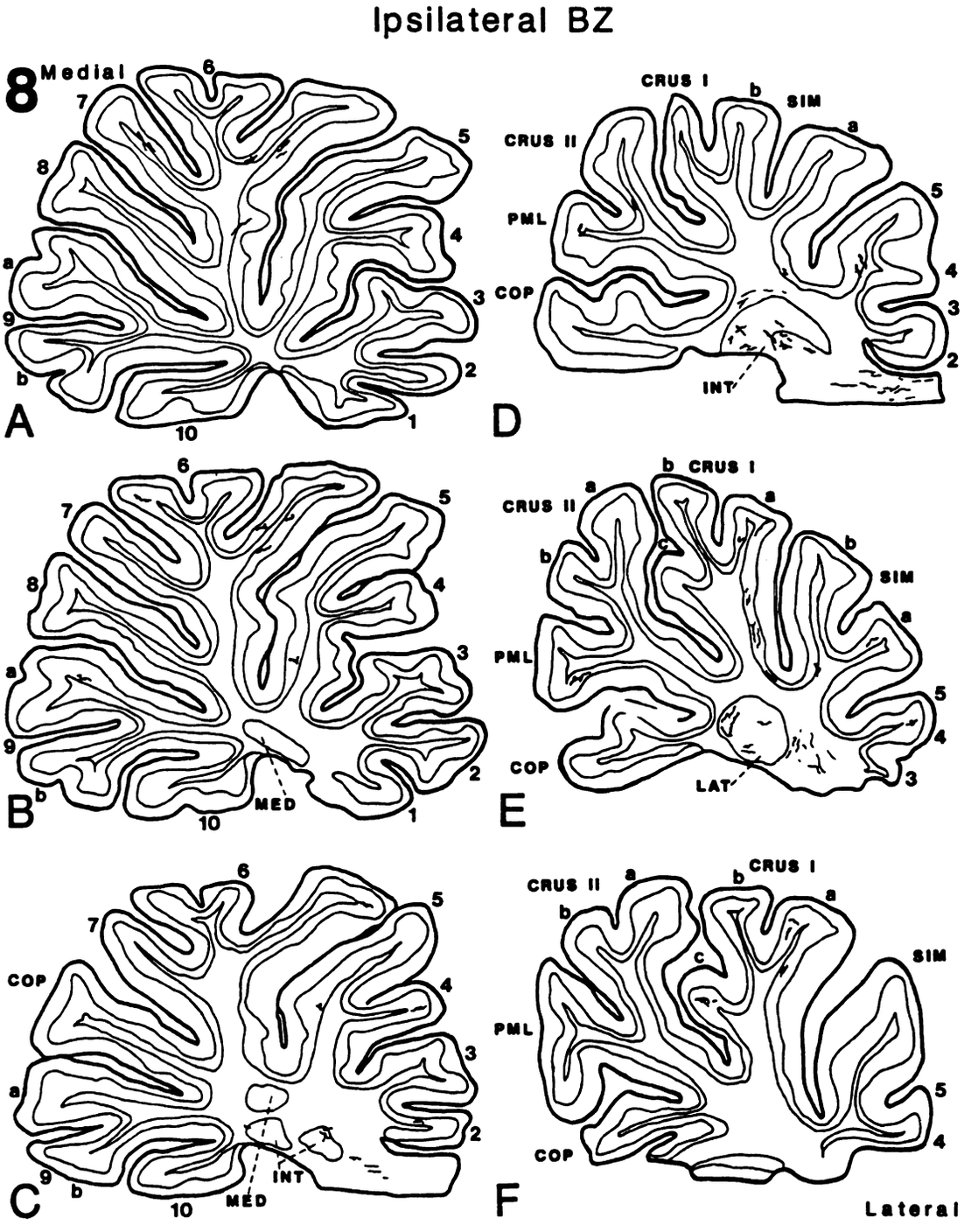
Ipsilateral BZ
8
Medial
A
D
B
E
C
F
Lateral
CRUS I
CRUS II
SIM
PML
COP
INT
MED
LAT

Figure 9: Camera lucida drawings of representative sagittal sections through the medial one-third (A, B), middle one-third (C, D), and lateral one-third (E, F) portions of contralateral rat cerebellum. These drawings illustrate the distribution and relative density of anterogradely labeled fibers and terminal arborizations after BZ injections with some spread into dorsal VL. Only a few axons form plexuses in the posterior one-half of the vermis and ventral folial wall of PML.

FIGURE 9

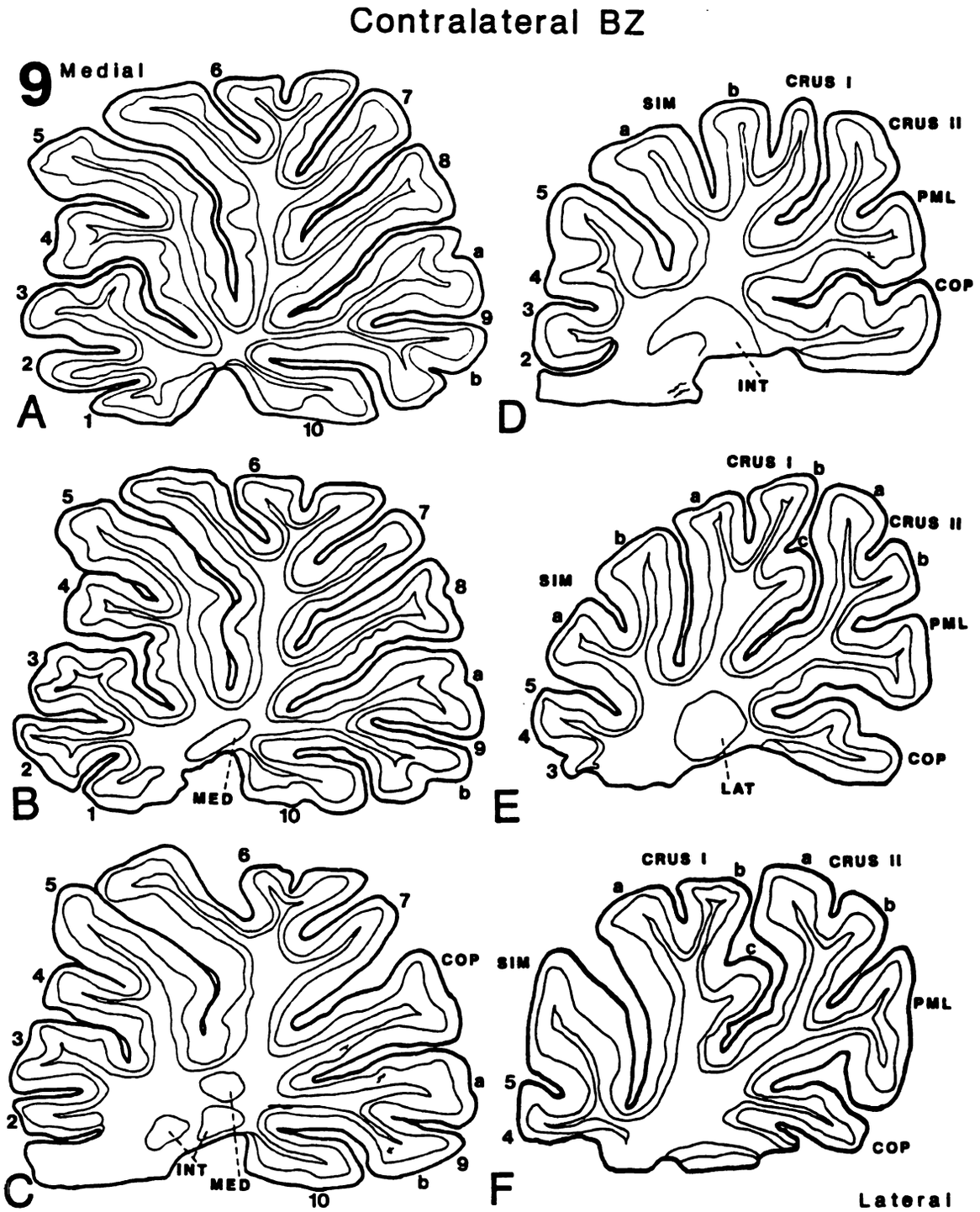
Contralateral BZ
9
Medial
A
B
C
D
E
F
SIM
CRUS I
CRUS II
PML
COP
INT
MED
LAT
Lateral

Figure 10: Representative drawings of the three types of Vo efferent terminal axonal arborizations located in the granule cell layer (GCL) of the cerebellar cortex. One type, GCL-Simple (1-3), is characterized by a thin terminal strand (ts) that terminates in bulbous fusiform-shaped boutons (b). The second type, GCL-Complex (4-5), is characterized by a thicker terminal strand which forms massive irregularly shaped boutons from which twisted and angular appendages ensue. The third type, GCL-Filamentous (6), is characterized by thick terminal strands terminating in irregularly shaped boutons which emit several recurving thin bouton bearing filamentous processes closely approximating Purkinje cell somata.

FIGURE 10

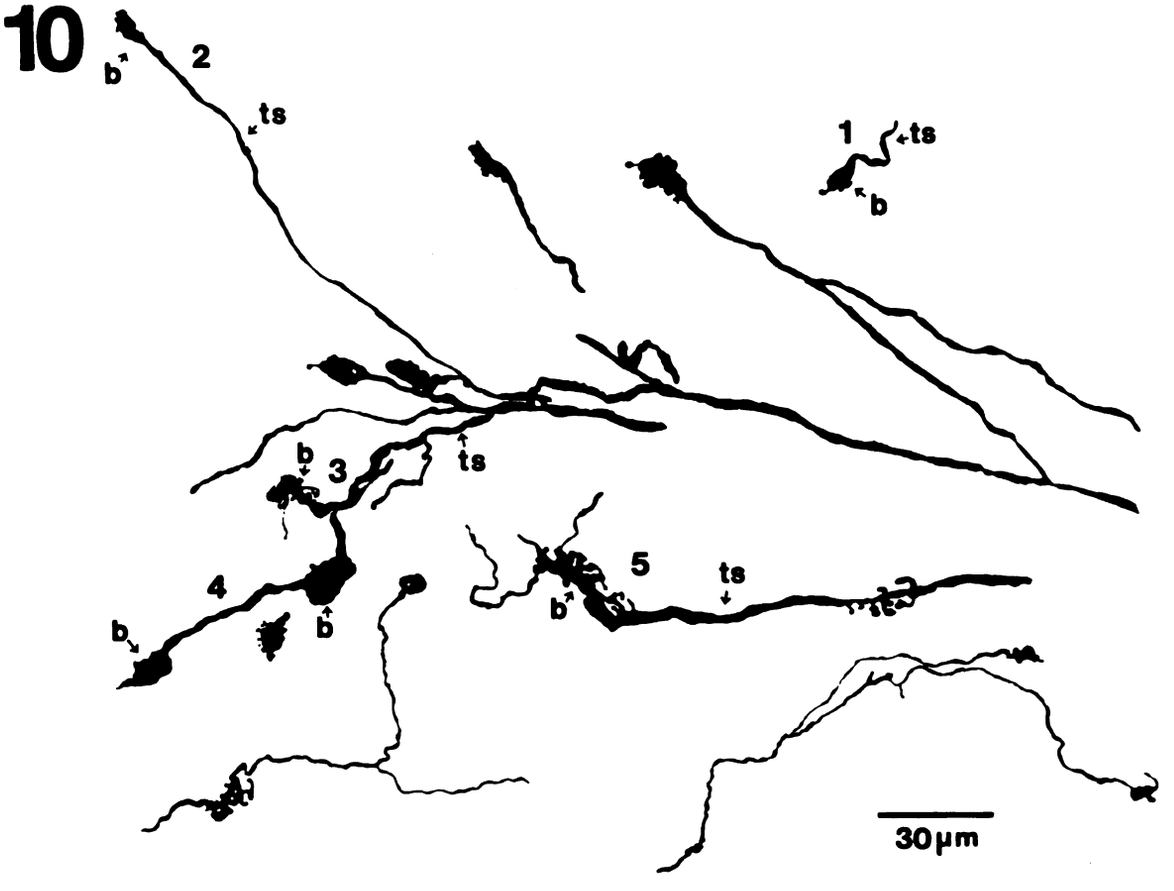

Figure 11: Representative drawings of the two types of Vo efferent terminal axonal arborizations located in the Purkinje cell layer (PCL) of the cerebellar cortex. One type, PCL-Simple (1-2), is characterized by a thin terminal strand (ts) which terminates in either short side branches capped by a bouton (b) or as a single bouton bearing branch. The second type, PCL-Complex (3-4), is characterized by a thick terminal strand with several recurving filamentous processes extending well into PCL. Dashed lines indicate the peripheral border of Purkinje cell bodies.

FIGURE 11

11

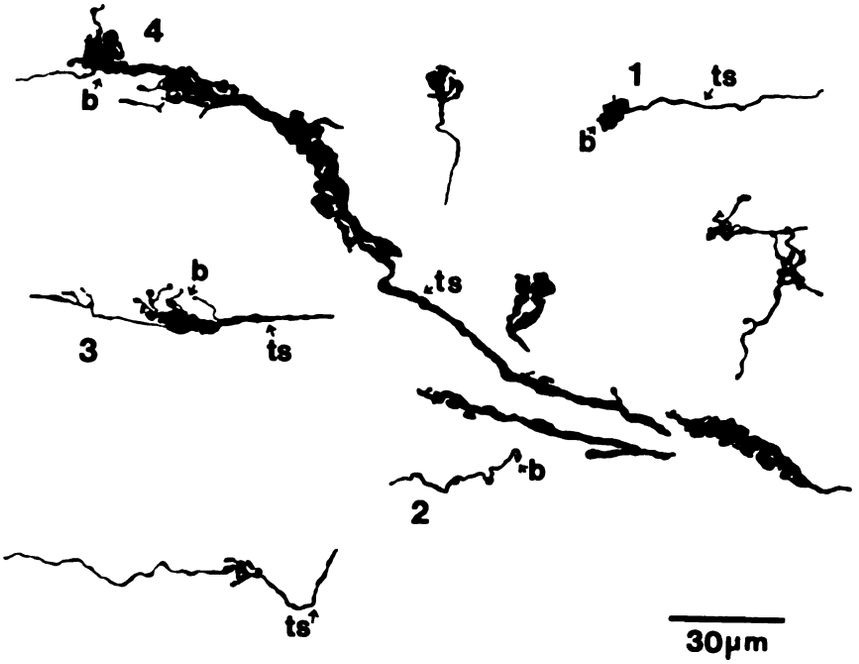

Figure 12: Representative drawings of the single type of Vo efferent terminal axonal arborization located in the medial, interposed and lateral cerebellar nuclei. Single collateral terminal strands (ts) emanate from parent fibers (1) as they course through the deep cerebellar nuclei on their way to the cerebellar cortex. The terminal strands give rise to several bouton bearing side branches capped by an end bouton (b).

FIGURE 12

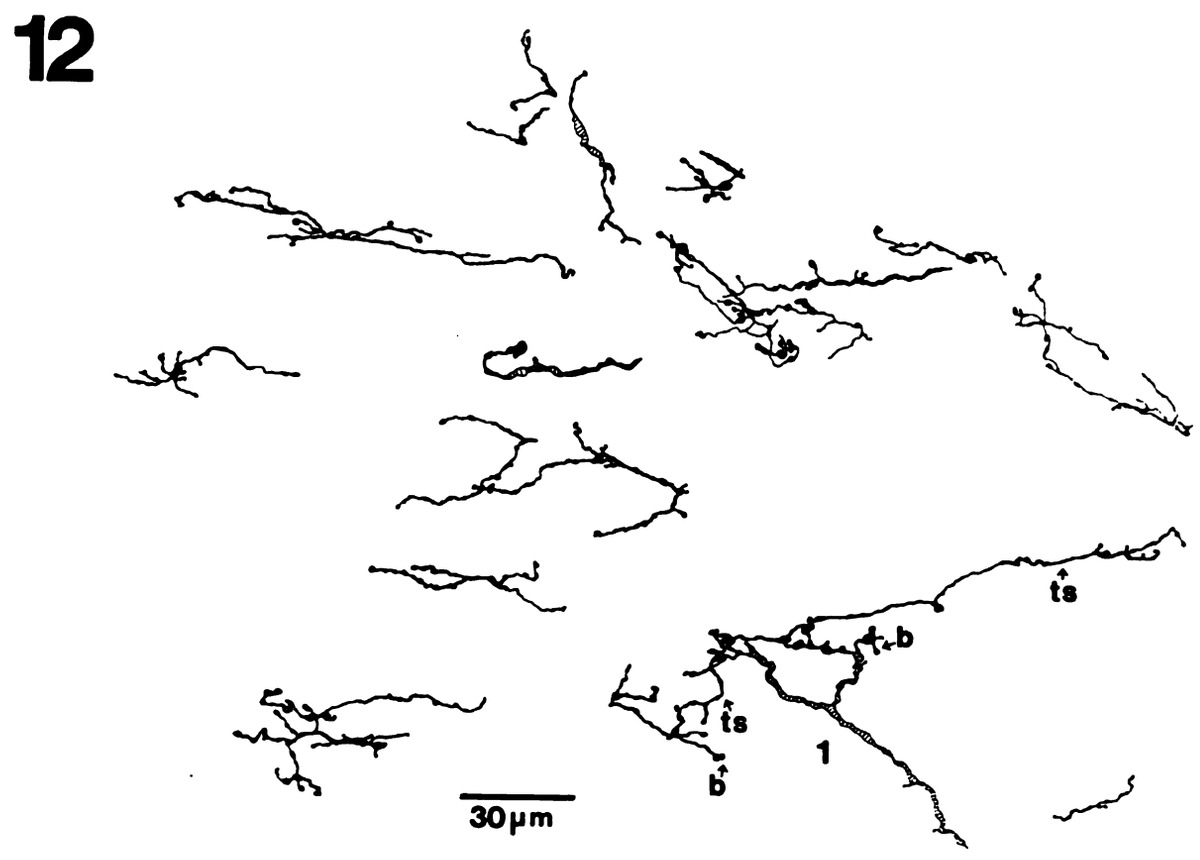

Figure 13: Photomicrographs that document the morphological characteristics of each type of Vo efferent terminal axonal arborization found in the various orofacial tactile regions of the cerebellum and deep cerebellar nuclei (dCN). (A) Representative spray of mossy fibers emerging from the white matter to enter and distribute throughout a folium within GCL and PCL. (B-F) Representatives of the types of morphologically distinct Vo efferent terminal axonal arborizations found in GCL and PCL; GCL-Simple (B), GCL-Complex (C), GCL-Filamentous (D), PCL-Complex (E), PCL-Simple (F). Representative type of morphologically distinct Vo efferent terminal axonal arborization found in dCN; single collaterals branch from parent fibers on their way to the cerebellar cortex (G), and terminate in (H) as single terminal strands (ts).

FIGURE 13

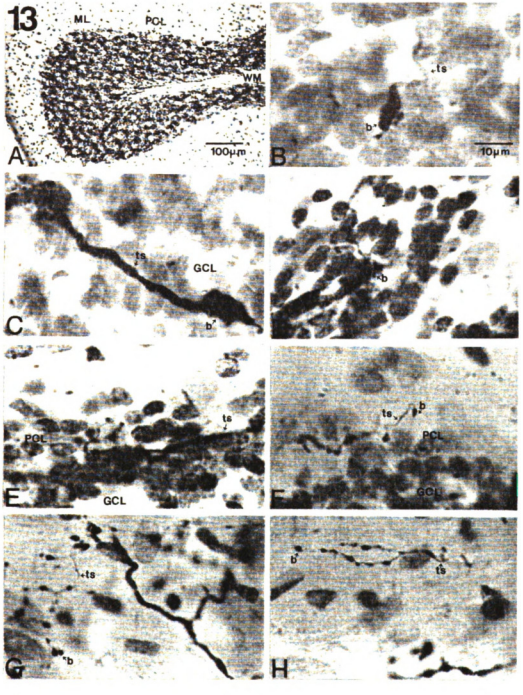
13
ML
POL
WM
100µm
A
ts
b
10µm
B
ts
GCL
b
C
b
POL
ts
GCL
E
ts
b
POL
GCL
F
ts
b
G
b
H

DATE DUE	DATE DUE	DATE DUE

TOPOGRAPHICAL DISTRIBUTION AND MORPHOLOGICAL FEATURES OF SECOND ORDER PROJECTIONS FROM IDENTIFIED SUBDIVISIONAL AREAS OF RAT TRIGEMINAL NUCLEUS ORALIS

VOLUME II

By

Lizabeth Ann Smith

A DISSERTATION

Submitted to
Michigan State University
in partial fulfillment of the requirements
for the degree of

DOCTOR OF PHILOSOPHY

Department of Anatomy

1992

THE D
IN C
SUB

Ne

Falls et

investiga

subdivisi

and func

axons wh

groups o

provide

dorsomed

synaptic

investiga

have est

originati

(SVN), i.

dorsal ho

'76; Burto

and Falls

CHAPTER III

THE DISTRIBUTION AND MORPHOLOGY OF AXONS TERMINATING IN CRANIAL NERVE NUCLEI FROM NEURONS IN IDENTIFIED SUBDIVISIONAL AREAS WITHIN RAT TRIGEMINAL NUCLEUS ORALIS

INTRODUCTION

Neuroanatomical studies in our laboratory (Falls, '84a; Falls, '86; Falls et al., '85; Falls and Alban, '86) and electrophysiological investigations (Hayashi, '82) have provided experimental evidence that each subdivision of rat trigeminal nucleus oralis (Vo) receives morphologically and functionally distinct groups of primary and non-primary afferent axons which are positioned to directly influence the activity of different groups of second order Vo projection neurons. These projection cells provide the efferent outflow from each of three Vo subdivisions; dorsomedial (DM), ventrolateral (VL) and border zone (BZ), and affect synaptic activity in numerous target areas along the neuraxis. Several investigations utilizing anatomical and electrophysiological methodology have established the existence of a direct trigeminospinal projection originating from neurons in each portion of the spinal trigeminal nucleus (SVN), i.e., Vo, trigeminal nucleus interpolaris (Vi) and the medullary dorsal horn (MDH; trigeminal nucleus caudalis) in rat (Burton and Loewy, '76; Burton and Lowey, '77; Leong et al., '84; Ruggiero et al., '81; Satoh, '79 and Falls, '83), hamster (Bruce et al., '84), cat (Burton et al, '79; Burton and

Loewy,

Matsus

et al.,

Martin,

Trigemi

project

Previous

and M

intertrig

'84a: Na

VI

'80). Ho

groups o

that the

pathway

continuir

contact is

obicularis

undertak

their ter

innervati

used a

notoneur

sensory n

vulgaris

previously

Loewy, '76; Craig, '78; Hayashi et al., '84; Kuypers and Maisky, '75; Matsushita et al., 82; Matsushita et al, '80; Matsushita et al., '81; Rustioni et al., '84; Tohyama et al., '79), dog (Craig, '78), opossum (Cabana and Martin, '84; Crutcher et al., '78), and monkey (Burton and Loewy, '77). Trigeminal projection neurons have been shown in retrograde studies to project to the facial nucleus (Nord, '67; Erzurumlu and Killackey, '80). Previous retrograde and anterograde transport studies have shown that Vi and MDH subdivisions within SVN send intratrigeminal and intertrigeminal projections (Gobel and Purvis, '72; Ikeda et al, '84; Falls, '84a; Nasution, '87).

VII receives afferent input from SVN (Erzurumlu and Killackey, '80). However, clear evidence for direct input from Vo neurons to specific groups of VII nucleus motoneurons is lacking. It is currently suggested that the consensual blink reflex is accomplished through a polysynaptic pathway originating in the ophthalmic division of the trigeminal nerve, continuing through SVN and the reticular formation before synaptic contact is achieved with VII motoneurons for bilateral eyelid closure via the obicularis oculi muscles. To date, no anatomical studies have been undertaken to examine the morphological features of efferent axons and their terminal arbors arising from neurons in each Vo subdivision and innervating the cranial motor and sensory nerve nuclei. In this study, we used a double-labeling technique to determine whether or not VII notoneurons innervating the obicularis oculi as well as cranial nerve and sensory nuclei are specific targets of Vo projection neurons. The Phaseolus vulgaris leuccoagglutinin (PHA-L) anterograde technique has been previously used to demonstrate the efferent projections from Vo to the

spin

'90a.

techn

popul

previo

'86).

morph

from n

identifi

quantit

includin

details o

present

relative

terminati

A prelim

Falls, '88

spinal cord, cerebellum and diencephalic nuclei (Smith and Falls, '88, '90a,b).

The anterograde Phaseolus vulgaris leuccoaglutinin (PHA-L) technique allows for comparison of projections from different neuronal populations, eg., spinal cord neurons, which have been identified previously using retrograde transport methods (Falls, '83; Falls, '84b; Falls, '86). This technique also allows for further characterization of morphological features of parent axons and terminal arborizations arising from neurons in each Vo subdivision and terminating in anatomically identified sensory, motor and autonomic areas in the brainstem. Detailed quantitative anatomical information about precise spatial features including source, destination, patterns of termination, and morphological details of Vo cranial nerve nuclei axonal connections is non-existent. In the present study, we have closely examined and compared the distribution, relative densities and morphological features of Vo efferent axons terminating in sensory, motor and parasympathetic cranial nerve nuclei. A preliminary report of these findings has been published (Smith and Falls, '88).

METHODS

Experiments were performed on twelve adult male Sprague Dawley albino rats (250-300) grams body weight. For PHA-L injections, a detailed protocol of the PHA-L method is given in a previous section (Chapt 1). All surgeries employed aseptic technique and all animals were housed, maintained and cared for according to federally prescribed guidelines (NIH Guide, '85). Under sodium pentobarbital anesthesia animals were placed in a stereotaxic apparatus and a small opening was made in the occipital bone and dura mater incised. A glass micropipette was used to deliver 2.5% PHA-L solution iontophoretically into DM, VL and BZ subdivisions of Vo. In a subpopulation, experimental animals were reanesthetized at 7-10 days following the PHA-L injections and pressure injections of 30% horseradish peroxidase (HRP, Sigma type VI) in 2% dimethylsulfoxide was delivered to the zygomatic branch of the facial nerve and the obicularis oculi muscle bilaterally. After PHA-L postinjection survival periods of 10-14 days and 48 hours following the HRP injections, animals were deeply anesthetized and perfused transcardially using a two stage procedure of Berod ('81). The brainstem was removed and postfixed overnight. The next day, 30 um thick coronal sections through the brainstem were obtained using an Oxford Vibratome. For PHA-L immunohistochemistry, sections were processed immediately according to a modification of the method of Gerfen and Sawchenko ('84). Sections were incubated in antibodies against PHA-L (1:2000; Vector Labs) and visualization of the PHA-L stain was insured once sections were processed with the avidin-biotinylated HRP (ABC) technique, (Hsu et al., '81) using a vectastain ABC kit (Vector Labs). The final peroxidase reaction was performed with a solution of 0.05%

di

Fo

slic

all

Lab

were

term

plotte

lucida

magni

magni

labeled

retrogra

HRP re

retrogra

locations

their cell

(25) phot

and their

VII neuro

diaminobenzidine in Tris buffer (0.05 M, pH 7.6) for 45-60 minutes. Following this, the sections were rinsed and mounted onto gelatin-coated slides. After counterstaining with cresyl violet acetate and coverslipping, all reacted sections were examined utilizing a light microscope (Leitz Laborlux 12) equipped with a drawing tube. Schematic reconstructions were made using an Aus Jena documator and each of the labeled fibers and terminal arborizations observed in the brainstem cranial nerve nuclei were plotted separately on representative drawings of the sections. Camera lucida drawings of labeled fibers and their terminal arbors were made at a magnification of 1,250 utilizing a 100X oil immersion objective. High magnification (100X) photomicrographs were made of representative labeled fibers and their terminals in the brainstem. For the analysis of retrogradely labeled cells, only those neurons demonstrating cytoplasmic HRP reaction product with a clearly visible nucleolus were identified as retrogradely labeled VII cells. Detailed drawings showing the precise locations of HRP-labeled neurons in Vo as well as the size and shape of their cell bodies were made at a magnification of 250X. High magnification (25) photomicrographs were made of representative PHA-L labeled fibers and their terminals which ended in close approximation to HRP labeled VII neurons.

RESULTS

INJECTION SITES

Unilateral PHA-L deposits were localized in discrete areas within each Vo subdivision (Figs. 1 and 2). Only areas containing densely filled neurons were considered to be effective zones from which efferent projections originated. Weak anterograde label was observed following injections in which PHA-L deposits only sparsely filled Vo projection neurons. In several cases (824, 826 and 750) PHA-L diffused into the spinal V tract (svt) and labeled numerous svt axons as far caudally as the MDH which serves to indicate that PHA-L may have been subject to uptake and transport by at least some fibers of passage. However, the potential problems of retrograde transport of PHA-L by fibers of passage published in other studies (Cliffer and Giesler, '88; Schofield, '90) did not play a significant role in the results of this study since cases of PHA-L deposition without spread into svt yielded similar results. The potential does exist for retrograde transport of PHA-L in that the labeled fibers found in svt could originate from VL neurons giving rise to spinal cord axonal projections since VL neurons have been shown to project through svt to the spinal cord (Falls, ' 83).

Most Labeled Vo efferent axons to cranial nerve nuclei coursed dorsomedially and medially through the gigantocellular (RFg) and parvocellular (RFp) reticular formation on their way to respective cranial nerve nuclei and the medial longitudinal fasciculus (mlf) bilaterally. In addition, a small contingency of Vo efferents coursed rostrally and caudally through Vms, Vi and MDH as they ascended and descended to these respective nuclei. Although the potential exists for possible labeling of

inter

and

distri

interf

previo

largely

(Cases

BZ inje

photogr

situated

slight s

rostrocau

injection

along the

distance

dorsoventr

Figs. 1,2 (

spread int

along the

700 um d

experimen

(Cases 739

in size to t

intertrigeminal fibers of passage originating from neurons located in Vi and MDH it was not thought to be significant in this study. The pattern of distribution and morphologies of labeled Vo intratrigeminal and intertrigeminal efferents were not identical in characteristics as described previously for Vi efferents to the spinal cord (Cook and Falls, '91).

In this study all twelve experiments resulted in injections of PHA-L largely restricted to either DM, VL or BZ. Three of the brains examined (Cases 734, 751 and 750) were used to illustrate representative DM, VL and BZ injection sites respectively in Fig. 1 A-C, schematically and Figs. 2 A-C, photographically. The DM injection site, Case 734 (Figs. 1,2 A), was situated in middle DM and partially filled dorsal and ventral zones with slight spread into dorsal BZ. The injection site measured 1180 um rostrocaudally, 850 um dorsoventrally and 400 um mediolaterally. The VL injection site, Case 751 (Figs. 1,2 B), was located approximately midway along the rostrocaudal length of Vo. The PHA-L deposit extended a short distance into BZ and measured 720 um rostrocaudally, 525 um dorsoventrally and 700 um mediolaterally. The BZ injection site, case 750 in Figs. 1,2 C was located in the dorsal two-thirds of the subdivision with some spread into the dorsal portion of VL. The injection site was located midway along the rostrocaudal extent of Vo and extended 1080 um rostrocaudally, 700 um dorsoventrally, and 300 um mediolaterally. In the additional six experiments injections were made at other locations in Vo subdivisions (Cases 739, 741, 751, 824, 826, and 860) and the injection sites were similar in size to those illustrated above and yielded similar results.

OVER

resulte
injecti
bilater
(SOL),
nucleu
contral
rostrall
trochlea
dorsal v
labeling
SOL, Vm
arbors w
arbors a
(Figs. 4
terminal
for the
Bilateral

PROJECT

OCULOM

Lab
level of th
rostrally t
following I

OVERALL PROJECTIONS TO THE CRANIAL NERVE NUCLEI

Ascending and descending projections form each Vo subdivision resulted in anterograde labeling in specific cranial nerve nuclei. Following injections into DM numerous axons formed dense terminal arborizations bilaterally in the trigeminal nuclear complex (SVC), solitary nucleus (SOL), trigeminal motor nucleus (Vmo), facial nucleus (VII), hypoglossal nucleus (XII), with fewer fibers terminating in the same nuclei contralaterally (Fig. 4). A smaller bilateral projection was observed rostrally in Edinger Westphal nucleus (EW), occulomotor nucleus (III), trochlear nucleus (IV), and nucleus abducens (VI) and caudally in the dorsal vagal nucleus (X) (Figs. 7 and 13). Injections into VL resulted in the labeling of terminal arbors bilaterally in sensory trigeminal complex SVC, SOL, Vmo, VII, and XII (Figs. 5, 8,9,10-12). Sparsely dispersed terminal arbors were found ipsilaterally in caudal X. The density of labeled terminal arbors appeared to be less than those observed following the DM injection (Figs. 4 and 5). Following an injection principally located in BZ, labeled terminal arbors were found to be predominately ipsilateral in SVC (except for the homologous area contralaterally in Vo), rostral SOL , Vmo. Bilateral projections were observed primarily in caudal SOL and VII.

PROJECTIONS TO CRANIAL NERVE MOTOR NUCLEI

OCULOMOTOR, TROCHLEAR AND ABDUCENS NUCLEI

Labeled parent axons coursed medially through the medulla at the level of the injection site to enter mlf bilaterally. Vo parent axons ascended rostrally to exit at appropriate levels to terminate in III and IV and VI following DM injections. Vo efferents were observed to give off collaterals

which

More r

trajecto

The ren

to enter

diffusely

were in

and in g

A

in each

0.2 to 0

terminal

umX 0.9

secondary

diameter

with its c

TRIGEMI

The

dorsal ro

following

axons of D

along the r

a band of

BZ injectio

enter ipsila

through th

which exited mlf in the pons and course laterally to enter VI bilaterally. More rostrally, labeled parent fibers were observed to continue on in their trajectory within mlf to exit in the mesencephalon and enter IV bilaterally. The remaining Vo axons in mlf were seen to exit and course rostromedially to enter III bilaterally. Labeled terminal arborizations were observed to be diffusely distributed along the rostrocaudal extent of these three nuclei and were in greater density ipsilaterally in VI, of equal density bilaterally in IV and in greater density contralaterally in III.

A single population of Vo efferent terminal arborizations was found in each of these nuclei. Upon entering each of these nuclei parent axons, 0.2 to 0.9 um in diameter continued as thin terminal strands. Each terminal strand was characterized by widely spaced boutons en passant 0.3 umX 0.9 um to 0.6 um X 1.1 um in diameter and occasionally emitted secondary side-branches which terminate in an end bouton (0.8-1.5 um in diameter). Sometimes these side branches are seen to redirect and course with its collateral branch.

TRIGEMINAL MOTOR NUCLEUS

The trajectory of parent fibers destined to innervate Vmo followed a dorsal route through the medullary and pontine reticular formation following injections into each Vo subdivision. At rostral Vo levels, parent axons of DM, VL and BZ neurons were observed to exit medially to course along the medial aspect of Vo within the reticular formation and give rise to a band of medially (following DM injections) or dorsally (following VL and BZ injections) directed labeled parent fibers. These fibers were observed to enter ipsilateral Vmo from its lateral and ventrolateral border, to course through the nucleus giving off collaterals along its dorsoventral and

medio

midlin

In adc

labelec

neurop

Vo effe

termina

contrala

were ob

projecti

in Vmo

describe

arboriza

distribut

Te

The term

is shown

bilaterall

measure

dorsomec

character

rise to ar

terminal

branches

um in dia

mediolateral extent, and to continue through the nucleus and cross the midline to enter the medial and ventromedial aspects of contralateral Vmo. In addition, following DM, VL and BZ injections, a small grouping of labeled efferent parent fibers was observed to course through the Vo neuropil and to the level of Vms and exit medially coursing with the other Vo efferents to innervate contralateral Vmo bilaterally. Labeled Vo efferent terminal arborizations were observed to be more diffusely distributed in contralateral Vmo. Although the labeled parent axons and terminal arbors were observed bilaterally following each subdivisional injection, the densest projection was always ipsilateral. Owing to the extremely sparse labeling in Vmo following a BZ injection, this subdivision is almost limited to being described as a predominately ipsilateral innervation of Vmo. Terminal arborizations were observed to be oriented in different planes, and were distributed somewhat homogeneously within the nucleus.

Terminal arbors from a single type of Vo efferent was found in Vmo. The terminal portions of the single population of Vo efferent axons to Vmo is shown in Fig. 8. Labeled terminal strands are found principally bilaterally after injections made in DM and VL. These terminal strands measure 0.2-1.3 um in diameter and are seen to run predominately in a dorsomedial direction for 80-300 um. The terminal strands are characterized by widely-spaced endings 0.8-2.0 um in diameter and giving rise to an occasional short side branch capped by an end bouton. These terminal strands frequently end in clusters of intermingling short branches bearing numerous boutons en passant and end boutons (1.5-3.0 um in diameter).

FACIA

were ob
within
the me
Parent
ventrall
labeled
the midl
found th
situated
density
neurons
neurons.

Tw
terminal
in latera
Parent a
type of V
terminal
mediolate
emitted s
branching
en passant
each other
efferent ter
lateral por

FACIAL MOTOR NUCLEUS

Following injections made into DM, VL and BZ labeled Vo axons were observed to issue from the dense area of labeled somata and axons within the injection site and course medially along a ventral path through the medullary reticular formation to ipsilateral and contralateral VII. Parent fibers were observed to course through the medulla and turn ventrally to enter ipsilateral VII from its dorsolateral aspect while other labeled axonal collaterals were seen to continue in their trajectory across the midline to terminate in contralateral VI. Terminal arborizations were found throughout the rostrocaudal extent of VII bilaterally and were situated in the lateral halves of VII bilaterally. A variation in the level of density of labeling for terminal arbors in VII was observed with DM neurons giving the densest innervation followed by VL and then BZ neurons.

Two morphologically distinct types of parent axons and their terminal arborizations were found to enter and intermingle with each other in lateral portions of VII following each subdivisional injection (Fig. 9). Parent axons giving rise to thin terminal strands characterized the first type of Vo-VII efferent and its terminal arbor. These bouton bearing terminal strands were 0.2 to 1.3 um in diameter and were found to course mediolaterally and dorsoventrally for 15-200 um. During their course they emitted several side branches which underwent secondary and tertiary branching. These side branches contained several multi-shaped boutons en passant and end boutons (0.9-2.4 um in diameter) and intermingled with each other to form small clusters of terminal fibers (Fig. 9). Type 1 Vo-VII efferent terminal arborizations were found dorsally in the intermediate and lateral portions of the nucleus. The second type of Vo-VII efferent was

found

These

diamet

(1.0-1.9

HYPOG

L

the ret

termina

neurons

aspect

labeled

medially

rostral a

medially

XII from

giving o

contralat

parent fi

the Vo n

with the

labeled V

DM injec

efferent t

Tw

XII origi

terminati

found ventrally in the intermediate and lateral portions of VII bilaterally. These strands ran dorsoventrally for 150-200 um and measure 0.2-1.0 um in diameter. They were sparsely branched and contain widely spaced small (1.0-1.9 um in diameter) axonal endings (Figs. 9 and 14).

HYPOGLOSSAL NUCLEUS

Labeled parent axons coursed dorsally and dorsomedially through the reticular formation and the neuropil subadjacent to SOL before terminating in XII. At caudal Vo levels, parent axons of DM and VL and neurons were observed to exit dorsomedially and medially along the medial aspect of Vo and course within the reticular formation as a bundle of labeled Vo efferent axons running dorsomedially at rostral Vi levels and medially at caudal Vi levels following DM injections and dorsomedially at rostral and caudal levels following VL injections. These dorsomedially and medially directed labeled parent fibers were observed to enter ipsilateral XII from its lateral or ventrolateral aspects, to course through the nucleus giving off collaterals and to cross the midline to enter the medial aspect of contralateral XII. Additionally, following DM and VL injections, labeled parent fibers were observed to course dorsomedially and medially through the Vo neuropil and exit at more caudal levels from Vi and MDH to course with the other Vo fibers to enter XII bilaterally. The greatest density of labeled Vo efferent terminal arborizations was always observed following DM injections and were ipsilateral to the injection site. No labeled Vo efferent terminal arbors were seen in XII following a BZ injection.

Two types of labeled Vo efferent terminal arborizations was seen in XII originating from DM and VL neurons. Type 1 terminal strands terminating in the rostral one-half of XII were observed to have a

dorsoventra
diameter) bo
Type 1 effer
to 3.5 um in
one-half of t
ran mediola
Several bout
along the st
branches be
and14).

PROJECTIO

SENSORY T

Follow
were located
seen coursin
terminal arb
homologous
labeled ter
contralateral
terminal arb
for the contr
ipsilaterally.
internuclear
referred to as
'84) which u

dorsoventral orientation and were characterized as thin (0.2-1.0 um in diameter) bouton bearing strands that emit few side branches. Frequently, Type 1 efferents would end in terminal clusters characterized by large (up to 3.5 um in diameter) irregularly shaped axonal endings. In the caudal one-half of the nucleus, Type 2 efferents had thin terminal strands which ran mediolaterally for 60-270 um and measured 0.2-1.0 um in diameter. Several boutons en passant (measuring 0.7-2.0 um in diameter) were seen along the strands that terminated in an end bouton. Occasional side branches bearing 1-7 endings emanated from the parent shaft (Figs. 10 and14).

PROJECTIONS TO CRANIAL SENSORY NUCLEI

SENSORY TRIGEMINAL NUCLEI

Following DM, VL and BZ injections, labeled terminal arborizations were located in the homonymous Vo subdivision. Parent fibers were also seen coursing within contralateral Vms, Vi and MDH and giving rise to terminal arborizationns located within an area of these SVC nuclei that is homologous to that of the injection site, eg., VL injections give rise to labeled terminal arbors situated in the ventrolateral portions of contralateral Vms, Vo, Vi and MDH. However, the density of labeled terminal arbors was always less compared to that seen ipsilaterally except for the contralateral Vo subdivision innervated by its homonymous area ipsilaterally. Vo efferent parent axons utilized three pathways to provide internuclear innervation. On pathway, utilized ipsilaterally, has been referred to as an "intranuclear" route (Gobel and Purves, ';72 Ikeda et al, '84) which uses the deep axon bundles running rostrocaudally through

SVC. Tw

al., ('84)

used for i

the area o

Axo

Vms, Vi a

ventrolater

DM neuron

characteriz

running do

few widely

short side b

shaft. Type

diameter) w

branches be

diameter, re

type of Vo e

SVC Type 2

contralatera

similar to th

ipsilateral V

arborization

there tende

present in ta

SVC. Two additional pathways taken by parent axons, referred by Ikeda et al., ('84) as "intertrigeminal" routes incorporated routes within the svt (used for ipsilateral projections) and the reticular formation subadjacent to the area of the injection site (utilized for contralateral projections).

Axons of Vo neurons projecting to contralateral Vo and bilaterally to Vms, Vi and MDH, were of two types which ran in dorsomedial and ventrolateral directions within SVC. Vo efferents of both types arising from DM neurons terminated in SVC bilaterally. The first type, SVC Type 1, is characterized by a single thin terminal strand (0.4-0.7 um in diameter) running dorsoventrally for approximately 80-100 um in length and emitting few widely spaced terminal endings (0.7-1.9 um in diameter) Occasionally short side branches bearing an end bouton would emanate from the parent shaft. Type 2 SVC Vo efferents had a thicker parent strand (0.6-1.0 um in diameter) which emitted several secondary and tertiary bouton bearing side branches bearing en passant and end boutons (0.6-1.3 um and 1.0-2.0 um in diameter, respectively). Following injections made in VL, the predominate type of Vo efferent terminal arborization is characterized as being of the SVC Type 2 which are found ipsilaterally in Vms, Vi and MDH and in contralateral SVC. Following injections made in BZ, terminal arbors similar to that of the SVC Type 1 are found in contralateral SVC and in ipsilateral Vms, Vi and MDH. Although both Type 1 and Type 2 terminal arborizations were found in SVC bilaterally following VL and BZ injections, there tended to be an overwhelming number of one or the other types present in target zones examined (Figs. 11 and 15).

PROJECT

The
described f
caudal Vo
reticular fo
in the med
reticular f
direction a
SOL levels
were obser
SOL. Vo
ipsilateral
mediolatera
density of la
seen followi
branches, al
XII to inne
innervation.
with the pr
axonal fiber
appropriate
directly acr
projections f
with those d

Termi
were of two
arborizations

PROJECTIONS TO SOLITARY NUCLEUS

The manner in which Vo efferents arrived at SOL is similar to that described for XII. Parent axons from DM, VL and BZ neurons exited from caudal Vo directly medial to their respective injection sites to course in the reticular formation directly adjacent to SVN. At appropriate caudal levels in the medulla, labeled parent fibers were observed coursing through the reticular formation and neuropil adjacent to SOL in a dorsomedial direction at rostral SOL levels and in a medioventral direction at caudal SOL levels following DM and BZ injections. Parent fibers of VL neurons were observed to course dorsomedially toward the rostrocaudal extent of SOL. Vo efferent fibers were observed to enter the lateral aspect of ipsilateral SOL and terminate throughout its rostrocaudal and mediolateral extent following DM, VL and BZ injections. The greatest density of labeled Vo efferent terminal arborizations in ipsilateral SOL was seen following DM injections followed by BZ and VL injections. Collateral branches, although fewer in number, coursed across the midline through XII to innervate contralateral SOL. DM neurons gave the heaviest innervation. SOL innervation was made equally by VL and BZ neurons. As with the preceeding descriptions, a small group of labeled Vo efferent axonal fibers were observed to course through caudal Vo to exit at appropriate Vi and MDH levels to exit the medial portions of SVN is an area directly across from the homologous SVN area receiving internuclear projections form Vo. Once in the reticular formation, these fibers mixed with those described earlier and coursed to SOL bilaterally.

Terminal arborizations within SOL arising from Vo parent axons were of two morphologically distinct types. Both types of terminal arborizations are seen bilaterally after DM, VL and BZ injections. In the

rostral ha
approxima
diameter.
the strands
caudally in
measuring
length. Nu
been observ
side branche

PROJECTIO

EDINGER-W

The t
described fo
observed to
enter the n
III a slight
terminal ar
gave rise to
um in diar
direction.
boutons en
observed to
terminal ar
diameter,
interval and

rostral half of SOL, thin terminal strands run mediolaterally for approximately 200 um and measure less than or equal to 0.4um in diameter. Widely spaced boutons (1-2 um in diameter) were found along the strands which emit widely spaced short side branches (Fig. 12). More caudally in SOL, terminal strands are also observed to run mediolaterally, measuring 0.5 um in diameter and extending approximatly 300um in length. Numerous, as many as thirty-nine widely spaced endings have been observed along the strands that emit occasional widely spaced short side branches (Fig. 12).

PROJECTIONS TO CRANIAL AUTONOMIC NUCLEI

EDINGER-WESTPHAL NUCLEUS

The trajectory of parent fibers innervating EW was similar to that described for Vo efferents innervating III and VI. Vo parent fibers were observed to course further rostrally in mlf to exit in the mesencephalon and enter the nucleus along its lateral borders bilaterally. Like that found in III a slight density gradient was found with a greater number of labeled terminal arbors found contralaterally. A single population of parent axons gave rise to the terminal arborizations (Fig. 13). Terminal strands 0.3-1.0 um in diameter were seen to course predominately in a dorsoventral direction. Each terminal strand was characterized by widely spaced boutons en passant 0.7-1.5 um in diameter and a few side branches were observed to emanate from the terminal strands. This type of Vo efferent terminal arborization was similar in its morphology as well as its axonal diameter, frequency of branching and characteristics of interbouton interval and bouton size to that found caudally in X.

that d
dorsom
subadja
parent a
and med
sites and
They gav
rostral V
following
following
parent fib
ventrolater
terminal ar
greater den
ipsilateral X
contralateral
single popula
terminal arbo
EW (Fig. 13).
and were see
bouton conta
bouton bearin

DORSAL VAGAL NUCLEUS

The manner at which Vo efferent axons arrived at X is similar to that described for SOL and VII. The parent axons coursed dorsally and dorsomedially through the reticular formation and the neuropil subadjacent to X prior to innervating ipsilateral X. At caudal Vo levels parent axons of DM and VL neurons were observed to exit dorsomedially and medially along the medial aspect of Vo from their respective injection sites and to course in the reticular formation in close proximity to SVN. They gave rise to a group of labeled Vo efferents which ran dorsomedially at rostral Vi levels and medially at caudal Vi and rostral MDH levels following DM injections and dorsomedially at rostral and caudal levels of X following VL injections. The dorsomedially and medially directed labeled parent fibers were observed to enter ipsilateral X from its lateral or ventrolateral aspect and course in and through the nucleus, giving off terminal arborizations along its dorsoventral and mediolateral extent. A greater density of labeled terminal arbors was observed more laterally in ipsilateral X. A sparse scattering of labeled terminal arbors was observed contralaterally in the caudal portion of X only following DM injections. A single population of parent axons (0.4-1.2 um in diameter) gave rise to terminal arborizations in X. These were of the same type which innervated EW (Fig. 13). Terminal strands measured approximately um in diameter and were seen to course predominately in a dorsoventral direction. Each bouton containing terminal strand was characterized as thin with a few bouton bearing side branches and widely spaced interbouton intervals.

ADDITIO

Vo e

(AMB) an

However, t

and diffus

identificatic

observed in

Vmes bilate

of axons ari

observed fo

distribution

injections fo

was observe

warrant the

projections.

ADDITIONAL PROJECTIONS

Vo efferent projections were observed to innervate nucleus ambiguus (AMB) and the trigeminal mesencephalic nucleus (Vmes) bilaterally. However, the labeled parent axons and terminal arbors were very sparse and diffusely distributed within these nuclei and precluded positive identification of actual termination. It is interesting that of the Vo efferents observed in these two nuclei, a greater majority were seen ventrally in Vmes bilaterally following BZ injections with an abrupt fall in the numbers of axons arising from DM and VL neurons. A similar situation was also observed for Vo efferents labeled in AMB. The densest pattern of distribution for labeled efferents in ipsilateral AMB was seen following BZ injections followed by DM and VL injections. Extremely sparse labeling was observed in contralateral AMB. It is thought that future studies warrant the investigation of these diffuse and sparse Vo efferent projections.

Vo INNER

The

III, IV an

underlying

orienting r

In particul

be a necess

already a r

ventral to

stratum alb

album profu

arises from

possibility t

turning of t

toward a no

efferents pr

deep layers

musculature

and Harding

pinnae move

pontomedulla

nuclei (Verte

Martin, '83; T

spinal cord (C

DISCUSSION

Vo INNERVATION OF OCULAR MOTOR NUCLEI

The demonstration of Vo efferent projections to cranial nerve nuclei III, IV and VI suggest that Vo may be part of a complex substrate underlying orienting reflexes. The precise pathways for execution of the orienting reflex are far from clear and include several contributing nuclei. In particular, the deep layers of the superior colliculus (SC) are thought to be a necessary element in eliciting orienting behaviors (Peterson, '80). It is already a matter of fact that SVN, especially Vi, projects to SC (those ventral to stratum opticum; including stratum griseum intermediale, stratum album intermediale, stratum griseum profundum and stratum album profundum) (Rhoades et al., '89). A Vo efferent projection to SC arises from DM, VL and BZ neurons, unpublished observation). The possibility that the orienting reflex which is manifested by a characteristic turning of the head, with concomitant movement of the eyes and pinnae toward a novel stimulus, may be executed directly through deep tectal efferents projecting to appropriate motor structures. Intermediate and deep layers of SC project to the upper cervical segments, innervating axial musculature involved in elicitation of head turning movements (Huerta and Harding, '82), to the cranial motor nuclei involved in extraocular and pinnae movements (Vidal et al., '88; Keller, '79; Graham, '77) and to the pontomedullary reticular formation which projects to these cranial motor nuclei (Vertes et al., "86; Kawamura and Hashikawa, '78; Panneton and Martin, '83; Takeuchi et al., '79). Since Vo projects to SC and the cervical spinal cord (Chapt 1) as well as the cranial nerve nuclei involved in eye and

pinna

activi

Vo IN

represe

muscle

and ner

'66; Dom

motoneu

dorsally,

subdivisio

dorsal inte

and Lodg

representat

al, '73). I

proboscis ar

intermediate

Hinrichsen a

Report

from Vo to

Killackey, '7

an ipsilatera

of VII (Hi

Trigeminofac

horn, are to

pinnae movements it is probable that it is well situated to modulate neural activity occurring during the orienting response.

Vo INNERVATION OF OROFACIAL MOTOR NUCLEI

The organization of rat VII has been mapped for nerve representation (Martin and Lodge, '77; Szekely and Matesz, '82) as well as muscle representation (Watson et al, '82). In addition, a general muscle and nerve pattern exists for a number of mammalian species (Courville, '66; Dom, '82; Kume et al., '78; Martin and Lodge, '77; Provis, '77). Facial motoneurons are organized so that dorsal muscles are represented dorsally, and ventral muscles ventrally (Provis, '77). Basically, six subdivisions are described; lateral, dorsolateral, ventral intermediate, dorsal intermediate, ventral medial and dorsal medial (Greene, '63; Martin and Lodge, '77; Papez, '27; Watson et al., '82). The zygomatic representation extends throughout the intermediate portion of VII (Dom et al, '73). It has been demonstrated that motoneurons innervating the proboscis are situated lateral within VII, oral and orbital motoneurons are intermediate, and pinnae and neck motoneurons are medial (Watson, '82; Hinrichsen and Watson, '83).

Reported projections from SVC to VII include ipsilateral projections from Vo to the lateral and intermediate divisions (Erzurumlu and Killackey, '79; Hinrichsen and Watson, '83; Travers and Norgren, '83) and an ipsilateral projection from MDH (medial lamina) to the medial division of VII (Hinrichsen and Watson, 83; Senba and Tohyama, '83). Trigeminofacial and spinofacial projections, originating from the dorsal horn, are topographically organized with facial motoneurons receiving

cutaneous
(Panneton
Vo p
an involvm
labeling p
originating
trigeminal
motoneuro
participatic
portions of
al., '82). La
nasolabial r
to whisk vib
muscles are
contributing
greater rol
movements.
projections t
Leu-e
Tohyama, '8
since enkep
al., '78; Urca
effects (Cha
illustrated (P
A clas
medial and
'56). SOL re

cutaneous input from areas overlying the muscles they innervate (Panneton and Martin, '83).

Vo projections to intermediate subdivisions of VII bilaterally suggest an involvment of these axons in the consensual blink reflex. The double-labeling portion of this study confirms that Vo efferent projections originating from VL, receiving input from the ophthalmic division of the trigeminal nerve, are situated in close proximity to retrogradely labeled VII motoneurons. Vo projections to ventral portions of VII suggests participation of these fibers in the pinnae orienting reflex since ventral portions of VII are innervated by the posterior auricular nerve (Watson et al., '82). Lateral projections may be contributing to finer adjustments of the nasolabial muscles. This is expected since rats use the nasolabial muscles to whisk vibrissae (a rapid and finely coordinated movement). Since facial muscles are not only involved in communication but also feeding and contributing to an open airway during breathing, Vo neurons may play a greater role than just providing for reflex responses or coordinated movements. This suggestion seems quite plausible in light of additional Vo projections to SOL and AMB.

Leu-enkephalin has been detected in axons in VII (Senba and Tohyama, '83) and it may be utilized by Vo neurons to affect motor functions since enkephalins have been shown to have epileptic properties (Frenk et al., '78; Urca et al., '78) and enkephalin receptors are related to behavioral effects (Chang et al., '80). Enkephalin-like Vo neurons have been illustrated (Bowker, '88).

A classical division of SOL exists that divides this nucleus into medial and lateral portions based on morphological differences (Torvick, '56). SOL receives afferents from V, VII, IX, and X cranial nerves, which

form

Senso

with V

part of

to the c

and XII

to X an

coereleu

cardiova

Vo

types of

suggests

the XII, V

form the solitary tract and terminate rostrocaudally within the nucleus. Sensory axons of VII terminate in the rostral portion of lateral SOL, along with V and IX afferents. X and some IX afferents terminate in the medial part of SOL at levels rostral to the obex and the lateral portion of SOL caudal to the obex. Axons originating in the rostral part of SOL project to VII, V, and XII. Those projections originating from the caudal part of SOL project to X and AMB. A substanital projection to the ventral medulla, locus coereleus, and parabrachial nuclei implicate SOL involvement in cardiovascular and respiratory control.

Vo efferent projections to SOL with two morphologically different types of terminal arbors terminating in rostral or caudal SOL portions suggests that Vo may be modulating the X output of SOL differently from the XII, V and VII outputs.

Figure 1:
injection s
A-C). Ar
zone (BZ)
DM, partly
VL. C. A
spread into
facial moto

Figure 1: Low power photomicrographs showing the location of PHA-L injection sites in the three subdivisions of rat trigeminal nucleus oralis (Vo; A-C). Arrows identify dorsomedial (DM), ventrolateral (VL) and border zone (BZ) subdivisions. A. An injection situated in the middle portion of DM, partly filling its dorsal and ventral zones. B. An injection located in VL. C. An injection located in the dorsal two-thirds of BZ with some spread into the dorsal area of VL and the spinal trigeminal tract (svt). VII, facial motor nucleus.

FIGURE 1

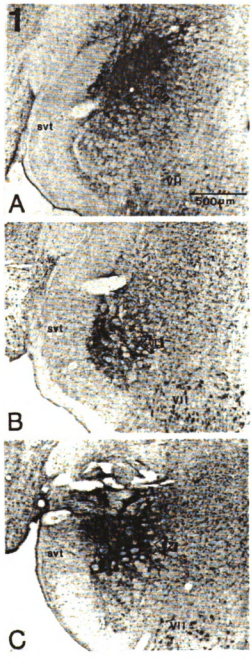

Figure 2:
which illus
A-C. A. A
illustration
injection sit

Figure 2: Camera lucida drawings of transverse sections through Vo (A-C) which illustrate the locations of the three injection sites shown in Figure 1 A-C. A. An illustration of an injection site contained within DM. B. An illustration of an injection site located in VL. C. An illustration of an injection site in BZ with slight spread into the dorsal portions of VL and svt.

Figure
injectio
bodies i
obicular
some spr
point to r
L labeled

Figure 3: Low power photomicrographs showing the locations of a PHA-L injection site and horseradish peroxidase (HRP) retrogradely labeled cell bodies in the facial motor nucleus (VII) following injections made into the obicularis oculi muscles bilaterally. A. An injection situated in VL with some spread into svt. B-C. Higher power photomicrographs of VII. Arrow point to retrogradely labeled cell bodies that are closely approached by PHA-L labeled VL terminal arborizations.

FIGURE 3

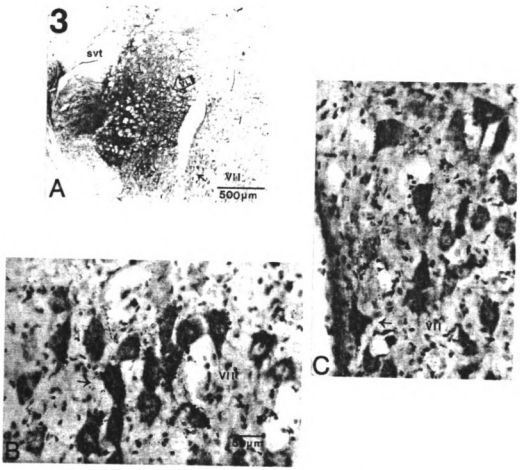

FIGUR
through
mesence
the medu
anterogra
injections
terminal a
nucleus (
bilaterally
abducens n
sensory com

FIGURE 4: Camera lucida drawings of coronal/transverse sections through different levels of the rat brainstem. A-C. Sections through the mesencephalon. E-F. Sections through the pons. G-H. Sections through the medulla. These sections illustrate the topographical organization of anterogradely labeled parent fibers and terminal arborizations after DM injections. Numerous axons are observed to form moderate to dense terminal arborizations primarily contralaterally in the Edinger Westphal nucleus (EW) and ipsilaterally in the dorsal vagal nucleus (X) and bilaterally in the oculomotor nucleus (III), trochlear mucleus (IV), abducens nucleus (VI), trigeminal motor nucleus (Vmo), VII, trigeminal sensory comples (SVC) and solitary nucleus (Sol).

4

PSLA

A

B

C

D

FIGURE 4

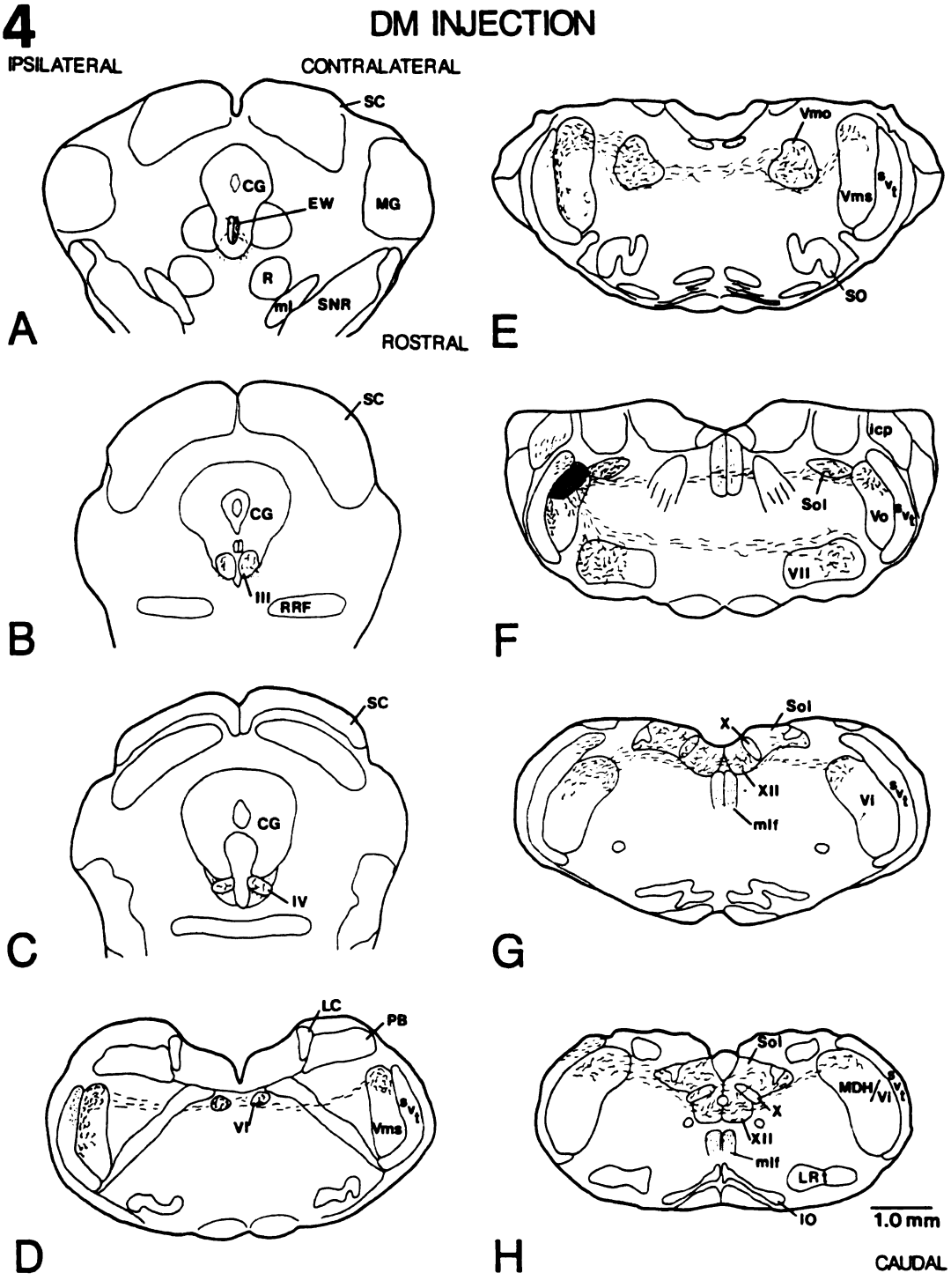
4
DM INJECTION
IPSILATERAL
CONTRALATERAL
SC
CG
EW
MG
R
ml
SNR
A
ROSTRAL
Vmo
Vms
SVt
SO
E
SC
CG
III
RRF
B
icp
Sol
Vo
SVt
VII
F
SC
CG
IV
C
Sol
X
XII
mlf
VI
SVt
G
LC
PB
SVt
Vms
VI
D
Sol
MDH/VI
SVt
X
XII
mlf
LRt
IO
1.0 mm
H
CAUDAL

Figure 5:
the rat br
the medul
anterograc
Numerous
bilaterally

Figure 5: Camera lucida drawings of coronal/transverse sections through the rat brainstem. A. Sections through the pons. B-D. Sections through the medulla. These sections illustrate the topographical organization of anterogradely labeled fibers and terminal arborizations after VL injections. Numerous axons form dense terminal arborizations ipsilaterally in X, bilaterally in Vmo, VII, XII, SVC and Sol.

FIGURE 5

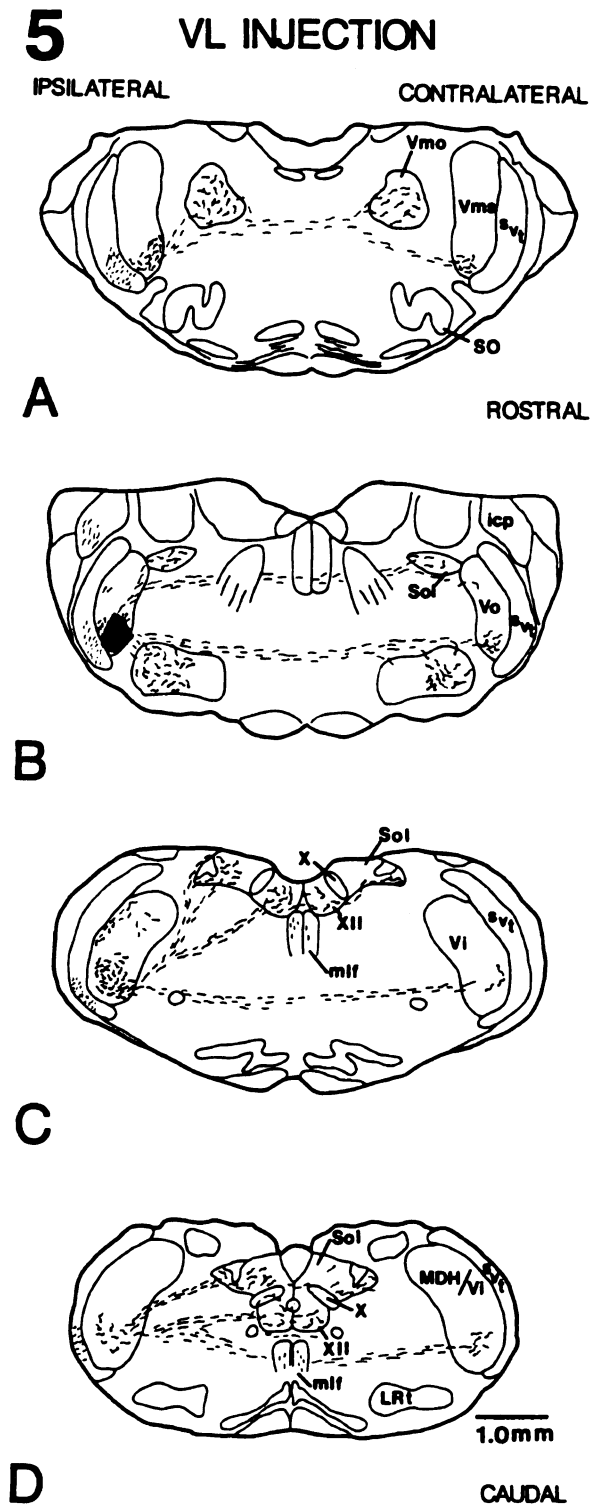
5
VL INJECTION
IPSILATERAL
CONTRALATERAL
Vmo
Vme
svt
so
A
ROSTRAL
icp
Sol
Vo
svt
B
Sol
X
XII
mlf
svt
Vl
C
Sol
MDH/Vl
svt
X
XII
mlf
LRt
1.0mm
D
CAUDAL

Figure 6

the rat b

medulla.

anterogra

Numerou

in Vmo a

SVC and

Figure 6: Camera lucida drawings of coronal/transverse sections through the rat brainstem. A. Section through the pons. B-D. Sections through the medulla. These sections illustrate the topographical organization of anterogradely labeled fibers and terminal arborizations after BZ injections. Numerous axons form dense terminal arborizations primarily ipsilaterally in Vmo and bilaterally (with a strong ipsilateral predominance) in VII, SVC and bilaterally in Sol.

FIGURE 6

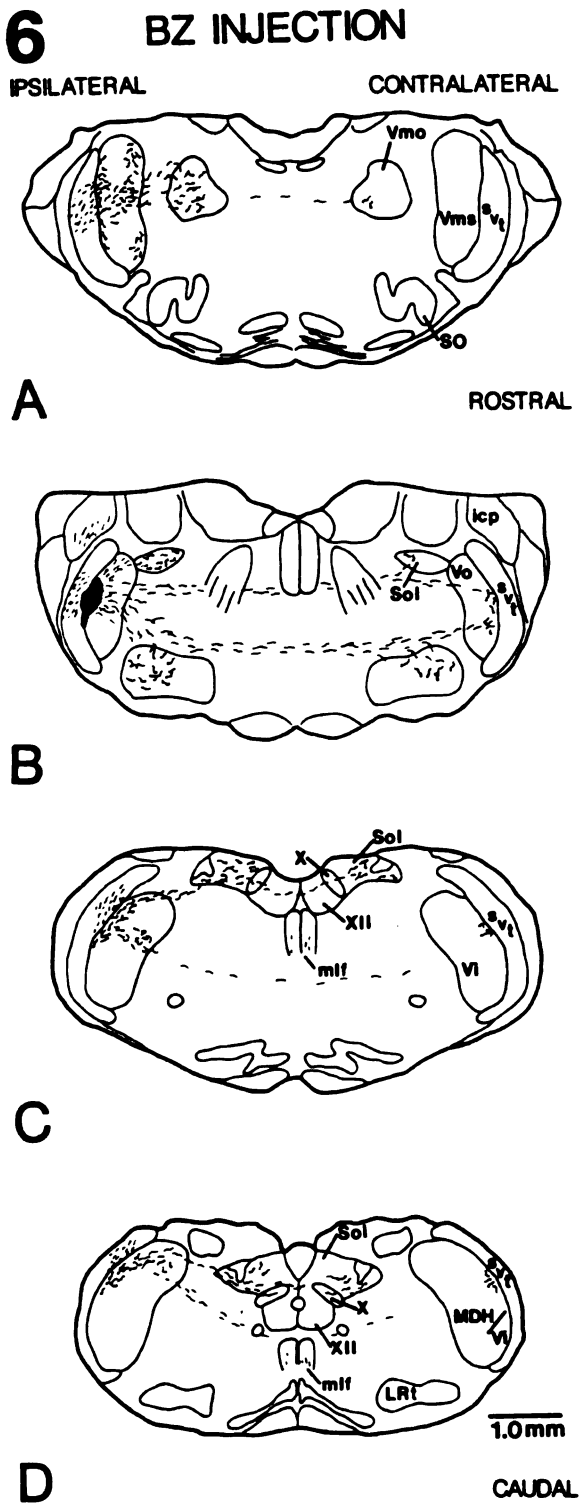
6
BZ INJECTION
IPSILATERAL
CONTRALATERAL
Vmo
Vms
SVt
SO
A
ROSTRAL
icp
Vo
Sol
SVt
B
Sol
X
XII
mlf
SVt
Vl
C
Sol
X
XII
mlf
LRt
MDH
Vl
SVt
1.0mm
D
CAUDAL

Figure 7
terminal
made in
and cont
to emit
end bout

Figure 7: A high power reconstruction of a single type of labeled Vo efferent terminal arborization found in III, IV and VI only following injections made in DM. Many terminal arbors can be found throughout ipsilateral and contralateral III, IV and VI. The thin terminal strands are observed to emit several short side branches bearing small boutons en passant and end boutons (b).

Figure

termir

the th

charac

giving

B. Th

short b

Figure 8: A high power reconstruction of a single type of labeled Vo efferent terminal arbor found in Vmo after an injection of PHA-L made into each of the three Vo subdivisions. A. The single type of terminal ending is characterized by a thicker terminal strand with widely spaced endings giving rise to an occasional short side branch capped by an end bouton (b). B. These terminal strands frequently end in clusters of intermingling short branches bearing numerous boutons en passant and end boutons (b).

FIGURE 8

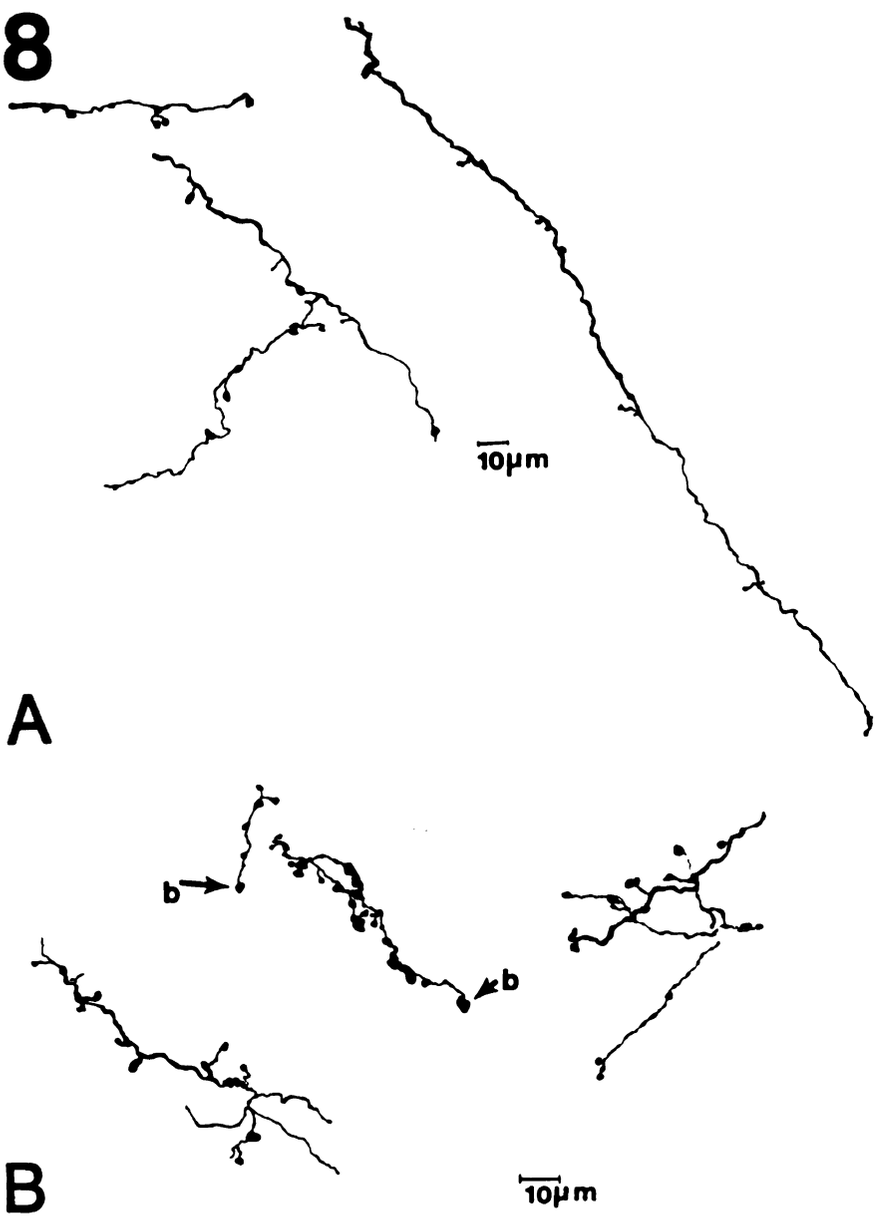

Figur

arbori

are tw

consis

severa

contai

B. Oc

with e

type o

VII. T

widely

Figure 9: A high power reconstruction of PHA-L labeled terminal arborizations in VII bilaterally following DM, VL and BZ injections. There are two morphologically distinct types of terminal strands. A. One type consists of a thin terminal strand located dorsally within VII which emits several side branches that undergo secondary and tertiary branching containing several multi-shaped boutons en passant and end boutons (b). B. Occasionally several side branches of the type shown in (A) intermingle with each other to form small clusters of terminal fibers. C. The second type of labeled Vo efferent terminal arborization is found ventrally within VII. This type of terminal arbor is thin and sparsely branched, containing widely spaced small axonal endings.

FIGURE 9

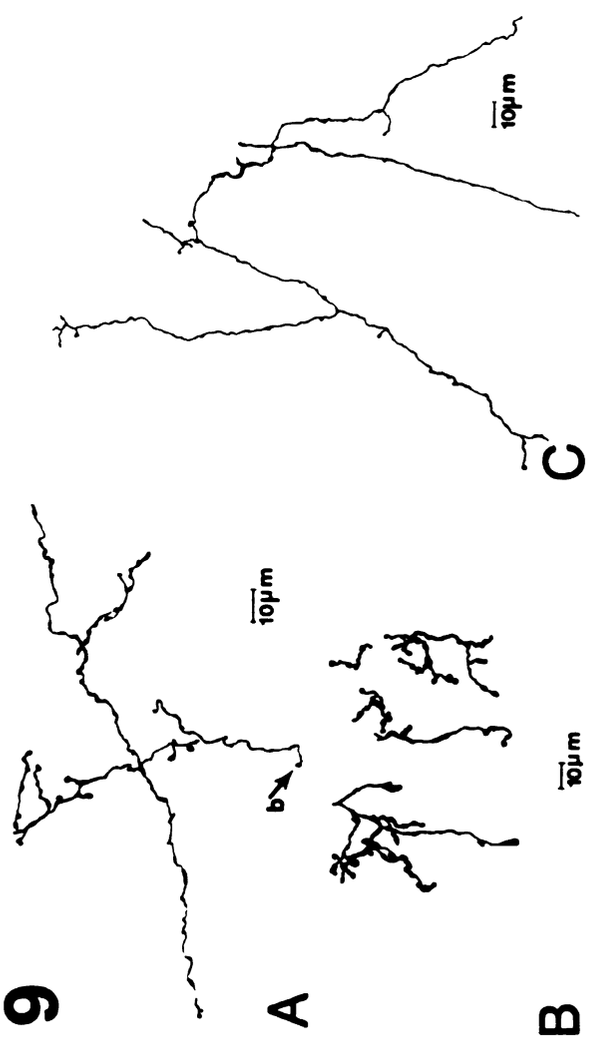

Figure 10: A high power reconstruction of two types of morphologically distinct labeled terminal arborizations found within XII bilaterally originating form DM and VL neurons. A. One type, terminating in the rostral one-half of XII, is characterized as a thin, bouton bearing, terminal strand which emits an occasional side branch. B. Frequently, the type of Vo efferent terminal arbor shown in (A) ends in a terminal cluster characterized by large irregularly shaped terminal end boutons (b). C. In the caudal one-half of XII, thin terminal strands are observed to frequently emit several side branches bearing 1-7 endings emanating from the parent shaft.

FIGURE 10

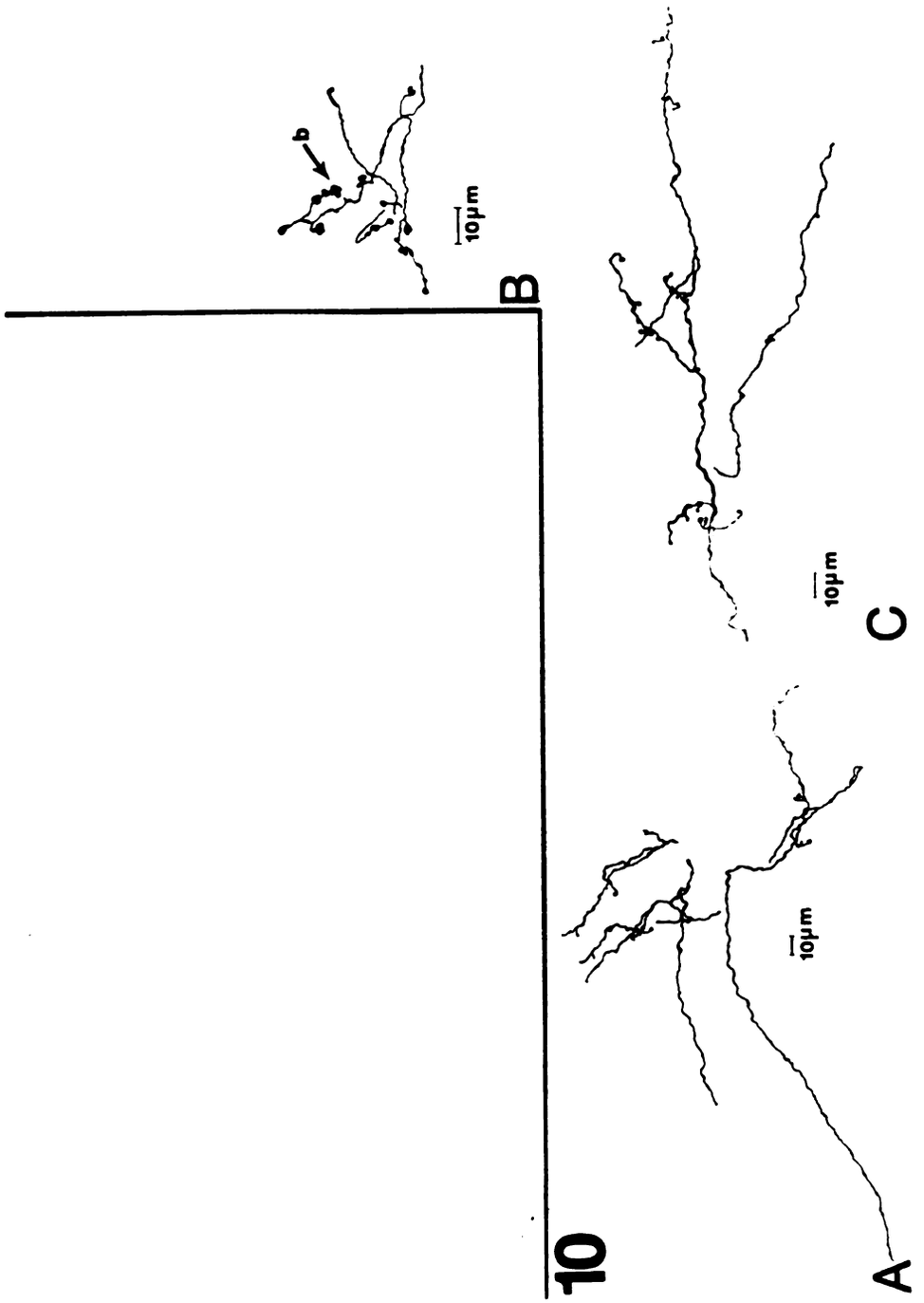

Figure 11: High power reconstructions of PHA-L labeled terminal arborizations in SVC following injections made in all three Vo subdivisions. A. Two morphologically distinct types of Vo efferents, following a DM injection, are observed in an area homologous to that of the injection site ipsilaterally in the main sensory trigeminal nucleus (Vms), trigeminal nucleus interpolaris (Vi) and medullary dorsal horn (MDH) and contralaterally in Vms, Vo, Vi and MDH. The first type (SVC Type 1) (arrowhead) is characterized by a thin terminal strand with a few widely spaced terminal endings while the second type (arrow, SVC Type 2) has a thicker parent strand and emits several secondary and tertiary side branches bearing boutons en passant and end boutons (b). B. Following VL injections, the predominate type of Vo efferent terminal arborization in SVC is characterized as being of the SVC Type 2. C. Following injections made in BZ, terminal arbors similar to the SVC Type 1 are found in SVC bilaterally.

FIGURE 11

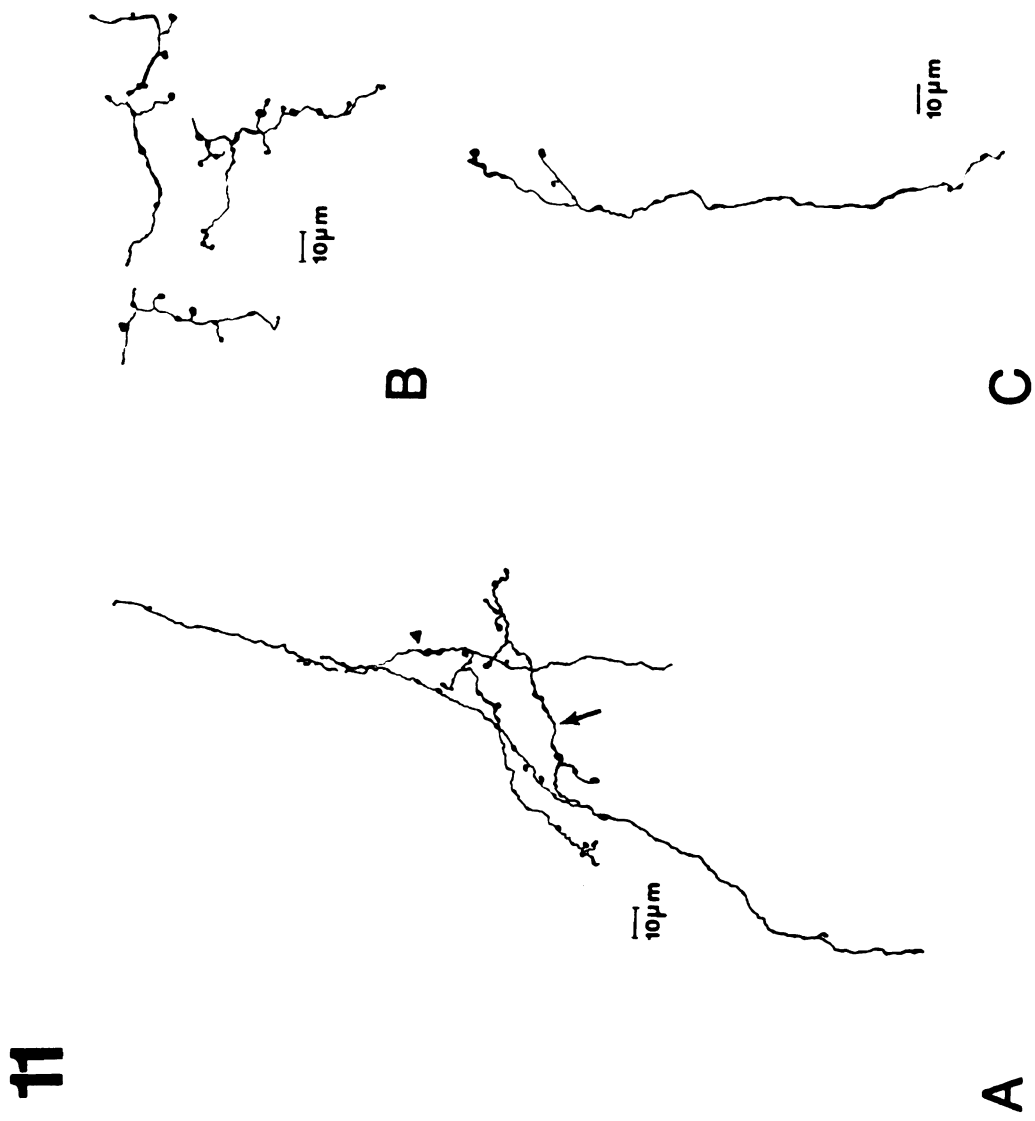

11

Figure 12: A high power reconstruction of two types of labeled Vo efferent terminal arborizations found in Sol following injections made into each of the three Vo subdivisions. A. Terminal arborizations within the rostral one-half of Sol are characterized by thin strands with widely spaced short side branches. B. More caudally in Sol, terminal strands are thinner and are observed to emit widely spaced endings.

FIGURE 12

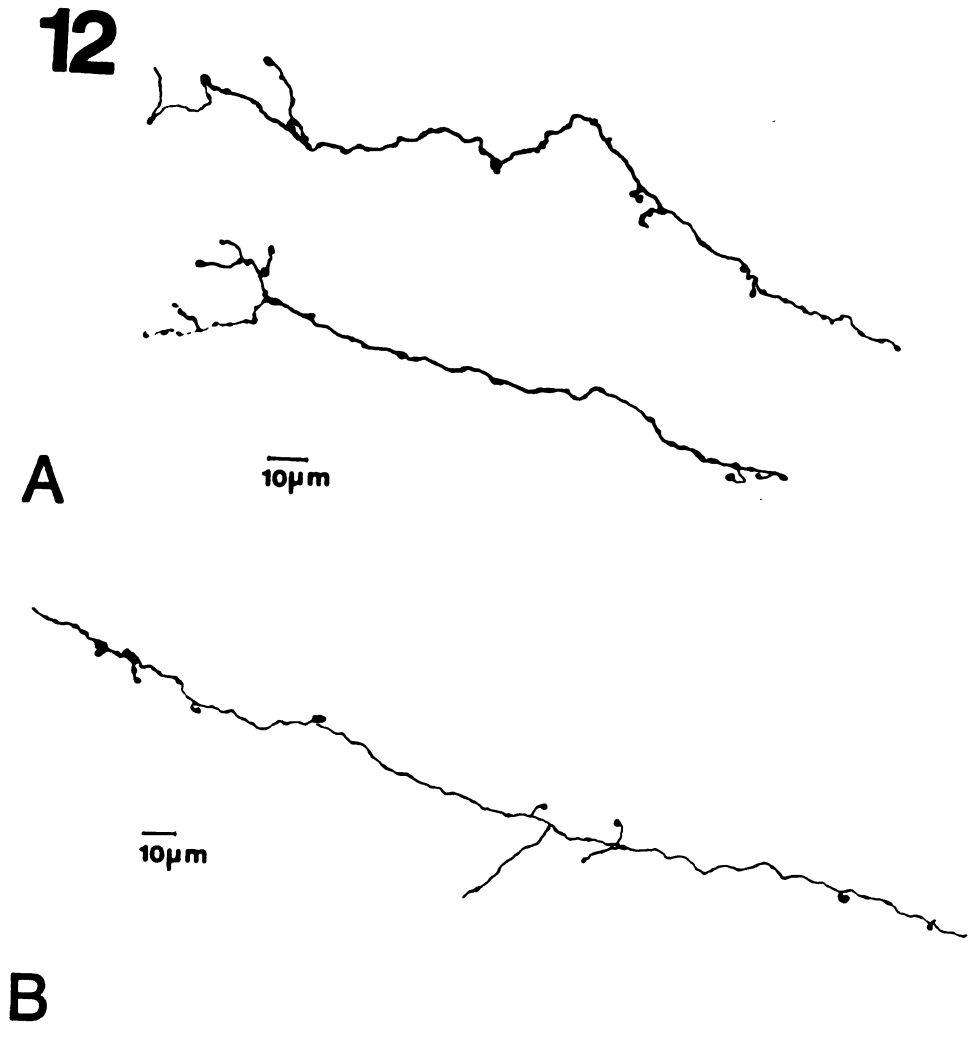

Figure 13: High power reconstruction of a single type of Vo efferent terminal arborization found in EW following DM injections and X following DM and VL injections. Each terminal strand is characterized by a few side branches and widely spaced boutons en passant.

Figure 14: Photomicrographs that document the morphological characteristics of each type of Vo efferent terminal arbor found in cranial nerve motor nuclei. A. The type of morphologically distinct terminal strands found in III, IV and VI. B. The single type of terminal strand arborizing in Vmo. C. The one type of Vo efferent ending which terminates dorsally in VII. D. The second type of Vo efferent terminating ventrally in VII. E. The type of Vo efferent terminal arbor terminating rostrally in XII. F. The second type of Vo efferent to XII, terminating caudally.

FIGURE 14

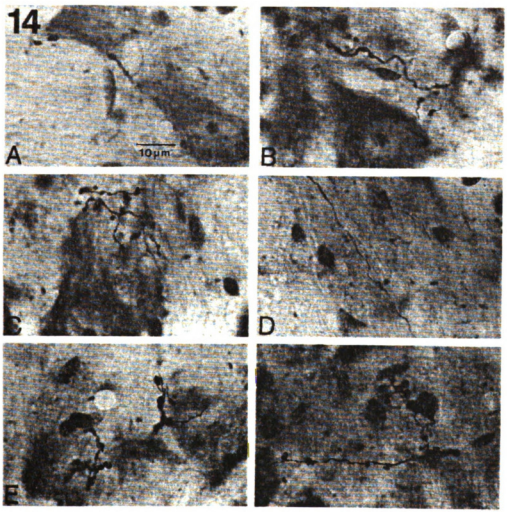

Figure 15: Photomicrographs that document the morphological characteristics of each type of Vo efferent in cranial nerve sensory and autonomic nuclei. A. The first type of terminal strand found in SVC bilaterally, SVC Type 1, following DM injections. B. The second type, SVC Type 2, of Vo efferent terminal arbor found in SVC bilaterally following DM injections. C. The first type, SVC Type 1, of Vo efferent terminal arborization found bilaterally in SVC following VL injections. D. The second type, SVC Type 2, of Vo efferent terminal arborization found bilaterally in SVC following BZ injections. E. The type of morphologically distinct terminal strand found bilaterally in rostral Sol. The type of terminal strand found caudally in Sol. G. The single type of Vo efferent terminal strand found on EW and X following DM injections and in X after VL injections.

FIGURE 15

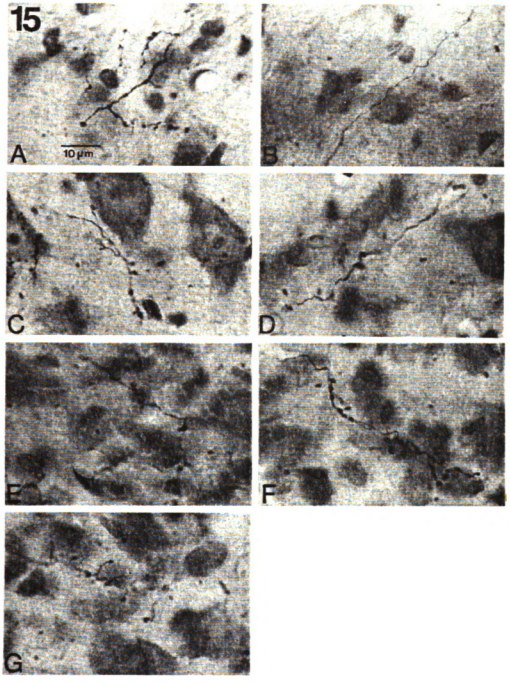

CHAPTER IV

EFFERENT PROJECTIONS TO THE VENTRAL POSTERIOR MEDIAL NUCLEUS OF THE THALAMUS AND OTHER DIENCEPHALIC NUCLEI FROM IDENTIFIED SUBDIVISIONAL AREAS OF RAT TRIGEMINAL NUCLEUS ORALIS.

INTRODUCTION

Trigeminothalamic projections in various mammals have been carefully analyzed electrophysiologically and anatomically, utilizing classical and more recent neuroanatomical tracing techniques, (Carpenter and Hanna, '61; Dunn and Matzke, '67; Lund and Webster, '67; Kruger et al., '77; Burton and Craig, '79; Fukushima and Kerr, '79; Erzurumlu et al., '80; Erzurumlu and Killackey, '80; Woolston et al. '82; Shigenaga et al., '83; Peschanski, '84; Silverman and Kruger, '85 Jacquin et al., '86; Bruce et al., '87; Mantle-St. John and Tracey, '87; Patrick and Robinson, '87; Chiaia et al., '91a,b; Phalen and Falls, '91b). The strongest projection has been demonstrated from the main sensory nucleus (Vms), with a substantial projection from trigeminal nucleus interpolaris (Vi) and a small contribution made by the medullary dorsal horn (MDH; nucleus caudalis). However, extremely sparse to no projections have been reported to arise from trigeminal nucleus oralis (Vo) neurons.

Anatomical studies (Falls, '83; Falls, '86; Falls and Alban, '86) and electrophysiological investigations (Hayashi, '82) have provided experimental evidence that each subdivision of rat Vo, receives morphologically and functionally distinct groups of primary and non-

primary afferent axons which are positioned to directly influence the activity of different groups of second-order projection neurons. Each subdivision contains second-order neurons which provide efferent outflow to affect synaptic activity at many locations along the neuraxis including the trigeminal, facial and hypoglossal motor nuclei (Ramon y Cajal, '09; Carpenter and Hanna, '61; Sessle and Kenny, '73; Greenwood and Sessle, '76; Dubner et al., '78; Erzurumlu and Killackey, '79; Smith and Falls, '90), the superior colliculus (Huerta et al., '83; Killackey and Erzurumlu, '81), cerebellum (Falls and Van Wagner, '84; Huerta et al., '83; Mantle-St. John and Tracey, '87; Matsushita et al., '82; and Smith and Falls, '90), and spinal cord (Falls, '83; Matsushita et al., '81; Matsushita et al., '82; Ruggiero et al., '81; and Smith and Falls, '88). Recent experiments in our laboratory (Smith and Falls, '90a,b), utilizing the anterograde tracer Phaseolus vulgaris leuccoagglutinin (PHA-L) have allowed for the demonstration of Vo efferent projections to areas along the neuraxis (eg. VPM and intralaminar diencephalic nuclei, Purkinje cell layer and deep cerebellar nuclei of the cerebellum, intermediolateral cell column of the thoracic spinal cord, rostral cranial nerve nuclei) that have been previously characterized as weak or non-existent.

The purpose of the present investigation is to examine the topographical organization of efferent projections to the diencephalon originating from the cytoarchitectonically defined subdivisions within Vo. We also sought to determine whether Vo trigeminothalamic (Vo-TT) efferents from neurons within different subdivisions demonstrated similar or different morphological features. Anterograde transport of PHA-L was employed to determine the overall course, distribution, relative density, organization and light microscopic morphology of efferent axons and their

terminal arborizations originating from neurons in each Vo subdivision and terminating in VPM and the diencephalon. A partial report of these findings has been previously reported (Smith and Falls, '90b).

METHODS

Eight adult male Sprague Dawley albino rats (250-300g) were utilized in this study and were treated according to NIH prescribed guidlines (NIH Guide, '85) . A detailed protocol of the PHA-L method used here is given in a previous section (Chapt. 1). To study the overall distribution and morphological features of Vo efferents to the diencephalon, small deposits of PHA-L were made iontophoretically under stereotaxic guidance into previously defined Vo subdivisions (Falls, '83, Falls, '84a; Falls, '86; Falls et al., '85; Falls and Alban, '86). After a survival period of 10-14 days, the rats were anesthetized with sodium pentobarbital and perfused according to a modification of the pH-shift method of Berod et al., ('81). Following postfixation, 30 um coronal sections were cut using an Oxford Vibratome. For the visualization of PHA-L staining, sections were incubated 48 hours in antibodies against PHA-L (1:2000) and then processed using the Vectastain kit (Vector laboratories) (Hsu et al., '81). The sections were processed in a solution of 0.05% diaminobenzidine in Tris buffer (0.05 M, pH 7.5) for 60 minutes, rinsed and mounted onto gelatin coated slides, stained with cresyl violet and coverslipped for light microscopic analysis. The distribution of PHA-L labeled axons was studied at the light microscopic level. For data presentation, the distribution of labeled Vo axons were illustrated in schematic drawings using an Aus Jena documator at the magnification of 17.5X onto which drawings of parent fibers and their terminal arbors were positioned utilizing a 2.5X objective lens attached to a Leitz Laborlux 12 microscope fitted with a drawing tube at a magnification of 31X. Detailed morphological features of parent axons and their terminal arbors were illustrated using a 100X oil immersion objective lens at a

magnification of 1,250X. Photomicrographs of corresponding sections were taken to illustrate morphological details.

RESULTS

INJECTION SITES

Deposits of PHA-L were localized to discrete areas within each of the three subdivisions of rat Vo. Photomicrographs demonstrating representative injection sites within the dorsomedial (DM; Case 734), ventrolateral (VL; Case 751) and border zone (BZ; Case 750) subdivisions are shown in Fig. 1 A-C. While the fields of diffuse PHA-L reaction product appeared to be extensive in several cases (Figure 2 A-C; Cases 739 and 840) much of each field was devoid of labeled cells. Only areas containing densely filled neurons were considered to be the effective zones from which efferent projections originated. Deposits of PHA-L which failed to label neurons at the injection sites often resulted in weak anterograde label. In two cases (734, 840) two of the PHA-L labeled cells were located two or more millimeters from the central zone of the injection site. The possibility exists that these cells were labeled as a result of retrograde transport of the lectin which has been reported for other systems (Lee et al., '87). In several cases (824, 826 and 750) PHA-L diffused into the spinal trigeminal tract (SVT) at the approximate rostrocaudal location of the mid-portion of the facial motor nucleus caudal to the point of entry of the sensory root of the trigeminal nerve into the brainstem. In these instances injections labeled numerous axons in SVT as far caudal as the MDH and serves to indicate that PHA-L is subject to uptake and transport by at least some fibers of passage (Cliffer and Giesler, '88). The potential problems of retrograde transport and transport of PHA-L by fibers of passage probably did not influence the results of this study since cases of PHA-L deposition without spread into SVT yielded the same results and only two retrogradely labeled cells have

been recorded in a total of eight experimental cases. It should be mentioned that labeling of parent axons and terminal arborizations located in the diencephalon following PHA-L injections into Vo would not involve the main axons of projection neurons which occur in more caudal portions of the brainstem, eg. Vi and MDH since most of the axons do not course through Vo as they ascend to the diencephalon. In this study injections of PHA-L were largely restricted to either DM, VL, or BZ, however, some cases included injections involving various aspects of either SVT (Fig. 1A, C; Cases 734, 750) or the pontine reticular formation (Fig. 2 B; Case 739). All of these cases yielded similar results. Of the eight brains examined, three were chosen for detailed description of the efferent projections to the diencephalon (Figs. 1 A-C and 2 A-C; stippled injection sites). The DM injection site was situated in middle DM and partially filled its dorsal and ventral zones as well as the dorsal one-half of BZ. This injection site measured 1180 um rostrocaudally, 850 um dorsoventrally and 400 um mediolaterally. The injection site located in VL was approximately two-thirds the distance along the rostrocaudal length of Vo. It measured 570 um rostrocaudally, 520 um dorsoventrally, and 480 um mediolaterally. The BZ injection site was located in the dorsal two-thirds of the subdivision with some spread into the dorsal portion of VL. The injection site was midway along the rostrocaudal extent of Vo and extended 1080 um rostrocaudally, 700 um dorsoventrally, and 300 um mediolaterally. In the five additional cases, PHA-L depositions were similar with respect to size and extent of those illustrated above and yielded similar results.

OVERALL PROJECTIONS TO THE DIENCEPHALON

Ascending efferent projections from each Vo subdivision resulted in anterograde axonal labeling in specific diencephalic nuclei. Following injections into DM numerous axons formed dense terminal arborizations in contralateral VPM, Po, PF, and ZI with fewer fibers terminating in the same nuclei ipsilaterally (Fig. 3 A-D). Terminal arbors were found in CM and bilaterally in CL with a contralateral predominance (Fig. 3 A-C). Injections into VL resulted in the labeling of terminal arbors bilaterally in Po, PF, and ZI and contralaterally in VPM (Fig. 4 A-D). The densities of the arbors appeared to be less than those observed following the DM injection (compare Figs. 3 A-D and 4 A-D). Sparsely dispersed terminal arbors were found in rostral CM. Following an injection principally located in BZ labeled terminal arbors were found bilaterally in Po and PF, with a contralateral predominance, and only contralaterally in VPM and ZI (Fig. 5 A-D). A small number of efferent axons were observed to terminate midway through CM.

PROJECTIONS TO VPM

Following injections into VL and BZ labeled Vo-TT axons were observed to course ventromedially from Vo at the level of the mid-facial nucleus, decussate and ascend contralaterally in an area bordered by the predorsal bundle and the gigantocellular reticular nucleus. Parent fibers were observed to course through the brainstem in the dorsal portion of the middle one-third of the contralateral medial lemniscus (ML). At caudal thalamic levels, fibers shifted to the lateral portion of ML and entered VPM caudally. Terminal arborizations were found throughout the rostrocaudal extent of contralateral VPM (Figs.4, 5). Ipsilateral VPM was devoid of Vo-

TT efferents and no parent axons were seen coursing in ipsilateral ML. Deposits of PHA-L in DM resulted in labeled axons ascending bilaterally in the same portion of ML with a marked contralateral predominance. Contralaterally terminal arbors were found throughout the rostrocaudal extent of VPM (Figs.4, 5). Labeled terminal arborizations in ipsilateral VPM were sparse and situated in the caudal portion of the nucleus. Within VPM terminal arborizations from DM, VL, and BZ neurons were observed to form definitive patches (Figs.3-5). Labeled axons of DM neurons were observed to terminate in patches located ventrolaterally in contralateral rostral VPM (Fig. 3 A-B). Proceeding caudally, terminal arbors were observed bilaterally in patches located in the lateral portion of the nucleus (Fig. 3 B-D). Terminal arbors from axons of VL neurons were located in patches situated dorsomedially in contralateral rostral VPM (Fig. 4 A-D). These patches moved to a central position in the nucleus at more caudal levels. Terminal arborizations from axons of BZ neurons formed patches laterally in contralateral rostral VPM which moved caudally to the medial border at the mid portion of the nucleus (Fig. 5 A-B). For each subdivision injected, the density of the terminal arbors within a patch became greater as one proceeded caudally through contralateral VPM (Figs. 3 C-D;4 A-D; 5 C-D).

The same two morphologically distinct types of parent axons and their terminal arborizations were found to enter and intermingle with each other in VPM patches following each subdivision injection (Fig.6,7). Parent axons measuring um in diameter and giving rise to thin terminal strands 0.5 um in diameter) characterized the first type of Vo-TT efferent and its terminal arbor (Figs.7;15C). These terminal strands were sparsly branched and coursed in all directions in VPM patches. Widely spaced

boutons en passant measuring approximately 0.5 um in diameter were found along the strands which often terminated in bulbous, irregularly shaped end boutons ranging in size from 1.0 X 1.0 um to 1.0 X 1.5 um. Terminal strands from this first type of Vo-TT efferent were also found along the periphery of a patch as well as diffusely coursing in adjacent areas of VPM neuropil. The second type of Vo-TT terminal arbor (Figs.7; 15B) was characterized by a thicker generally unbranched terminal strand (1.0-1.5 um in diameter) which gave rise to irregularly shaped boutons en passant and end boutons ranging from 2.5 X 3.0 um to 7.0 X 9.0 um in diameter. Within the patches these thin terminal strands were always observed in greater density than those of the first type of Vo-TT efferent.

PROJECTIONS TO Po

The trajectory of parent fibers to Po followed the same route to the thalamus as those described for VPM following injections into each Vo subdivision. At caudal thalamic levels parent axons of DM, VL, and BZ neurons were observed to exit the dorsal portion of the medial two-thirds of contralateral ML and course dorsally and laterally to terminate diffusely in Po (Figs. 3-5). Some parent fibers crossed caudal to the level of CM and terminated diffusely in ipsilateral Po (Fig.3-5; B-C). In addition, following DM injections, a few parent fibers were observed to leave the dorsal one-half of the medial portion of ipsilateral ML and enter the ipsilateral nucleus (Fig.3; B-D). Although the labeled parent axons and terminal arbors were observed bilaterally following each subdivisional injection, the densest projection was always contralateral. Terminal arborizations were observed to be oriented in different planes, were heavily concentrated in the ventral region of Po and were found in greatest density in more caudal portions of

the nucleus (Fig.3; C-D). Terminal arbors of two types of Vo-TT efferents were found in Po (Figs. 7,8,15D). One type was thicker, 0.8-1.2 um in diameter parent fiber with terminal strand measurements of 0.4-0.8 um in diameter. The second type is characterized as a thin parent fiber which upon entering Po continued as thin, sparsly branched terminal strand (approximately 0.5 um in diameter) ranging from 50-160 um in length. The terminal strands were observed to either run an isolated course through the Po neuropil or participate in small clusters of terminal strands with other Vo-TT efferents of the same type. Boutons en passant and end boutons measuring 0.5 X 1.0 to 3.0 X 5.5 in diameter were found along the terminal strands (Figs. 8; 15D).

PROJECTIONS TO CM

Labeled parent axons coursed through the brainstem from neurons located in each Vo subdivision to reach the caudal thalamus in the medial one-half of contralateral ML. Labeled fibers exited and ran medially and dorsally to enter the caudal portion of CM (Fig.3-5;A-C). A few Vo-TT efferents from DM neurons were also seen to emerge from the medial one-third of ipsilateral ML and course dorsomedially to enter CM (Fig.3;A-C). A single population of Vo-TT efferents was observed to terminate in CM after injections into each Vo subdivision (Fig.3 B). Upon entering CM, parent axons continued as thin terminal strands measuring approximately 0.5 um in diameter. These terminal strands maintained a mediolateral trajectory for 50-350 um (Figs. 11A; 15G). Each terminal strand was characterized by widely spaced boutons en passant 0.5 X 1.0 to 1.5 X 3.4 um in diameter and an occasional short side branch capped by an end bouton.

PROJECTIONS TO CL

Following DM injections labeled parent axons destined for CL intermingled and coursed bilaterally in ML with a contralateral predominance along with those axons destined for CM. Contralateral Vo-TT efferents entered contralateral CL with a few fibers crossing the midline caudal to CM to terminate in the ipsilateral nucleus. A few Vo efferents from ipsilateral ML terminated sparsely in ipsilateral CL. Terminal arborizations were observed bilaterally in CL. Axons entering CL showed a predominately dorsal orientation and ended in a single population of terminal strands (0.5-1.0 um in diameter). These terminal strands were found in the caudal two-thirds of the nucleus and coursed mediolaterally and dorsoventrally for 20-110 um (Fig. 11B; 15G). Each terminal strand was characterized by several multi-shaped boutons en passant and end boutons (0.5 X 1.0 to 1.5 X 2.0 um in diameter). Occasionally, a side branch terminated in an irregularly shaped bouton.

PROJECTIONS TO PF

The pathway taken by parent fibers terminating in PF was similar to that for Vo-TT efferents projecting to CL except that all three subdivisions were observed to project to this nucleus. The level at which parent axons entered PF was situated more caudally in the thalamus than those entering CL (Fig.3-5;D). The densest labeling followed DM injections while labeling was more sparse after VL and BZ injections (Figs.3-5;D). Terminal strands were found bilaterally in the lateral-most regions of each PF with the greatest density contralaterally. A single population of parent axons gave rise to terminal arborizations (Fig. 11C; 15G). Terminal strands measured approximately 0.5 um in diameter and were seen to course predominately

in a dorsomedial direction for 90-210 um. Each terminal strand was characterized by widely spaced endings 0.5 X 0.5 to 0.5 X 1.5 um in diameter and an occasional short side branch terminating in an end bouton.

PROJECTIONS TO ZI

The manner in which Vo efferents arrived at ZI is similar to that described for VPM. The parent axons from DM, VL, and BZ neurons exited from the medial one-half of contralateral ML and coursed ventromedially to contralateral ZI (Fig.3-5;B-D). Some labeled axons from DM, and VL neurons decussated caudal to CM and coursed ventrolaterally to ipsilateral ZI (Fig.3,4;D). In addition, a few parent fibers from DM neurons exited from the medial one-half of ipsilateral ML and coursed ventrally to ipsilateral ZI (Fig.3;B-D). Following each subdivisional injection, labeled parent axons and terminal arborizations were considerably more dense in contralateral ZI (Figs.3-5:A-C). Two morphologically distinct types of Vo efferents terminated in ZI and intermingled with each other. The first type of parent axon was situated ventrally in ZI, coursed ventromedially for 30-220 um through the ZI neuropil and terminated as a thin terminal strand approximately 0.5 um in diameter. These terminal strands were sparsely branched and were seen to have widely-spaced small (1.0 X 1.0 to 2.5 X 2.5 um in diameter) axonal endings (Figs. 10; 15F). The second type of terminal arborization (Fig. 10; 15E) emanated from a parent axon was found dorsally and ventrally in ZI. The thin, bouton bearing, terminal strands ranged from 0.5-1.0 um in diameter and coursed mediolaterally and dorsoventrally through ZI for appoximately 70 um. These terminal strands emitted several side branches which underwent secondary

branching and contained several multi-shaped boutons en passant and end boutons (1.5 X 1.5 to 3.0 X 3.5 um in diameter).

Additional diencephalic projections included those to reiniens thalamic nucleus (Re), nucleus of the fields of Forel (F) and to nucleus submedius (G).

DISCUSSION

This study shows that there are fiber connections between Vo and selected thalamic and diencephalic nuclei and that the pattern of efferent projections differs somewhat from those reported in previous investigatons (Kruger et al. '77; Erzurumlu and Killackey, '80; Erzurumlu et al., '80; Mantle-St. John and Tracey, '87). Major thalamic and diencephalic nuclei receiving input from Vo neurons were found to include VPM, Po, CL-PF, and ZI. Other previously unreported projections of Vo were also observed, including efferents to CM, CL, PF, Re, SubP, G, Gu. The data presented here demonstrate that terminal axonal arborizations from neurons located within each Vo subdivision are clustered in discrete patches within VPM and that this patch-like topography is apparent throughout most of the rostrocaudal extent of the nucleus with the greatest density located caudally. The data also show that DM neurons project bilaterally to VPM while innervation from VL and BZ neurons was contralateral. Other thalamic nuclei receiving bilateral projections from Vo subdivisions are Po, Pf, and CL (only from DM). Bilateral projections were also found to ZI from each Vo subdivision. Midline thalamic nuclei, CM and Re, receive projections from DM, VL, and BZ. These results indicate that the efferent projections from Vo are topographically organized within and across its cytoarchitectonic subdivisions. The significance of topographically organized and restricted projections from rat Vo is discussed in light of physiological and anatomical studies indicating the functional heterogeneity of this nucleus.

Methodological Limitations

The uptake and subsequent transport of PHA-L were originally shown to be restricted to cell bodies and dendrites at the site of injection (Gerfen and Sawchenko, '84). However, a recent study indicates that PHA-L may be taken up by fibers of passage within the spinal cord (Cliffer and Giesler, '88; Schofield, '90). Such a mechanism is not likely to account for the present findings, since neither injections of PHA-L into the white matter of svt nor deposits of PHA-L into the Vo neuropil, which failed to result in cellular uptake, produced any anterograde labeling. Therefore, the localization of cells filled with PHA-L was used to determine the limits of the effective site within Vo from which anterograde transport occurred. This ability to make well defined and restricted PHA-L injection sites facilitated the delineation of the topographical organization of Vo efferent projections, both within and across the cytoarchitectonic subdivisions of this nucleus.

In most instances in this study it was possible to limit the uptake of PHA-L to cells situated within the myelo- and cytoarchitectonically defined DM and VL subdivisions of Vo. However, deposits of PHA-L restricted to cells comprising BZ could seldom be achieved without some slight spread of reaction product into DM and VL. This was apparently due to the narrow width of BZ and the fact that injections could not be contained within such a small area. Target regions which exhibited a comparable density of labeling after discretly placed PHA-L injections within Vo subdivisions ie., cerebellum, cranial nerve nuclei, and spinal cord (Smith and Falls,'88,'90a, 90b) have been shown in retrograde tracing studies to receive Vo afferents (Falls, '84a,c; Falls, '86, Falls and Van Wagner, '84, Falls et al., '85; Erzurumlu and Killackey, '79; Erzurumlu and Bates, '80).

Conversly, projections which showed only weakly retrogradely labeled cells in Vo after partial and large VPM injections (Kruger et al., '77) are shown in this study to be more robust which is consistent with a more intense uptake of PHA-L by neuronal cell bodies. The ability to recognize morphological features associated with terminal axon arborizations at the light microscopic level represents a significant advantage of the PHA-L method over other anterograde techniques (Gerfen and Sawchenko, '84; Wouterlood and Groenewegen, '85). In the present study, it was often possible to distinguish between axon terminal arbors and fibers of passage in Vo target sites for which previously existing data were incomplete. However, the unequivocal demonstration of Vo terminations onto target cells requires electron microscopic verification. The PHA-L anterograde tracing method appears to be more sensitive than autoradiographic techniques, particularly with regard to minor projections (Ter Horst, '84). We observed a number of efferent projections from Vo which, to the best of our knowledge, have previously been unreported in the rat eg., Re, G, sub P, PF, and CM-CL. Furthermore, the PHA-L method permitted a more detailed examination of projections which had been recognized but otherwise uncharacterized.

Vo PROJECTIONS TO THE LATERAL THALAMUS

Recent retrograde transport studies (Peschanski, '84; Erzurumlu and Killackey, '80) have shown that several diencephalic nuclei receive efferent input from the contralateral Vms, Vi and MDH. These trigeminal nuclei have been demonstrated to project to VPM, the medial portion of the medial geniculate body, the ventral area of ZI and nucleus lateralis posterior, pars lateralis. The results presented in this study illustrate that

Vo neurons project to a widespread area of the thalamus as well as associated diencephalic nuclei. In many ways Vo projections are similar to both Vms and Vi in their distribution to VPM and Pom. Similarities are also seen with respect to the pattern of innervation observed for MDH neurons in that both Vo and MDH project to medial thalamic nuclei i.e., CM, CL, PF, SubP, G (submedius).These similarities may reflect the fact that Vo neurons receive a substantial proportion of primary pain afferents as well as cutaneous input from peri-oral and facial structures.

PROJECTIONS TO VENTRAL POSTERIOR MEDIAL NUCLEUS

In many mammalian species, including the rat, VPM is recognized as the main diencephalic nucleus for receiving efferent innervation from Vms, Vi, and MDH (Lund and Webster, '67; Smith, '73; Smith '75; Mizuno, '70; Erzurumlu, '80; Stewart and King, '63; Burton et al., '79; Peschanski, '84). Trigeminothalamic projections are completely contralateral in the rat, although interspecies differences are reported (Erzurumlu et al.,'80; Smith, '73, '75). Furthermore, there does not seem to be a segregation of VPM inputs from rat Vms and SVN and neurons from the different trigeminal nuclei probably innervate/interact with the same VPM neurons. Some of the terminal arborizations in VPM following injections into Vms, Vi and MDH are found to exhibit a similar morpohology resembling the "bushy arborization" found in the ventrobasal complex (Ramon y Cajal, '09; Scheibel and Scheibel, '66; McAlister and Wells, '81). A similar situation exists for the appearance for Vo-TT efferent terminal arborizations within VPM. Vo-TT efferents to VPM are characterized based on fiber diameter, terminal branching pattern and end bouton size and consist of two distinct types. One of which appears similar to that described for the "bushy

arborization" described above, while the second type of VPM terminal arborization is much thinner with fewer terminal swellings of a much smaller diameter.

Trigeminothalamic projections terminate in VPM in a somatotopic pattern (Erzurumlu and Killackey, '80). This corresponds to the strict somatotopy in SVN as shown electrophysiologically (Nord and Kyler, '68, Emmers, '65) and in VPM (Waite, '73). In the cat, facial representation from SVN (somatotopy inverted and medially rotated) is represented in VPM as an expanded representation of maxillary sinus hairs (Waite, '73). The ratculus representation in VPM is upright and medially rotated 225° with respect to the facial representation in Vi (Erzurumlu and Kilackey, '80). WGA-HRP injections restricted to dorsal parts of Vms and Vi resulted in efferent projections grouped ventromedially in VPM while efferents originating from ventral portions of these trigeminal nuclei (Peschanski, '84) terminated dorsally in VPM. Results of the present study support an anatomical separation between oral and peri-oral representation in the ventromedial portion of VPM with the facial vibrissae representation dorsally. Furthermore, the present results are in agreement with earlier electrophysiological mapping studies of trigeminal input to the ventrobasal complex (Emmers, '65; Kirkpatrick and Kruger, '75; Nord, '67; Shigenaga, '73; Waite, '73). While Peschanski ('84) refers to a separation of topographically specific inputs caudally in VPM following large injections of WGA-HRP into Vms and Vi, the present study suggests that for Vo each subdivision carrying vibrissal-facial and oro-facial information projects in a topographical manner that is separate and distinct in the rostral area of termination (caudal 1/5th of the rostral end of VPM). The entire trigeminal representation in VPM does not extend as far rostrally as that of the body

wall in cat (Saporta and Kruger, '77). Neurons labeled following PHA-L injections in DM (receiving orofacial tactile and pain primary afferent input from svt) project to ventromedial portions of rostral VPM while cells labeled after injections made in VL (reception area for facial-vibrissal tactile primary afferent input from svt) project to dorsomedial areas within rostral VPM. As labeled axons are followed caudally, Vo-TT efferent projections are observed to shift in their position and converge in contralateral VPM to occupy a position centrally in its most caudal portions. In caudal VPM, terminal arbors of efferent projections originating from second-order DM cells receiving oral cavity input are positioned subadjacent to VPL while efferent projections from cells innervated by vibrissae or facial hairs terminate medially to DM terminal arborizations. This shift in locale and apparent convergence of Vo-TT efferent terminal arbors suggests a repositioning of the somatotopic map of the ratculus caudally in VPM. It is also at this point of convergence of Vo-TT efferents in contralateral VPM that an ipsilateral projection from DM neurons can be seen in an approximately similar representation. Such a shift in position of the face as well as a proposal for a bilateral representation of SVN receptive fields in VPM has been proposed by Emmers ('65). In his electrophysiological studies, Emmers ('65) found neurons located in the caudal ventrobasal complex, referred to as SII, which responded to stimuli applied to large often bilateral receptive fields including the face. Emmers ('65) was able to map out two separate representations of a ratculus one similar to that reported by Erzurumlu and Killackey, ('80), termed SI, and another smaller representation more caudally in VPM, SII, which shifted in space to be positioned more centrally with a ratculus demonstrating vibrissal representation medial to

a peri-oral representation. Another electrophysiological study in rat has demonstrated a bilateral oral and perioral representation in caudal VB (Bombardiere et al., '75) and a double representation in the human ventrobasal thalamus has been observed as well (Emmers and Tasker, '75). Guilbaud et al. ('80) has found neurons positioned in more caudal areas of the ventrobasal complex that are excited by noxious stimuli applied to large areas of the body and face bilaterally. Erumzurlu and Killackey ('80) do not agree with Emmers' ('65) topographical map and state that the figure he presented underrepresents the face area and places it too medial, and that the trunk representation is placed largely within a portion of VPM. Other contradictory studies show no support for an SII representation in VPM by observing atrophic ventrobasal neurons, secondary to an SI lesion, retrogradely labeled by SII HRP injections (Jones and Leavitt, '73). Wise and Jones ('76) have suggested that the SII zone of ventrobasal neurons with bilateral receptive fields (Emmers, '65) and a bilateral midline ventrobasal receptive field (Donaldson et al., '75) may represent an area within the ventrobasal thalamus that projects to the commissurally connected cortical field caudal to SI.

This rostrocaudal pattern of termination in VPM for Vo-TT efferents originating from DM, VL and BZ is also suggested for Vi neurons situated in similar regions (Cook and Falls, '89,'90). However, the pattern of terminal label produced by Vi neurons may be more complex due to the six cytoarchitectonically and functionally distinct subregions reported for this nucleus (Phalen and Falls, '89, '91a,b).

This is the first anatomical study to show that a substantial contribution is made by rat Vo to trigeminothalamic efferent projections, and to demonstrate a bilateral projection, from DM to VPM. It is possible

that the results reflected in previous studies, utilizing lesion techniques or those using the anterograde transport of WGA-HRP, are the consequence of large or near total nuclear injections or that injections were confined to subdivisions not projecting bilaterally to VPM i.e., VL and BZ. It is also possible that PHA-L offers a superior method for demonstrating weak or small projections that would otherwise have been missed.

It is interesting that the characteristic pattern for the termination of vibrissal input from cells located in VL is shifted in VPM to occupy a central location in more caudal sections. This new position is in register with electrophysiologic maps within VPM which describe a columnar arrangement of clusters of neurons receiving projections from individual vibrissae (Sugitani et al., '90). A columnar arrangement is described for VPM neurons receiving second-order trigeminal afferent input from individual vibrissae in rat such that rows of cells extend from an anterior-dorsomedial position to a posterior-ventrolateral position. Sugitani ('90) also suggested a somatotopic representation of individual vibrissae i. e., the ventralmost row of vibrissae project rostrally and the dorsalmost row project caudally in VPM while the caudalmost vibrissae of each row project to dorsolateral parts of VPM and rostrally situated vibrissae project ventromedially. Sugitani ('90) suggests that the anterio-posterior/mediolateral orientation of these columns excludes the complete representation of all vibrissae within these rows in any one coronal plane and this opinion is supported by HRP studies (Saporta and Kruger, '77; Hoogland et al., '87).

Vo vibrissal information is projected by VL neurons to a more centralized location in caudal VPM while Vi neurons are observed (Cook and Falls, '90) to terminate in or nearby the marginal or shell-like area of

VPM dorsoventrally. According to Sugitani ('90) the spatial distribution of recording sites of VPM multi-receptive vibrissal neurons, with receptive field properties, considered to be derived from projections from Vi (Woolston et al., '82; Jacquin et al., '86; Rhoades et al., '87) are located along the marginal area of rat VPM while single-receptive vibrissal neurons, thought derived from Vms afferent input, typically showing single vibrissal receptive fields (Nord, '68; Waite, '84), distributed within the inner portion of VPM. Subtle differences to the results of the above studies have been reported for response properties of second-order vibrissal driven neurons in Vo and Vi. According to Gibson ('87) rat Vi neurons are found to have smaller receptive fields than vibrissal driven Vo neurons while Vo neurons are shown to have lower displacement thresholds and greater sensitivity. This suggests functional differences between the two types of SVN neurons. Vo neurons would likely be concerned with detection of and response to weak stimuli whereas, Vi neurons would be concerned primarily with high spatial resolution.

PROJECTIONS TO THE POSTERIOR NUCLEUS OF THE THALAMUS

A somatic part of Po has described to exist in a discrete region confined to the ventral part of the medial division (Curry and Gordon, '72). Neurons situated in rat Po (anteromedial portion) are topographically organized in a manner that mirrors the somesthetic map in VPM (Fabri and Burton, '91). A crude ratculus is illustrated to show the snout subadjacent to the medial "shell region" of VPM with forelimbs and hindlimbs extending dorsomedially eg., as if the two figures were standing head on head facing medially and ventrally toward the third ventricle. Trigeminal projections to the medial portion of Po (Pom) have been

demonstrated for Vms, Vi and MDH (Stewart and King, '63; Burton et al., '79; Ganchrow, '78; Erzurumlu and Killackey, '80; Chiaia et al., '91a,b). A large part of the medial portion of Pom is innervated by spinothalamic fibers (Mehler, '66,'69; Boivie, '79; Berkley, '80). Studies utilizing retrograde tracing techniques in cat suggest that the spinothalamic axons may originate from dorsal horn cells which have different characteristics compared with those projecting to VPM (Carstens and Trevino, '78). In rat Pom, spinothalamic endings are not as densly distributed (Lund and Webster, '67b).

Po neurons are thought to function in the transmission of somesthetic inputs, and have been shown to receive input from multimodal afferents (Neylon and Haight, '83; Roger and Cadusseau, '84). Po neurons have large bilateral receptive fields and some show a convergence between light mechanical, auditory and noxious inputs (Darian-Smith, '64; Perl and Whitlock, '61; Poggio and Mountcastle, "60; Rowe and Sessle, '68). The receptive fields for vibrissa-sensitive cells in Pom are larger than those for VPM (Chiaia et al., '91a, b).

The fact that Vo neurons project to Po in a widespread manner in contrast to restricted terminations in VPM has been supported in other studies for Vms and Vi neurons (Chiaia et al., '91a, b). While most VPM cells in their study responded to deflection to one or more mystacial vibrissae with the remainder activated by guard hairs or skin, less than half of the neurons located in Pom were activated by vibrissa deflection while the majority of cells were excited by stimulation of skin, mucosa or activation of muscle-related afferents. Only small percentages of these cells responded only to noxious stimulation. Although Pom projects to the SI cortex (Fabri and Burton, '91; Carvell and Simons, '87; Spreafico et al., '87)

it does not seem to project to the receptive fields of layer IV "barrel" neurons (Armstrong-James et al., '91). Chiaia et al. ('91b) suggest that Pom neurons are specialized for processing global aspects of tactile stimulation and not devoted to the detection of stimulus magnitude or precise somotopic locale.

Clinical studies report that stimulation of the middle meningeal artery and superior sagittal sinus result in painful sensations which are referred to defined facial regions (Feindel et al., '60; Northfield, '38; Penfield and McNaughton, '40; Ray and Wolff, '40; Wirth and Van Buren, '71). The medial division of Po is thought to be involved with the processing of nociception (Albe-Fessard et al.,'85). Cells located in Pom were excited by stimulation of the middle meningeal artery or superior sagittal sinus (Davis and Dostrovsky, '88) and have been shown to receive trigeminal inputs (Curry, '72; Dong and Wagman, '76; Feindel et al., '60; Poggio and Mountcastle, '60). However, the role of Pom neurons in the appreciation of pain is still undetermined.

Peschanski ('84) equated trigeminal terminations in VPM with "bushy arbors" observed by Schiebel and Schiebel ('66) and reported that terminations in the lateral portion of Po were not the same type. Chiaia et al., ('91a) suggest that their trigeminothalamic terminal endings in Pom are in an area similar to that described by Peschanski ('84) as lateral Po. Vms and Vi neurons are not thought to give rise to collateral projections to both VPM and Pom, instead, arbors arise from separate populations of neurons, based on the restricted pattern observed for terminations in VPM and the widespread termination of trigeminothalamic efferents in Pom Chiaia et al., '91a). That Vo-TT efferent terminations in Po are observed to be of two types originating from medium and thin diameter parent axons

suggest that perhaps more than one type of input is being relayed to Po. Vo neurons probably do not differ in respect to Vms and Vi cell bodies in that they most likely arise from separate populations of neurons and are not specifically collateralizations of axon terminals projecting to VPM. Vo has been reported to receive noxious as well as tactile input from the face and oral cavity. It is possible that the two types of Po terminal arborizations convey different information to Po.

PROJECTIONS TO ZONA INCERTA

Although ZI has been parcelled into antero-polar, dorsal, ventral, magnocellular, caudal and postero-polar parts (Watanabe and Kawana, '82; Kawana and Watanabe, '81), it is grossly observed to be segregated dorsoventrally with respect to afferent and efferent connectivity. A topographical organization exists in ZI as terminal arborizations from somesthetic areas are observed to terminate ventrally. Degeneration and autoradiographic studies in different mammalian species, including the rat, have demonstrated afferent projections to ZI originating from the somatosensory cortex (Price and Webster, '72), dorsal column nuclei (Hand and Liu, '72; Lund and Webster, '67; Boivie, '71; Jane and Schroeder, '71; Schroeder and Jane, '71; Hazlett et al., '72; Hand and Van Winkle, '77; Berkley and Hand. '78) Vms (Mizuno, '70; Smith, '72, '73; Peschanski, '84) SVN (Erzurumlu and Killackey, '80; Peschanski, '84) and the lateral cervical nucleus (Lund and Webster, '67b). No reports of a Vo trigeminocertal projection have been made. The massive projections from Vms, Vi and the sensory cortex as well as those from the dorsal column nuclei and lateral cervical nucleus terminate in a narrow band along the ventral half of ZI (Roger and Cadusseau, '85; Peschanski, '84). The

contingent somatosensory input demonstrates a large degree of overlap between the endings originating from different somatosensory areas. Axonal labeling following cortical injections reveals terminal fields caudally in ventral ZI while other somatosensory centers were observed to project and terminate further rostrally. The overlap of terminal endings from the different somatosensory systems was greatest in density in caudal ZI. Efferent connections arising from neurons located within ZI have been shown to distribute in a widespread manner to motor-related centers including globus pallidus, precerebellar nuclei, mesencephalic premotor nuclei, pretectum (Ricardo, '81; Watanabe and Kawana. '82).

Labeled terminal endings from the somatosensory cortex, dorsal column nuclei and trigeminal complex demonstrate a high degree of overlap which suggests the existence of a somatosensory receptive zone within ventral ZI. Receptive fields within ZI have been mapped (Nicolelis et al., '91) and reveal a crude somatotopic map of the rat's body which parallels the map in VPM and is mainly characterized by large contralateral receptive fields.

Electrophysiological studies in ZI suggest that this diencephalic nucleus plays a role in processing somesthetic information and perhaps participates in the transmission of noxious stimuli (Kruger and Albe-Fessard, '60; Kaelher and Smith, '79). Other electrophysiological and behavioral studies suggest that ZI shares similar functions with the reticular formation with regard to nonspecific activating properties. Following lesions placed in ZI, an animal's level of vigilance decreases (Starzl et al., '51; Naquet et al., '66; Santacana and Delacour, '68; McGinty, '69; Lindsley et al., '70). In consideration of the massive somatosensory input into ZI, it is possible that a reduction in sensory stimuli from the body

as well as visual afferents from the lateral geniculate nucleus and superior colliculus (Roger, '85; Watanabe and Kawana, '82) could lend the animal unresponsive to external environmental events.

The trigeminal system is implicated as being involved in diving reflex mechanisms which involve reflex cardiovascular changes including bradycardia following the application of tactile and thermal (cold) stimuli to the face. Projections from neurons situated in all three subdivisions of Vo terminate in ventral ZI and are also reported to terminate in the interomediolateral cell column of the thoracic spinal cord (Chapt 1) and dorsal vagal nucleus (Chapt 3). Vo efferent projections to ZI may not only participate in forwarding somesthetic information regarding the head but may also be providing ZI with parallel signals regarding internal homeostasis (Vo afferents have been reported to innervate cranial dura mater as well as the sagittal sinus and middle meningeal artery) of the head that perhaps will also be relayed independently to the dorsal vagal nucleus and intermediolateral cell column. The potential also exists for recriprocal incertotrigeminal inputs to participate in the integrative control of autonomic responses associated with different normal behaviors as well as during locomotor and consumptive behaviors. This speculative projection from ZI has yet to be elucidated. The fact that Po, which is densely innervated by terminal endings from Vo, sends a strong projection to ventral ZI (Roger and Cadusseau, '85; Cadusseau and Roger, '85), suggest for the further intergration of direct and indirect trigeminal input that may be involved in the relay of ZI specific information in the control of autonomic responses.

Vo PROJECTIONS TO THE MEDIAL THALAMUS

Recent studies utilizing neuroanatomical techniques have shown additional labeling of several medial thalamic nuclei from MDH (Peschanski, '84; Erzurumlu and Killackey, '80). MDH neurons have been observed to project bilaterally to nucleus submedius (G in this study), the intralaminar nuclei (CM, CL) and the subparafascicular area of the mesodiencephalic junction (SubP in this study). In the present study, Vo-TT efferent projections are shown to distribute within the diencephalon in a manner similar to that of MDH.

Recent anterograde and retrograde transport studies have established that the intralaminar nuclei eg., CM, CL, PF, G (submedius) of mammals project densly upon the striatum and diffusely over widespread areas of the cerebral cortex (Krettek and Price, '77; Sato et al., '79; Herkenham and Pert, '81; Macchi et al., '84). Intralaminar neurons are shown (Albe-Fessard and Besson, '73) to have large receptive fields, demonstrate spatial and modality convergence, respond to noxious stimuli and are thought to play a role in nociception. Electrophysiological studies (Applebaum et al., '79; Giesler et al., '81) reveal the termination of spinothalamic fibers in the region of the intralaminar nuclei in monkeys. Spinothalamic neurons projecting to the intralaminar nuclei are characterized as having high-threshold or wide dynamic-range properties and bilateral receptive fields. The cells with collaterals to the ventral posterior nucleus receive both A and C fiber input, have small excitatory fields, surrounding larger inhibitory areas and discharge characteristics of high-threshold cells suggesting they mediate discriminative aspects such as intensity, location and duration of noxious cutaneous stimulation (Jones, '85).

Electrophysiological studies have identified MDH neurons excited by middle meningeal artery stimulation (Davis and Dostrovsky, '86a; Davis and Dostrovsky, '86b; Strassman et al., '86) and by noxious stimulation over the periorbital skin. MDH neurons receive a good portion of the nociceptive input from the head and face (Dubner et al., '78).The rostral nuclei in SVN are thought to be associated mainly with processing non-noxious information but may play a role in nociception for oral and dental pain (Azerad et al., '82; Broton and Rosenfeld, 82; Broton and Rosenfeld, '86; Eisenman et al., '63; Falls, '86; Hayashi et al., '84; Nord and Young, '79; Sessle and Greenwood, '86; Vyklicky et al., '77; Young, '82). A retrograde axonal study (Shigenaga et al., '83) indicates that neurons in Vo project to CL whereas MDH neurons terminate in other more lateral thalamic nuclei. Davis and Dostrovsky ('88) suggest separate pathways for information from the cranial vasculature to reach MDH neurons and Vo/Vi neurons based on differences in receptive field properties. Thus sensory experiences and reflexive behavior resulting from information processing in the caudal and rostral trigeminal nuclei may differ. The results illustrated in the present study supports the premise of Vo involvement in nociceptive pathways to intralaminar nuclei, specifically as it demonstrates labeled Vo-TT efferent projections to the same medial thalamic nuclei as MDH which has been identified electrophysiologically (Strassman, '86; Davis and Dostrovsky, '88).

VO PROJECTIONS TO THALAMIC VISCEROSOMATIC NEURONS

Trigeminal primary afferent projections that innervate the dura mater are thought to convey nociceptive information during episodes of migraine (Moskowitz, '84) or cluster headache (Hardebo, '84). The pain

reported during these types of headaches is usually referred along a trigeminal peripheral receptive field. The demonstration of the referral of pain from arterial and dural stimulation in man shows that widespread areas of the dura mater and dural sinuses give rise to referred pain in the eye, forehead, temple and neck regions (Penfield and McNaughton, '40; Ray and Wolff, '40; Wirth and Van Buren, '71). Fay ('32) reported that stimulation of the proximal portion of the middle cerebral artery produces pain ipsilaterally in the forehead as well as behind the eye.

Rat dura mater is richly innervated by unmyelinated C and poorly myelinated Ad axons which course in relation to cerebral vessels (Penfield and McNaughton, '40, Andres, '87). At the electron microscopy level, single A axons and C fiber bundles are observed to intertwine along their final course within a schwann cell to culminate in multiaxonal units or terminations of approximately 15 endings (Andres, '87). Unencapsulated Ruffini-like receptors have been identified associated with the A axons found in the dura mater along areas where superficial cerebral vessels enter the sagittal sinus and at the confluens of sinuses. The unencapsulated Ruffini-like terminals innervating the dura mater are thought to be stretch receptors (Andres, '87).

Some dural innervation is thought to arise from nociceptors which refer noxious input to a cutaneous field in the ipsilateral trigeminal area of distribution. This view is based on reports from patients of painful sensations following neurosurgical procedures that involve stimulation of the dura mater at the margins of the dural sinuses and along the middle meningeal artery (Penfield, '35; Penfield and McNaughton, '40; Ray and Wolff, '40; Wirth and Van Buren, '71). Pain was the only sensation felt by these patients, regardless of whether the dura mater was stimulated by

pressure, traction, heat or electric current. Dural sites found to induce painful sensations were restricted to regions overlying the superior sagittal sinus, branches of the middle meningeal artery and sites where cerebral vessels enter the dural sinuses. Dural innervation was absent in patients with lesions of the trigeminal nerve or trigeminal ganglion (Penfield and McNaughton, '40) Substance P immunoreactive fibers are found within the walls of the superior sagittal sinus and meningeal artery of guinea pigs (Furness et al., '82) and rat (Matsuyama, '85). A functional correlation is thought to exist in the role played by trigeminal innervation by allowing for the generation of conscious perception of headache, via trigeminothalamic projections.

Anatomical studies indicate that the trigeminal nerve provides sensory innervation to the middle cerebral artery, middle meningeal artery and superior sagittal sinus (Andres, et a., '87; Borges and Moskowitz, '83; Mayberg et al., '84; Steiger et al., '82 O'Connor and van der Kooy, '86). Using retrograde tracing techniques, O'Connor and van der Kooy ('86) reported that cells situated in the ophthalmic division of the trigeminal ganglion that innervate the forehead tend to be clumped around individual cells that innervate the middle cerebral artery. In their study, a significant population of cells that innervate the middle cerebral artery were also found to project to other cerebral arterial branches via collateral branches as well as innervating the surrounding dura mater. In electrophysiological studies, (Borges and Moskowitz, '83; Davis and Dostrovsky, '87a, b; Strassman et al., '86) neurons within the SVN were activated by stimulation of either the middle meningeal artery or superior sagittal sinus suggesting that these neurons may mediate the painful sensation associated with vascular head pain.

Increasing evidence has been given for viscerosomatic convergence at spinal cord levels (Cervero, '83) where painful sensations arising from visceral organs are often referred to a specific portion of the body surface, (Chapt 1). Referral of visceral pain to somatic regions may result from a convergence of somatic and visceral afferent input onto nociceptive relay neurons that project to the thalamus (Ruch, '46). Electrophysiological studies have demonstrated that in certain spinal cord laminae, neurons receive converging visceral and somatic afferent input Cervero, '80; Cervero, '83; Hancock and Rigamonti, '73; Pomeranz et al., '68; Selzer and Spencer, '69). In the thoracic cord at caudal levels, neurons are found that can be activated following electrical stimulation of the splanchnic nerve (Foreman et al., '81), while spinothalamic cells located at more rostral levels receive afferent input from cardiac viscera (Ammons et al., '84; Blair et al., '81). All spinothalamic cells in these and similar studies that receive visceral afferent input also have a cutaneous receptive field located within the somatic dermatome corresponding to the segmental location of the neuron. Spinal viscerosomatic neurons which are responsive to nociceptive cutaneous stimulation are classified as nociceptive specific or wide dynamic range neurons depending on their response to natural cutaneous stimulation within their receptive field. Wide dynamic range neurons receive both rapid and slowly conducting cutaneous afferent input with visceral input arriving by Ad and C fibers (Ammons et al., '84; Blair, '81; Foreman et al, '81; Hancock et al., '75).

The responses of SVN neurons that receive a dural input are similar to those of spinothalamic neurons which receive convergent input. Many SVN neurons responsive to stimulation of the dura mater also have cutaneous receptive fields in the region supplied by the ophthalmic division

of the trigeminal nerve. The fact that only painful responses can be elicited from clinical manipulation of the dura mater is consistent with the finding that dural responses are found in cells receiving nociceptive cutaneous inputs. Strassman ('86) found that following electrical stimulation of the dura mater in or near sites where major vessels run, receptive fields recorded from cells in medullary SVN are all centered within the cutaneous area supplied by the first division of the ipsilateral trigeminal nerve. The functional significance of his finding is attributed to a possible physiological basis for clinical observations that dural pain from stimulation of the midsagittal sinus or middle meningeal artery is referred to the ipsilateral forehead and eye. Just as electrical stimulation of the raphe nucleus magnus supresses responses of neurons located in the thoracic dorsal horn to cardiac visceral stimulation (Chapman et al., '85), the response of SVN cells to dural stimulation can be supressed following electrical shock stimuli to the periaqueductal gray (Strassman et al., '86). This finding providings evidence for periaqueductal gray control of visceral sensory responses of trigeminal neurons.

Sensory innervation of dural vessels has been suggested to play a major role (Penfield and Naughton, '40) in the pathogenesis of pain in certain forms of headache. There is evidence that alterations in the extracranial vascular tone are associated with the different phases of headache (Ostfeld et al., '57).

Strassman et al., ('86) reported that several MDH nociceptive neurons excited by dural stimulation could be antidromically activated by the ventrobasal complex. Various thalamic nuclei; VPL, VPM, Pom, CL, and submedius are thought to be involved on the processing of different components of nociception (Albe-Fessard et al., '85). Nociceptive neurons in

cat MDH have been antidromically activated following stimulation within VPM (Angerbaur and Dostrovsky, '84; Azerad et al., 82; Henry et al., '77; Hu et al., '81). Anatomical studies utilizing retrograde and anterograde techniques have demonstrated that trigeminothalamic fibers terminate in VPM (Albe-Fessard et al., '85; Berkley, '80; Burton and Craig, '79; Burton et al., '79; Shigenaga et al., '83; Yasui et al., '83), Pom (Albe-Fessard et al., '85; Berkley, '80; Burton et al., '79; Shigenaga et al., '83), ZI (Berkley, '80), PF (Berkley, '80), and submedius (Albe-Fessard et al, '85; Craig and Burton, 81). Several electrophysiological studies have revealed trigeminal nociceptive thalamic neurons, including some with input from the teeth, in several nuclear groups: intralaminar (Dong et al., 78; Yakota et al., '85; Rydenhag and Roos, '86; Yakota, '88), Pom(Woda et al., '75; Matsumoto et al., '88), VPM (Yakota and Matsumoto, '83a,b; 'Yakota et al., '85; Rydenhag and Roos, '86; Yakota et al., '86) and submedius (Craig and Burton, '81; Craig, '87; Dostrovsky et al., 87). Cells with nociceptive receptive fields were often found in the periphery or "shell" region of cat VPM (Zugami and Lambert, '90).

The electrophysiologic properties of thalamic neurons activated by stimulation of the middle meningeal artery and/or the superior sagittal sinus has been reported (Davis and Dostrovsky, '87, '88a; Zigami and Lambert, '90; Zugami et al. '87; Strassman et al., '86). Following stimulation in VPM, Strassman et al., ('86) antidromically activated 9 out of 23 MDH neurons responding to dural vessel stimulation in the cat. Davis and Dostrovsky ('88a) activated neurons in several thalamic nuclei including VPM, Pom, ZI and VL following electrical stimulation of the middle meningeal artery and superior sagittal sinus. The latencies reported following activation of these vessels suggested the involvement of

small, myelinated primary afferent fibers. Of the neurons tested for the existence of orofacial inputs, all were found to have an excitatory receptive field on the face and usually involved the ophthalmic division. However, Davis and Dostrovsky ('88) reported that only one neuron was excited by stimulation of the cornea while twenty-four cells were activated by pinch or tap stimuli applied to the face. The firing properties and receptive field properties of these thalamic neurons implicate a role in the appreciation of cerebrovascular pain.

Thalamic neurons located in Pom and ZI are also activated by stimulation of the middle meningeal artery and superior sagittal sinus (Davis and Dostrovsky, '88a). Anatomical studies have demonstrated trigeminal inputs to VPM, Pom, and ZI (Berkley, '80; Burton and Craig, '79; Burton and Craig, '83; Burton et al., '79; Shigenaga, '83;). Electrophysiological studies have demonstrated tactile responses of neurons in VPM (Yakota et al., '85; Yakota et al., '87; Yakota and Matsumoto, '83a,b; Zigami and Lambert, '90) and Pom (Curry, '72; Guilbaud et al., '77; Poggio and Mountcastle, '60; Yakota and Matsumoto, '83b;) following stimulation of facial skin, confirming the existence of trigeminal inputs to these nuclei. A population of MDH nociceptive neurons with orofacial receptive fields has been antidromically activated from ZI (Angerbaur and Dostrovsky, '84).

MDH is considered to be an important relay center for oro-facial pain sensations (Dubner, '78) and is thought to be the most likely region to receive nociceptive sensory information from the cranial vasculature. Davis and Dostrovsky ('88b) reported that a group of neurons in MDH were activated by middle meningeal artery stimulation. MDH neurons activated by stimulation of the middle meningeal artery were almost always excited

by noxious stimulation of the cornea and/or periorbital skin. Nociceptive specific neuronal populations in cat have been located electrophysiologically in Vo and the caudal portion of Vi which respond to electrical stimulation to both the middle meningeal artery and superior sagittal sinus (Davis and Dostrovsky, '88b). In their study, Davis and Dostrovsky ('88b), were able to histologically reconstruct recording sites to demonstrate that MDH neurons were concentrated in the lateral one-half of laminae III-V while neurons in Vo and the rostral portion of Vi were not confined to any particular region. Although migrainous head pain is often felt in and around the eyes and temple region, and is thought to be explained by convergence of somatic and visceral inputs on SVN neurons. However, some anatomic inconsistencies are apparent. The dura mater of the middle cranial fossa is largely supplied by the middle meningeal artery which courses with the meningeal branch of the mandibular nerve, the nervus spinosis. Since mandibular primary afferents transmit somatic information from the jaw, one would think that noxious stimulation of these primary afferents would terminate in those portions of MDH and Vo which contain cells responding to mandibular cutaneous input with subsequent referral of noxious cerebrovascular manipulation to the jaw.

Vo has been shown to receive trigeminal primary afferents conveying noxious information from the oral cavity (Falls, '84c). It is interesting that the present study shows DM (receiving mandibular primary afferent input) to project most densely to thalamic nuclei reported to be involved with the reception of nociceptive input from cranial vasculature. The results in our study suggest that Vo cells, which have been demonstrated electrophysiologically to innervate areas of the thalamus receiving noxious input from the dura mater are projecting to those identified thalamic nuclei

which have been determined to receive second-order trigeminal input from intracranial structures.

PROJECTIONS TO ADDITIONAL THALAMIC NUCLEI

The ventroposterior nucleus, parvocellular part (VPPC) or referred by Paxinos and Watson ('86) as the Gustatory nucleus (G). In cat, nucleus ventralis posteromedialis parvocellularis, lateral (VPMpcl), adjacent to VPM proper, has been shown to receive somatosensory input from the ipsilateral intraoral structures, primarily tongue, rather than gustatory input (Nishikawa et al., '88). The oral cavity contains a specialized mechanoceptor in the periodontal ligament which has be reported to be included in the trigeminal somatosensory representation in VPM (Darian-Smith, '73; Woda et al, '75; Yakota, et al., 86). The distribution of peridontal units in cat VPM was studied (Yakota et al, '88). Peridontal units receiving contralateral inputs were located in the medial portion of VPM proper while those units receiving ipsilateral inputs were found in the lateral subdivision of VPMpcl (ipsilateral tongue units were also observed in this region). Within Vms and SVN is the representation of the peridontum (Eisenman et al., '63; Kawamura and Nishiyama, '66; Khyyat et al., '75; Kruger and Mitchel, '62; Nord and Young, '75; Sessel and Greenwood, '76; Yasui et al., '83). Yasui et al ('83) found that SVN and the ventral division of Vms project contralaterally to VPM while the dorsal division of Vms projects to VPMpcl. An electrophysiological study has shown that dorsal Vms contains peridontal units together with tongue units. Emmers ('66) found tactile, pressure and thermal units within the medially located lingual nerve projection zone of cat VPM. The present study suggests a bilateral projection with a contralateral predominance to more medial

portions of rat VPM which are situated within the defined boundaries of Gu. The possibility for Vo-TT inputs carrying periodontal or tongue information is speculative but certainly plausible. Although previous studies in cat report an ipsilateral projection of peridontal and tongue input to more medial regions outside of VPM proper, it is possible that interspecies differences may exist and that the more snouted animal may have a stronger contralateral projection from more caudal SVN nuclei in comparison to Vms.

Nucleus submedius (G) receives dense projections from spinothalamic tract neurons and trigeminothalamic tract neurons in cat, rat, and monkey (Craig asnd Burton, '81; Peschanski, '84). Input from MDH in cat originates almost exclusively from neurons located lamina I (Craig and Burton, '91), projects to the medial half of G and is nociceptive specific (Craig and Kniffki, '85; Dostrovsky and Broton, '85). Neurons in G in turn project topographically to the middle layers of the ventral lateral orbital cortex (Craig et al., '82). Recently, electrophysiological studies (Dostrovsky and Guilbaud, '88; Miletic and Coffield, '89; Craig, '90) have demonstrated nociceptive-specific neurons in G of the cat and rat. As a result of these studies, G has been proposed to act as a nociceptive substrate involved in the affective aspect of pain (Craig and Burton, 81; Craig, '87).

The results presented in the present study illustrate Vo-TT efferent projections from cells situated in the orofacial reception area of Vo which send their axons to the medial aspect of G in a similar manner described for MDH. It is likely that these Vo-TT efferent terminal arbors are conveying noxious input obtained from thermoreceptors and mechanoreceptors located in the oral cavity. This notion is supported by other electrophysiological studies that show numerous neurons, located in

the rostral portion of SVN, respond to noxious stimulation of tooth pulp, oral mucosa, or perioral skin (Azerad et al., '82; Campbell et al., '84; Davis et al., '71; Eisenman et al., '63; Greenwood, '73; Hayashi et al., '84; Lisney, '78; Nord, '76; Nord and Young, '79; Sessle and Greenwood, '76; Tamarova et al., '73; Vyklicky et al., '73; Young and Perryman, 86).

MORPHOLOGICALLY DISTINCT CELL TYPES AND TERMINAL ARBORIZATIONS

A population of terminal arborizations in VPM following injections into Vms, Vi and MDH is found to exhibit a similar morpohology resembling the "bushy arborization" found in the ventrobasal complex (Ramon y Cajal, '09; Scheibel and Scheibel, '66; McAlister and Wells, '81).

A functional homology with respect to that observed for terminal endings from neurons in the dorsal column nuclei and spinal cord in VPL has also been suggested for Vms, Vi and MDH neurons terminating in VPM (Darian-Smith, '73). "Bushy arbors" have been associated with DCN afferents while spinothalamic afferents have been recognized as a loosely arranged network of thin collaterals (Scheibel and Scheibel, '66; McAllister and Wells, '81). However, some spinothalamic afferent terminals, have been illustrated using the anterograde technique of WGA-HRP to resemble "bushy arbors" (Peshanski, '83). In the present study, a similar observation is made. Two distinct morphological types, large or globular terminal arborizations in punctate arrangement within VPM and thin terminal arbors diffusely spread throughout the VPM neuropil, are observed for V0-TT efferent endings. "Bushy arbors" are thought to be a common feature of some terminal arborizations of afferents originating in different structures and may have functional significance in that they could operate in

generating an intense stimulus, representing some localizing feature in the periphery, among the VPM postsynaptic elements. Spinothalamic, DCN and trigeminal projections to the ventrobasal complex have been demonstrated electron microscopically to terminate in a similar manner onto proximal dendrites and cell bodies of ventrobasal neurons (Lee et al., '81; McAlister and Wells, '81; Peschanski et al., '81; Tripp and Wells, '78). Inputs relayed through Vms and Vi are thought to transmit non-noxious information (Kirkpatrick and Kruger, '75) while inputs from neurons in MDH convey noxious or temperature sensitive information (Mosso and Kruger, '73; Poulos and Moult, '77; Price et al., '76; Yakota, '76). The results presented here and in another anterograde study (Peschanski, '84) suggest that noxious signals could be transmitted to VPM neurons via terminal endings with morphological features comparable to those conveying non-noxious inputs. However, it is tempting to speculate that noxious inputs are conveyed by the thinner population of Vo-TT efferent projections considering that pain afferents are characteristically small myelinated and unmyelinated fibers.

FUNCTIONAL CONSIDERATIONS

TRIGEMINAL MODULATION OF SOMATOSENSORY AND PAIN CENTERS

Tactile information from somatosensory events in the limbs, trunk and neck is conveyed by dorsal root afferents and forwarded rostrally to the diencephalon via the dorsal column nuclei-medial lemniscal pathway, as well as spinothalamic, spinomesencephalic, spinoreticulothalamic and spinocervicothalamic pathways. A parallel system for relaying tactile and

pain information from the face, scalp and oral cavity to rostral brain structures is the trigeminothalamic pathway.

Clinical evidence has accumulated to support the concept of several pain centers in the thalamus and that each may be associated with different aspects of pain sensation. It is thought that the lateral thalamus is involved with discriminative aspects of pain, while the medial thalamus is involved with the motivational, affective and arousal aspects of pain. Restricted portions of human VPL respond to clinical stimulation generating conscious sensations of sharp pain that is discretely localized, while stimulation in portions of the medial thalamus elicit reports of diffuse, burning pain. Lesions in VPL provide only temporary analgesia with severe disruption of other tactile modalities including proprioception. Destruction of medial thalamus (CM, CL, PF), will have a more prominent disrupt effect on nociception.

Meningeal innervation has been the subject of many classical neuroanatomical studies (Crosby et al, '62) and the results of these ardent searches have provided evidence for trigeminal visceral sensory innervation of the dura mater. One of the first observations of innervation of the dura mater described "nervi tentorii" issuing from the first division of the trigeminal nerve (Arnold, 1826). Additional trigeminal dura mater innervation was observed as branches, "nervous spinosus" off the third division of the trigeminal nerve, which coursed along the middle meningeal artery toward the sagittal sinus (Luschka, 1850). Functional aspects of meningeal innervation were speculated by Alexander (1875) to provide a pain function via myelinated nerves, "nervi proprii", whereas, unmyelinated nerves were thought to be associated with vasomotor activity. Later studies utilizing silver impregnation methods (Rossi and Scevola, 35)

differentiated two types of nerve plexuses; one found situated in dural tissue and another within perivascular connective tissue. Modern axonal transport techniques have demonstrated innervation of the the cerebral arteries arising from the circle of Willis and to the dura mater from neurons in the ophthalmic and mandibular portions of the trigeminal ganglion (Steiger et al., '82; Mayberg et al., '84). However, Mayberg et al., ('81;'84) believe all three divisions of the trigeminal nerve innervate the dura mater and arise from small and medium sized neurons in the trigeminal ganglion while sympathetic innervation of the dura mater arises from the superior cervical ganglion.

Fibers innervating the dura mater are thought to carry nociceptive information during episodes of migraine (Moskowitz, '84) or cluster headache (Hardebo, '84). The pain reported during these types of headaches is usually referred along a trigeminal peripheral receptive field. The demonstration of the referral of pain from arterial and dural stimulation in man shows that widespread areas of the dura and dural sinuses give rise to referred pain in the eye, forehead, temple and neck regions (Penfield and McNaughton, '40; Ray and Wolff, '40; Wirth and Van Buren, '71). Fay ('32) reported that stimulation of the proximal middle cerebral artery produces pain ipsilaterally in the forehead as well as behind the eye.

MDH is considered to be an important relay center for oro-facial pain sensations (Dubner, '78)and is thought to be the most likely region to receive nociceptive sensory information from the cranial vasculature. Davis and Dostrovsky ('88b) reported a group of neurons in MDH were excited by middle meningeal artery stimulation. MDH neurons activated by stimulation of the middle meningeal artery were almost always excited by

by noxious stimulation of the cornea and/or periorbital skin. Nociceptive specific neuronal populations in cat have been located electrophysiologically in Vo and the caudal portion of Vi which respond to electrical stimulation to both the middle meningeal artery and superior sagittal sinus (Davis and Dostrovsky, '88b). In this particular study, Davis and Dostrovsky ('88b) were able to histologically reconstruct recording sites to demonstrate that MDH neurons were concentrated in the lateral one-half of laminae III-V while neurons in Vo and the rostral portion of Vi were not confined to any particular region. Although migrainous head pain is often felt in and around the eyes and temple region, and is thought to be explained by convergence of somatic and visceral inputs on SVN neurons. However, some anatomic inconsistencies are apparent. The dura mater of the middle cranial fossa is largely supplied by the middle meningeal artery which courses with the meningeal branch of the mandibular nerve, the nervus spinosis. Since mandibular primary afferents transmit somatic information from the jaw, one would think that noxious stimulation of these primary afferents would terminate in those portions of MDH and Vo which contain cells responding to mandibular cutaneous input with subsequent referral of noxious cerebrovascular manipulation to the jaw.

It is interesting that the present study shows DM (receiving mandibular primary afferent input) to project most densely to thalamic nuclei reported to be involved with the reception of nociceptive input from cranial vasculature. Vo as well as MDH neurons may play a role in maintaining cerebrovascular homeostasis through monitoring changes in vessel diameter (stretch receptors) with adverse changes possibly being relayed to the thalamus as well as the autonomic nervous system. The observation that some trigeminothalamic neurons receive somatic as well

as visceral information provides for conscious perception of of pain (headache) along areas of the face innervated by the three divisions of the trigeminal nerve.

Figure 1: Low-power photomicrographs showing the location of PHA-L injection sites in the three subdivisions of rat trigeminal nucleus oralis (Vo), (A-C). Arrows indicate dorsomedial (DM), ventrolateral (VL), and border zone (BZ) subdivisions. A. An injection situated in the middle portion of DM (MDM), partially filling its dorsal (MDMd) and ventral (MDMv) zones. B. An injection located in VL. C. An injection located in the dorsal two-thirds of BZ with some spread into the dorsal portion of VL and the spinal trigeminal tract (svt).

FIGURE 1

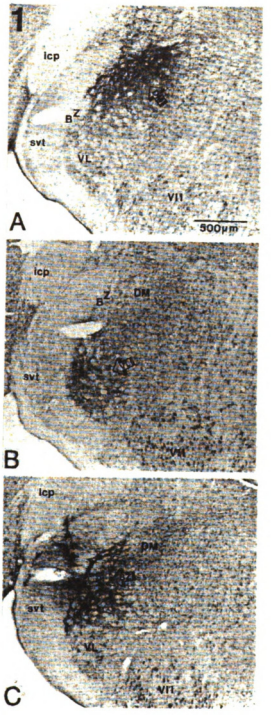

Figure 2: Camera lucida drawings of transverse sections through Vo (A-C) illustrate the locations of the three injection sites shown in Figure. 1 A-C as well as additional injection sites in the Vo subdivisions. A. An illustration of three injections contained within DM. B. An illustration of three injections located in VL. C. An illustration of two injections in BZ, both showing slight spread into either DM, VL or svt. VII, facial motor nucleus.

Figure 3: Camera lucida drawings of coronal sections through the rostral (A), middle (B-C), and caudal (D) extent of the rat ventrobasal complex of the thalamus to illustrate the topographical organization of anterogradely labeled fibers and terminal arborizations after injections made in DM. Numerous axons form dense terminal arborizations in contralateral VPM, Po, PF, and ZI with fewer fibers terminating in the same nuclei ipsilaterally. Terminal arbors were found in CM and Re and bilaterally in CL with a contralateral predominance. Sparse labeling was also noted in G.

FIGURE 3

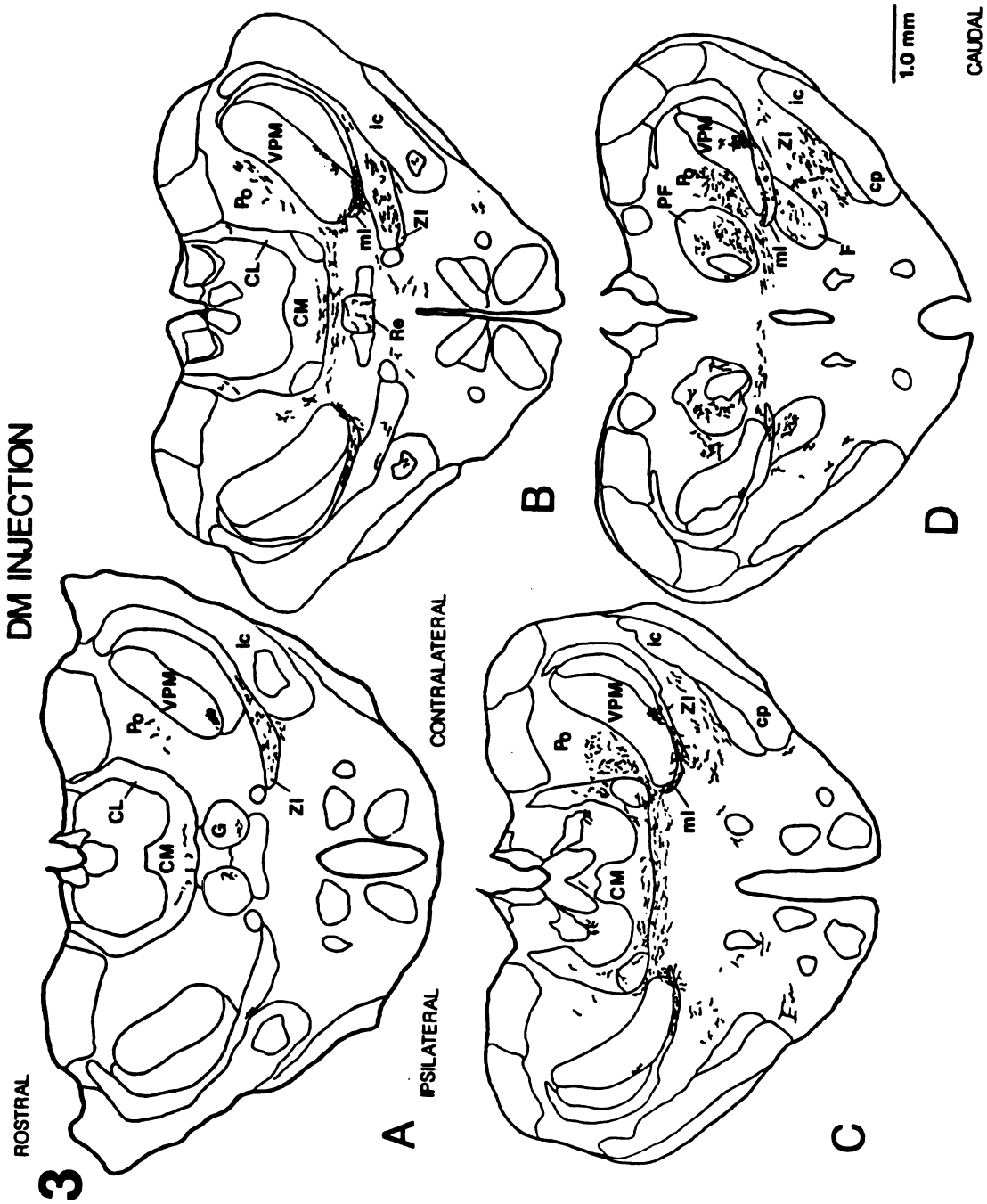
3
DM INJECTION
ROSTRAL
CAUDAL
IPSILATERAL
CONTRALATERAL
A
B
C
D
CL
CM
G
Po
VPM
Ic
ml
ZI
Re
PF
cp
1.0 mm

Figure 4: Camera lucida drawings of coronal sections through the rostral (A), middle (B-C), and caudal (D) extent of the rat ventrobasal complex of the thalamus to illustrate the topographical organization of anterogradely labeled fibers and terminal arborizations after injections made in VL. Terminal arbors were observed bilaterally in Po, PF, and ZI and contralaterally in VPM. The densities of the terminal arborizations appear to be less than those observed following DM injections. Sparsely dispersed terminal arbors were found in rostral CM and in Re while no labeling was noted in CL.

FIGURE 4

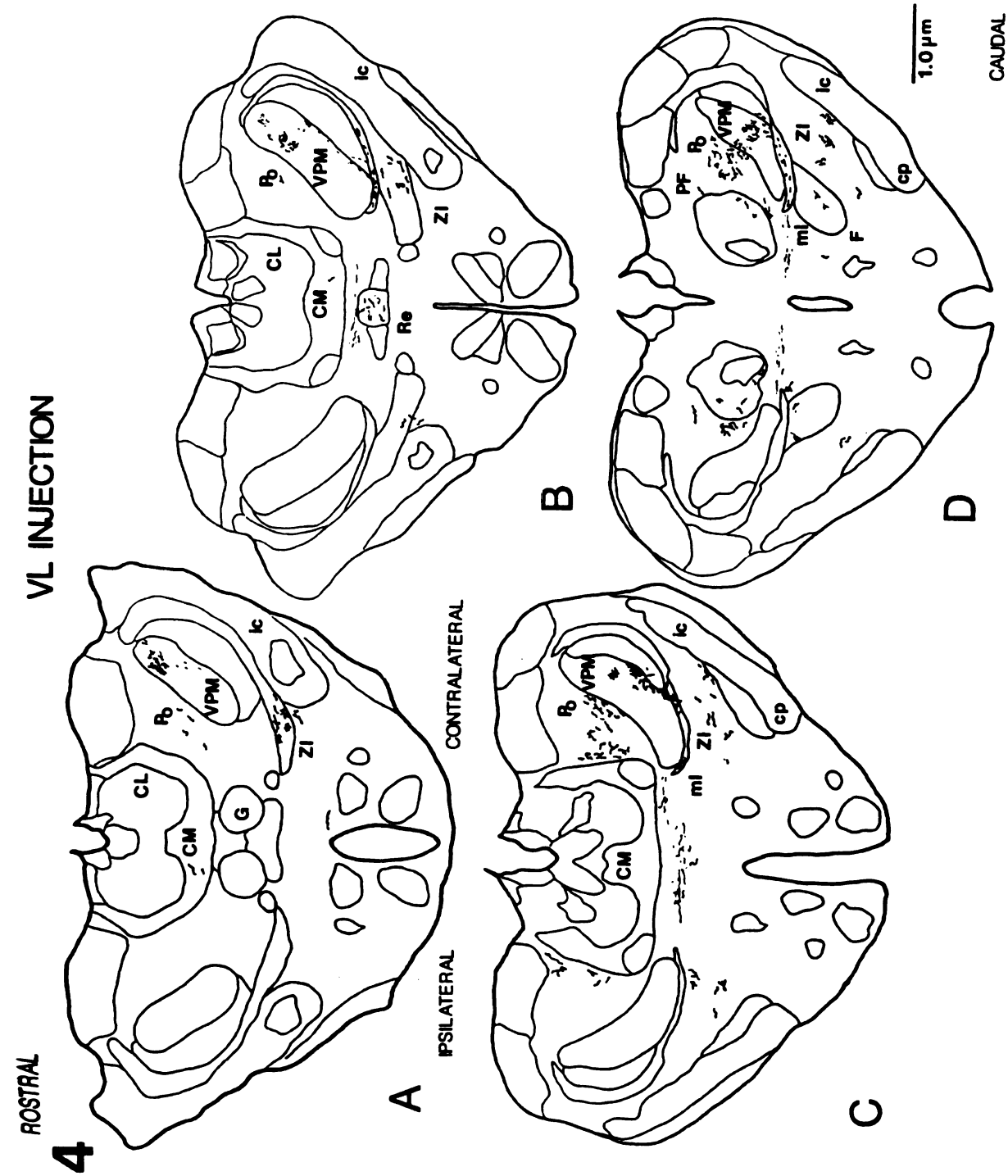
4
ROSTRAL
VL INJECTION
A
B
C
D
IPSILATERAL
CONTRALATERAL
CAUDAL
1.0 µm
CL
CM
G
Rb
VPM
Ic
ZI
Re
ml
cp
PF
F

Figure 5: Camera lucida drawings of coronal sections through the rostral (A), middle (B-C), and caudal (D) extent of the rat ventrobasal complex of the thalamus to illustrate the topographical organization of anterogradely labeled fibers and terminal arborizations after injections made in BZ. Labeled terminal arbors were found bilaterally in Po and PF, with a contralateral predominance, and only contralaterally in VPM and ZI. A small number of trigeminal afferent axons were observed to terminate midway through CM and in Re. No labeling was observed in CL.

FIGURE 5

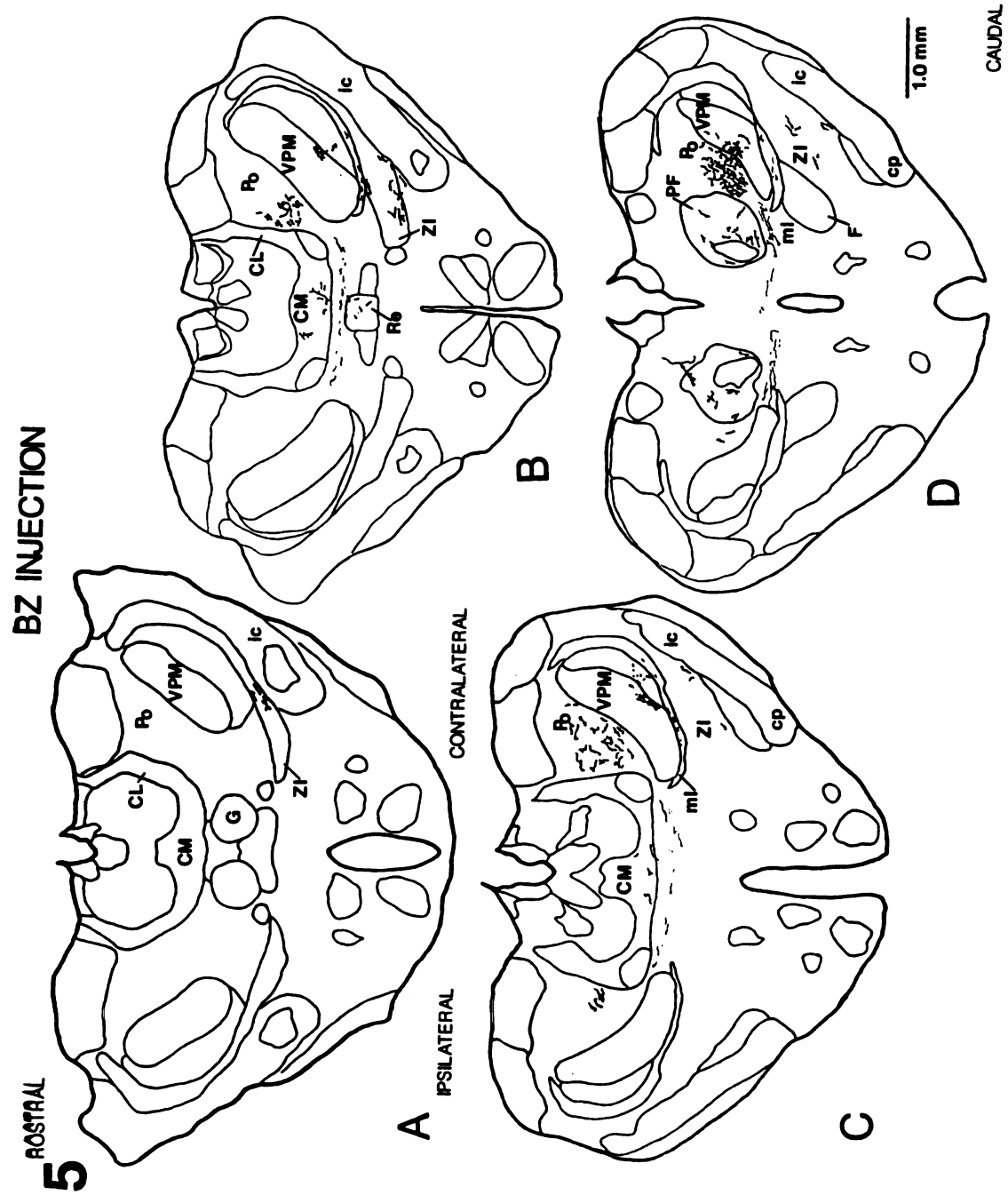
5
ROSTRAL
BZ INJECTION
A
IPSILATERAL
CONTRALATERAL
B
C
D
CAUDAL
1.0 mm
CL
CM
G
Rb
VPM
Ic
ZI
ml
cp
PF
F

Figure 6: Camera lucida drawing illustrating injection sites in (A) for DM, VL and BZ subdivisions and corresponding coronal sections in rostral (B) and caudal (C) levels of the ventral posteromedial nucleus of the thalamus (VPM). The topographical distribution of Vo efferent terminal arbors observed in rostral VPM following injections made in all three subdivisions is seen to shift at caudal VPM levels and occupy a central position with efferent terminal arbors from neurons in DM, VL and BZ subdivisions overlapping centrally along the mediolateral axis of VPM.

FIGURE 6

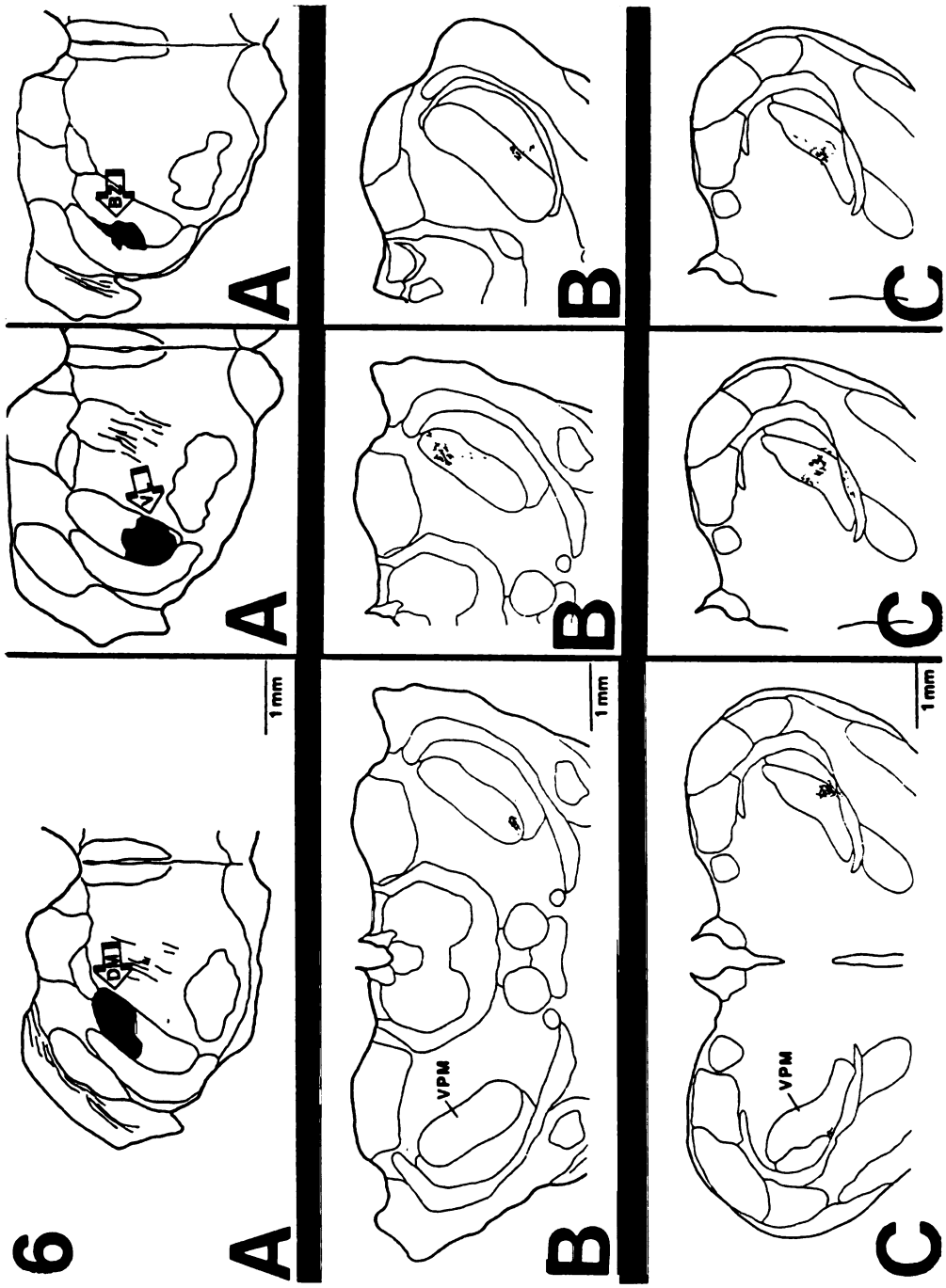

Figure 7: A: A high power reconstruction of two patch-like arrangements of labeled trigeminal afferents in contralateral VPM after an injection of PHA-L into VL. This characteristic arrangement of terminal strands is also observed following injections made in DM and BZ. Both arrangements contain two types of Vo-VPM efferents, a thin relatively unbranched terminal strand containing widely spaced oval boutons (arrow 1) as well as a thicker strand with large bulbous irregularly shaped boutons (arrow 2). B. High power reconstruction to illustrate the two distinct populations of terminal arborizations within the VPM patches.

FIGURE 7

Fig. 8. A high power reconstruction of the two types of Vo-Po efferent labeled after injection of PHA-L into each of the three Vo subdivisions. Numerous terminal arbors can be found throughout ipsilateral and contralateral Po. The first type is characterized by thin terminal strands which are observed to emit a few short side branches bearing small boutons en passant and end boutons (arrows). The second type of terminal arborization ensues from a thicker terminal strand from which secondary and tertiary side branches are observed as the parent axon terminates in a bulbous end bouton (b).

Fig. 9. A high power reconstruction of PHA-L labeled terminal arborizations in contralateral ZI following DM, VL, and BZ injections. There are two morphologically distinct types of terminal strands. One type (arrow 1) consists of a thinner terminal strand primarily situated ventrally in ZI which exhibits sparse branching and widely-spaced small axonal endings. The second type (arrow 2) is found both dorsally and ventrally within ZI and is characterized by a thicker terminal strand with numerous side branches. These branches and terminal strands contain several multi-shaped boutons en passant and end boutons.

Fig.10. A-D High power reconstructions of terminal strands which arise from the single type of Vo efferent found to terminate in CM, CL, PF, and Re following injections of PHA-L into each of the three Vo subdivisions. The thin terminal strands are sparsely branched and contain several widely spaced axonal endings. A. Representative Vo-CM terminal strands. B. Representative Vo-CL terminal strands. There is an absence of labeling in CL following VL and BZ injections. C. Representative Vo-PF terminal strands. D. Representative Vo-Re terminal strands.

FIGURE 10

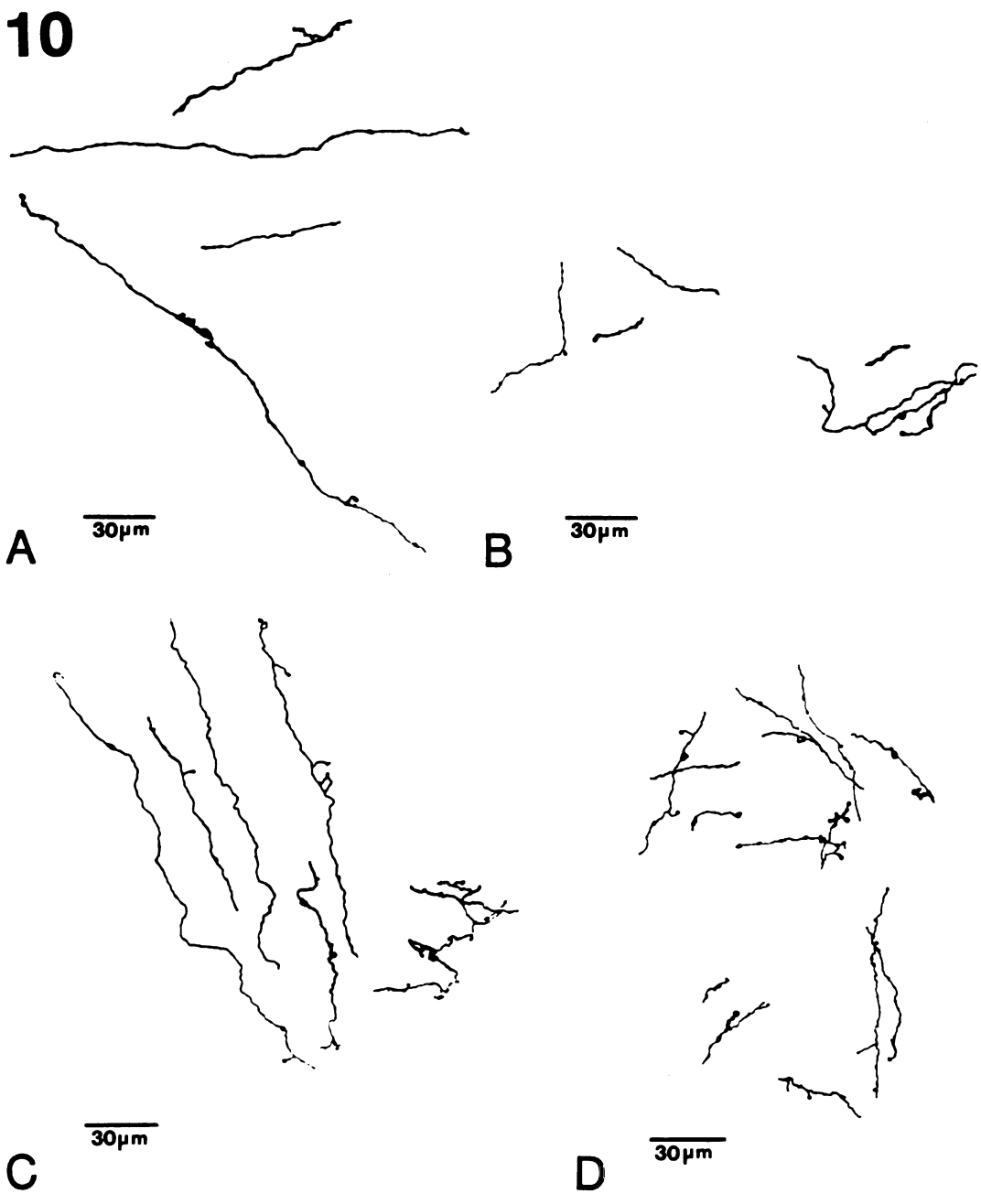

Fig. 11: Photomicrographs illustrating labeled terminal strands in diencephalic nuclei following PHA-L injections into Vo subdivisions (except for the absence of efferents in CL following injections in VL and BZ). A. An aggregate of labeled terminal strands ending in patch-like clusters in contralateral VPM. B. Labeled terminal strands in contralateral VPM illustrating one of the two representative types of Vo-VPM efferents. Large, bulbous, irregularly shaped boutons (arrows) are characteristic of this type of efferent fiber. C. The second type of Vo-VPM afferent characterized by a thin terminal strand capped by an oval bouton (arrow). D. Labeled terminal strands of the second type of Vo efferent terminal ending in Po is shown bearing several boutons en passant. E. A terminal portion of one of the two types of Vo-ZI afferent fibers exhibiting several boutons, one of which closely approximates a cell body. F. Labeled terminal strands seen in close approximation (arrows) to ZI neuronal cell bodies illustrate the second type of Vo-ZI efferent. G. Labeled terminal strands (arrows) in CL characteristic of the single type of efferent found in CM, CL, PF and Re. H. A labeled terminal strand closely approximates a cell body in Re (arrow).

FIGURE 11

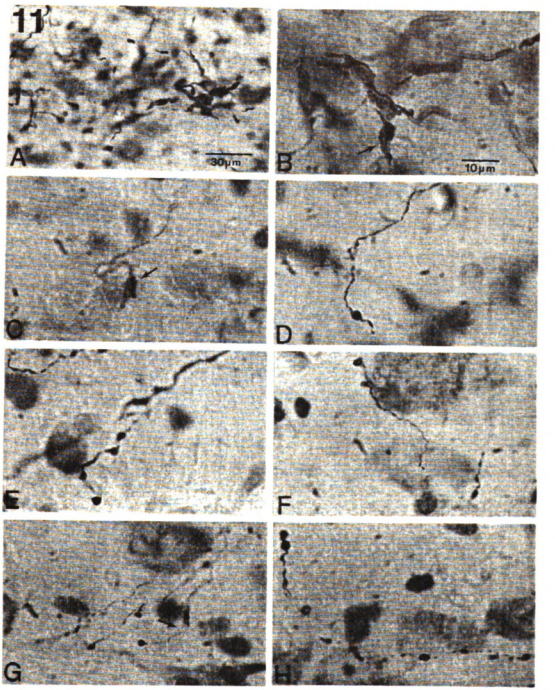

Figure 12: Photomicrograph illustrating a labeled terminal strand in Po following PHA-L injections into Vo subdivisions. The terminal arborization shown is of the first type of terminal strand found in Po and is characterized by a thin diameter axon with very sparse side branches and boutons en passant

FIGURE 12

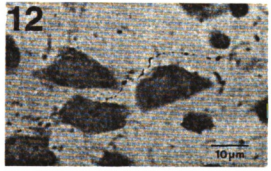

CONCLUDING REMARKS

Studies on the functional organization of SVN with respect to its involvement with chronic pain states (e.g., trigeminal neuralgia) have focused on the medullary dorsal horn (MDH) in light of its involvement with the reception, central processing and modification and relay of nociceptive information from orofacial structures. MDH is thought to be anatomically similar to the spinal cord dorsal horn, which is also involved in the reception, central processing and modification of nociceptive input to be relayed from the trunk and limbs (Gobel et al., '77) Clinical observations concerning trigeminal tractotomy in humans (Kunc, '70; Sjoqvist, '38) following severing the svt at the level of the obex, include an ipsilateral analgesis and thermanalgesia, while tactile sensations remain uninterrupted. Of the studies, in rat (Shigenaga et al., '88; Denny-Brown and Yanagisawa, '73), cat (Azerad, '82; Dickenson et al., '81; Hu and Sessle, '84; Sessle and Greenwood,'75; Yakota and Nishikawa, '82) and monkey (Bushnell et al., '84; Hoffman et al., '81; Price et al., '76), utilizing techniques to stimulate orofacial receptive fields by noxious stimuli, have recorded from neurons responding within MDH. The rostral portion of SVN, e.g., nucleus oralis (Vo) is also involved in the reception, central processing with modification and transmission of nociceptive inputs arising from oral and perioral regions. The fact that neurosurgical procedures in humans involving trigeminal tractotomy will preserve sensations for the oral cavity, tooth pulp and the central portion of the face is supported in animal research. Animal studies utilizing behavioral or

reflex models to study nociceptive reactions induced by dental, oral, and perioral (Azerad and Woda, '76; Broton and Rosenfeld, '85; Dallel et al, '88; Denny-Brown and Yanagisawa, '73; Sumino, '71; Young et al, '81; Young and Perryman, '84) or by facial stimulation (Dallel et al., '88; Borke et al., '83) have demonstrated that sensation in these areas area maintained following tractotomy. Lesions in the rostral SVN (Young and Perryman, '84; Pickoff-Matuk, et al., '86) without svt involvement, and lesion experiments that sever Vo efferent pathways (Broton and Rosenfeld, '82; Broton and Rosenfeld, '86) have shown decreases in rat behavioral responses to dental, oral and perioral noxious stimulation. Anatomical studies utilizing the transganglionic transport of HRP following into rat and cat tooth pulp, reveal that labeled primary trigeminal tooth pulp afferents project to all three portions of the SVN and the main sensory nucleus with the heaviest density being found in Vo (Arvidsson and Gobel, '81; Marfurt and Turner, '84; Westrum et al., '81). HRP injections into the sensory root of the trigeminal nerve demonstrate that rat Vo receives primary trigeminal axons with parent branches displaying morphology and size range accepted for Ad and C primary axons (Falls, '88). In addition, electrophysiological studies strongly suggest Vo is not only involved in the sensory aspect of pain but in motor activities or motivational affective mechanisms (Melzack and Casey, '68) related to pain (Azerad and Woda, '76; Dubner et al., '78; Hu and Sessle, '84; Matthew[illegible]al., '76). Electrophysiological and anatomical evidence in mammals [illegible]s that Vo receives innocuous inputs from primary trigeminal neurons which conduct in the Ad and Ab ranges and innervate peripheral receptive fields located in the oral cavity and on the face (Azerad et al., '82; Eisenman et al., '63; Greenwood, '73; Hayashi, '82; Khayyat et al., '75; Marfurt and Turner,

'84; Sessle and Greenwood, '76; Sessle and Hu, '81; Westrum et al., '81). These inputs also activate second order Vo and Vms projection neurons and non-relay cells, many of which receive nociceptive inputs. These non-relay cells have been considered to serve as interneurons mediating the excitatory and inhibitory influences of noxious information on tongue and jaw reflexes (Azerad and Woda, '76; Sar et al., '78; Sessle and Greenwood, '75). Complex interactions occur in Vo not only between non-primary afferents and nociceptive and mechanoceptive primary trigeminal axonal endings, but also between various non-primary inputs suggesting that Vo does not merely relay nociceptive and mechanoceptive inputs from the orofacial regions to other brain and spinal cord areas, since it is positioned to participate in the transmission of this input after subjecting it to central processing and modification.

Based on the results of the present study, Vo projection neurons target a larger area of the neuraxis than previously reported and their contribution to the modulation of motor expression is a certain possibility via their positions in the brainstem, cerebellum and spinal cord regions. Not only are cell bodies within the three subdivisional areas of Vo able to influence the output cells within the ventral horn of the spinal cord but they are also able to modify incoming afferent input in the dorsal horn thereby manipulating reflex circuitry as well as ascending sensory inputs. Many reflexes utilizing the afferent limb of trigeminal primary afferents have been reported clinically, e.g., diving reflex. The diving reflex or depressor reflex has been explored in various mammals, including man with the common report of a profound fall in arterial pressure and slowing of the heart rate following stimulation within the spinal trigeminal nucleus (Kumada et al., 75). However, the exact circuitry for these reflexes are not

certain. For the first time, this study provides some of the anatomical substrates which may be utilized in determining one of the possible efferent arms for observed clinical reflexes. It is known that paroxysmal supraventricular tachycardia (PST) in children, a treatable cardiac emergency, is not reversed by such maneuvers as reflex vagal stimulation, carotid massage, unilateral ocular pressure, induction of vomiting or the Valsalva maneuver. However, stimulation of the diving reflex by immersion of the face in cold water has been noted to terminate the attacks of supraventricular tachycardia in adults (Wildenthal et al., 75; Pickering and Bolton-Maggs, '75; Whayne, '76) as well as children (Whayne, '76; Whitman and Zakeosian, '76), with one report of the successful use of the diving reflex to terminate PST in two infants (Whitman et al., '77). In Chapt I, with the demonstration of an extensive projection pathway from DM to caudal levels of the spinal cord, the suggestion was made for exuberant trigeminal pathways along the neuraxis, but predominately in the spinal cord, as a result of other studies in human fetus experimentation (Hooker and Davenport, '59) and in Chapt III the extensive connections that DM makes with most of the cranial nerve nuclei suggests for the possibility of a new role for Vo as a reflex center within SVC. The dominant interaction that the trigeminal system has on the motor, sensory and autonomic nervous system in adults and children as illustrated here further suggests for its possible participation in pathological states that mimic a depressor-type response in the nervous system of children, e.g., sudden infant death syndrome. Certainly as more information regarding the neuronal circuitry of the trigeminal system is revealed, many unexplained syndromes may someday be better understood.

FIGURE 1: Overall Vo efferent distribution

FIGURE 1

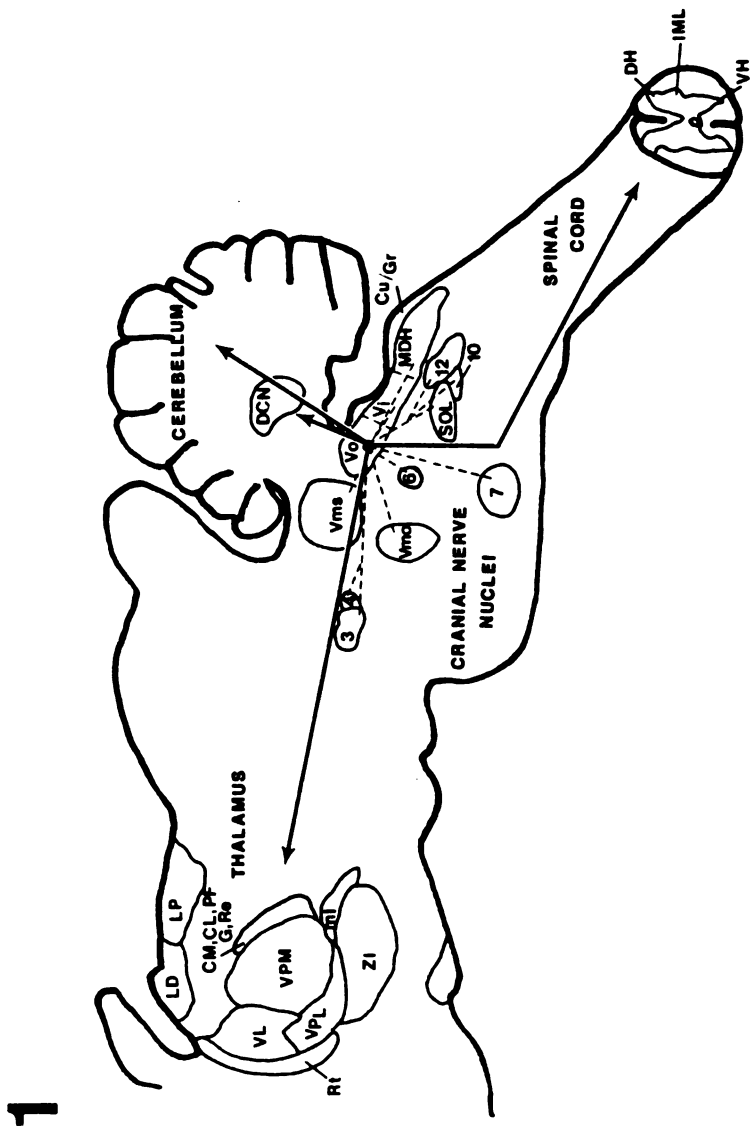

Vo EFFERENT PROJECTIONS

BIBLIOGRAPHY

BIBLIOGRAPHY

Abols, I. A., A. I. Basbaum (1981) Afferent connections of the rostral medulla of the cat: A neural substrate for midbrain-medullary interactions in the modulation of pain. J. Comp. Neurol. 201:285-297.

Abrahams, V. C., and P. K. Rose (1975) Projections of extraocular, neck muscle, and retinal afferents to superior colliculus in the cat: Their connections to cells of origin of tectospinal tract. J. Neurophysiol. 38:10-18.

Abrahams, V. C., G. Anstee, F. J. R. Richmond, and P. K. Rose (1979) Neck muscle and trigeminal input to the upper cervical cord and lower medulla of the cat. Can. J. Physiol. Pharmacol. 57:642-651.

Aker, F. D., and E. J. Reith (1980) Localization and quantification of neuron cell bodies innervating a rat mandibular molar tooth. Anat. Rec. 196:6A.

Albe-Fessard, D., A. Levante, and Y. Lamour (1974) Origin of spinothalamic tract in monkeys. Brain Res. 65:503-509.

Albe-Fessard, D., and J. M. Besson (1973) Convergent thalamic and cortical projections the non-specific system. In. Handbook of Sensory Physiology, Vol II: Somatosensory System. (A. Iggo, ed.) Springer, Berlin, pp. 490-560.

Albe-Fessard, D., K. J. Berkley, L. Kruger, H. J. Ralston, III., and W. D. Willis, Jr. (1985) Diencephalic mechanisms of pain sensation. Brain Res. Rev. 9:217-296.

Albright, B. C., and D. E. Haines (1978) Dorsal column nuclei in a prosimian primate (*Galago senegalensis*): II. Cuneate and lateral cuneate nuclei: Morphology and primary afferent fibers from cervical and upper thoracic spinal segments. Brain Behav. Evol. 15:165-184.

Aldskogius, H., and J. Arvidsson (1978) Nerve cell degeneration and death in the trigeminal ganglion of the adult rat following peripheral nerve transection. J. Neurocytol. 7:229-250.

Alexander, W. T. (1875) Bemerkungen uber die Nerven der mater. Arch. Mikr. Anat. XI. pp. 231-234.

Allen, F. D., and E. J. Reith (1924) Localization in the ganglion semilunare of the cat. J. Comp. Neurol. 38:1-24.

Amandt, K., J. Czachurski, K. Dembowsky, and H. Seller (1979) Bulbospinal projections to the interomediolateral cell column: A neuroanatomical study. J. Autonom. Nerv. Syst. 1:103-117.

Ammann, B., J. Gottschall, and W. Zenker (1983) Afferent projections from the rat longus capitus muscle studied by transganglionic transport of HRP. Anat. Embryol. 166:275-289.

Ammons, W. S., N.-M. Girardot, and R. D. Foreman (1985) Characteristics of T2-T5 spinothalamic neurons with viscerosomatic convergent inputs projecting to medial thalamus. J. Neurophysiol. 54:73-89.

Ammons, W. S., R. W. Blair, and R. D. Foreman (1984) Greater splanchnic excitation of primate T1-T5 spinothalamic neurons. J. Neurophysiol. 51:592.

Anden, N. E., M. G. M. Jukes, A. Lundberg, and L. Vyklicky (1966) The effect of DOPA on the spinal cord. I. Influence on transmission from primary afferents. Acta Physiol. Scand. 67:373-386.

Andersen, H. T. (1966) Physiological adaptations in diving vertebrates. Physiol. Rev. 46:212-243.

Andersen, P., J. C. Eccles, R. F. Schmidt, and T. Yokota (1964) Identification of relay cells and interneurons in the cuneate nucleus. J. Neurophysiol. 27:1080-1095.

Anderson, K. V., G. S. Pearl, and C. Honeycutt (1976) Behavioral evidence showing the predominance of diffuse pain stimuli over discrete stimuli in influencing perception. J. Neurosci. Res. 2:283-289.

Anderson, K., and H. Rosing (1977) Location of feline trigeminal ganglion cells innervating maxillary canine teeth: A horseradish peroxidase analysis. Exp. Neurol. 57:302-306.

Anderson, M. E., M. Yoshida, and V. J. Wilson (1971) Influence of superior colliculus on cat neck motoneurons. J Neurophysiol. 34:898-907.

Anderson, M. E., M. Yoshida, and V. J. Wilson (1972) Tectal and tegmental influences on cat forelimb and hindlimb motoneurons. J. Neurophysiol. 35:462-470.

Andres, K. H., M. Von During, K. Muszynsky, and R. F. Schmidt (1987) Nerve fibers and their terminals in the dura mater encephali of the rat. Anat. Embryol. 175:289-301.

Andrezik, J. A., V. Chan-Palay, and S. L. Palay (1981) The nucleus paragigantocellularis lateralis in the rat. Demonstration of afferents by the retrograde transport of horseradish peroxidase. Anat. Embryol. 161:373-390.

Angerbauer, C., and J. O. Dostrovsky (1984) A nociceptive projection from the medullary dorsal horn to the thalamus. Pain Suppl. 2:S282.

Angulo y Gonzales, A. W. (1940) The differentiation of the motor cell columns in the cervical cord of albino rat fetuses. J. Comp. Neurol. 73:469-488.

Appel N. M., and R. P.Elde (1988) The intermediolateral cell column of the thoracic spinal cord is comprised of target-specific subnuclei: Evidence from retrograde transport studies and immunohistochemistry. J. Neurosci. 8(5):1767-1775.

Applebaum, A. E., R. B. Leonard, D. R. Kenshalo, Jr., R. F. Martin, and W. D. Willis (1979) Nuclei in which functionally identified spino-thalamic tract neurons terminate. J. Comp. Neurol. 188:575-585.

Aprison, M. H., R. P. Shank, and R. A. Davidoff (1969) Glycine: A transmitter suspect in different areas of the brain and spinal cord in seven different vertebrates. Comp. Biochem. Physiol. 28:1345-1355.

Arends, J. J. A., T. J. H. Ruigrok, T. A. Henderson, and M. F. Jacquin (1990) Trigeminocerebellar projections in the adult rat. Soc. Neurosci. Abstr. 16:223.

Arieff, A. J., and S. W. Pyzik (1953) The ciliospinal reflex in injuries of the cervical spinal cord in man. A. M. A. Arch. Neurol. Psychiat. 70:621-629.

Armstrong, D. M., and R. F. Schild (1978a) An investigation of the cerebellar corticonuclear projections in the rat using an autoradiographic tracing method. I. Projections from the vermis. Brain Res. 141:1-19.

Armstrong, D. M., and R. F. Schild (1978b) An investigation of the cerebellar corticonuclear projections in the rat using an autoradiographic tracing method. II. Projections from the hemisphere. Brain Res. 141: 235-249.

Armstrong, D. M., N. C. Campbell, S. A. Edgley, R. F. Schild, and J. R. Trott (1982) Investigations of the olivocerebellar and spino-olivary pathways. In S. L. Palay, and V. Chan-Palay (eds): The Cerebellum-New Vistas. New York: Springer-Verlag. pp. 194-232.

Armstrong, R., L. Blesovsky, R. Corsiglia, and G. Gordon (1979) Descending projections form the cat's dorsal column nuclei. J. Physiol. (London). 296:43P.

Armstrong-James, M., C. A. Callahan, and M. A. Freidman (1991) Thalamocortical processing of vibrissal information in the rat. I. Intracortical origin of surround but not centre-receptive fields of layer-IV neurons in the rat S-I barrel field cortex. J. Comp. Neurol. 303:193-210.

Arnold, F. (1860) Icones nervorum capitus. Heidelberg, J. C. B. Mohr. pp. 34.

Arvidson, J. (1975) Location of cat trigeminal ganglion cells innervating dental pulp of upper and lower canines studied by retrograde transport of horseradish peroxidase. Brain Res. 99:135-139.

Arvidsson, B (1977) Retrograde axonal transport of HRP from cornea to the trigeminal ganglion. Acta Neuropathol. 38:49-52.

Arvidsson, J (1982) Somatotopic organization of vibrissae afferents in the trigeminal and spinal ganglia investigated by transganglionic transport of HRP. J. Comp. Neurol. 211:84-92.

Arvidsson, J., and G. Grant (1979) Further observations on transganglionic degeneration in trigeminal primary sensory neurons. Brain Res. 162:1-22.

Arvidsson, J., and S. Gobel (1981) An HRP study of the central projections of primary trigeminal neurons which innervate tooth pulps in the cat. Brain Res. 10:1-16.

Asanuma, C., W. T. Thach, and E. G. Jones (1983a) Cytoarchitectonic delineation of the ventral lateral thalamic region in monkeys. Brain Res. Rev. 5:219-235.

Asanuma, C., W. T. Thach, and E. G. Jones (1983b) Anatomical evidence for segregated focal groupings of efferent cells and their terminal ramifications in the cerebellothalamic pathway of the monkey. Brain Res. Rev. 5:267-297.

Asanuma, C., W. T. Thach, and E. G. Jones (1983c) Distribution of cerebellar terminations and their relation to other afferent terminations in the thalamic ventral lateral region of the monkey. Brain Res. Rev. 5:237-265.

Aschner, B. (1908) Uber einer bisher noch nicht beschriebenen Reflex vom Auge auf Kreislauf und Atmung. Verschwinden des Radialispulses bei Druck auf Auge. Wein. Klin. Wschr. 21:1529-1530.

Azerad, J., A. Woda, and D. Albe-Fessard (1982) Physiological properties of neurons in different parts of the cat trigeminal sensory complex. Brain Res. 246:7-21.

Azerad, J., and A. Woda (1976) Tooth pulp projection to the trigeminal complex and jaw opening reflex in the cat. J. Biol. Bucc. 4:109-115.

Barber, R. P., J. E. Vaughn, E. Robert (1982) The cytoarchitecture of GABAergic neurons in rat spinal cord. Brain Res. 238:305-328.

Barber, R. P., J. E. Vaughn, J. R. Slemmon, P. M. Salvaterra, E. Roberts, and S. E. Leeman (1979) The origin, distribution and synaptic relationships of substance P axons in rat spinal cord. J. Comp. Neurol. 184:331-352.

Basbaum, A. I. (1980 The anatomy of pain and pain modulation. In: H. W. Kosterlitz and L. Y. Terenius (eds.): Pain and Society. Weinheim: Verlag Chemie, pp. 91-122.

Basbaum, A. I., and H. L. Fields (1979) The origin of descending pathways in the dorsolateral funiculus of the spinal cord of the cat and rat: Further studies on the anatomy of pain modulation. J. Comp. Neurol. 187:513-532.

Basbaum, A. I., and P. J. Hand (1973) Projections of cervicothoracic dorsal roots to the cuneate nucleus of the rat, with observations on cellular "bricks". J. Comp. Neurol. 148:347-360.

Basbaum, A. I., C. H. Clanton, and H. L. Fields (1978) Three bulbospinal pathways from the rostral medulla of the cat: An autoradiographic study of pain modulating systems. J. Comp. Neurol. 178:209-224.

Bates, C. A., and H. P. Killackey (1985) The organization of the neonatal rat's brainstem trigeminal complex and its role in the formation of central trigeminal patterns. J. Comp. Neurol. 240:265-287.

Beadreau, D. E., and C. Jerge (1968) Somatotopic representation in the gasserian ganglion of tactile peripheral fields in the cat. Arch. Oral Biol. 13:247-256.

Beaudet, A., and C. Sotelo (1980) Synaptic remodeling of serotonin axon terminals in rat agranular cerebellum. Brain Res., 206:305-330.

Beitz, A. J. (1982) Structural organization of the fastigial nucleus. Exp. Brain Res. Supl. 6:233-246.

Belford, G. R., and H. P. Killackey (1979) Vibrissae representation in subcortical trigeminal centers of the neonatal rat. J. Comp. Neurol. 183:305-322.

Bennett, G. J., Z. Seltzer, G. W. Lu, N. Kishikawa, and R. Dubner (1983) The cells of origin of the dorsal column projection in the lumbosacral enlargements of cats and monkeys. Somatosens. Res. 1:131-149.

Bentivolgio, M., and H. G. J. M. Kuypers (1982) Divergent axon collaterals from the rat cerebellar nuclei to diencephalon, mesencephalon, medulla oblongata and cervical cord: A fluorescent double-labeling study. Exp. Brain Res. 46:339-356.

Berkley, K. J. (1975) Different targets of different neurons in nucleus gracilis of the cat. J. Comp. Neurol. 163:285-304.

Berkley, K. J. (1980) Spatial relationships between the terminations of somatic sensory and motor pathways in the rostral brainstem of cats and monkeys. I. Ascending somatic sensory inputs to lateral diencephalon. J. Comp. Neurol. 193:283-317.

Berkley, K. J. (1983) Afferent projections to and near the ventrobasal complex in the cat and monkey. In Somatosensory Integration in the Thalamus. A Re-evaluation based on New Methodological Approaches (eds. Macchi G., Rustionii A. and Spreafico R.), pp. 43-62. Elsevier, Amsterdam.

Berkley, K. J., A. Bloomqvist, A. Pelt, and R. Fink (1980) Differences in the collaterization of neuronal projections from the dorsal column nucleus and lateral cervical nucleus to the thalamus and tectum in the cat: An anatomical study using two different double labeling techniques. Brain Res. 202:273-290.

Berkley, K. J., and P. J. Hand (1978a) Projections to the inferior olive of the cat: II. Comparisons of input from the gracile, cuneate and the spinal trigeminal nuclei. J. Comp. Neurol. 180:253-264.

Berkley, K. J., and P. J. Hand (1978b) Efferent projections of the gracile nucleus in the cat. Brain Res. 153:263-283.

Berkley, K. J., R. J. Budell, A. Bloomqvist, and M. Bull (1986) Output systems of the dorsal column nuclei in the cat. Brain Res. 11:199-225.

Berod, A., B. K. Hartman, and J. F. Pujol (1981) Importance of fixation in immunohistochemistry: use of formaldehyde at variable pH for the localization of tyrosine hydroxylase. J. Histochem. Cytochem. 29:844-850.

Biedenbach, M. A. (1972) Cell density and regional distribution of cell types in the cuneate nucleus of the rhesus monkey. Brain Res. 45:1-14.

Bijlani, F., and N. H. Keswani (1961) The phrenic nucleus in the spinal cord of monkey (*Macaca mulatta*). Ind. J. Med. Res. 49:648-655.

Bjorkeland, M. (1983) Projections from the dorsal column nuclei and spinal cord to the pontine nuclei in cat. Abstr. Eur. Neurosci.

Bjorkeland, M., and J. Boivie (1985) Anatomy of the midbrain projections from the lateral cervical nucleus in the cat. In M. Rowe, and W. D. Willis, Jr., (eds.) Development, Organization, and Processing in Somatosensory Pathways. New York. A. R. Liss Inc., pp. 203-214.

Bjorkeland, M., and J. Bovie (1984) An anatomical study of the projections from the dorsal column nuclei to the midbrain in the cat. Anat. Embryol. 170:29-43.

Bjorklund, A., and G. Skagerberg (1979) Evidence for a major spinal cord projection from diencephalic A11 dopamine cell group in the rat using transmitter-specific fluorescent retrograde tracing. Brain Res. 177:170-175.

Blair, R. W., R. N. Weber, and R. D. Foreman (1981) Characteristics of primate spinothalamic tract neurons receiving viscerosomatic convergent inputs in T3-T5 segments. J. Neurophysiol. 46:797-811.

Blomqvist, A. (1980) Gracilo-diencephalic relay cells: A quantitative study in the cat using retrograde transport of horseradish peroxidase. J. Comp. Neurol. 193:1097-1125.

Blomqvist, A., R. Fink, D. Bowsher, S. Griph, and J. Westman (1978) Tectal and thalamic projections of dorsal column and lateral cervical nuclei: A quantative study in the cat. Brain Res. 141:335-341.

Boivie, J. (1970) The termination of the cervicothalamic tract in the cat. An experimental study with silver impregnation methods. Brain Res. 19:333-360.

Boivie, J. (1971) The termination in the thalamus and zonal incerta of fibers from the dorsal column nuclei (DCN) in the cat. An experimental study with silver impregnation methods. Brain Res. 28:459-490.1

Boivie, J. (1978) Anatomical observations on the dorsal column nuclei. Their thalamic projection and the cytoarchitecture of some somatosensory thalamic nuclei in the monkey. J. Comp. Neurol. 178:17-48.

Boivie, J. (1979) An anatomical reinvestigationof the termination of the spinothalamic tract in the monkey. J. Comp. Neurol. 186:343-370.

Boivie, J. (1980) Thalamic projections from lateral cervical nucleus in the monkey. A degeneration study. Brain Res. 198:13-26.

Boivie, J., and E. R. Perl (1975) Neural substrates of somatic sensation. In: MTP International Review of Science, Physiology Series One. Vol. 3, Neurophysiology. C. C. Hunt ed. University Park Press, Baltimore. pp.303-411.

Bombardieri, R. A., Jr., J. I. Johnson, Jr., and G. B. Campos (1975) Species differences in mechano-sensory projections from the mouth to the ventrobasal thalamus. J. Comp. Neurol. 163:41-64.

Borges, L. F., and M. A. Moskowitz (1983) Do intracranial and extracranial trigeminal afferents represent divergent axon collaterals? Neurosci Lett. 35:265-270.

Borke, R. C., M. E. Nau, and R. L. Ringer (1983) Brain stem afferents of hypoglossal neurons in the rat. Brain Res. 269:47-55.

Bower, J. M., D. H. Beerman, J. M. Gibson, G. M. Shambes, and W. Welker (1981) Principles of organization of a cerebro-cerebellar circuit: Micromapping projections from cerebral (SI) to cerebellar (granule cell) tactile areas of rats. Brain Behav. Evol. 18:1-18.

Bowker, R. M., H. W. M. Steinbusch, and J. D. Coulter (1981) Serotonin and peptidergic projections to the spinal cord demonstrated by a combined retrograde HRP histochemical staining method. Brain Res. 211:412-417.

Bowker, R. M., L. C. Abbott, and R. P. Dilts (1988) Peptidergic neurons in the nucleus raphe magnus and the nucleus gigantocellularis: their distributions, interrelationships, and projections to the spinal cord. Prog. in Brain Res. 77:95-127.

Brink, E. E., J. I. Morrell, and D. W. Pfaff (1979) Localization of lumbar epaxial motoneurons in the rat. Brain Res. 170:23-41.

Brodal , A., and P. A. Drablos (1963) Two types of mossy fiber terminals in the cerebellum and their regional distribution. J. Comp. Neurol. 121:173-187.

Brodal, A. (1980) Olivocerebellocortical projection in the cat as determined with the method of retrograde axonal transport of horseradish peroxidase. II. Topographical pattern in relation to the longitudinal subdivision of the cerebellum. In J. Courville, C. de Montigny and Y. Lamarre, (Eds.), The inferior olivary nucleus: Anatomy and physiology, Raven press, New York, pp187-206.

Brodal, A., and K. Kawamura (1980) Olivocerebellar projection: A review. Adv. Anat. Embryo. Cell Biol. 64:1-40.

Brodal, A., and R. Rexed (1953) Spinal afferents to the lateral cervical nucleus in the cat. J. Comp. Neurol. 98:179-211.

Brodal. A. (1974) Anatomy of the vestibular nuclei and their connections. In H. H. Kornhuber (ed.) Handbook of Sensory Physiology: Vestibular System. Springer-Verlag, Berlin, Vol. 6:239-352.

Broton, J. G., and J. P. Rosenfeld (1982) Rostral trigeminal projections signal perioral facial pain. Brain Res. 243:395-400.

Broton, J. G., and J. P. Rosenfeld (1985) Effects of trigeminal tractotomy on facial thermal nociception in the rat. Brain Res. 333:63-72.

Broton, J. G., and J. P. Rosenfeld (1986) Cutting rostral trigeminal nuclear complex projections preferentially affects perioral nociception in the cat. Brain Res. 397:1-8.

Brown, A. G (1981) Organization in the spinal cord. Springer Verlag, Heidelberg.

Brown, A. G. (1973) Ascending and long spinal pathways: dorsal columns, spinocervical tract and spinothalamic tract. In: Handbook of Sensory Physiology. Vol. II, Somatosensory System. (A. Iggo, ed). Springer, New York. pp. 315-338.

Brown, A. G. (1977) Cutaneous axons and sensory neurons in the spinal cord. Brit. Med. Bull. 33:109-112.

Brown, A. G., and D. N. Franz (1969) Responses of spinocervical tract neurons to natural stimulation of identified cutaneous receptors. Exp. Brain Res. 7:231-249.

Brown, A. G., C. R. House, P. K. Rose, and P. J. Snow (1976) The morphology of spinocervical tract neurones in the cat. J. Physiol. (Lond). 260:719-738.

Brown, J. W. (1956a) The development of subnucleus caudalis of the nucleus of the spinal tract of V in human embryos of 6 1/2 to 8 1/2 weeks of menstrual age. Anat. Rec. 124:265-266.

Brown, J. W. (1956b) The development of the nucleus of the spinal tract of V in human fetuses of 14 to 21 weeks of menstrual age. J. Comp. Neurol. 106:393-424.

Brown, J. W. (1958) The development of subnucleus caudalis of the nucleus of the spinal tract of V. J. Comp. Neurol. 110:105-134.

Brown, L. T., Jr. (1971) Projections and termination of the corticospinal tract in rodents. Exp. Brain Res. 13:432-450.

Brown, M. R., and L. A. Fisher (1984) Brain peptide regulation of adrenal epinepherine secretion. Am. J. Physiol. 247:E41-E46.

Brown, P. A. (1980) The inferior olivary connections to the cerebellum in the rat studied by the retrograde axonal transport of horseradish peroxidase. Brain Res. Bull. 5:267-275.

Bruce, L. L., J. G. McHaffie and B. E. Stein (1984) Organization of the hamster trigeminal complex: Projections to superior colliculus, thalamus, and spinal cord. Soc. Neurosci. Abstr. 10:483.

Bruce, L. L., J. G. McHaffie and B. E. Stein (1987) The organization of trigeminotectal and trigeminothalamic neurons in rodents: A double-labeling study with fluorescent dyes. J. Comp. Neurol. 262:315-330.

Brunner, R., P. Zimmerman, and F. W. Klubmann (1980) Localization and neurophysiological properties of motorneurones of the M triceps surae of the rat after retrograde labelling with evans blue. Cell and Tissue Res. 212:73-81.

Brushart, T. M., and M. M. Mesulam (1980) Alteration in connections between muscle and anterior horn motoneurons after peripheral nerve repair. Science 208:603-605.

Bryan, R. N., D. L. Trevino, J. D. Coulter, and W. D. Willis (1973) Location and somatotopic organization of the cells of origin of the spino-cervical tract. Exp. Brain Res. 17:177-189.

Budell, R. J., and K. J. Berkley (1983) Differences in thalamic- and spinal-projecting neurons in cat dorsal column nuclei. Soc. Neurosci. Abstr. 9:920.

Bull, M. S., and K. J. Berkley (1984) Differences in the neurons that project from the dorsal column nuclei to the diencephalon, pretectum and tectum in the cat. Somatosen Res. 1:281-300.

Burgen, A. S. V., and L. M. Chipman (1951) Cholinesterase and succinic dehydrogenase in the central nervous system of the dog. J. Physiol. (Lond.), 114:296-305.

Burton, H. and A. D. Lowey (1976) Descending projections from the marginal cell layer and other regions of the monkey spinal cord. Brain Res. 116:485-491.

Burton, H., A. D. Jr. Craig, D. A. Poulos, and Molt (1979) Efferent projections form temperature-sensitive recording loci within the marginal zone of the nucleus caudalis of the spinal trigeminal complex in the cat. J. Comp. Neurol. 183:753-778.

Burton, H., and A. D. Craig, Jr. (1979) Distribution of trigeminothalamic projection cells in cat and monkey. Brain Res. 161:515-521.

Burton, H.., and A. D. Loewy (1977) Projections to the spinal cord from medullary somatosensory relay nuclei. J. Comp. Neurol. 173:773-792.

Bushnell, M. C., G. H. Duncan, R. Dubner, and L. F. He (1984) Activity of trigeminothalamic neurons in medullary dorsal horn of awake monkeys trained in a thermal discrimination task. J. Neurophysiol. 52:170-187.

Cabana, T. and G. F. Martin (1984) Developmental sequence in the origin of descending spinal pathways. Studies using retrograde transport techniques in the North American Opossum (Didelphis virginiana). Dev. Brain Res. 15:247-263.

Cadusseau, J., and M. Roger (1985) Description d'une connexion re´´ciproque entre la zona incerta et le noyau poste´rieus du thalamus. Etude anatomique chez le Rat. C. R. Acad. Sci. (Paris) 300 (se.III):643-646.

Campbell, E. J. M., E. Agostoni, and Newsom-Davis (1972) The respiratory muscles: Mechanics and neural control. London: W. B. Saunders.

Campbell, N. C., R. W. Clarke, and B. Matthews (1984) Neurons in trigeminal subnucleus oralis (VSNO) with inputs from tooth-pulp in the cat. J. Dent. Res. 63:518.

Carpenter, M. B., and G. R. Hanna (1961) Fiber projections from the spinal trigeminal nucleus in the cat. J. Comp. Neurol. 117:117-132.

Carpenter, M. B., and J. Sutin (1983) The autonomic nervous system. In: Human Neuroanatomy, 8th edn., Williams and Wilkins, Baltimore pp. 209-231.

Carpenter, M. B., B. M. Stein, and J. E. Shriver (1968) Central projections of spinal dorsal roots in the monkey. II. Lower thoracic, lumbosacral and coccygeal dorsal roots. Am. J. Anat. 123:75-118.

Carstens, E., and D. L. Trevino (1978) Laminar origins of spinothalamic projections in the cat as determined by the retrograde transport of horseradish peroxidase. J. Comp. Neurol. 182:151-166.

Carvell, G. E., and D. J. Simons (1987) Thalamic and corticocortical connections of the second somatic sensory area of the mouse. J. Comp. Neurol. 265:409-427.

Cervero, F. (1982) Noxious intensities of visceral stimulation are required to activate viscero-somatic multireceptive neurons in the thoracic spinal cord of the cat. Brain Res. 240:350-352.

Cervero, F. (1983a) Somatic and visceral inputs to the thoracic spinal cord of the cat: Effects of noxious stimulation of the biliary system. J. Physiol. (Lond). 337:51-67.

Cervero, F. (1983b) Supraspinal connections of neurones in the thoracic spinal cord of the cat: Ascending projections and effects of descending impulses. Brain Res. 275:251-261.

Cervero, F. (1983c) Mechanisms of visceral pain. In Persistent Pain Vol 4. Grune and Stratton, New York pp. 1-19.

Cervero, F., and A. Iggo (1978) Natural stimulation of urinary bladder afferents does not affect transmission through lumbosacral spinocervical tract neurones in the cat. Brain Res. 156:375-379.

Cervero, F., and L. A. Connell (1984) Fine afferent fibers from viscera do not terminate in the substantia gelatinosa of the thoracic spinal cord. Brain Res. 294:370-374.

Cervero. , F., A. Iggo, and V. Molony (1977) Responses of spinocervical tract neurones to noxious stimulation of the skin. J. Physiol. 267:537-558.

Chalmers, J. P. (1975) Brain amines and models of experimental hypertension. Circulation Res. 36:469-480.

Chan-Palay, V. (1975) Fine structure of labeled axons in the cerebellar cortex and nuclei of rodents and primates after intraventricular infusions with tritiated serotonin. Anat. Embryol. 148:235-265.

Chan-Palay, V., and S. L. Palay (1977) Ultrastructural identification of substance P cells and their processes in rat sensory ganglia and their terminals in the spinal cord by immunocytochemistry. Proc. Natl. Acad. Sci., USA 74:4050-4054.

Chan-Palay, V., S. L. Palay, J. T. Brown, and C. V. Itallie (1977) Sagittal organization of olivocerebellar and reticulocerebellar projections: Autoradiographic studies with S-Methionine. Exp. Brain Res. 30:561-576.

Chaouch, A., D. Menetrey, D. Binder, and J. M. Besson (1983) Neurons at the origin of the medial component of the bulbopontine spinoreticular tract in the rat: An anatomical study using horseradish peroxidase retrograde transport. J. Comp. Neurol. 214:309-320.

Chapman, C. D., W. S. Ammons, and W. D. Foreman (1985) Raphe magnus inhibition of feline T1-T4 spinoreticular tract cell responses to visceral and somatic inputs. J. Neurophysiol. 53:773-785.

Cheek, M. D., A. Rustioni, and D. L. Trevino (1975) Dorsal column nuclei projections to the cerebellar cortex in cats as revealed by the use of the retrograde transport of horseradish peroxidase. J. Comp. Neurol. 164:31-46.

Chiaia, N. L., R. W. Rhoades, C. A. Bennett-Clarke, S. E. Fish, and H. P. Killackey (1991a) Thalamic processing of vibrissal information in the rat. I. Afferent input to the medial ventral posterior and posterior nuclei. J. Comp. Neurol. 314:201-216.

Chiaia, N. L., R. W. Rhoades, S. E. Fish, and H. P. Killackey (1991b) Thalamic processing of vibrissal information in the rat: II. Morphological and functional properties of medial ventral posterior nucleus and posterior nucleus neurons. J. Comp. Neurol. 314:217-236.

Christensen, B. N., and E. R. Perl. (1970) Spinal neurones specifically excited by noxious or thermal stimuli: Marginal zone of the dorsal horn. J. Neurophysiol. 33:293-307.

Chung, J. M., K. Chung, and R. D. Wurster (1975) Sympathetic preganglionic neurons of the cat spinal cord: Horseradish peroxidase study. Brain Res. 91:126-131.

Chung, K., J. M. Chung, F. W. LaVelle, and R. D. Wurster (1979) The anatomical localization of descending pressor pathways in the cat spinal cord. Neurosci. Lett. 15:71-75.

Clark, W. B., and D. Bowsher (1962) Terminal distribution of primary afferent trigeminal fibers in the rat. Exp. Neurol. 6:372-383.

Cliffer, K. D., and G. J. Jr. Giesler (1988) PHA-L can transported anterogradely through fibers of passage. Brain Res. 458:185-191.

Cody, F. W. J., and H. C. Richardson (1978) Response of cerebellar interpositus nuclear neurons to trigeminal inputs in the cat. J. Physiol. (Lond.) 277:62p-63p.

Coffey, G. L. (1971) The distribution of respiratory motoneurons in the thoracic spinal cord pf the cat. Ph.D. Thesis. University of London.

Coleridge, H. M., and J. C. G. Coleridge (1979) Afferents of the pulmonary vascular bed and their role. In: Integrative Functions of the Autonomic Nervous System. C. McC. Brooks, K. Koizumi, and A. Sato (eds.). New York, University of Tokyo Press, Tokyo; and Elsevier-North Holland, New York. pp. 98-110.

Coleridge, H. M., Coleridge, J. C. G., and C. Kidd (1964) Cardiac receptors in the dog, with particular reference to two types of afferent endings in the ventricular wall. J. Physiol. (Lond.) 174:323-339.

Cook M. S. , and W. M. Falls. (1990) Efferent projections of neurons in the ventrolateral magnocellular region of rat trigeminal nucleus interpolaris. Anat. Rec. 226:22A.

Cook, M. S., and W. M. Falls (1991) Distribution and morphology of efferent projections from neurons in dorsomedial subdivisions of rat trigeminal nucleus interpolaris. Soc. Neurosci. Abstr. 17:290.

Cooke, J. D., B. Larson, and B. Sjolund (1971b) Organization of afferent connections to cuneocerebellar tract. Exp. Brain Res. 13:359-377.

Cooke, J. D., B. Larson, O. Oscarsson, and B. Sjolund (1971a) Organization and termination of cuneocerebellar tract. Exp. Brain Res. 13:339-358.

Corbin, K. B., and J. C. Hinsey (1935) Intramedullary course of the dorsal root fibers of the first four cervical nerves. J. Comp. Neurol. 63:119-126.

Corbin, K. B., W. T. Lhamon, D. W. Petit (1937) Peripheral and central connections of the upper cervical dorsal root ganglia in the rhesus monkey. J. Comp. Neurol. 66:405-414.

Corvaja, N., I. Grofova, O. Pompeiano, and F. Walberg (1977) The lateral reticular nucleus in the cat. I. An experimental anatomical study of its spinal and supraspinal afferent connections. Neuroscience 2:537-553.

Courville, J. (1966) The nucleus of the facial nerve: The relation between cellular groups and peripheral branches of the nerve. Brain Res. 1:338-354.

Craig, A. D, Jr. (1976) Spinocervical tract cells in cat and dog, labeled by the retrograde transport of horseradish peroxidase. Neurosci. Lett. 3:173-177.

Craig, A. D. (1982) The thalamocortical projection of nucleus submedius in the cat. J. Comp. Neurol. 206:28-48.

Craig, A. D. (1990) Nociceptive neurons in the nucleus submedius (Sm) in the medial thalamus of the cat. Pain Suppl 5:S492.

Craig, A. D., and J. O. Dostrovsky (1991) Thermoreceptive lamina I trigeminothalamic neurons project to the nucleus submedius in the cat. Exp. Brain Res. 85:470-474.

Craig, A. D., and K.-P. Kniffki (1985) Spinothalamic lumbosacral lamina I cells responsive to skin and muscle stimulation in the cat. J. Physiol. (Lond.) 365:197-221.

Craig, A. D., and S. Mense (1983) The distribution of afferent fibers from the gastrocnemius-soleus muscle in the dorsal horn of the cat, as revealed by the transport of HRP. Neurosci. Lett. 41:233-238.

Craig, A. D., jr. (1978) Spinal and medullary input to the lateral cervical nucleus. J. Comp. Neurol. 181:729-744.

Craig, A. D., jr. (1987) Medial thalamus and nociception: the nucleus submedius. In: J.-M. Besson, G. Guilbaud, and M. Psechanski (eds.). Thalamus and Pain. Elsevier, Amsterdam. pp.227-243.

Craig, A. D., jr., and D. N. Tapper (1978) The lateral cervical nucleus in the cat: Functional organization and characteristics. J. Neurophysiol. 41:1511-1534.

Craig, A. D., jr., and H. Burton (1979) The lateral cervical nucleus in the cat: Anatomic organization of cervicothalamic neurons. J. Comp. Neurol. 185:329-346.

Craig, A. D., jr., and H. Burton (1981) Spinal cord medullary lamina I projection to nucleus submedius in medial thalamus: a possible pain center. J. Neurophysiol. 45(3):443-466.

Crutcher, K. A., A. O. Humbertson and G. F. Martin (1978) The origin of brainstem-spinal pathways in the North American Opossum (*Didelphis virginiana*). Studies using the horseradish peroxidase method. J. Comp. Neurol. 179:169-194.

Csillik, B., F. Joo and P. Kasa (1963) Cholinesterase activity of archicerebellar mossy fiber apparatuses. J. Histochem. Cytochem. 11:113-114.

Culberson, J. L. (1987) Projection of cervical dorsal root fibers to the medulla oblongata in the bush-tailed possum (*Trichosurus vulpecula*). Amer. J. Anat. 179:232-242.

Culberson, J. L., and D. L. Kimmel (1975) Primary afferent fiber distribution at brachial and lumbosacral spinal cord levels in the opossum (*Didelphis marsupialis virginiana*). Brain Behav. Evol. 12:229-246.

Culberson, J. L., D. E. Haines, D. L. Kimmel, and P. B. Brown (1979) Contralateral projection of primary fibers to mammalian spinal cord. Exp. Neurol. 64:83-97.

Cummings, J. F. (1969) Thoracolumbar preganglionic neurons and adrenal innervation in the dog. Acta Anat. 73:27-37.

Cummings, J. F., and J. M. Petras (1977) The origin of spinocerebellar pathways: I. The nucleus cervicalis centralis of the cranial cervical spinal cord. J. Comp. Neurol. 173:655-692.

Curry, M. J., and G. Gordon (1972) The spinal input to the posterior group in the cat. An electrophysiological investigation. Brain Res. 44:417-437.

Dallel, R., P. Raboisson, P. Auroy, and A. Woda (1988) The rostral part of the trigeminal sensory complex is involved in orofacial nociception. Brain Res. 448:7-19.

Dalsgaard, C. J., and L. G. Elfvin (1979) The spinal orgin of preganglionic fibers projecting onto the superior cervical ganglion and inferior mesenteric ganglion of the guinea pig, as demonstrated by the horseradish peroxidase technique. Brain Res. 172:139-143.

Dalsgaard, C. J., T. Hokfelt, O. Johnsson, and R. Elde (1981) Somatostatin immunoreactive cell bodies in the dorsal horn and the parasympathetic intermediolateral nucleus of the rat spinal cord. Neurosci. Lett. 27:335-339.

Darian-Smith, I (1973) The trigeminal system. In: Handbook of Sensory Physiology, Vol. II, Somatosensory System. A. Iggo (ed.). New York. Springer. pp. 271-314.

Darian-Smith, I. (1964) Cortical projections of thalamic neurones excited by mechanical stimulation of the face of the cat. J. Physiol. (Lond.) 171:339-360.

Darian-Smith, I., and G. Mayday (1969) Somatotopic organization within the brainstem trigeminal complex of the cat. Exp. Neurol. 2:290-309.

Darian-Smith, I., P. Mutton, and R. Proctor (1965) Functional organization of tactile cutaneous afferents within the semilunar ganglion and trigeminal spinal tract of the cat. J. Neurophysiol. 28:682-694.

Dart, A. M. (1971) Cells of the dorsal column nuclei projecting down into the spinal cord. J. Physiol. (London). 219:29-30.

Davidson, N. (1965) The projection of afferent pathways on the thalamus of the rat. J. Comp. Neurol. 124:377-390.

Davies, W. I. R., D. Scott, Jr., K. Vesterstrom, and L. Vyklicky (1971) Depolarisation of the tooth pulp afferent terminals in the brain stem of the cat. J. Physiol. (Lond.) 218:515-532.

Davis, K. D., and J. O. Dostrovsky (1986a) Activation of trigeminal brain-stem nociceptive neurons by dural artery stimulation. Pain 25:395-401.

Davis, K. D., and J. O. Dostrovsky (1986b) Electrophysiological evidence for convergence of sagittal sinus, dural artery and cutaneous sensory information onto trigeminal neurons in the cat. Soc. Neurosci. Abstr. 12:230.

Davis, K. D., and J. O. Dostrovsky (1987a) Neurons in the rostral spinal nucleus excited by stimulation of the middle meningeal artery and superior sagittal sinus. In R. F. Schmidt, H. G. Schaible and C. Vahle-Hinz (Eds.). Fine Afferent Nerve Fibers and Pain. VCH. Weinheim, pp. 367-374.

Davis, K. D., and J. O. Dostrovsky (1987b) Thalamic neurons excited by stimulation of the sagittal sinus and middle meningeal artery. Pain 4:S264.

Davis, K. D., and J. O. Dostrovsky (1988a) Responses of feline trigeminal spinal tract nucleus neurons to stimulation of the middle meningeal artery and sagittal sinus. J. Neurophysiol. 59:648-666.

Davis, K. D., and J. O. Dostrovsky (1988b) Cerebrovascular application of bradykinin excites central sensory neurons. Brain Res. 446:401-406.

Denny-Brown, D., and N. Yanagisawa (1973) The function of the descending root of the fifth nerve. Brain 96:783-814.

Dickenson, A. H., R. F. Hellon, and C. J. Woolf (1981) Tooth pulp input to the spinal trigeminal nucleus: A comparison of inhibitions following segmental and raphe magnus stimulation. Brain Res. 214:73-87.

Dietrichs, E. (1981a) Cerebellar corticonuclear and nucleocortical projections in the cat as studied with anterograde and retrograde transport of horseradish peroxidase. III. The anterior lobe. Anat. Embryol. 162:223-247.

Dietrichs, E., (1981b) The cerebellar corticonuclear and nucleocortical projections in the cat as studied with anterograde and retrograde transport of horseradish peroxidase. IV. The paraflocculus. Exp. Brain Res. 44: 235-242.

Dietrichs, E., and F. Walberg (1979) The corticonuclear and nucleocortical projections in the cat as studied with anterograde and retrograde transport of horseradish peroxidase. I. The paramedian lobule. Anat. Embryol. 158:13-39.

Dietrichs, E., and F. Walberg (1980) Cerebellar corticonuclear and nucleocortico projections in the cat as studied with anterograde and retrograde transport of horseradish peroxidase. II. Lobulus Simplex, Crus I and II. Embryol. (Berl.) 161:83-103.

DiFiglia, M., M. Aronin, and S. E. Leeman (1984) Ultrastructural localization of immunoreactive neurotensin in the monkey superficial dorsal horn. J. Comp. Neurol. 225:1-12.

DiTirro, F. J., G. F. Martin, and R. H. Ho (1983) A developmental study of substance P, somatostatin, enkephalin, and serotonin immunoreactive elements in the spinal cord of the North American opossum. J. Comp. Neurol. 213:241-261.

Dom, R. M. (1982) Topographical representation of the peripheral nerve branches of the facial nucleus of the opossum: A study utilizing horseradish peroxidase. Brain Res. 246:281-284.

Dom, R. W. Falls, and G. F. Martin (1973) The motor nucleus of the facial nerve in the opossum (*Didelphis marsupialis virginiana*): Its organization and connections. J. Comp. Neurol. 152:373-402.

Donaldson, L., P. J. Hand, and A. R. Morrison (1975) Corticothalamic relationships in the rat. Exp. Neurol. 47:448-458.

Dong, W. K., H. Ryu, and I. H. Wagman (1978) Nociceptive responses of neurones in medial thalamus and their relationship to spinothalamic pathways. J. Neurophysiol. 41:1592-1613.

Dostrovsky, J. O., and G. Guilbaud (1988) Noxious stimuli excite neurons in nucleus submedius of the normal and arthritic rat. Brain Res. 460:269-280.

Dostrovsky, J. O., and J. G. Broton (1985) Antidromic activation of neurons in the medullary dorsal horn from stimulation in nucleus submedius. Soc. Neurosci. Abstr. 11:411.

Dostrovsky, J. O., J. G. Broton, and N. K. Warma (1987) Functional properties of subnucleus caudalis lamina I neurons projecting to nucleus submedius. In: R. F. Schmidt, H.-G. Schaible, C. Vahle-Hinz (eds.). Fine Afferent Nerve Fibers and Pain. VCH. Weinheim. pp.357-366.

Dubner, R., B. J. Sessle, and A. T. Storey (1978) The Neural Basis of Oral and Facial Function. New York: Plenum Press, pp. 74-100.

Dunn, J. D., and H. A. Matzke (1967) Efferent fiber connections of the marmoset (*Oedipomidas oedipus*) trigeminal nucleus caudalis. J. Comp. Neurol. 133:429-438.

Ebbesson, S. O. E. (1968) A connection between the dorsal column nuclei and the dorsal accessory nuclei. Brain Res. 8:393-397.

Eccles, J., M. Ito and J. Szentagothai (1967) The cerebellum as a neuronal machine. Berlin-Heidelberg-New York: Springer.

Edwards, S. B. (1972) The ascending and descending projections of the red nucleus in the cat: An experimental study using an autoradiographic tracing method. Brain Res. 48:45-63.

Eisenman, J., S. Landgren, and D. Novin (1963) Functional organization in the main sensory trigeminal nucleus in the rostral subdivision of the nucleus of the spinal trigeminal tract in the cat. Acta Physiol. Scand. 59 Suppl 214:1-14.

Eller, T., and V. Chan-Palay (1976) Afferents to the cerebellar lateral nucleus. Evidence from retrograde transport of horseradish peroxidase after pressure injections through micropipettes. J. Comp. Neurol. 166:285-302.

Elliott, H. C. (1942) Studies on the motor cells of the spinal cord. I. Distribution in the normal human cord. Am. J. Anat. 70:95-117.

Ellis, L., and A. Rustioni (1981) A correlative HRP, Golgi, and EM study of the intrinsic organization of the feline dorsal column nuclei. J. Comp. Neurol. 197:341-367.

Emmers, R. (1965) Organization of the first and second somesthetic regions (SI and SII) in the rat thalamus. J. Comp. Neurol. 124:215-228.

Emmers, R. (1966) Separate relay of tactile, pressure, thermal, and gustatory modalities in the cat thalamus. Proc. Soc. Exp. Biol. Med. 12:527-531.

Emmers, R., and R. R. Tasker (1975) The human somesthetic thalamus. Raven Press, New York.

Erzurumlu, R. S., and H. P. Killackey (1979) Efferent connections of the brainstem trigeminal complex with the facial nucleus of the rat. J. Comp. Neurol. 188:75-86.

Erzurumlu, R. S., C. A. Bates, and H. P. Killackey (1980) Differential organization of thalamic projection cells in the brain stem trigeminal complex of the rat. Brain Res. 198:427-433.

Erzurumlu. R. S., and H. P. Killackey (1980) Diencephalic projections of the subnucleus interpolaris of the brainstem trigeminal complex in the rat. Neurosci. 5:1891-1901.

Escolar, J. (1948) The afferent connections of the 1st, 2nd, 3rd cervical nerves in the cat. J. Comp. Neurol. 89:79-92.

Ezure, K., S. Sasaki, Y. Uchino, and V. J. Wilson (1978) Frequency-response analysis of vestibular-induced neck reflex in cat. II. Functional significance of cervical afferents and of tectospinal tract. J. Neurophysiol. 41:459-471.

Fabri, M., and H. Burton (1991) Topography of connections between primary somatosensory cortex and posterior complex in rat: a multiple fluorescent tracer study. Brain Res. 538:351-357.

Falls, W. M. (1983) Light and EM analysis of identified trigeminospinal projection neurons in rat trigeminal nucleus oralis. Anat. Rec. 205:55A.

Falls, W. M. (1984a) Termination in trigeminal nucleus oralis of ascending intratrigeminal axons originating from neurons in the medullary dorsal horn: An HRP study in the rat employing light and electron microscopy. Brain Res. 290:136-140.

Falls, W. M. (1984b) Axonal endings terminating on dendrites of identified large trigeminospinal projection neurons in rat trigeminal nucleus oralis. Brain Res. 324:335-341.

Falls, W. M. (1984c) The morphology of neurons in trigeminal nucleus oralis projecting to the medullary dorsal horn (trigeminal nucleus caudalis): A retrograde horseradish peroxidase and Golgi study. Neuroscience 13:1279-1298.

Falls, W. M. (1986) Morphology and synaptic connections of myelinated primary axons in the ventrolateral region of rat trigeminal nucleus oralis. J. Comp. Neurol. 244:96-110.

Falls, W. M. (1987) Direct connections of primary trigeminal afferent axons with trigeminocerebellar projection neurons in the border zone of rat trigeminal nucleus oralis. Neurosci. Letts. 83:247-252.

Falls, W. M. (1988) The synaptic organization of trigeminal primary axons in nucleus oralis. J. Electron. Microscopy Tech. 10:213-227.

Falls, W. M., and J. P. Van Wagner (1984) Orofacial projections to cerebellar tactile areas from the rat spinal trigeminal nucleus. Anat. Rec. 208:54A.

Falls, W. M., and M. M. Alban (1986) Morphological features of identified trigeminocerebellar projection neurons in the border zone of rat trigeminal nucleus oralis. Somatosen. Res. 4:1-12.

Falls, W. M., R. E. Rice, and J. P. Van Wagner (1985) The dorsomedial portion of trigeminal nucleus oralis (Vo) in the rat: Cytology and projections to the cerebellum. Somatosens. Res. 3:89-118.

Faull, R. L. M., and J. B. Carman (1978) The cerebellofugal projections in the brachium conjunctivum of the rat. I. The contralateral ascending pathways. J. Comp. Neurol. 178:495-518.

Fay, T. (1936) The mechanism of headache. Trans. Am. Neurol. Assn. 62:74-77.

Feindel, W., W. Penfield, and F. McNaughton (1960) The tentorial nerves and localization of intracranial pain in man. Neurology 10:555-563.

Feldberg, W., and M. Vogt (1948) Acetylcholine synthesis in different regions of the central nervous system. J. Physiol. (Lond.), 107:372-381.

Feldman, S. G., and L. Kruger (1980) An axonal transport study of the ascending projection of medial lemniscal neurons in rat. J. Comp. Neurol. 192:427-454.

Ferraro , A., and S. E. Barrera (1935) Posterior column fibers and their termination in Macacus rhesus. J. Comp. Neurol. 62:507-530.

Fields, H. L. , A. I. Basbaum, C. H. Clanton, and S. D. Anderson (1977a) Nucleus raphe magnus inhibition of spinal cord dorsal horn neurons. Brain Res. 126:441-453.

Fields, H. L., C. H. Clanton, and S. D. Anderson (1977b) Somatosensory properties of spinoreticular neurons in the cat. Brain Res. 120:49-66.

Fields, H. L., G. M. Wagner, and S. D. Anderson (1975) Some properties of spinal neurons projecting to the medial brain-stem reticular formation. Exp. Neurol. 47:118-134.

Fisher, D. A., and M. R. Brown (1980) Somatostatin analog: Plasma catecholamine supression mediated by the central nervous system. Endocrinology. 107:714-718.

Foreman, R. D., and C. A. Ohata (1980) Effect of coronary artery occlusion on thoracic spinal neurones receiving viscero-somatic inputs. Am. J. Physiol. 238:H667-H674.

Foreman, R. D., and R. N. Weber (1980) Responses from neurons of the primate spinothalamic tract to electrical stimulation of afferents from the cardiopulmonary region and somatic structures. Brain Res. 186:463-468.

Foreman, R. D., M. B. Hancock, and W. D. Willis (1981) Responses of spinothalamic tract cells in the thoracic spinal cord of the monkey to cutaneous and visceral inputs. Pain 11:149-162.

Foreman, R. D., R. F. Schmidt, and W. D. Willis (1979a) Field potentials and excitation of primate spinothalamic neurones in response to volleys in muscle afferents. J. Physiol. (Lond.). 286:197-214.

Foreman, R. D., R. F. Schmidt, and W. D. Willis (1979b) Effects of mechanical and chemical stimulation of fine muscle afferents upon primate spinothalamic tract cells. J. Physiol. (Lond.). 286:215-231.

Fukushima, T., and F. W. L. Kerr (1979) Organization of trigeminothalamic tracts and other thalamic afferent systems of the brainstem in rat: presence of gelatinosa neurons with thalamic connections. J. Comp. Neurol. 183:169-184.

Furness, J. B., R. E. Papka, N. G. Della, M. Costa and R. L. Eskay (1982) Substance P-like immunoreactivity in nerves associated with the vascular system of guinea pig. Neuroscience 7:447-459.

Fuxe, K. (1965) Evidence for the existence of monoamine neurons in the central nervous system. Acta Physiol. Scand. (Suppl.) 247:39-85.

Fuxe, K., D. Ganten, T. Hokfelt, and P. Bolme (1976) Immunohistochemical evidence for the existence of angiotensin-II containing nerve terminals in the brain and spinal cord in the rat. Neurosci. Lett. 2:229-234.

Ganchrow, D. (1978) Intratrigeminal and thalamic projections of nucleus caudalis in the squirrel monkey (*Saimiri sciureus)* : A degeneration and autoradiographic study. J. Comp. Neurol. 178:281-312.

Gardner, E, and F. Morin (1957) Projection of fast afferents to the cerebral cortex of monkey, Amer.J. Physiol. 189:152-158.

Gerfen, C. R., and P. E. Sawchenko (1984) An anterograde neuroanatomical tracing method that shows the detailed morphology of neurons, their axons and terminals: Immunohistochemical localization of the axonally transported plant lectin, Phaseolus vulgaris leucoagglutinin (PHA-L). Brain Res. 290:219-238.

Gerhart, K. D., R. P. Yezierski, G. J. Giesler, Jr., and W. D. Willis (1981) Inhibitory receptive fields of primate spinothalamic tract cells. J. Neurophysiol. 46(6):1309-1325.

Gerrits, N. M., A. H. Epema, and J. Voogd (1984) The mossy fiber projection of the nucleus reticularis tegmenti pontis to the flocculus and adjacent ventral paraflocculus in the cat. Neurosci. 11:627-644.

Gerrits, N. M., and J. Voogd (1981) Cerebellar efferents of the nucleus reticularis tegmenti pontis in the cat. Acta. Morph. Neerl.-Scand. 19:57.

Gibson, J. M. (1987) A quantative comparison of stimulus-response relationship of vibrissae-activated neurons in subnuclei oralis and interpolaris of the rat's trigeminal sensory complex: Receptive field properties and threshold distributions. Somatosen. Res. 5:135-155.

Gibson, S. J., J. M. Polak, S. R. Bloom, and P. D. Wall (1981) The distribution of nine peptides in rat spinal cord with special emphasis on the substantia gelatinosa and on the area around the central canal (Lamina X). J. Comp. Neurol. 201:65-79.

Giesler, G. J. ,Jr., R. P. Yezierski, K. D. Gerhart, and W. D. Willis (1981b) Spinothalamic tract neurons that project to medial and/or lateral thalamic nuclei: Evidence for a physiologically novel population of spinal cord neurons. J. Neurophysiol. 46:1285-1308.

Giesler, G. J., D. Menetrey, and A. I. Basbaum (1979a) Differential origins of spinothalamic tract projections to medial and lateral thalamus in the rat. J. Comp. Neurol. 184:107-126.

Giesler, G. J., Jr., D. Menetrey, G. Gilbaud, and J. M. Besson (1976) Lumbar cord neurons at the origin of the spinothalamic tract in the rat. Brain Res. 118:320-324.

Giesler, G. J., Jr., G. Urca, J. T. Cannon, and J. C. Liebeskind (1979b) Response properties of neurons of the lateral cervical nucleus in the rat. J. Comp. Neurol. 186:65-78.

Giesler, G. J., Jr., H. R. Spiel, and W. D. Willis (1981a) Organization of spinothalamic tract axons within the rat spinal cord. J. Comp. Neurol. 195:243-252.

Giesler, G. J., R. L. Nashin, and A. M. Madsen (1984) Postsynaptic dorsal column pathway of the rat. I. Anatomical studies. J. Neurophysiol. 51:260-275.

Glazer, E. J., and A. I. Basbaum (1981) Immunohistochemical localization of leucine-enkephalin in the spinal cord of the rat: Enkephalin containing marginal neurons and pain modulation. J. Comp. Neurol. 196:377-389.

Gobel, S. (1979) Neural circuitry in the substantia gelatinosa of Rolando: Anatomical insights. In: Advances in Pain Research and Therapy. J. J. Bonica, J. C. Liebeskind, and D. G. Albe-Fessard(eds). New York: Raven. pp. 175-195.

Gobel, S., and M. B. Purvis (1972) Anatomic studies of the organization of the spina V nucleus: the deep bundles and the spinal V tract. Brain Res. 48:27-44.

Gobel, S., S. Hockfield, and M. A. Ruda (1981) Anatomical similarities between medullary and spinal dorsal horns. In. Oral-Facial Sensory and Motor Functions. Y. Kawamura, and R. Dubner (eds.). Tokyo. Quintessence. pp.211-223.

Gobel, S., W. M. Falls, and S. Hockfield (1977) The division of the dorsal and ventral horns of the mammalian caudal medulla into eight layers using anatomical criteria. In: Pain in the Trigeminal Region. D. J. Anderson, and B. Mathews (eds.). Amsterdam: Elsevier/North-Holland. pp443-453.

Goering, G. H. (1928) An experimental analysis of the motor-cell columns in the cervical enlargement of the spinal cord in the albino rat. J. Comp. Neurol. 46:125-153.

Gokin, A. P. (1970) Synaptic activation of interneurones in the thoracic spinal cord by cutaneous muscle and visceral afferents. Neurofiziologiia (Moscow). 2:563-572.

Goodman, D. C. and J. T. Simpson, jr. (1961) Functional localization in the cerebellum of the albino rat. Expl. Neurol. 3:174-188.

Goodman, D. C., R. E. Hallet, and R. B. Welch (1963) Patterns of localization in the cerebellar corticonuclear projections of the albino rat. J. Comp. Neurol. 121:51-67.

Gordon, G., and C. H. Paine (1960) Functional organization in nucleus gracilis of the cat. J. Physiol. (Lond). 153:311-349.

Gordon, G., and M. G. M. Jukes (1964) Dual organization of the exteroceptive components of the cat's gracile nucleus.. J. Physiol. (Lond). 173:263-290.

Goshgarian, H. G. (1981) The role of cervical afferent nerve fiber inhibition of the crossed phrenic phenomenon. Exp. Neurol. 72:211-225.

Goshgarian, H. G., and J. A. Rafols (1981) The phrenic nucleus of the albino rat: A correlative HRP and Golgi study. J. Comp. Neurol. 201:441-456.

Graham, J. (1977) An autoradiographic study of the efferent connections of the superior colliculus in the cat. J. Comp. Neurol. 173:629-654.

Grant, G. (1962) Spinal course and somatotopically localized termination of the spinocerebellar tracts. An experimental study in the cat. Acta Physiol. Scand. 56(Suppl 193):1-45.

Grant, G., and J. Arvidsson (1975) Transganglionic degeneration in trigeminal primary sensory neurons. Brain Res. 95:265-279.

Grant, G., and Y. Ygge (1981) Somatotopic organization of the thoracic spinal nerve in the dorsal horn demonstrated with transganglionic degeneration. J. Comp. Neurol. 202:357-364.

Green, E. C. (1963) Anatomy of the rat. Hafner, New York.

Greenwood, L. F. (1973) An electrophysiological study of the central connections of primary afferent nerve fibers from the dental pulp in the cat. Arch. Oral. Biol. 18:771-785.

Greenwood, L. F., and B. J. Sessle (1976) Pain, brainstem mechanisms, and motor function. In B. J. Sessle and A. G. Hannam (eds): Mastication and Swallowing: Biological and Clinical Correlate. Toronto: University of Toronto Press. pp. 108-119.

Gregg, J. M., and A. D. Dixon (1973) Somatotopic organization of the trigeminal ganglion in the rat. Arch. Oral Biol. 18:487-498.

Groenewegen, H. J., and J. Voogd (1977) The parasagittal zonation within the olivocerebellar projection. I. Climbing fiber distribution in the vermis of the cerebellum. J. Comp. Neurol. 174:417-488.

Groenewegen, H. J., J. Voogd and S. L. Freedman (1979) The parasagittal zonation within the olivocerebellar projection. II. Climbing fiber distribution in the intermediate and hemispheric parts of cat cerebellum. J. Comp. Neurol. 183:551-602.

Grossman, M. L., A. I. Basbaum, and H. L. Fields (1982) Afferent and efferent connections of the rat tail flick reflex (A model used to analyze pain control mechanisms). J. Comp. Neurol. 206:9-16.

Guilbaud, G., G. Benelli, and S. M. Besson (1977) Response of thoracic dorsal horn interneurones to cutaneous stimulation and to the administration of algogenic substrates into the mesenteric artery in the spinal cat. Brain Res. 124:437-448.

Guilbaud, G., M. Peschanski, M. Gautron, and D. Binder (1980) Neurones responding to noxious stimulation in VB complex and caudal adjacent regions in the thalamus of the rat. Pain 8:303-318.

Gulley, R. L., (1973) Golgi studies of the nucleus gracilis in the cat. Anat. Rec. 177:325-342.

Gura, E. V., and Y. P. Limanskii (1977) Antidromic and synaptic potentials of motoneurons of the cat accessory nerve nucleus. J. Neurophysiol. 41:459-471.

Gwyn, D. G.., and H. A. Waldron (1968) The nucleus of the dorsolateral funiculus of the spinal cord of the rat. Brain Res. 10:342-351.

Ha, H. (1971) Cervicothalamic tract in the Rhesus monkey. Exp. Neurol. 33:205-212.

Ha, H., and F. Morin (1964) Comparative anatomical observations of the cervical nucleus, N. cervicalis lateralis, of some primates. Anat. Rec. 148:374-375.

Ha, H., S. T. Kitai, and F. Morin (1965) The lateral cervical nucleus of the raccoon. Exp. Neurol. 11:441-450.

Ha, H., T. Kao, and E. C. Tan (1980) Muscle sensory neurons in the spinal ganglia in the rat determined by the retrograde transport of horseradish peroxidase. Exp. Neurol. 70:438-445.

Haber, L. H., B. D. Moore, and W. D. Willis (1982) Electrophysiological response properties of spinothalamic neurons in the monkey. J. Comp. Neurol. 207:75-84.

Haines, D. E. and J. A. Rubertone (1979) Cerebellar corticonuclear fibers of the dorsal culminate lobule (anterior lobe-lobule V) in a prosimian primate, Galago senegalensis. J. Comp. Neurol. 186:321-342.

Haines, D. E., and G. W. Patrick (1981) Cerebellar corticonuclear fibers of the paramedian lobule of tree shrew (Tupaia glis) with comments on zones. J. Comp. Neurol. 201:99-119.

Haines, D. E., and J. A. Rubertone (1977) Cerebellar corticonuclear fibers: evidence of zones in the primate anterior lobe. Neurosci. Lett. 6:231-236.

Haines, D. E., and R. H. Whitworth (1978) Cerebellar cortical efferent fibers of the paraflocculus of tree schrew (Tupaia glis). J. Comp. Neurol. 182:137-150.

Haines, D. E., and S. L. Koletar (1979) Topography of cerebellar corticonuclear fibers of the albino rat. Vermis of anterior and posterior lobes. Brain Behav. Evol. 16:271-292.

Haines, D. E., J. L. Culberson, and G. F. Martin (1976) Laterality and topography of cerebellar cortical efferents in the opposum (Didelphis marsupialis virginiana). Brain Res. 106:152-158.

Hainsworth, R., C. Kidd, and R. J. Linden (eds) (1979) Cardiac Receptors. Cambridge, England. Cambridge University Press.

Hamilton, J., D. Moodie, and J. Levy (1979) The use of the diving reflex to terminate supraventricular tachycardia in a 2-week-old infant. Am. Heart J. 97(3):371-374.

Hancock, H. B., and B. Rigamonti (1973) Convergence in lumbar spinal cord pathways activated by splanchnic nerve and hindlimb cutaneous nerve stimulation. Exp. Neurol. 38:337.

Hancock, M. B., and C. A. Peveto (1979a) A preganglionic autonomic nucleus in the dorsal gray commissure of the lumbar spinal cord of the rat. J. Comp. Neurol. 183:65-72.

Hancock, M. B., and C. A. Peveto (1979b) Preganglionic neurons in the sacral spinal cord of the rat: An HRP study. Neurosci. Lett. 11:1-5.

Hancock, M. B., R. D. Foreman, and W. D. Willis (1975) Convergence of visceral and cutaneous input onto spinothalamic tract cells in the thoracic spinal cord of the cat. Exp. Neurol. 47:240-248.

Hand, P. J. (1966) Lumbosacral dorsal root terminations in the nucleus gracicis of the cat. Some observations on terminal degeneration in other medullary sensory nuclei. J. Comp. Neurol. 126:137-156.

Hand, P. J., and C. N. Liu (1966) Efferent projections of the nucleus gracilis. Anat. Rec. 154:353.

Hand, P. J., and T. Van Winkle (1977) The efferent connections of the feline nucleus cuneatus. J. Comp. Neurol. 171:83-110.

Hanna, B. D., F. Lioy, and C. Polosa (1981) Role of carotid and central chemoreceptors in the CO2 response of sympathetic preganglionic neurons. J. Auton. Nerv. Syst. 3:421-435.

Hardebo, J. E. (1984) The involvement of trigeminal substance P neurons in cluster headache. An hypothesis. Headache 24:294-304.

Hayashi, H. (1982) Differential terminal distribution of single large cutaneous afferent fibers in the spinal trigeminal nucleus and in the cervical spinal dorsal horn. Brain Res. 244:173-177.

Hayashi, H., R. Sumino and B. J. Sessle (1984) Functional organization of trigeminal subnucleus interpolaris: Nociceptive and innocuous afferent inputs, projections to thalamus, cerebellum, and spinal cord, and descending modulation from periaqueductal gray. J. Neurophysiol. 51:890-905.

Hayes, N. L., and A. Rustioni (1979) Dual projections of single neurons are visualized simultaneously: Use of enzymatically inactive (3H) HRP. Brain Res. 165:321-326.

Hazlett, J. C., R. Dom, and G. F. Martin (1972) Spino-bulbar, spino-thalamic and medial lemniscal connections in the American opossum, *Didelphis marsupialis virginiana*. J. Comp. Neurol. 146:95-118.

Hebb, C. O., (1959) Chemical agents of the nervous system. Int. Rev. Neurobiol. 1:165-193.

Hebb, C. O., and A. Silver, (1956) Choline acetylase in the central nervous system of man and some other mammals. J. Physiol. (Lond.), 134:718-728.

Lee, C. L., D. J. McFarland, and J. R. Wolpaw (1987) Retrograde transport of the lectin Phaseolus vulgaris leucoagglutinin by rat spinal motoneurons. Soc. Neurosci. Abstr. 13:676.

Lee, C. L., M. Peschanski, and H. J. Ralston, III. (1981) Morphophysiology of neurons of the rat ventrobasal thalamic complex. An intracellular HRP study. Pain Suppl. 1:S210.

Lende, R., and D. Poulos (1970) Functional localization in the trigeminal ganglion in the monkey. J. Neurosurg. 32:336-343.

Leong, S. K., J. Y. Shieh and W. C. Wong (1984) Localizing spinal-cord-projecting neurons in adult albino rats. J. Comp. Neurol. 228:1-17.

Liebman, J. M., D. J. Mayer, and J. C. Liebskind (1970) Mesencephalic central gray lesions in fear motivated behavior in rats. Brain Res. 23:353-370.

Light, A. R., and E. R. Perl (1979a) Reexamination of the dorsal root projection to the spinal dorsal horn including observations on the differential terminations of coarse and fine fibers. J. Comp. Neurol. 186:117-132.

Light, A. R., and E. R. Perl (1979b) Spinal termination of functionally identified primary afferent neurones with slowly conducting myelinated fibers. J. Comp. Neurol. 186:133-150.

Light, A. R., D. L. Trevino, and E. R. Perl (1979) Morphological features of functionally defined neurones in the marginal zone and substantia gelatinosa of the spinal dorsal horn. J. Comp. Neurol. 186:151-172.

Lima, D., and A. Coimbra (1989) Morphological types of spinomesencephalic neurons in the marginal zone (lamina I) of the rat spinal cord, as shown after retrograde labelling with cholera toxin subunit B. J. Comp. Neurol. 279:327-339.

Linden, R. J. (1975) Reflexes from the heart. Prog. Cardiovasc. Dis. 18:201-221.

Lindsey, D. F., R. J. Barton, and R. J. Atkins (1970) Effects of subthalamic lesions on peripheral and central thresholds in cats. Exp. Neurol. 26:109-119.

Lisney, S. J. W. (1978) Some anatomical and electrophysiological properties of tooth-pulp afferents in the cat. J. Physiol. (Lond.) 284:19-36.

Loewy, A. D., and H. Burton (1978) Nuclei of the solitary tract: efferent connections to the lower brain stem and spinal cord of the cat. J. Comp. Neurol. 181:421-450.

Loew

Loew

Loew

Loga

Lund

Lund

Lusch

Macch

Mallia

Mallia

Manni

Mantle

Marfur

Loewy, A. D., and S. McKellar (1980) The neuroanatomical basis of central cardiovascular control. Fed. Proc. 39:2495-2503.

Loewy, A. D., and S. McKellar (1981) Serotonergic projections from the ventral medulla to the interomedial cell column in the rat. Brain Res. 211:146-152.

Loewy, A. D., S. McKellar, and C. B. Saper (1979) Direct projections from the A5 catecholamine cell group to the interomediolateral cell column. Brain Res. 174:309-314.

Logan, K. and L. T. Robertson (1986) Somatosensory representation of the cerebellar climbing fiber system in the rat. Brain Res. 372:290-300.

Lund, R. D., and K. E. Webster (1967a) Thalamic afferents from the dorsal column nuclei. An experimental anatomical study in the rat. J. Comp. Neurol. 130:301-311.

Lund,R. D. and K. E. Webster (1967b) Thalamic afferents from the spinal cord and trigeminal nuclei. An experimental anatomical study in the rat. J. Comp. Neurol. 130:313-328.

Luschka, H. von (1850) Die nerven der harten Hirnhaut. Laupp H. Tubingen.

Macchi, G., M. Bentivoglio, M. Molinari, and D. Minciacchi (1984) The thalamo-caudate versus thalamo-cortical projections as studied in the cat with fluorescent retrograde double labeling. Exp. Brain Res. 54:225-239.

Malliani, A. (1979) Afferent cardiovascular sympathetic nerve fibers and their function in the neural regulation of the circulation. In: Cardiac Receptors. R. Hainsworth, C. Kidd, and P. L. Linden (eds.). Cambridge University Press. Cambridge, England. pp.319-338.

Malliani, A., F. Lombardi, and M. Pagani (1981) Functions of afferents in cardiovascular sympathetic nerves. J. Auton. Nerv. Syst. 3:231-236.

Manni, E., G. Palmeri, R. Marini, and V. E. Pettorossi (1975) Trigeminal influences on extensor muscles of the neck. Exp. Neurol. 47:330-342.

Mantle-St. John, L. A., and D. J. Tracey (1987) Somatosensory nuclei in the brainstem of the rat: Independent projections to the thalamus and cerebellum. J. Comp. Neurol., 255:259-271.

Marfurt, C. F. (1981a) The somatotopic organization of the cat trigeminal ganglion as determined by the horseradish peroxidase technique. Anat. Rec. 201:105-118.

Marfurt, C. F. (1981b) The central projection of trigeminal primary afferent neurons in the cat as determined by the transganglionic transport of horseradish peroxidase. J. Comp. Neurol. 203:785-798.

Marfurt, C. F., and D. F. Turner (1984) The central projections of tooth pulp afferent neurons in the rat as determined by the transganglionic transport of horseradish peroxidase. J. Comp. Neurol. 223:535-547.

Marley, P. D., J. I. Nagy, P. C. Emson, and J. F. Rehfeld (1982) Cholecystokinin in the rat spinal cord: Distribution and lack of effect of neonatal capsaicin treatment and rhizotomy. Brain Res. 238:494-498.

Martin, M. R., and D. Lodge (1977) Morphology of the facial nucleus of the rat. Brain Res. 123:1-12.

Matsumoto, N., T. Sato, H. Sawano, A. Tochinai, and T. A. Suzuki (1988) Characteristics of tooth pulp-driven neurons in the posterior group of the cat thalamus. Neurosci. Lett. 93:253-358.

Matsushita, M., and T. Tanami (1983) Contralateral termination of primary afferent axons in the sacral and caudal segments of the cat, as studied by anterograde transport of horseradish peroxidase. J. Comp. Neurol. 220:206-218.

Matsushita, M., and Y. Hosoya (1979) Cells of origin of the spinocerebellar tract in the rat, studied with the method of retrograde transport of horseradish peroxidase. Brain Res. 173:185-200.

Matsushita, M., M. Ikeda and N. Okado (1982) The cells of origin of the trigeminothalamic, trigeminospinal and trigeminocerebellar projections in the cat. Neuroscience 7:1439-1454.

Matsushita, M., N. Okada, M. Ikeda and Y. Hosoya (1980) Identification of spinal projecting neurons in the cat trigeminal spinal and mesencephalic nuclei using the retrograde horseradish peroxidase technique. In Integrative control functions of the brain, Vol. III. (eds. Ito M., Tsukahara N, Kubota K, and Yagi K.), pp. 161-163, Elsevier North Holland Biomedical Press, Amsterdam.

Matsushita, M., N. Okado, M. Ikeda and Y. Hosoya (1981) Descending projections from the spinal and mesencephalic nuclei of the trigeminal nerve to the spinal cord in the cat. A study with the horseradish peroxidase technique. J. Comp. Neurol. 196:173-187.

Matsushita, M.,and M. Ikeda (1975) The central cervical nucleus as cell origin of a spinocerebellar tract arising from the cervical cord: A study in the cat using horseradish peroxidase. Brain Res. 100:412-419.

Matsuyama, T., S. Shiosaka, A. Wanaka, S. Yoneda, K. Kimura, T. Hayakawa, P. C. Emson, and M. Tohyama (1985) Fine structure of peptidergic and catecholaminergic nerve fibers in the anterior cerebral artery and their interrelationship: An immuno electronmicroscopic study. J. Comp. Neurol. 223:46-56.

Matthews, B., J. Baxter, and S. Watts (1976) Sensory and reflex responses to tooth pulp stimulation in man. Brain Res. 113:83-94.

Maunz, R. A., M. G. Pitts, and B. W. Peterson (1978) Cat spinoreticular neurons: Locations responses and changes in responses during repetitive stimulation. Brain Res. 148:365-379.

May, J. G., and K. J. Berkley (1983) Anatomic characteristics of pontine-projecting neurons within the dorsal column nuclei of the cat. Soc. Neurosci. Abstr. 9:870.

Mayberg, M. R., N. T. Zervas, and M. A. Moskowitz (1984) Trigeminal projections to supratentorial pial and dural blood vessels in cats demonstrated by horseradish peroxidase histochemistry. J. Comp. Neurol. 223:46-56.

Mayberg, M., R. S. Langer, N. T. Zervas, and M. A. Moskowitz (1981) Perivascular meningeal projections from cat trigeminal ganglia: Possible pathway for vascular headaches in man. Science 213:228-230.

Mazza, J., and A. Dixon (1972) A histological study of chromatolytic cell groups in the trigeminal ganglion of the rat. Arch. Oral Biol. 17:377-387.

McAllister, J. P., and J. Wells (1981) The structural organization of the ventral posterolateral nucleus in the rat. J. Comp. Neurol. 197:271-301.

McComas, A. J. (1963) Responses of rat dorsal column system to mechanical stimulation of the hindpaw. J. Physiol. (Lond). 166:435-488.

McCouch, G. P., I. D. Deering, and T. H. Ling (1951) Location of receptors for tonic neck reflexes. J. Neurophysiol. 14:191-195.

McCreery, D. B., J. R, Bloedel, and E. G. Hames (1979a) Excitability changes in lumbosacral spinothalamic neurons produced by non-noxious mechanical stimuli and by graded stimuli applied to the face. Brain Res. 177:253-263.

McCreery, D. B., J. R. Bloedel, and E. G. Hames (1979b) Effects of stimulating in raphe nuclei and in reticular formation on repsonse of spinothalamic neurons to mechanical stimuli. J. Neurophysiol. 42:166-182.

McDonald, R. L., and D. Cohen (1970) Cells of origin of sympathetic and pre- and postganglionic cardioacceleratory fibers in the pigeon. J. Comp. Neurol. 140:343-358.

McGinty, D. J. (1969) Somnolence recovery and hyposomnia following ventromedial diencephalic lesions in the rat. Electroenceph. Clin. Neurophysiol. 26:70-79.

McHanwell, S., and T. J. Biscoe (1981) The localization of the motoneurons supplying the hindlimb muscles of the mouse. Philos. Trans. R. Soc. Lond. (B) 293:477-508.

McIntosh, F. C. (1941) The distribution of acetylcholine in the peripheral and central nervous system. J. Physiol. (Lond.) 99:436-442.

McLaughlin, B. J., R. Barber, K. Saito, E. Roberts, and Y. J. Wu (1975) Immunocytochemical localization of glutamate decarboxylase in rat spinal cord. J. Comp. Neurol. 164:305-322.

McLauglin, B. J., J. G. Wood, K. Saita, R. Barber, J. E. Vaugh, E. Roberts, and J. Y. Wu (1974) The fine structural localization of glutamate decarboxylase in synaptic terminals of rodent cerebellum. Brain Res. 76:377-392.

Mehler, W. R. (1966) The posterior thalamic region in man. Confin. Neurol. 27:18-29.

Mehler, W. R. (1969) Some neurological species differences-a posteriori. Ann. N. Y. Acad. Sci. 167:424-468.

Mehler, W. R. (1971) Idea of a new anatomy of the thalamus. J. Psychiatr. Res. 8:203-217.

Melzack, R., and K. L. Casey (1968) Sensory, motivational and central control determinants of pain. In: D. R. Kenshalo (ed.) The Skin Senses. Thomas, Springfield, IL. pp. 423-443.

Melzack, W. R., W. A. Stotler, and W. K. Livingston (1958) Effects of discrete brain stem lesions in cats on perception of noxious stimulation. J. Neurophysiol. 21:353-367.

Menetrey, D., A. Chaouch, and J. M. Besson (1980) Location and properties of dorsal horn neurons at origin of spinoreticular tract in lumbar enlargement of the rat. J. Neurophysiol. 44:862-877.

Menetrey, D., A. Chaouch, D. Binder, and J. M. Besson (1982) The origin of the spinomesencephalic tract in the rat: An anatomical study using the retrograde transport of horseradish peroxidase. J. Comp. Neurol. 206:193-207.

Menetrey, D., F. Roudier, and J. M. Besson (1983) Spinal neurons reaching the lateral reticular nucleus as studied in the rat by retrograde transport of horseradish peroxidase. J. Comp. Neurol. 220:439-452.

Menetrey, D., G. J. Giesler, Jr., and J. M. Besson (1977) An analysis of response properties of spinal cord dorsal horn neurones to nonnoxious and noxious stimuli in the spinal rat. Exp. Brain Res. 27:15-33.

Mense, A., A. R. Light, and E. F. Perl (1981) Spinal terminations of subcutaneous high-threshold mechanoreceptors, in: Spinal Cord Sensation (A. G. Brown and M. Rethelyi, eds.), Scottish Academic Press, Edinburgh. pp. 79-86.

Messing, R. B., and L. D. Lytle (1977) Serotonin containing neurons: Their possible role in pain and analgesia. Pain 4:1-21.

Mesulam, M.-M., and T. M. Brushart (1979) Transganglionic and anterograde transport of horseradish peroxidase across dorsal root ganglia: A tetramethylbenzidine method for tracing central sensory connections of muscle and peripheral nerves. Neurosci. 4:1107-1117.

Miletvic, V., and J. A. Coffield (1989) Responses of neurons in the rat nucleus submedius to noxious and innouous mechanical cutaneous stimulation. Motor. Res. 6:567-588.

Millar, J. (1973) The topography and receptive fields of ventroposterolateral thalamic neurons excited by afferents projecting through the dorsolateral funiculus of the spinal cord. Exp. Neurol. 49:281-290.

Millar, J., and A. J. Basbaum (1975) Topography of the projection of the body surface of the cat to cuneate and gracile nuclei. Exp. Neurol. 49:281-290.

Milne, R. J., R. D. Foreman, G. J. Giesler, jr., and W. D. Willis (1981) Convergence of cutaneous and pelvic visceral nociceptive inputs into primate spinothalamic neurones. Pain. 11:153-184.

Mizuno, N. (1970) Projection fibers from the main sensory trigeminal nucleus and the supratrigeminal region. J. Comp. Neurol. 139:457-472.

Mizuno, N., K. Nikano, M. Imaizumi, M. Okamoto (1967) The lateral cervical nucleus of the japanese monkey (*Macaca fuscata*). J. Comp. Neurol. 129:375-384.

Molander, C., Q. Xu, and G. Grant (1984) The cytoarchitectonic organization of the spinal cord in the rat. I. The lower thoracic and lumbosacral cord. J. Comp. Neurol. 230:133-141.

Molander, C., Q. Xu, C. Rivero-Melian, and G. Grant (1989) Cytoarchitectonic organization of the spinal cord in the rat: II. The cervical and upper thoracic cord. J. Comp. Neurol. 289:375-385.

Molinari, H. H. (1983) Nucleus gracilis projections to the medial and dorsal accessory olives of the cat: A retrograde tracing study. Soc. Neurosci. Abstr. 9:1083.

Molinari, H. H. (1984) Ascending somatosensory projections to the dorsal accessory olive: An anatomical study in cats. J. Comp. Neurol. 223:110-123.

Molony, F., W. M. Steedman, F. Cervero, and A. Iggo (1981) Intracellular marking of identified neurons in the superficial dorsal horn of the cat spinal cord. J. Q. Exp. Physiol, 66:211-223.

Morgan, C. W., I. Nadelhaft, and W. C. deGroat (1978) Anatomic localization of corneal afferent cells in the trigeminal ganglion. Neurosurgery 2:252-258.

Morgan, C., I. Nadelhaft, W. de Groat (1981) The distribution of visceral primary afferents from the pelvic nerve to Lissauer's tract and the spinal gray matter and its relationship to the sacral sympathetic nucleus. J. Comp. Neurol. 201:415-440.

Morin, F., H. G. Schwartz, and J. L. O'Leary (1951) Experimental study of the spinothalamic and related tracts. Acta Psychiatr. Neurol. 26:371-396.

Moskowitz, A. S., S. M. Breedlove, A. P. Arnold, and J. C. Liebeskind (1982) Distribution of enkephalin-like immunoreactivity in the rat spinal cord: an immunohistochemical study. Soc. Neurosci. Abstr. 8:100.

Moskowitz, M. A. (1984) The neurobiology of vascular head pain. Ann. Neurol. 16:157-168.

Mosso, J. A., and L. Kruger (1973) Receptor categories represented in spinal trigeminal nucleus caudalis. J. Neurophysiol. 36:472-488.

Mugnaini, E. and P. Forstronen (1967) Ultrastructural studies on the cerebellar histogenesis. I. Differentiation of granule cells and development of glomeruli in the chick embryo. Z. Zellforsch. 77:115-143.

Mysicka, A., and W. Zenker (1981) Central projections of muscle afferents from the sterno-mastoid nerve in the rat. Brain Res. 211:257-265.

Nagata, T. and L. Kruger (1979) Tactile neurons of the superior colliculus of the cat: Input and physiological properties. Brain Res. 174:19-37.

Nagy, J. I., S. P. Hunt, L. Iversen, and P. C. Emson (1981) Biochemical and anatomical observations on the degeneration of peptide-containing primary afferent neurons after neonatal capsaicin. Neuroscience 6:1923-1934.

Nakano, K. (1970) The cytoarchitectonic study of the spinal cord in the dog. Mie. Med. J. 20:185-226.

Naquet, R., N. Denavit, and D. Albe-Fessard (1966) Comparison entre le role du subthalamus et cehie des differentes structures bulbomesence-phaliques dans le maintain de la vigilance. Electroenceph. Clin. Neurophysiol. 20:149-164.

Nasution, I. D., and Y. Shigenaga (1987) Ascending and descending internuclear projections within the trigeminal sensory nuclear complex. Brain Res. 425:234-247.

Neylon, L., and J. R. Haight (1983) Neocortical projections of the suprageniculate and posterior thalamic nuclei in the marsupial brush-tailed possum, Trichosorus vulpecula (*Phalangeridae*), with a comparative commentary on the organization of the posterior thalamus in marsupial and placental mammals. J. Comp. Neurol. 217:357-375.

Nicolelis, J., K. Chaplin, and C. S. Liu (1991) Connectivity and physiology of the rat zona incerta. World Congress Neuroscience Abstr.

Nicoll, R. A., G. R. Siggins, N. Ling, F. E. Bloom, and R. Guillemin (1977) Neuronal actions of endorphins and enkephalins among brain regions: A microiontophoretic study. Proc. Natl. Acad. Sci. U. S. A., 74:2584-2588.

Nicolopoulos-Stournaras, S., and J, F, Iles (1983) Motor neuron columns in the lumbar spinal cord of the rat. J. Comp. Neurol. 217:75-85.

NIH Guide for the Care and Use of Laboratory Animals. NIH, 9000 Rockville Pike, Bethesda MD. 20892, 1985.

Nishikawa, Y., N. Koyama, and T. Yakota (1988) Ipsilateral somatosensory tongue representation within the lateral subdivision of the nucleus ventralis posteromedialis parvocellularis of the cat thalamus. Brain Res. 458:394-396.

Nishimori, T., M. Sera, S. Suemune, A. Yoshida, K. Tsuru, Y. Tsuiki, T. Akisaka, T. Okamoto, Y. Dateoka, and Y. Shinenaga (1986) The distribution of muscle primary afferents from the masseter nerve to the trigeminal sensory nuclei. Brain Res. 372:375-381.

Noordenbos, W., and P. D. Wall (1976) Diverse sensory functions with an almost totally divided spinal cord. A case of spinal cord transection with preservation of part of one anterolateral quadrant. Pain 2:185-195.

Nord S. G. (1967) Somatotopic organization of trigeminal nucleus, the dorsal column nuclei, and related structures in the rat. J. Comp. Neurol. 130:343-356.

Nord, S. G. (1976) Responses of neurons in rostral and caudal trigeminal nuclei to tooth pulp stimulation. Brain Res. Bull. 1:489-492.

Nord, S. G., and H. J. Kyler (1968) A single unit analysis of trigeminal projections to bulbar reticular nuclei of the rat. J. Comp. Neurol. 134:485-499.

Nord, S. G., and R. F. Young (1975) Projection of tooth pulp afferents to the cat trigeminal nucleus caudalis. Brain Res. 90:195-204.

Nord, S. G., and R. F. Young (1979) Effects of chronic descending tractotomy on the response patterns of neurons in trigeminal nuclei principalis and oralis. Exp. Neurol. 65:355-372.

Norris, J. R. and H. P. Killackey (1988) Neurons in the dorsal column nuclei of rat which project to ipsilateral thalamus. Soc. Neurosci. Abstr. 14:123.

Northfield, D. W. C. (1938) Some observations on headache. Brain 61:133-162.

Nygren, L. G., and L. Olson (1977) A major projection form locus coeruleus: The main source of noradrenergic nerve terminals in the ventral and dorsal columns of the spinal cord. Brain Res. 132:85-93.

O'Connor, T., and D. van der Kooy (1986) Pattern of intracranial and extracranial projections of trigeminal ganglion cells. J. Neurosci. 6:2200-2207.

Odutola, A. B. (1977) On the location of reticular neurons projecting to the cuneo-gracile nuclei in the rat. Exp. Neurol. 54:54-59.

Ogawa, T., N. C. Jefferson, and H. Necheles (1959) Phrenic cross innervation of the hemidiaphragm in the dog. Am. J. Physiol. 194:355-358.

Olfield, B. J., and G. M. McLachlan (1981) An analysis of the sympathetic preganglionic neurons projecting from the upper thoracic spinal roots of the cat. J. Comp. Neurol. 196:329-345.

Ostapoff, E. M., and J. I. Johnson (1988) Distribution of cells projecting to thalamus vs. those projecting to cerebellum in subdivisions of the dorsla column nuclei in racoons. J. Comp. Neurol. 267:211-230.

Ostfeld, A. M., D. J. Reis, H. Goodell, and H. G. Wolff (1957) Headache and hydration. Arch, Intern. Med. 96:142-152.

Oswaldo-Cruz, E., and C. Kidd (1964) Functional properties of neurons in the lateral cervical nucleus of the cat. J. Neurophysiol. 27:1-14.

Otsuka, M., and S. Konishi (1975) Substance P and excitatory transmitter of primary sensory neurons. Cold Spring Harbor Symp. Quant. Biol., 40:135-143.

Otsuka, M., K. Obata, Y. Miyata, and Y. Tanaka (1971) Measurement of v-aminobutyric acid in isolated nerve cells of cat central nervous system. J. Neurochem., 18:287-295.

Paintal, A. S. (1973) Vagal sensory receptors and their reflex effects. Physiol. Rev. 53:159-227.

Palay, S. L. and V. Chan-Palay (1974) Cerebellar cortex: cytology and organization. Berlin, Springer.

Palkovits, M., and L. Zaborsky (1977) Neuroanatomy of central cardiovascular control. Nucleus tractus solitarii: Afferent and efferent neuronal connections in relation to the baroreceptor reflex arc. Prog. Brain Res. 47:9-34.

Panneton, W. M., and G. F. Martin (1983) Brainstem projections to the facial nucleus of the opossum: A study using axonal transport techniques. Brain Res. 267:19-33.

Panneton, W. M., B. G. Klein, and M.F. Jacquin (1991) Trigeminal projections to contralateral dorsal horn originate in midline hairy skin. Somatosen. Mot. Res. 8(2):165-173.

Papez, J. W. (1927) Subdivisions of the facial nucleus. J. Comp. Neurol. 43:159-171.

Papez, J. W. (1929) Comparative Neurology. Crowell, New York.

Patrick, G. W., and D. E. Haines (1982) Cerebellar afferents to paramedian lobule from the trigeminal complex in *Tupaia glis*: A horseradish peroxidase (HRP) study. J. Morph. 172:209-222.

Patrick, G. W., and M. A. Robinson (1987) Collateral projections from trigeminal sensory nuclei to ventrobasal thalamus and cerebellar cortex in rats. J. Morphol. 192:229-236.

Paxinos, G, and C. Watson (1986) The Rat Brain in Stereotaxic Coordinates. New York: Academic Press.

Pearl, G. S., K. Anderson, and H. S. Rosing (1977) Anatomic evidence revealing extensive transmedian innervation of feline canine teeth. Exp. Neurol. 54:432-443.

Pearson, A. A. (1938) The spinal accessory nerve in human embryos. J. Comp. Neurol. 68:243-266.

Penfield, W. (1935) A contribution to the mechanism of intracranial pain. Res. Nerv. Ment. Dis. 15:399-436.

Penfield, W., and F. McNaughton (1940) Dural headache and the innervation of the dura mater. Arch. Neurol. Psychiat. 44:43-75.

Perl, E. R., and D. G. Whitlock (1961) Somatic stimuli exciting spinothalamic projections to thalamic neurons in cat and monkey. Exp. Neurol. 3:256-296.

Peschanski, M. (1984) Trigeminal afferents to the diencephalon in the rat. Neuroscience 12:465-487.

Peschanski, M., and H. J. Ralston (1985) Light and electron microscopic evidence of transneuronal labeling with WGA-HRP to trace somatosensory pathways to the thalamus. J. Comp. Neurol. 236:29-41.

Peschanski, M., C. L. Lee, and H. J. Ralston, III. (1981) Neurons of the rat ventrobasal thalamic complex responsive to stimuli applied to the face or to the limbs. An intracellular HRP study with electron microscopy. Neurosci. Lett. Suppl 7:S136.

Peschanski, M., P. W. Mantyh, and J. M. Besson (1983) Spinal afferents to the ventrobasal complex of the rat thalamus. An anatomical study using WGA-HRP. Brain Res. 278:240-244.

Peterson, B. W. (1979) Distribution of neuronal responses to tilting within vestibular nuclei of the cat. J. Neurophysiol. 33:750-767.

Peterson, B. W. (1980) Participation of pontomedullary reticular neurons in specific motor activity. In: The Reticular Formation Revisited, J. A. Hobson and M. Brazier (eds.). Raven Press, New York, pp. 171-192.

Petras, J. M., and A. I. Faden (1978) The origin of sympathetic preganglionic neurons in the dog. Brain Res. 144:353-357.

Petras, J. M., and J. F. Cummings (1972) Autonomic neurons in the spinal cord of the rhesus monkey: A correlation of the findings of cytoarchitectonics and sympathectomy with fiber degeneration following dorsal rhizotomy. J. Comp. Neurol. 146:189-218.

Petras, J. W. (1965) Afferent peripheral nerve fibers to the spinal cord and dorsal column nuclei in the cat. An analysis and comparison with the distribution of terminal efferent brain fibers to the spinal cord. Anat. Rec. 151:399-400.

Petras, J. W. (1966) Afferent fibers to the spinal cord. The terminal distribution of dorsal root and encephalospinal axons. Med. Serv. J. (Canada)22:688-694.

Peyronnard, J. M., and L. Charron (1983) Motoneuronal and motor axonal innervation in the rat hindlimb: A comparative study using horseradish peroxidase. Exp. Brain Res. 50:125-132.

Pfaller, K., and J. Arvidsson. (1988) Central distribution of trigeminal and upper cervical primary afferents in the rat studied by anterograde transport of horseradish peroxidase conjugated to wheat germ agglutinin. J. Comp. Neurol. 268:91-108.

Phelan, K. D., and W. M. Falls (1989) An analysis of the cyto-and myeloarchitectonic organization of trigeminal nucleus interpolaris in the rat. Somatosen. Res. 6(4):333-366.

Phelan, K. D., and W. M. Falls (1991a) The spinotrigeminal pathway and its spatial relationship to the origin of trigeminospinal projections in the rat. Neuroscience 40:477-496.

Phelan, K. D., and W. M. Falls (1991b) A comparison of the distribution and morphology of thalamic, cerebellar and spinal projection neurons in rat trigeminal nucleus interpolaris. Neuroscience 40:497-511.

Pickering, R., and P. Bolton-Maggs (1975) Treatment of supraventricular tachycardia. Lancet 1:340.

Pickoff-Matuk, J. F., J. P. Rosenfeld, and J. G. Broton (1986) Lesions of the mid-spinal trigeminal complex are effective in producing perioral thermal hypoalgesia. Brain Res. 382:291-298.

Poggio, G. F., and V. B. Mountcastle (1960) A study of the functional contributions of the lemniscal and spinothalamic systems to somatic sensibility. Bull. John's Hopk. Hosp., 106:266-316.

Polosa, C. (1967) Silent period of sympathetic preganglionic neurons. Can. J. Physiol. Pharmacol. 45:1033-1045.

Pomeranz, B., P. D. Wall, and W. V. Webber (1968) Cord cells responding to fine myelinated afferents from viscera, muscle and skin. J. Physiol. (Lond). 199:511-532.

Porter, J. D., and R. F. Spencer (1982) Localization and morphology of cat extraocular muscle afferent neurons identified by retrograde transport of horseradish peroxidase. J. Comp. Neurol. 204:56-64.

Poulos, D. A., and J. T. Molt (1977) Thermosensory mechanisms in the spinal trigeminal nucleus of cats. In Pain in the Trigeminal Region. (eds. D. J. Anderson and B. M. Mathews) Elsevier, Amsterdamn, pp. 443-453.

Precht, W. (1974) Physiology of the vestibular nuclei. In Handbook of Sensory Physiology, vol. VI, Vestibular system, Part I, Basic Mechanisms. H. H. Kornhuber (ed.), Springer Verlag, Berlin-Heidelberg-New York.

Prechtl, K. F. R. (1953) Die kletterbewegungen beim saugling. Monatschr. Kinderheilk. 101:519-521.

Preiss, G., and C. Polosa (1977) The relation between end-tidal CO2 and discharge patterns of sympathetic preganglionic neurons. Brain Res. 122:255-269.

Price, D. D., R. Dubner, and J. W. Hu (1976) Trigeminothalamic neurons in nucleus caudalis responsive to tactile, thermal and nociceptive stimulation of the monkey's face. J. Neurophysiol. 39:936-953.

Proshansky, E., and M. D. Egger (1977) Staining of the dorsal root projection to the cat's dorsal horn by anterograde movement of horseradish peroxidase. Neurosci. Lett. 5:103-110.

Provis, J. (1977) The organization of the facial nucleus of the brushed-tailed possum (*Trichosurus vulpecula*). J. Comp. Neurol. 172:177-188.

Ramon y Cajal, S. (1909) Histologu de systeme nerveux de l'homme et des vertebres. Norbert Maloine, Paris. 2 vols.

Rando, T. A., C. W. Bowers, and R. G. Zigmond (1981) Localization of neurons in the rat spinal cord which project to the superior cervical ganglion. J. Comp. Neurol. 196:73-83.

Ranson, S. W., H. K. Davenport, and E. A. Doles (1932) Intramedullary course of the dorsal root fibers of the first three cervical nerves. J. Comp. Neurol. 94:1-12.

Rao, G. S., R. P. Saigal, and S. Sahu (1972) The phrenic nerve and the localization of phrenic nucleus in the spinal cord of the buffalo (*Bubalus bubalia*). Acta Anat. 83:468-477.

Ray, B. S., and H. G. Wolff (1940) Experimental studies on headache. Pain sensitive structures of the head and their significance in headache. Arch. Surg. 41:813-856.

Reis, D. J., N. Doba, D. W. Snyder, and M. A. Nathan (1977) Brain lesions and hypertension: Chronic lability and elevation of arterial blood pressure produced by electrolytic lesions and 6-hydroxydopamine treatment of nucleus tractus solitarii (NTS) in rat and cat. Prog. Brain Res. 47:169-188.

Renaud, L. P., J. B. Martin, and P. Braueau (1975) Depressant action of TRH, LH-RH and somatostatin on activity of central neurons. Nature, 255:233-235.

Rethelyi, M., D. L. Trevino, and E. R. Perl (1979) Distribution of primary afferent fibers within the sacrococcygeal dorsal horn: An autoradiographic study. J. Comp. Neurol. 185:603-622.

Rexed, B. (1951) The nucleus cervicalis lateralis, a spinocerebellar relay nucleus. Acta Physiol. Scand. Suppl 89:67-68.

Rexed, B. (1952) The cytoarchitectonic organization of the spinal cord in the cat. J. Comp. Neurol. 96:415-496.

Rexed, B. (1954) A cytoarchitectonic atlas of the spinal cord. J. Comp. Neurol. 100:297-397.

Rexed, B. (1964) Some aspects of the cytoarchitectonics and synaptology of the spinal cord. Prog. Brain Res. 11:58-92.

Rexed, R., and A. Brodal (1951) The nucleus cervicalis lateralis. A spinocerebellar relay nucleus. J. Neurophysiol. 14:300-407.

Rhoades, R. W., S. E. Fish, N. L. Chiaia, C. Bennett-Clarke, and R. D. Mooney (1989) Organization of the projections from the trigeminal brainstem complex to the superior colliculus in the rat and hamster: Anterograde tracing with Phaseolus vulgaris leucoagglutinin and Intra-axonal injection. J. Comp. Neurol. 289:641-656.

Ribak, C. E., and A. Peter (1975) An autoradiographic study of the projections from the lateral geniculate body of the rat. Brain Res. 92:341-368.

Ricardo, J. A. (1981) Efferent connections of the subthalamic regions in the rat. II. The zona incerta. Brain Res. 214:43-60.

Richardson, H. C., F. W. J. Cody, V. E. Paul, and A. G. Thomas (1978) Convergence of trigeminal and limb inputs onto cerebellar interpositus nuclear neurones in the cat. Brain Res. 156:355-359.

Richmond, F. J. R., and V. C. Abrahams (1975) Morphology and enzyme histochemistry of dorsal muscles of the cat neck. J. Neurophysiol. 38:1312-1321.

Richmond, F. J. R., D. Scott, and V. C. Abrahams (1978) Distribution of motoneurons to the neck muscles biventer cervicis, splenius and complexus in the cat. J. Comp. Neurol. 181:451-464.

Riedel, W., and M. Iriki (1979) Autonomic nervous control of temperature homeostasis. In: Integrative Functions of the Autonomic Nervous System. C. McC. Brooks, K. Koizumi, and A. Sato (eds.). University of Tokyo Press, Tokyo and Elsevier-North Kolland, New York. pp. 399-414.

Ring, G., and D. Ganchrow (1978) Projections of nucleus caudalis and spinal cord to brainstem and diencephalon in the hedgehog (*Erinaceus europaeus* and *Paraechinus aethiopicus*): A degeneration study. J. Comp. Neurol. 216:132-151.

Ritchie, T. C., L. J. Roos, B. J. Williams, and R. B. Leonard (1984) The descending and intrinsic serotonergic innervation of an elasmobranch spinal cord. J. Comp. Neurol. 224:395-406.

Ritz, L. A., J. L. Culberson, and P. B. Brown (1985) Somatotopic organization in cat spinal cord segments with fused dorsal horns: Caudal and thoracic levels. J. Neurophysiol. 54:1167-1177.

Rivnik, E., and F. Walberg (1975) Studies on the cerebellar projections from the main and external cuneate nuclei in the cat by means of retrograde axonal transport of horseradish peroxidase. Brain Res. 95:371-381.

Robards, M. J., M. Stritzel, and R. T. Robertson (1980) Ventral horn cells of the cervical cord project to neck muscles and brain. Brain Res. 189:519-523.

Robards, M., D. Watkins, and R. B. Masterton (1976) An anatomical study of some somesthetic efferents to the intercollicular zone of the midbrain of the opossum. J. Comp. Neurol. 170:499-524.

Robertson, L. T. (1985) Somatosensory representation of the climbing fiber system in the rostral intermediate cerebellum. Exp. Brain Res. 61:73-86.

Robertson, L. T. and K. D. Laxer (1981) Localization of cutaneously elicited climbing fiber response in lobule V of the monkey cerebellum. Brain Behav. Evol. 18:157-168.

Robertson, L. T.(1984) Topographic features of climbing fiber input in the rostral anterior lobe of the cat cerebellum. Exp. Brain Res. 55:445-454.

Robertson, L. T., K. D. Laxer and D. S. Rushmer (1982) Organization of climbing fiber input from mechanoreceptors to lobule V vermal cortex of the cat. Exp. Brain Res. 46:281-291.

Roger, M., and J. Cadusseau (1984) Afferent connections of the nucleus posterior thalami in the rat, with some evolutionary and functional considerations. J. Hirnforsch. 25:473-485.

Roger, M., and J. Cadusseau (1985) Afferents to the zona incerta in the rat: A combined retrograde and anterograde study. J. Comp. Neurol. 241:480-492.

Romagnano, M. A., and R. W. Hamill (1984) Spinal sympathetic pathways: an enkephalin ladder. Science 225:737-739.

Romanes, G. J. (1951) The motor cell columns of the lumbosacral spinal cord of the cat. J. Comp. Neurol. 94:313-364.

Romanes, G. J. (1964) The motor pools of the spinal cord. Prog. Brain Res. 11:93-119.

Rose, P. K., and N. Sprott (1979) Proprioceptive and somatosensory influences on neck muscle motoneurons. Progress in Brain Res. Reflex Control of Posture and Movement. R. Granit and O. Pompeiano (eds.), Elsevier, North-Holland, Biomed Press, Amsterdam/New York.

Rose, P. K., and V. C. Abrahams (1977) Tectospinal and tectoreticular cells. Their distribution and afferent connections. Canad. J. Physiol. Pharmacol. 56:650-658.

Rosen, I. (1967) Functional organization of Group I activated neurons in the cuneate nucleus of the cat. Brain Res. 6:770-772.

Rossi, F., and D. Scevola (1935) Contributo alla conoscenza della distribuzione della fibre nervose nella dura madre encefalica. Monitore Zool. Ital. 45:289.

Rowe, M. J., and B. J. Sessle (1968) Somatic afferent input to posterior thalamic neurones and their axon projection to cerebral cortex in the cat. J. Physiol. (Lond.) 196:19-35.

Rubin, E., and D. Purves (1980) Segmental organization of sympathetic preganglionic neurons in the mammalian spinal cord. J. Comp. Neurol. 192:163-174.

Ruch, T. C. (1947) Visceral sensation and referred pain. In J. F. Fulton (ed.), Howell's Textbook of Physiology, 15th ed., Saunders, Philadelphia. pp. 385-401.

Ruda, M. A., J. Coffield, and H. W. M. Steinbusch (1982) Immunocytochemical analysis of serotonergic axons in laminae I and II of the lumbar spinal cord of the cat. J. Neurosci. 2:1660-1671.

Ruggiero, D. A., C. A. Ross and D. J. Reis (1981) Projections from the spinal trigeminal nucleus to the entire length of the spinal cord in the rat. Brain Res. 225:225-233.

Rushmer, D. S., M. H. Wollacott, L. T. Robertson and K. D. Laxer (1980) Somatotopic organization of climbing fiber projections from low threshold cutaneous afferents to pars intermedia of cerebellar cortex in the cat. Brain Res. 181:17-30.

Russchen, F. T., H. J. Groenewegen, and J. Voogd (1976) Reticulocerebellar connections in the cat. An autoradiographic study. Acta. Morph. Neerl.-Scand. 14:245-246.

Rustioni, A. (1973) Non-primary afferents to the nucleus gracilis from the lumbar cord of the cat. Brain Res. 51:81-95.

Rustioni, A. (1974) Non-primary afferents to the cuneate nucleus in the brachial dorsal funiculus of the cat. Brain Res. 75:247-259

Rustioni, A., and A. B. Kaufman (1977) Identification of cells of origin of non-primary afferents to the dorsal column nuclei of the cat. Exp. Brain Res. 27:1-14.

Rustioni, A., and G. Macchi (1968) Distribution of dorsal root fibers in the medulla oblongata of the cat. J. Comp. Neurol. 134:113-126.

Rustioni, A., and N. L. Hayes (1981) Corticospinal tract collaterals to the dorsal column nuclei of cats. Exp. Brain Res. 43:237-245.

Rustioni, A., D. E. Schmechel, S. Cheema and D. Fitzpatrick (1984) Glutamic acid decarboxylase-containing neurons in the dorsal column nuclei of the cat. Somatosen. Res. 1:329-357.

Rustioni, A., N. L. Hayes, and S. O'Neill (1979) Dorsal column nuclei and ascending spinal afferents in macaques. Brain. 102:95-125.

Rydenhag, B., and A. Roos (1986) Projections of tooth pulp afferents to the thalamus of the cat. II. Distribution and characteristics of single units. Exp. Brain Res. 64:49-58.

Saigal, R. P., A. N. Karamanlidis, J. Voogd, O. Managana, and H. Michaloudi (1980) Secondary trigeminocerebellar projections in sheep studied with the horseradish peroxidase tracing method. J. Comp. Neurol. 189:537-553.

Sant. 'Ambrogio, G., D. T. Frazier, M. F. Wilson, and E. Agostoni (1963) Motor innervation and pattern of activity of cat diaphragm. J. Appl. Physiol. 18:43-46.

Santacana, M. P., and J. Delacour (1968) Effects, chez le rat, des lesions de la zona incerta, et des corps mamillaries, sur un condition nemert defensif. Neuropsychologia 6:115-124.

Saporta, S., and L. Kruger (1977) The organization of the thalamocortical relay neurons in the rat ventrobasal complex studied by the retrograde transport of horseradish peroxidase. J. Comp. Neurol. 174:187-208.

Sar, M., W. E., Stumpf, R. J. Miller, K. J. Chang, and P. Cuatrecasas (1978) Immunohistochemical localization of enkephalin in rat brain and spinal cord. J. Comp. Neurol. 182:17-38.

Sato, A., and R. F. Schmidt (1971) Spinal and supraspinal components of the reflex discharges into lumbar and thoracic white rami. J. Physiol. (Lond). 212:839-850.

Sato, M., K. Itoh, N. Mizuno (1979) Distribution of thalamo-caudate neurons in the cat as demonstrated by horseradish peroxidase. Exp. Brain Res. 34:143-154.

Satoh, K. (1979) The origin of reticulospinal fibers in the rat: A HRP study. J. Hirnforsch. 20:313-332.

Satoh, K., A. Kashiba, H. Kimura, and T. Maeda (1982) Noradrenergic axon terminals in the substantia gelatinosa of the rat spinal cord. Cell Tissue Res. 222:359-378.

Scheibel, A. B., (1977) Sagittal organization of mossy fiber terminal systems in the cerebellum of the rat: A Golgi study. Exp. Neurol. 57:1067-1070.

Scheibel, M. A., and A. B. Scheibel (1958) Structural substrates for integrative patterns in the brainstem reticular core. In Jasper H. H., L. D. Proctor, R. S. Knighton, and W. C. Noshay (eds.): Reticular formation of the brain. Boston: Little Brown and Co., pp. 31-35.

Scheibel, M. E., and A. B. Scheibel (1966) Patterns of organization in specific and non-specific thalamic fields. In The Thalamus (eds. D. P. Purpura and M. D. Yahr) Columbia University Press, New York, pp. 13-46.

Schlafke, M. E., and W. R. See (1980) Ventral medullary surface stimulus response in relation to ventilatory and cardiovascular effects. In: Central Interactions Between Respiratory and Cardiovascular Control Systems. H. P. Kopechen, S. M. Hilton, and A. Trzebski (eds.). Berlin. Springer-Verlag. pp. 56-63.

Schofield, B. R. (1990) Uptake of Phaseolus vulgaris leucoagglutinin (PHA-L) by axons of passage. J. Neurosci. Methods 35:47-56.

Schramm, L., J. R. Adair, J. Stribling, and L.Gray (1975) Preganglionic innervation of the adrenal gland of the rat: A study using horseradish peroxidase. Exp. Neurol. 49:540-553.

Schroder, H. D. (1980) Organization of the motoneurons innervating the pelvic muscles of the male rat. J. Comp. Neurol. 192:567-587.

Schroder, H. D. (1984) Somatostatin in the caudal spinal cord: An immunohistochemical study of the spinal centers involved in the innervation of pelvic organs. J. Comp. Neurol. 223:400-414.

Schroeder, D. M., and J. A. Jane (1971) Projection of dorsal column nuclei and spinal cord to brainstem and thalamus in the tree shrew, *Tupaia glis*. J. Comp. Neurol. 142:309-350.

Schulman, J. A., T. E. Finger, N. C. Brecha, and H. J. Karten (1981) Enkephalin immunoreactivity in Golgi cells and mossy fibers of the mammalian, avian, amphibian and teleost cerebellum. Neuroscience, 6:2407-2416.

Schultzberg, M., J. M. Lundberg, T. Hokfelt, L. Terenius, J. Brandt, R. P. Elde, and M. Goldstein (1978) Enkephalin-like immunoreactivity in gland cells and nerve terminals of the adrenal medulla. Neuroscience 3:1169-1186.

Schultzberg, M., T. Hokfelt, L. Terenius, L. G. Elfvin, J. M. Lundberg, J. Brandt, R. Elde, and M. Goldstein (1979) Enkephalin immunoreactive nerve terminals and cell bodies in sympathetic ganglia of the guinea pig and rat. Neuroscience 4:249-270.

Sears, T. A (1976) The neural architecture of movements of the rib cage, a multi-segmented laminated motor system. Exp. Brain Res. (Suppl) 1:450-454.

Selzer, M., and W. A. Spencer (1969) Convergence of visceral and cutaneous afferent pathways in the lumbar spinal cord. Brain Res. 14:331-348.

Senba, E., and M. Tohyama (1983a) Leucine-enkephalin-containing neuron system in the facial nucleus of the rat with special reference to its fine structure. Brain Res. 274:17-23.

Senba, E., and M. Tohyama (1983b) Reticulo-facial enkephalinergic pathway in the rat: An experimental immunohistochemical study. Neurosci. 10:831-839.

Sessle, B. J., and D. J. Kenny (1973) Control of tongue and facial motility. In J. Bosma (ed): Fourth Symposium on Oral Sensation and Perception: The Mouth of the neonati. Bethesda, Maryland:DHEW. pp. 222-231.

Sessle, B. J., and J. W. Hu (1981) Raphe-induced supression of the jaw-opening reflex and single neurons in trigeminal subnucleus oralis, and influence of naloxone and subnucleus caudalis. Pain 10:19-36.

Sessle, B. J., and L. F. Greenwood (1975) Effects of trigeminal tractotomy and of carbamazepine on single trigeminal sensory neurons in cat. J. Dent. Res. 54:B201-B206.

Sessle, B. J., and L. F. Greenwood (1976) Inputs to trigeminal brain stem neurones from facial, oral, tooth pulp and pharyngolaryngeal tissues. I. Responses to innocuous and noxious stimuli. Brain Res. 117:211-226.

Sessle, B. J., and L. F. Greenwood (1986) Inputs to trigeminal brainstem neurons from facial, oral, tooth and pharyngolaryngeal tissues. I. Responses to innocuous and noxious stimuli. Brain Res. 117:211-216.

Seybold, V. S., and R. P. Elde (1982) Neurotensin immunoreactivity in the superficial laminae of the dorsal horn of the rat: I. Light microscopic studies of cell bodies and proximal dendrites. J. Comp. Neurol. 204:89-100.

Shambes, G. M., D. H. Beerman, and W. Welker (1978a) Multiple tactile areas in cerebellar cortex: Another patchy cutaneous projection to granule cell columns in rats. Brain Res. 157:123-128.

Shambes, G. M., J. M. Gibson, and W. Welker (1978b) Fractured somatotopy in granule cell tactile areas of the rat cerebellar hemispheres revealed by micromapping. Brain Behav. Evol. 15:94-140.

Shigenaga, Y., I. C. Chen, S. Suemune, T. Nishimori, I. D. Nasution, A., Yoshida, H. Sato, T. Okamoto, M. Sera, and M. Hosoi (1986) Oral and facial representation within the medullary and upper cervical dorsal horns in the cat. J. Comp. Neurol. 243:388-408.

Shigenaga, Y., M. Sera, T. Nishimori, S. Suemune, M. Nishimura, A. Yoshida, and K. Tsuru (1988) The central projection of masticatory afferent fibers to the trigeminal sensory nuclear complex and upper cervical cord. J. Comp. Neurol. 268:489-507.

Shigenaga, Y., Z. Nakatani, T. Nishimori, S. Suemune, R. Kuroda, and S. Matano (1983) The cells of origin of cat trigeminothalamic projections: especially in the caudal medulla. Brain Res. 277:201-222.

Shriver, J. E., B. M. Stein, and M. B. Carpenter (1968) Central projections of spinal dorsal roots in the monkey. 1. Cervical and upper thoracic dorsal roots. Amer. J. Anat. 123:27-74.

Shute, C. C. and P. R. Lewis (1965) Cholinesterase-containing pathways of the hindbrain; Afferent cerebellar and centrifugal cochlear fibers. Nature (Lond.) 205:242-246.

Silverman, J. D., and L. Kruger (1985) Projections of the rat trigeminal sensory nuclear complex demonstrated by multiple fluorescent dye retrograde transport. Brain Res. 361:383-388.

Simantov, R., M. J. Kuhar, G. R. Uhl, and H. Snyder (1977) Opioid peptide enkephalin: Immunohistochemical mapping in rat central nervous system. Proc. Natl. Acad. Sci. 74:2167-2171.

Simon, E., and W. Riedel (1975) Diversity of regional sympathetic nerve activity in integrative cardiovascular control patterns and metabolism. Brain Res. 87:323-333.

Sjoqvist, O. (1938) Studies on pain conduction in the trigeminal nerve; contribution to surgical treatment of facial pain. Acta Psychiatr. Scand. Suppl. 17:1-139.

Smith, C. L. (1983) The development and postnatal organization of primary afferent projections to the rat thoracic spinal cord. J. Comp. Neurol. 220:29-43.

Smith, C. L., and M. Hollyday (1983) The development and postnatal organization of motor nuclei in the rat thoracic spinal cord. J. Comp. Neurol. 220:16-28.

Smith, L. A., and W. M. Falls (1987) Efferent projections to cranial nerve nuclei from rat trigeminal nucleus oralis. Anat Rec. 220:91A.

Smith, L. A., and W. M. Falls (1988) Efferent projections to rat spinal cord from trigeminal nucleus oralis utilizing the method of PHA-L. Soc. Neurosci. Abstr. 14:697.

Smith, L. A., and W. M. Falls (1990a) Projections from rat trigeminal nucleus oralis to the cerebellum. Soc. Neurosci. Abstr. 16:895.

Smith, L. A., and W. M. Falls (1990b) Thalamic projections from neurons in rat trigeminal nucleus oralis. Anat. Rec. 226:94-95A.

Smith, R. L. (1972) Fiber projections from the principal sensory trigeminal nucleus in the monkey. Anat. Rec. 172:409.

Smith, R. L. (1973) The ascending fiber projections from the principal sensory trigeminal nucleus in the rat. J. Comp. Neurol. 148:423-446.

Smith, R. L. (1975) Axonal projections and connections of the principal sensory trigeminal nucleus in the monkey. J. Comp. Neurol. 163:347-376.

Snyder, R. L., R. L. M. Faull, and W. R. Mehler (1978) A comparative study of the neurons of origin of the spinocerebellar afferents in the rat, cat and squirrel monkey based on the retrograde transport of horseradish peroxidase. J. Comp. Neurol. 181:833-852.

Somana, R. and F. Walberg (1979) Cerebellar afferents from the nucleus of the solitary tract. Neurosci. Lett. 11:41-47.

Somana, R., N. Kotchabhakdi, and F. Walberg (1980) Cerebellar afferents from the trigeminal sensory nuclei in the cat. Exp. Brain Res. 38:57-64.

Somiya, H., and T. Tonoue (1984) Neural peptides as central integrators of autonomic nerve activity: Effects of TRH, SRIF, VIP, and bombesin on gastric and adrenal glands. Reg. Pept. 9:47-52.

Sotgiu, M. L., and G. Marini (1977) Reticulo-cuneate projections as revealed by horseradish peroxidase axonal transport. Brain Res. 128:341-345.

Spreafico, R., and P. Barbaresi, R. J. Weinberg, and A. Rustiono (1987) SII-projecting neurons in the rat thalamus: a single-and double-retrograde tracing study. Somatosen. Res. 4:359-375.

Spyer, K. M., (1981) Neural organization and control of baroreceptor reflex. Rev. Physiol. Biochem. Pharmacol. 88:23-124.

Starzl, T. E., C. W. Taylor, and H. W. Magoun (1951) Ascending conduction in the reticular activating system, with special reference to the diencephalon. J. Neurophysiol. 14:461-477.

Steiger, G. J., J. M. Tew, and J. T. Keller (1982) The sensory innervation of the dura mater in the trigeminal ganglion of the cat. Neurosci Lett. 31:231-236.

Steindler, D. A. (1977) Trigemino-cerebellar projections in normal and reeler mutant mice. Neurosci. Lett. 6:293-300.

Sterling, P., and H. G. J. M. Kuypers (1967) Anatomical organization of the brachial spinal cord of the cat. II. The motoneuron plexus. Brain Res. 4:16-32.

Stewart, W. A., and R. B. King (1963) Fiber projections from the nucleus caudalis of the spinal trigeminal nucleus. J. Comp. Neurol. 121:271-286.

Strassman, A., P. Mason, M. Moskowitz, and R. Maciewicz (1986) Response of brainstem trigeminal neurons to electrical stimulation of the dura. Brain Res. 379:242-250.

Sugitani, M., J. Yano, T. Sugai, and H. Ooyama (1990) Somatotopic organization and columnar structure of vibrissae representation in the rat ventrobasal complex. Exp. Brain Res. 81:346-352.

Sumal, K. K., V. M. Pickel, R. J. Miller, and D. J. Reis (1982) Enkephalin-containing neurons in substantia gelatinosa of spinal trigeminal complex: Ultrastructure and synaptic interaction with primary sensory afferents. Brain Res. 248:223-236.

Sumino, R. (1971) Central neural pathways involved in the jaw-opening reflex in the cat. In: R. Dubner and Y. Kawamura (eds.), Oral Facial Sensory and Motor Mechanisms. Appleton-Century-Crofts, New York. pp. 315-331.

Sumino, R., and S. Nozaki (1977) Trigemino-neck reflex-its peripheral and central organisation. In Pain inthe trigeminal region. D. S. Anderson and B. Mathews (eds.), Elsevier, Amnsterdam pp. 365-375.

Swanson, L. W., and H. G. J. M. Kuypers (1980) The paraventricular nucleus of the hypothalamus: Cytoarchitectonic subdivision and organization of projections to the pituitary, dorsal vagal complex, and spinal cord as demonstrated by retrograde fluorescence double-labeling methods. J. Comp. Neurol. 194:555-570.

Swanson, L. W., and S. McKellar (1979) The distribution of oxytocin and neurophysin stained fibers in the spinal cord of the rat and monkey. J. Comp. Neurol. 188:87-106.

Szekely, G., and C. Matesz (1982) The accessory motor nuclei of the trigeminal, facial, and abducens nerves in the rat. J. Comp. Neurol. 210:258-264.

Taber, E. (1961) The cytoarchitecture of the brainstem of the cat. 1. Brainstem nuclei of the cat. J. Comp. Neurol. 116:27-69.

Takeuchi, Y., H. Kimura and Y. Sano (1982) Immunocytochemical demonstration of serotonin-containing nerve fibers in the cerebellum. Cell Tiss. Res. 226:1-12.

Takeuchi, Y., M. Uemura, K. Matsuda, R. Matsushima, and N. Mizuno (1980) Parabrachial nucleus neurons projecting to the lower brainstem and the spinal cord. A study in the cat by the Fink-Heimer and the Horseradish peroxidase methods. Exp. Neurol. 70:403-413.

Tamarova, Z. A., A. I. Shapovalov, and L. Vyklicky (1973) Projection of tooth pulp afferents in the brain stem of rhesus monkey. Brain Res. 64:442-445.

Tan, C. K. and A. R. Lieberman (1978) Identification of thalamic projection cells in the rat cuneate nucleus: A light and electron microscopic study using horseradish peroxidase. Neurosci. Lett. 10:19-22..

Tan, C. K., and W. C. Wong (1982) The structure and connections of the dorsal column nuclei. In Progress in Anatomy, vol. 2 (eds. Harrison R. J. and Navaratnam V.), pp.161-177. Cambridge University Press, Cambridge.

Ter Horst, G. J., H. J. Groenwegen, H. J. Krast, and P. G. M. Liuten (1984) Phaseolus vulgaris leuco-agglutinin immunohistochemistry. A comparison between autoradiographic and lectin tracing of neuronal efferents. Brain Res. 307:370-383.

Tohyama, M., K. Sakai, M. Touret, D. Salvert and M. Jouvet (1979) Spinal projections from the lower brain stem in the cat as demonstrated by the horseradish peroxidase technique. II. Projections from the dorsolateral pontine tegmentum and raphe nuclei. Brain Res. 176:215-23.

Tonoue, T., H. Hata, T. Ohnishi, N. Kido, and T. Nakamura (1985) Somatostatin and GABA correlate with cervical autonomic nerve activity. Regul. Pept. 10:299-307.

Torvik, A. (1956) Afferent connections to the sensory trigeminal nuclei, the nucleus of the solitary tract and adjacent structures: An experimental study in rat. J. Comp. Neurol. 106:51-142.

Travers, J. B., and R. Norgren (1983) Afferent projections to the oral motor nuclei in the rat. J. Comp. Neurol. 220:280-298.

Trevino, D. L., J. D. Coulter, and W. D. Willis (1973) Location of cells of origin of spinothalamic tract in lumbar enlargement of the monkey. J. Neurophysiol. 36:750-761.

Trevino, D. L., R. A Maunz, R. N. Bryan, and W. D. Willis (1972) Location of cells of origin of the spinothalamic tract in the lumbar enlargement of cat. Exp. Neurol. 34:64-77.

Trevino,D. L. (1978) The origin and projections of a spinal nociceptive and thermoreceptive pathway. In Zotterman, Y. (ed) Sensory Functions of the Skin in Primates, with Special Reference to Man. New York, Pergamon Press, pp. 367-376.

Tripp, L. N., and J. Wells (1978) Formation of new synaptic terminals in the somatosensory thalamus of the rat after lesions of the dorsal column nuclei. Brain Res. 155:362-367.

Truex, R. C., M. J. Taylor, M. Q. Smythe, and P. L. Gildenberg (1970) The lateral cervical nuclei of cat, dog and man.J. Comp. Neurol. 139:92-104.

Uhl, G. R., R. R. Goodman, M. J. Kuhar, S. R. Childers, and S. H. Snyder (1979) Immunohistochemical mapping of enkephalin containing cell bodies, fibers and nerve terminals in the brain stem of the rat. Brain Res. 166:75-94.

Ullah, M. (1978) Localization of the phrenic nucleus in the spinal cord of the rabbit. J. Anat. 125:377-386.

Umetani, T., T. Tabuchi, and R. Ichimura (1986) Cerebellar corticonuclear and corticovestibular fibers from the posterior lobe of the albino rat, with comments on zones. Brain, Behav. Evol. 29:54-67.

Valverde, F. (1966) The pyramidal tract in rodents. A study of its relations with the posterior column nuclei, dorsolateral reticular formation of the medulla oblongata, and cervical spinal cord (Golgi and electron microscopic observations). Z. Zellforsch. 71:297-363.

Van Loon, G. R., N. M. Appel, and D. Ho (1981) B-Endorphin-induced increase in plasma epinepherine, norepinepherine and dopamine in rats: Inhibition of adrenomedullary response by intracerebral somatostatin. Brain Res. 212:207-214.

van Rossum, J. (1969) Corticonuclear and corticovestibular projections in the cerebellum. An experimental investigation of the anterior lobe, the simple lobule and the caudal vermis in the rabbit. Dissertation, Leiden.

Vertes, R. P., G. F. Martin, and R. Waltzer (1986) An autoradiographic analysis of ascending projections from the medullary reticular formation in the rat. Neuroscience 19(3):873-898.

Vidal, P. P., P. J. May, and R. Baker (1988) Synaptic organization of the tecto-facial pathways in the cat: Synaptic potentials following collicular stimulation. J. Neurophysiol. 60(2):769-797.

Vlklicky, L., and D. Keller (1973) Central projection of tooth pulp primary afferents in the cat. Acta. Neurobiol. Exp. 33:803-809.

Voogd, J. and F. Bigare (1980) Topographical distribution of olivary and corticonuclear fibers in the cerebellum: a review. In de Montigny, and Courville (eds): Anatomy and physiology of the inferior olivary nucleus. New York: Raven Press. pp. 207-234.

Vyklicky, L., O. Keller, P. Jastreboff, L. Vyklicky, Jr., and S. M. Butkhuzi (1977) Spinal trigeminal tractotomy and nociceptive reactions evoked by tooth pulp stimulation in the cat. J. Physiol. Paris 73:379-386.

Waite, P. M. (1973) Somatotopic organization of vibrissal responses in the ventrobasal complex of the rat thalamus. J. Physiol. (Lond.) 228:527-540.

Walberg, F. (1980) Olivocerebellar projection in the cat as determined with the method of retrograde axonal transport of horseradish peroxidase. I. topographical pattern; in de Montigny, Courville, Anatomy and Physiology of the inferior olivary nucleus. Raven press, New York, pp. 169-186.

Walberg, F., and A. Brodal (1979) The longitudinal zonal pattern in the paramedian lobule of the cat's cerebellum: an analysis based on a correlation of recent HRP data with results of studies with other methods. J. Comp. Neurol. 187:581-588.

Wall, P. D., and A. Taub (1962) Four aspects of trigeminal nucleus and a paradox. J. Neurophysiol. 25:110-126.

Warwick, R., and P. L. Mitchell (1956) The phrenic nucleus of the macaque. J. Comp. Neurol. 105:553-585.

Warwick, R., and P. L. Williams (1973) Gray's Anatomy. 35th ed. London:Longman.

Watanabe, K., and E. Kawana (1982) The cells of origin of the incertofugal projections to the tectum, thalamus, tegmentum and spinal cord in the rat. A study using the autoradiographic and horseradish peroxidase methods. Neuroscience 7:2389-2406.

Watson, C. R. R., and R. C. Switzer III (1978) Trigeminal projections to cerebellar tactile areas in the rat-origin mainly from n. interpolaris and n. principalis. Neurosci. Lett. 10:77-82.

Watson, C. R. R., S. Sakai, and W. Armstrong (1982) Organization of the facial nucleus in the rat. Brain Behav. Evol. 20:19-28.

Webber, C. L., Jr., R. D. Wurster, and J. M. Chung (1979) Cat phrenic nucleus architecture as revealed by horseradish peroxidase mapping. Exp. Brain Res. 32:1-12.

Webster, K. E., and S. K. Kemplay (1987) Distribution of primary afferent fibers from the forelimb of the rat to the upper cervical spinal cord in relation to the location of spinothalamic neuron populations. Neurosci. Lett. 76:-18-24.

Weinberg, R. J., and A. Rustioni (1989) Brainstem projections to the rat cuneate nucleus. J. Comp. Neurol. 282:142-156.

Welker, W. I (1990) The significance of folliation and fissuration of cerebellar cortex. The cerebellar folium as a fundamental unit of sensorimotor integration. Arch. ital. Biol. 128: 87-109.

Westrum, L. E., R. C. Canfield, and T. A. O'Conner (1980) Projections from dental structures to the brainstem trigeminal complex as shown by transganglionic transport of horseradish peroxidase. Neurosci. Lett. 20:31-36.

Westrum, L. E., R. C. Canfield, and T. A. O'Connor (1981) Each canine tooth projects to all brain stem trigeminal nuclei in cat. Exp. Neurol. 74:787-799.

Whayne, M. (1976) Conversion of paroxysmal atrial tachycardia by facial immersion in ice water. JACEP 5:434.

White, J. C., and W. H. Sweet (1955) Pain, its mechanisms and neurosurgical control. Springfield, Il.: Thomas.

Whitman, V., and G. Zakeosian (1976) The diving reflex in termination of supraventricular tachycardia in childhood. J. Pediatr. 89:1032.

Whitman, V., Z. Friedman, W. Berman, and M. J. Maisels (1977) Supraventricular tachycardia in newborn infants: An approach to therapy. J. Pediatr. 90:304.

Wiksten, B. (1979a) The central cervical nucleus in the cat. I A golgi study. Exp. Brain Res. 36:143-154.

Wiksten, B. (1979b) The central cervical nucleus in the cat. II. The cerebellar connections studied with retrograde transport of horseradish peroxidase. Exp. Brain Res. 36:155-173.

Wiksten, B. (1979c) The central cervical nucleus in the cat. III. The cerebellar connections studied with anterograde transport of 3H-Leucine. Exp. Brain Res. 36:175-189.

Wiksten, B., and G. Grant (1983) The central cervical nucleus in the cat. IV. Afferent fiber connections : An experimental anatomical study. Exp. Brain Res. 1983:405-412.

Wilcox, T. K., R. P. Yezierski, K. D. Gerhart, and W. D. Willis (1980) A study of the response properties of medial brainstem cells projecting to the spinal cord in monkeys. Soc. Neurosci. Abstr. 6:40.

Wildenthal, K., J. Atkins, S. Leshin, and C. L. Skelton (1975) The diving reflex used to treat paroxysmal atrial tachycardia. Lancet 1:12.

Willis, W. D., and R. E. Coggeshall (1978) Sensory Mechanisms of the Spinal Cord, John Wiley and Sons, New York. p. 477.

Willis, W. D., D. R. Kenshalo, and R. B. Leonard (1979) The cells of origin of the primate spinothalamic tract. J. Comp. Neurol. 188:543-574.

Willis, W. D., L. H. Haber, and R. F. Martin (1977) Inhibition of spinothalamic tract cells and interneurons by brain stem stimulation in the monkey. J. Neurophysiol. 40:968-981.

Wilson, V. J., and B. W. Peterson (1978) Peripheral and central substrates of vestibulo spinal reflexes. Physiol. Rev. 58:80-105.

Windle, W. F. (1933) Neurofibrillar development in the central nervous system of cat embryos between 8 and 12 mm long. J. Comp. Neurol. 58:643-723.

Windle, W. F., and M. F. Austin (1936) Neurofibrillar development in the central nervous system of chick embryos up to 5 days of incubation. J. Comp. Neurol. 63:431-463.

Winter, D. L. (1965) N. gracilis of cat. Functional organization and corticofugal effects. J. Neurophysiol. 28:48-70.

Wirth, F. P., Jr., and M. Van Buren (1971) Referral of pain from dural stimulation in man. J. Neurosurg. 34:630-642.

Wise, S. P., and E. G. Jones (1976) The organization and postnatal development of the commissural projection of the rat somatic sensory cortex. J. Comp. Neurol. 168:313-343.

Wise, S. P., E. A. Murray, and J. D. Coulter (1979) Somatotopic organization of corticospinal and corticotrigeminal neurons in the rat. Neurosci. 4:65-78.

Woda, A., J. Azerad, G. Guilbaud, and J. M. Besson (1975) E´´tude microphysiologique des projections thalamiques de la pulpe dentaire chez le chat. Brain Res. 89:193-213.

Woolston, D. C., J. Kassel, and J. M. Gibson (1981) Trigeminocerebellar mossy fiber branching to granule cell layer patches in the rat cerebellum. Brain Res. 209:255-269.

Woolston, D. C., J. R. LaLonde, and J. M. Gibson (1982) Comparison of response properties of cerebellar- and thalamic- projecting interpolaris neurons. J. Neurophysiol. 48:160-173.

Wouterlood, F. G., and H. J. Groenewegen (1985) Neuroanatomical tracing by use of Phaseolus vulgaris-leucoagglutinin (PHA-L): electron microscopy of PHA-L-filled neuronal somata, dendrites, axons and axon terminals. Brain Res. 326:188-191.

Yakota, T. (1976) Two types of tooth pulp units in the bulbar lateral reticular formation. Brain Res. 104:325-329.

Yakota, T. (1988) Anatomy and physiology of intra-and extracranial nociceptive afferents and their central projections. In J. Olesen and L. Edvinsson (eds.). Basic Mechanisms of Headache. Elsevier, Amsterdam. pp.117-126.

Yakota, T., and N. Matsumoto (1983a) Somatotopic distribution of trigeminal nociceptive specific neurons within the caudal somatosensory thalamus of the cat. Neurosci. Lett. 39:125-130.

Yakota, T., and N. Matsumoto (1983b) Location and functional organization of trigeminal wide dynamic range neurons within the nucleus ventralis posteromedialis of the cat. Neurosci. Lett. 39:231-236.

Yakota, T., and Y. Nishikawa (1982) Responses in the cat caudal medulla by stimulation of tooth pulp. In: B. Matthews and R. G. Hill (eds.). Anatomical Physiological and Pharmacological Aspects of Trigeminal Pain. Excerpta Medica, Amsterdam. pp. 119-135.

Yakota, T., N. Kayama, Y. Nishikawa, and A. Hasegawa (1988) Dual somatosensory representation of the peridontium in nucleus ventralis posteromedialis of the cat thalamus. Brain Res. 475:187-191.

Yakota, T., N. Koyama, N. Matsumoto (1985) Somatotopic distribution of trigeminal nociceptive neurons in ventrobasal complex of cat thalamus. J. Neurophysiol. 53:1387-1400.

Yakota, T., T. Masuda, H. Taguchi, and N. Koyama (1987) Viscerosomatic convergence onto nociceptive neurons in the shell region of nucleus ventralis posterolateralis. In: R. F. Schmidt, H. G. Schaible, and C. Vahle-Hinz (eds.). Fine Afferent Nerve Fibers and Pain. VCH, Weinheim. pp. 427-437.

Yakota, T., Y. Nishikawa, N. Koyama (1986) Toothpulp input to the shell region of nucleus ventralis posteromedialis of the cat thalamus. J. Neurophysiol. 56:80-98.

Yasui, Y., K. Itoh, N. Mizuno, S. Nomura, M. Takada, A. Konishi, and M. Kudo (1983) The posteromedial ventral nucleus of the thalamus (VPM) of the cat: Direct ascending projections to the cytoarchitectonic subdivisions. J. Comp. Neurol. 220:219-228.

Yee, J., and K. B. Corbin (1939) The intramedullary course of the upper five, cervical, dorsal root fibers in the rat. J. Comp. Neurol. 70:297-304.

Ygge, J., and G. Grant (1983) The organization of the thoracic nerve projection in the rat dorsal horn demonstrated with transganglionic transport of horseradish peroxidase. J. Comp. Neurol. 216:1-9.

Yokota, T. (1976) Two types of tooth pulp units in the bulbar lateral reticular formation. Brain Res. 104:325-329.

Yoss, R. E. (1953) Studies of the spinal cord. Part 3. Pathways for deep pain within the spinal cord and brain. Neurology 3:163-175.

Young, R. F. (1982) Effects of trigeminal tractotomy on dental sensation in humans. J. Neurosurg. 56:812-818.

Young, R. F., and K. M. Perryman (1984) Pathway for orofacial pain sensation in the trigeminal brain-stem nuclear complex of the macaque monkey. J. Neurosurg. 61:563-568.

Young, R. F., and K. M. Perryman (1986) Neuronal responses in rostral trigeminal brain-stem nuclei of macaque monkeys after chronic trigeminal tractotomy. J. Neurosurg. 65:508-516.

Young, R. F., T. D. Oleson, and K. M. Perryman (1981) Effect of trigeminal tractotomy on behavioral response to dental pulp stimulation in the monkey. J. Neurosurg. 55:420-430.

Zucker, E., and W. I. Welker (1969) Coding of somatic sensory input by vibrissae neurons in the rat's trigeminal ganglion. Brain Res. 12:138-156.

Zugami, A. S., and G. A. Lambert (1990) Stimulation of cranial vessels excites nociceptive neurones in several thalamic nuclei of the cat. Exp. Brain Res. 81:552-566.

Zugami, A. S., G. A. Lambert, and J. W. Lance (1987) Studies in the cat for the pathway for vascular head pain. Cephalgia Suppl 6:26.